

Antibacterial prenylated isoflavonoids and stilbenoids

*Quantitative structure-activity relationships
and mode of action*

Carla Araya-Cloutier

Propositions

1. The site of action of antibacterial prenylated phenolic compounds is the cytoplasmic membrane.
(this thesis)
2. After hydrophobicity, molecular shape is the most important feature of antibacterial prenylated phenolic compounds.
(this thesis)
3. Evaluation of assumptions advances science more than their prolonged use.
4. Personalized medicine may be effective, but not efficient.
5. "Carbon neutrality" is at its best a delayed "carbon correction".
6. The current use of referenda in the EU does not serve democracy.
7. Confirmation bias flourishes in the social media environment.

Propositions belonging to the thesis entitled:

"ANTIBACTERIAL PRENYLATED ISOFLAVONOIDS AND STILBENOIDS
Quantitative structure-activity relationships and mode of action."

Carla M. Araya-Cloutier

Wageningen, 13 April 2017

Antibacterial prenylated isoflavonoids and stilbenoids

**Quantitative structure-activity relationships and
mode of action**

Carla Araya-Cloutier

Thesis committee

Promotors

Prof. Dr H. Gruppen
Professor of Food Chemistry
Wageningen University & Research

Co-promotors

Dr J-P. Vincken
Associate professor, Laboratory of Food Chemistry
Wageningen University & Research

Dr H.M.W. den Besten
Associate professor, Laboratory of Food Microbiology
Wageningen University & Research

Other members

Prof. Dr J.T. Zuilhof, Wageningen University & Research
Prof. Dr O.P. Kuipers, University of Groningen
Prof. Dr B.H. ter Kuile, University of Amsterdam
Prof. Dr P.J.G.M. de Wit, Wageningen University & Research

This research was conducted under the auspices of the Graduate School VLAG (Advanced studies in Food Technology, Agrobiotechnology, Nutrition and Health Sciences).

Antibacterial prenylated isoflavonoids and stilbenoids

**Quantitative structure-activity relationships and
mode of action**

Carla Araya-Cloutier

Thesis

submitted in fulfilment of the requirements for the degree of doctor

at Wageningen University

by the authority of the Rector Magnificus,

Prof. Dr A.P.J. Mol,

in the presence of the

Thesis Committee appointed by the Academic Board

to be defended in public

on Thursday 13 April 2017

at 11 a.m. in the Aula.

Carla Araya-Cloutier

Antibacterial prenylated isoflavonoids and stilbenoids

Quantitative structure-activity relationships and mode of action,

200 pages.

PhD thesis, Wageningen University, Wageningen, the Netherlands (2017)

With references, with summary in English

ISBN 978-94-6343-036-4

DOI 10.18174/400170

Abstract

Prenylated phenolic compounds, i.e. those bearing a C₅-isoprenoid (*prenyl*) substituent, are abundant in plants from the Fabaceae (legume) family and are potential natural antibacterial agents against resistant pathogenic bacteria. To understand the antibacterial properties of these compounds, (quantitative) structure-activity relationships and mode of action of these molecules were investigated against Gram positive and negative bacteria.

Compounds belonging to the flavonoid, isoflavonoid and stilbenoid classes were studied. Antibacterial activity was modulated by the (sub)class of phenolic compound, as well as by the configuration, position and number of prenyl groups. Prenylated isoflavones were found to be better antibacterials than prenylated pterocarpan and prenylated stilbenoids. It was also shown that chain prenylation increased the antibacterial activity more than pyran-ring prenylation. Diprenylated compounds were among the most active antibacterials with minimum inhibitory concentrations of less than 10 µg/mL against *Listeria monocytogenes*. The main molecular characteristics defining antibacterial activity were molecular shape (including flexibility and globularity) and hydrophobicity. Regarding the mode of action of these compounds, it was shown that prenylated phenolic compounds can disrupt the integrity of the membrane by permeabilization very quickly. Interestingly, some good antibacterial prenylated (iso)flavonoids showed good permeabilization capacity whereas others not (including diprenylated molecules), highlighting potential differences in their interactions with the bacterial membrane. Likewise, it was shown that Gram negative intrinsic resistance towards prenylated phenolic compounds is primarily due to the activity of efflux pump systems and that it can be overcome by using an efflux pump inhibitor in combination with antibacterial prenylated compounds. Last, *in vitro* production of prenylated phenolic compounds was performed with microbial prenyltransferase SrCloQ and novel C- and O-prenylated compounds were produced.

Table of contents

Chapter 1	General Introduction	1
Chapter 2	The position of prenylation of isoflavonoids and stilbenoids from legumes (Fabaceae) modulates the antimicrobial activity against Gram positive pathogens	29
Chapter 3	Rapid membrane permeabilization of <i>Listeria monocytogenes</i> and <i>Escherichia coli</i> induced by prenylated phenolic compounds: influence of skeleton structure and prenyl configuration	65
Chapter 4	QSAR-based molecular signatures of prenylated (iso)flavonoids underlying antimicrobial potency against and membrane-disruption in Gram positive and Gram negative bacteria: <i>Listeria monocytogenes</i> and <i>Escherichia coli</i>	97
Chapter 5	Structural basis for non-genuine phenolic acceptor substrate specificity of <i>Streptomyces roseochromogenes</i> prenyltransferase CloQ from the ABBA/PT-barrel superfamily	135
Chapter 6	General Discussion	161
Summary		189
Acknowledgments		193
About the author		197

Chapter 1

General Introduction

Phenolic compounds comprise an extensive family of plant secondary metabolites. Based on the number of phenolic rings, compounds have been classified as simple phenolic compounds (single phenolic ring) or polyphenols (two or more phenolic rings). Phenolic compounds can be substituted with multiple hydroxyl groups or other groups (e.g. methyl, glycosyl), increasing their chemical diversity. Phenolic compounds are known to be produced in plants as part of their defense system against pathogens. In the Fabaceae (Leguminosae) family, substitution of phenolic compounds with a five-carbon *prenyl* group is known to be one of the main defense responses to pathogens. These prenylated phenolics have the potential to be used as natural antibacterials against pathogenic bacteria. Prenylated phenolic compounds are structurally diverse as a result of different phenolic skeletons, different configuration of prenylation, different positions at which the prenyl groups can be attached, and the presence of other substituents. This large molecular diversity has made it difficult to establish clear structure-activity relationships (SAR) for this family of compounds with regard to antibacterial activity.

Systematic SAR of prenylated phenolic compounds as antibacterials need to be established. To understand the molecular features relevant for antibacterial activity, an array of different prenylated phenolic compounds needs to be considered. In line with this, due to lack of commercially or otherwise available pure prenylated compounds, production of sufficient amounts of structurally diverse prenylated phenolic compounds has to be studied as well. Likewise, it is important to define the mode of action of these natural compounds. The current need for new antibacterials, the potential of prenylated phenolic compounds as antibacterial agents and their production methods will be discussed in this chapter.

ANTIBACTERIAL DRUGS

Discovery of and resistance development to antibacterial drugs

Resistance is inevitable. It is not a question of 'if' but rather a question of 'when' (Walsh et al., 2014)

Natural products have played an essential role in the discovery and development of therapeutic agents since ancient times.^[1] Most antimicrobials were originally isolated by screening soil-derived actinomycetes during the golden era of antimicrobial discovery (1930s-1960s) (**Figure 1.1**).^[2] Later came the golden era of medicinal chemistry, where optimization of existing molecular scaffolds created successive generations of important antibiotic classes. This approach was successful in dealing with the succeeding waves of resistant bacterial pathogens.^[3] In the 1990s, target-based high-throughput screening of synthetic compound libraries was performed. However, these chemical libraries proved to be inefficient in generating lead compounds that could effectively penetrate bacterial cells.^[2] The synthetic chemicals often lacked the extensive functional group chemistry and chirality that natural products display.^[4] This resulted in a significant discovery void.^[3] Misuse of antibiotics, lack of discovery and innovation has led to the so-called resistance era faced today.^[5]

Resistance to common bacteria has reached alarming levels in many parts of the world,^[7] due to the almost inevitable selection of antimicrobial-resistant bacteria that arise after widespread use of a new antibiotic, both for veterinary and human use.^[3] The emergence of multidrug-resistant pathogens (i.e. resistant to multiple antibacterial drugs) with a variety of resistance mechanisms is characteristic of the resistance era.^[8] Despite the boom of genomic sciences, target-based high-throughput screening and advances in rational drug design,^[2] interest in natural product revitalized as a result of a pressing need for new antimicrobial scaffolds.^[9,10] This thesis deals with the potency, spectrum of activity and mode of action of phenolic compounds from legume plants as antibacterial agents.

Bacterial cell envelope architecture

The cell envelope of bacteria is the first barrier antibacterials need to cross in order to reach their targets (with the exception of antibacterials acting on the cell envelope itself) (**Figure 1.2**). In Gram positive bacteria, the cell envelope is composed of a cytoplasmic membrane (phospholipid bilayer) and a thick, rigid cell wall. The cell wall is composed of crosslinked layers of peptidoglycans associated with anionic polymers, called teichoic acids, and surface proteins. The function of the cell wall is primarily to confer shape and mechanical strength to bacteria.^[11] Gram negative bacteria have an extra outer membrane (OM) composed of a special lipid bilayer: the outer leaflet of the OM is composed of glycolipids, mainly lipopolysaccharides (LPS), instead of phospholipids. LPS molecules bind each other tightly, especially if divalent cations (Ca^{2+} and Mg^{2+}) are present to screen the negative charge of phosphate groups present on the molecules.

The acyl chains are largely saturated, which facilitates tight packing. These structural features make the OM very impermeable, specially to hydrophobic molecules.^[12,13] Furthermore, outer membrane proteins (OMPs) can be associated to the OM and function as channels for the diffusion of small molecules. The peptidoglycan cell wall in Gram negatives is relatively thin without teichoic acids.^[14]

For any antibacterial action, four main steps are required: (i) uptake of the antibacterial from solution, (ii) penetration to the target site, (iii) accumulation in target, and (iv) effective interaction with target.^[11] The uptake of an antibacterial across the OM in Gram negatives is often determined by its overall physical character (size, charge, hydrophobicity or amphiphilicity) rather than by specific chemical structure.^[11] Crossing can occur by (i) channel-mediated diffusion through porins (i.e. water-filled channels with low substrate selectivity), (ii) by lipid-mediated diffusion through OM bilayer (although occurrence of this type of influx is expected to be very slow in healthy cells)^[13], (iii) by carrier-mediated diffusion via substrate-specific transporters, or (iv) by self-promoted uptake (as pore-forming cationic peptides).^[11] Passage across the cell wall in both Gram positives and negatives is not restricted, as this open network conveys little barrier to most antibacterials (up to 30-57 kDa).^[15] For antibacterials with targets inside the cytosol, passage across the cytoplasmic membrane in both Gram positive and negative bacteria is usually mediated by active, carrier-mediated transport systems.^[16]

Bacteria can be intrinsically resistant to antibacterials, i.e. have the ability to resist the antibacterial action as a result of inherent structural and functional characteristics.^[18] Main causes of intrinsic resistance are (i) absence of a susceptible target (bacteria may lack the structural factors essential for the antibacterial action, e.g. Gram negatives lack the Ca^{2+} -rich environment in the cytoplasmic membrane essential for daptomycin binding and activity),^[19] (ii) prevention of access to targets (e.g. antibacterials may be unable to cross the OM of Gram negatives due to their size), or (iii) active efflux of the antibacterial preventing the effective accumulation in the target.^[18] In addition to intrinsic resistance, bacteria can acquire or develop resistance to antimicrobials by (i) genetic or post-translational modification of the target, (ii) chemical inactivation (e.g. hydrolysis of the antimicrobial), or (iii) modification of the cell envelope to reduce influx (e.g. alteration of the LPS layer, alteration of or reduction in porin density) or increase the efflux (e.g. induction of efflux pumps).^[18]

Gram negative bacteria are known to have a higher intrinsic resistance towards antimicrobials than Gram positive bacteria. This is primarily due to the limited permeability conferred by LPS, especially for hydrophobic molecules, and size restrictions of porins (generally $\text{MW} < 600\text{-}700$).^[11,13] In addition, double-membrane-spanning intrinsic efflux pumps keep an effective excretion of antibacterials across the double membrane of Gram negatives.^[17] Efflux pumps are transport proteins with broad substrate specificity involved in the expulsion of toxic substances. Studies indicate that recognition and uptake of substrates by the efflux pumps in Gram negatives can take place directly from the periplasm, from the outer leaflet of the inner membrane or from the cytoplasm.^[20,21]

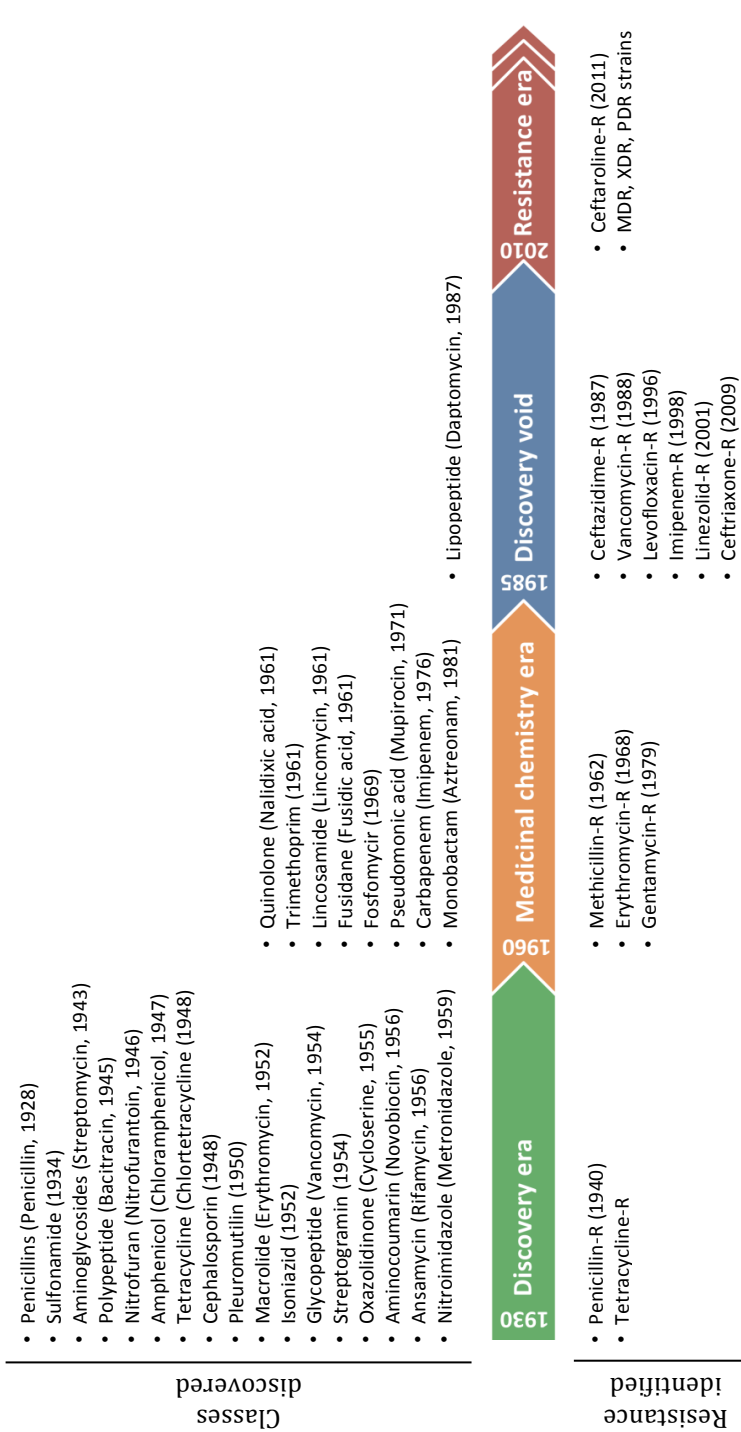


Figure 1.1. Time line of different eras of antimicrobial discovery and development. Upper side of time line: classes of antimicrobials discovered with name of representative agent and year of discovery between brackets; lower side of time line: resistance detection for some clinically-relevant antimicrobials. R, resistance; MDR, multidrug-resistant (resistant to ≥ 3 classes of antimicrobial agents); XDR, extensively-drug resistant (resistant to all but 1-2 classes of antimicrobial agents among those regarded as potentially effective for the respective pathogen); HDR, pan-drug resistant (resistant to all antimicrobial agents in all classes) (based on and adapted from Walsh et al.^[3], Ventola^[14]; WHO^[6]).

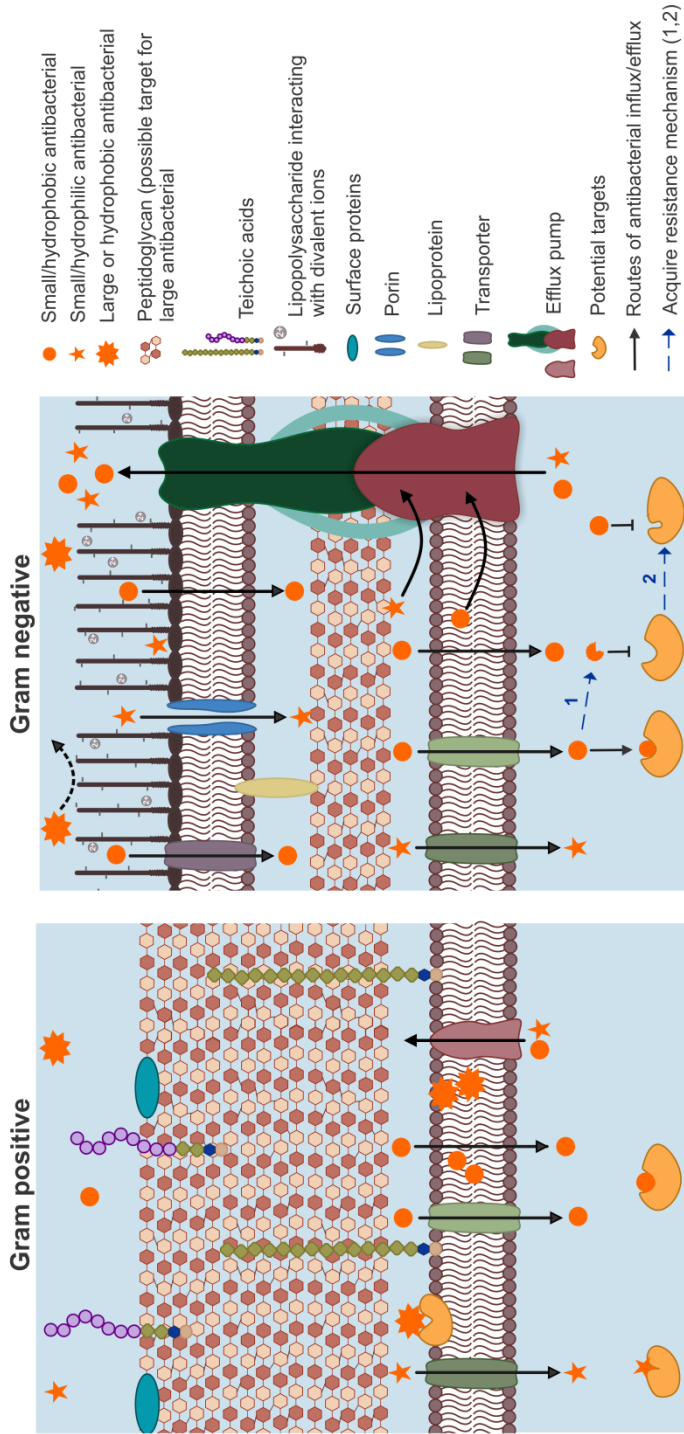


Figure 1.2. Routes of influx and efflux of antibacterials. Targets can be located at the cell envelope (e.g. peptidoglycan, cytoplasmic membrane or penicillin binding proteins), cytosol (e.g. ribosomes), or inside organelles (e.g. DNA gyrase). Acquired resistance mechanisms, i.e. inactivation of antibacterial (1) or modification of target (2) are shown in the Gram negative. Based on Li et al.^[1,9] and Silhavy et al.^[1,3]

In this thesis, we investigated the mode of action of prenylated phenolic compounds by studying their effects on the cytoplasmic membrane integrity (proposed target site of these compounds) and their expulsion by the efflux pump systems.

ANTIBACTERIAL PHYTOCHEMICALS FROM LEGUMES

Historically, natural extracts have been used as safe and effective remedies for infections in traditional medicine. Because nature can more effectively provide stereochemical and functional group diversity than synthetic chemistry,^[22] natural sources, like marine organisms, plants and uncultured bacteria, are extensive sources of new antibacterials.^[2] The majority of the antibacterials introduced to the market during the discovery era and since the 1980s has been derived from natural compounds.^[23]

Within natural products, plant extracts have displayed high effectiveness, low toxicity and low resistance development, probably due to their multiple mechanisms of action derived from the plethora of structurally diverse compounds produced by secondary plant metabolism.^[24,25] Some of the major antimicrobial compounds produced by plants are phenolic compounds (e.g. phenolic acids, flavonoids, isoflavonoids, tannins), quinones, coumarins, alkaloids, lectins, polypeptides and terpenoids.^[26]

The Fabaceae (Leguminosae) is the second largest family of medicinal plants (i.e. plants containing substances with therapeutic activity, which are known to be safe and effective based on its long historical use), containing over 490 medicinal plant species.^[27] This family was the top plant family associated with drug interventions in clinical trials in 2013, with anti-infective agents (i.e. antibacterial, antifungal, antiparasitic or antiviral) being the major drug category investigated.^[28] Phenolic compounds and saponins (triterpenoid glycosides) are two major groups of secondary metabolites in legumes.^[29,30] In fact, these two groups of phytochemicals are considered to be responsible for the wide range of biological activities of plants used in traditional Chinese medicine (TCM).^[31] Known examples of these type of phytochemicals include glyceollins (phenolic compound) and soyasaponins from soybean,^[24,32] and glabridin (phenolic compound) and glycyrrhizin (saponin) from licorice.^[33] Phenolic compounds and saponins have shown diverse biological activities, such as (anti)estrogenic,^[34,35] haemolytic,^[36] anti-inflammatory^[37] and antimicrobial activity.^[38,39]

In legumes, saponins are denoted as pre-formed barriers against pathogens, known as *phytoanticipins*.^[40] The amphiphilic nature of saponins, resulting from the triterpenoid skeleton substituted with glycosyl chains, enables them to interact with membrane sterols. This interaction results in disruption of membranes and, therefore, in antimicrobial activity.^[40] Antimicrobial activity of saponins has been reported especially against fungi and Gram positive bacteria.^[38] Legumes mainly contain oleanane-class soyasaponins, with members of the A, B and E groups.^[41] Group A soyasaponins contain two glycosyl chains, attached at C3 and C22 of soyasapogenol A. Group B and E soyasaponins contain only one glycosyl chain attached at C3 of soyasapogenol B or soyasapogenol E, respectively. Further structural diversification of soyasaponins is

derived from different levels of oxidation of the skeleton and different types of substituents, such as the DDMP (2,3-dihydro-2,5-dihydroxy-6-methyl-4H-pyran-4-one) substituent in group B saponins, different glycosyl moieties (e.g. glucuronic acid, galactose, glucose, rhamnose, xylose), and the presence of acetyl groups attached to those glycosyl moieties.^[42,43]

Prenylated phenolic compounds, i.e. those bearing an isoprenoid substituent attached to the skeleton, are often produced in response to plant infection, acting as *phytoalexins*.^[44] The Fabaceae family is one of the few families producing these compounds.^[45] Prenylation increases the antimicrobial activity of a molecule by increasing its affinity towards biological targets, such as membranes and proteins.^[46] Structural diversity of prenylated phenolic compounds in legumes is extensive, derived from the different classes of phenolic compounds and many possible substitutions (see below).

As both saponins and prenylated phenolic compounds are known to be plant antimicrobials, in this thesis we investigated the contribution of these two main groups of phytochemicals on the antibacterial properties of legume seedling extracts against human pathogens. Nevertheless, production of prenylated phenolic compounds is directly related to counteracting infection, in contrast to saponins which are constitutively produced. Therefore, this thesis is focused mainly on the antibacterial properties of prenylated phenolic compounds.

Structural diversity of prenylated phenolic compounds in legumes

Classes of phenolic compounds

Isoflavonoids are the main class of prenylated phenolic compounds produced in legumes. Flavonoids and, to a lesser extent, stilbenoids have also been found in some legume species.^[44,47] This thesis describes the antibacterial properties of compounds belonging to these three classes of phenolic compounds.

All these compounds are derived from the prenylpropanoid pathway (**Figure 1.3**).^[48] The flavonoid backbone (2-phenyl benzopyran) is formed after elongation (chalcone synthase, EC 2.3.1.74) of *p*-coumaroyl CoA with three molecules of malonyl-CoA, followed by intramolecular Claisen condensation (EC 2.3.1.74) and subsequent ring closure (chalcone isomerase, EC 5.5.1.6). These reactions result in the 2-phenyl benzopyran or flavonoid structure (C₆-C₃-C₆ backbone).^[49,50] The flavanones formed, naringenin or liquiritigenin, are further transformed into an array of flavonoid derivatives, belonging to 8 different subclasses, depending on the level of oxidation of the C-ring (**Figure 1.4**).^[51]

Isoflavonoids (3-phenyl benzopyrans) are formed after the aryl rearrangement (isoflavanone synthase, EC 1.14.13.136) from the C2 to the C3 of the benzopyran moiety of the flavonoid, followed by a dehydration step (isoflavanone dehydratase, EC 4.2.1.105) to obtain the basic isoflavones genistein or daidzein.^[53] These compounds are the precursor of a large variety of isoflavonoid compounds, belonging to 13 different subclasses, depending on the level of oxidation of the C-ring and the occurrence of an additional heterocyclic ring (**Figure 1.4**).^[47,54]

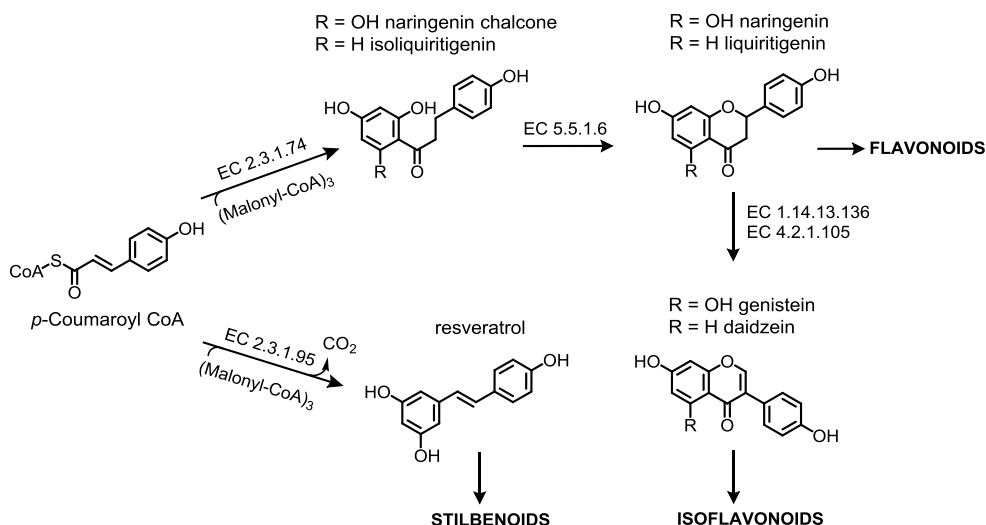


Figure 1.3. Biosynthetic pathway of phenolic compound classes studied in this thesis (adapted from Kodan et al.^[52]).

The stilbenoid skeleton (1,2-diphenylethene, C₆-C₂-C₆ backbone) derives from an aldol condensation and decarboxylation of the malonyl elongated CoA-activated phenolic acid (all done by the same enzyme, stilbene synthase, EC 2.3.1.95). The most common stilbene, resveratrol, derives from *p*-coumaroyl CoA (as shown in **Figure 1.3**).^[50] Other stilbenoids are formed from different CoA-activated phenolic acids: pinosylvin is formed from cinnamoyl CoA; piceatannol is formed from caffeoyl CoA and isorhapontigenin is formed from feruloyl CoA.^[55] Unlike (iso)flavonoids, diversification of stilbenoids consists of polymerization reactions involving usually 2 out of 4 different monomeric stilbenoids resulting in a large number of oligomeric structures.^[56]

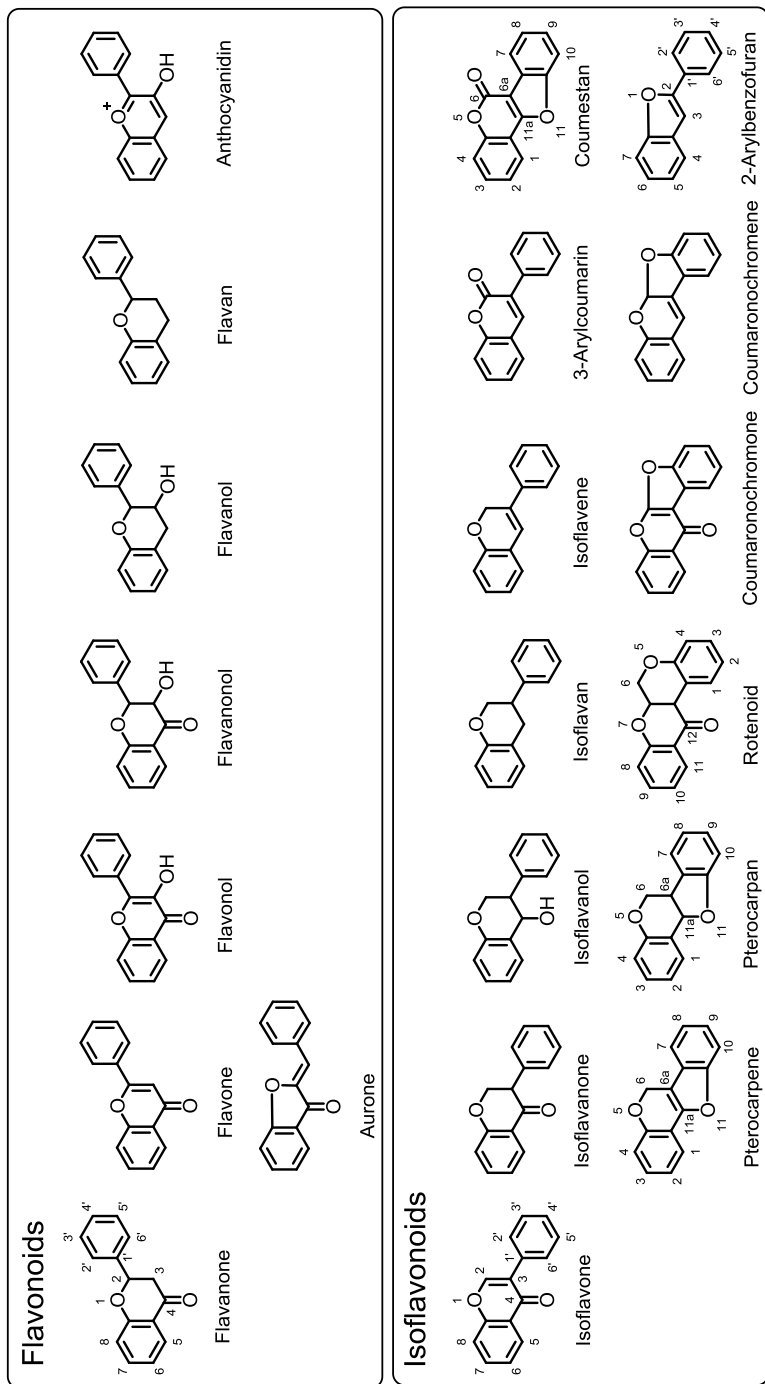


Figure 1.4. Flavonoid and isoflavonoid subclasses from which molecular diversification starts. IUPAC numbering of the different subclasses is shown (skeletons without numbering system are numbered similarly as the first skeleton of their class).

Decoration of phenolic compounds

Further diversification of phenolic compounds involves addition of different substituents to the main skeleton, mainly hydroxyl, O-methyl, glycosyl and prenyl groups.

Prenylation is used as a generic term for substitution with a five-carbon (prenyl group), ten-carbon (geranyl or lavandulyl) or fifteen-carbon (farnesyl) isoprenoid group.^[54] In this thesis, compounds bearing the five-carbon isoprenoid or prenyl unit are investigated. Prenyl groups are found in nature in different configurations: as a chain, or as a five- or six-membered ring coupled to a neighboring hydroxyl group (**Figure 1.5**).^[57] Further modifications, such as addition of hydroxyl groups or modification of the unsaturation pattern, have also been found in naturally-occurring phenolic compounds.^[58,59]

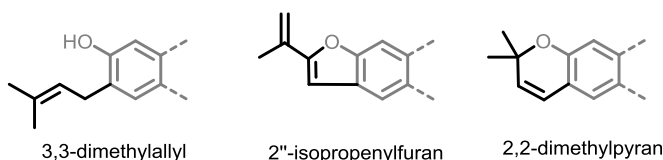


Figure 1.5. Most frequent configurations of prenyl groups (in black).

Prenyl groups are added to phenolic compounds by prenyltransferase.^[58] The prenyl groups are mainly attached to C-atoms, although O-prenylation has also been reported in few cases.^[47] There are four main carbon positions at which the prenyl group can be attached.^[60] As IUPAC carbon numbering is different between phenolic subclasses, Simons et al.^[54] introduced a different annotation system to describe the position of the prenyl group in an isoflavonoid skeleton, independent of the subclass. This system can be extended to flavonoids and stilbenoids, as shown in **Figure 1.6**.

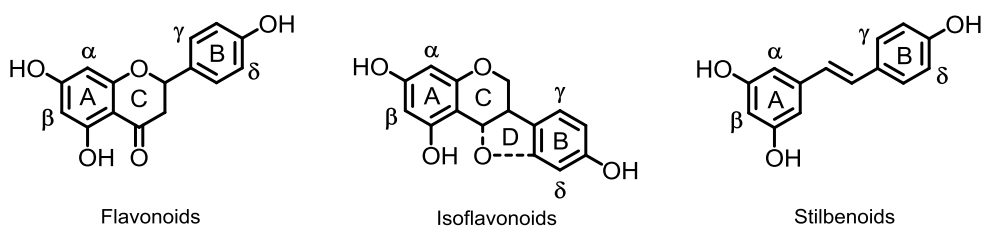


Figure 1.6. Prenyl positions within a phenolic compound skeleton indicated by Greek letters.

This thesis deals with the main prenylated phenolic compounds in legumes, belonging to the flavonoid, isoflavonoid and stilbenoid classes prenylated at three main positions (i.e. α , β and δ) in three main configurations (i.e. chain, pyran and furan).

Antimicrobial activity of prenylated phenolic compounds

Studies on antibacterial properties of prenylated phenolic compounds have mainly focused on Gram positive antibacterial activity, including clinical and foodborne pathogens, such as *Staphylococcus aureus* (*S. aureus*), *Streptococcus mutans* (*S. mutans*), *Enterococcus faecalis* (*E. faecalis*),^[61-63] and *Listeria monocytogenes* (*L. monocytogenes*).^[64,65] Although with much less examples, some prenylated phenolic compounds have shown moderate/good antibacterial activity against Gram negative bacteria, such as *Escherichia coli* (*E. coli*), *Salmonella Typhimurium*, *Klebsiella* spp. and *Shigella* spp.^[1,66-69]

Often, antibacterial activity is measured quantitatively by the broth (micro)dilution assay, where serial dilutions of the compound of interest are tested against a bacterial suspension (often standardized based on turbidity).^[70,71] Growth (**Step 1, Figure 1.7**) is usually determined visually (i.e. presence of turbidity) or spectrophotometrically (i.e. measurement of absorbance or “optical density”), after 24 h of cell exposure to antibacterial, at 35 ± 2 °C.^[71] The time to detection (TTD) of growth, i.e. the time to reach a specific absorbance value,^[72] can be used as an indication of inhibition. The minimum inhibitory (MIC) and bactericidal (MBC) concentrations are determined after the exposure period (**Step 2**). The MIC is usually defined as the lowest concentration of the compound that prevented visible growth of the bacteria.^[73] It is generally used as a standard for expressing the susceptibility of a microorganism to an antibacterial agent.^[74] The MBC of the compound is often defined as the lowest concentration of antibacterial that resulted in no bacterial growth after sub-culturing the antibacterial-exposed cells to antibacterial-free media.^[75] Both the MIC and the MBC are dependent on the initial inoculum size. Additionally, absorbance measurements have detection limits of around 10^7 CFU/mL or higher, depending on the microorganism.^[76] Therefore, plate count is a more accurate, alternative method used in this thesis. Both inoculum and MIC/MBC values are determined based on plate counts, as illustrated in **Figure 1.7**.

Natural compounds with MIC values equal or lower than $15 \mu\text{g/mL}$ are considered as compounds with very good antibacterial activity; compounds with MIC values from 15 up to and including $25 \mu\text{g/mL}$ are considered as having good activity, whereas compounds with MIC values from 25 up to and including $100 \mu\text{g/mL}$ are considered as having moderate antibacterial activity.^[77] Pure compounds with MIC values higher than $100 \mu\text{g/mL}$ are usually considered as having low activity, and thereby irrelevant.^[77]

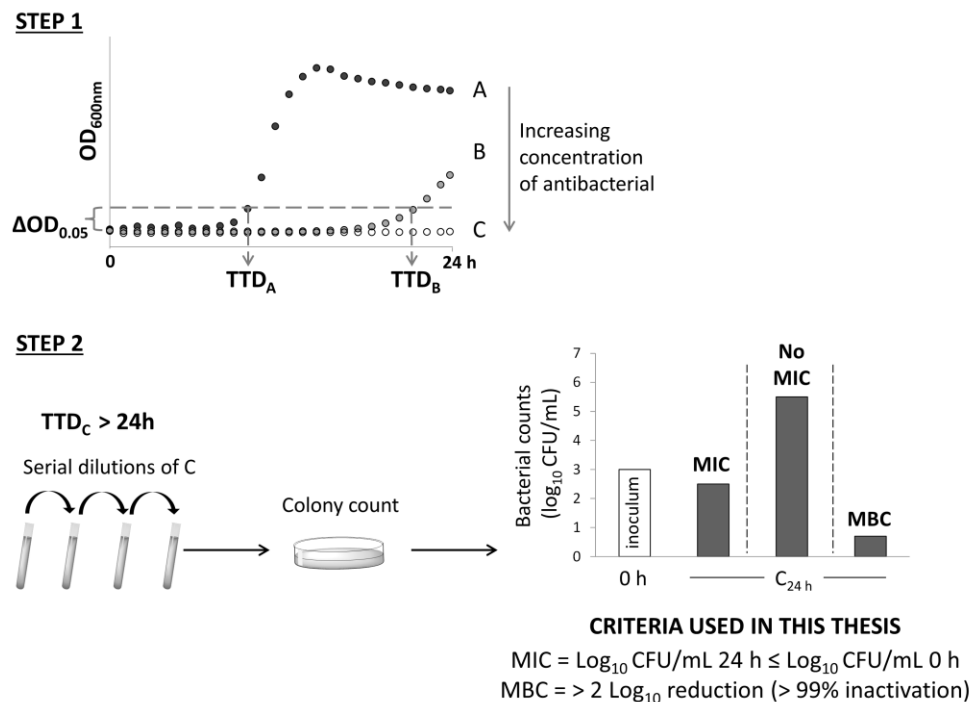


Figure 1.7. Schematic representation of the antibacterial susceptibility test used in this thesis. Step 1) The time to detection (TTD) of bacterial growth is the time required to observe a specific change in the optical density (OD) in 24 h. Increasing concentrations of antibacterial are tested. Step 2) For samples with a TTD > 24 h, serial dilutions are made and plated. After incubation, bacterial colonies (CFU/mL) are counted and MIC and MBC are determined according to the criteria defined.

Prenylated phenolic compounds have been demonstrated to have significant antibacterial activity, especially against Gram positive pathogens. MICs can be at the same levels as those of some traditional antibacterials.^[78-80] For example, eryvarin W, a double prenylated pterocarpene, had a MIC of 1.6-3.1 $\mu\text{g}/\text{mL}$ against 13 strains of methicillin-resistant *S. aureus* (MRSA), whereas the antibiotic vancomycin had a MIC of 0.8-3.1 $\mu\text{g}/\text{mL}$ against the same strains.^[61] The majority of potent prenylated phenolic compounds found have two prenyl groups attached to their skeleton. Some examples of such promising prenylated phenolic compounds are shown in **Figure 1.8** and **Table 1.1**. These active prenylated compounds had MICs below 12.5 $\mu\text{g}/\text{mL}$ against Gram positive or Gram negative bacteria. The active compounds belonged to a variety of (iso)flavonoid subclasses and contained either a prenyl chain or a pyran ring.

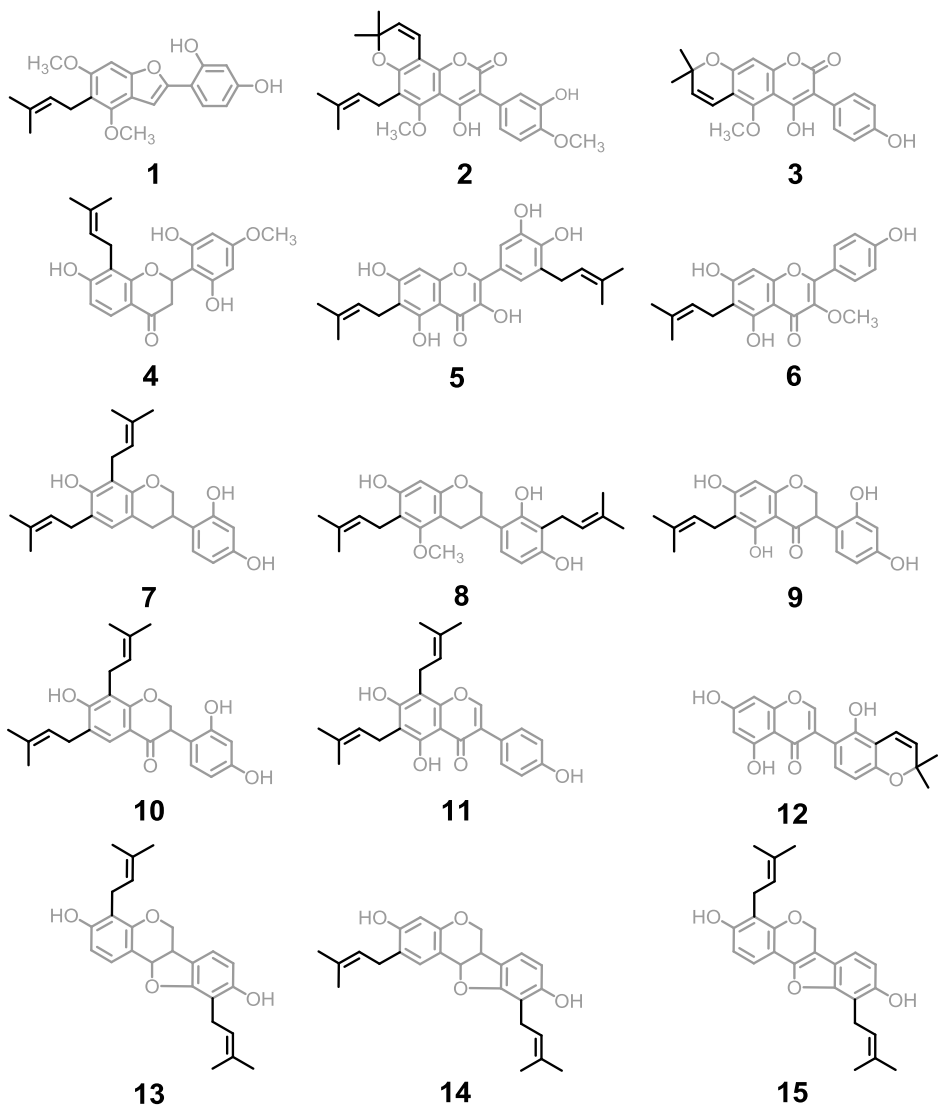


Figure 1.8. Examples of prenylated phenolic compounds with high antibacterial activity. Prenyl group is highlighted in black. Numbers refer to those mentioned in **Table 1.1**.

Table 1.1. Antibacterial prenylated phenolic compounds. ^a

No.	Subclass	Compound	Source ^b	Target bacteria ^c	MIC ^d	Conventional antibacterial, MIC ^d	Ref.
1	2-Arylbenzofuran	Gancaonin I	<i>G. uralensis</i>	<i>B. subtilis</i> <i>M. luteus</i> <i>S. aureus</i> MRSA	3.1 3.1 1.6-3.1 1.6-3.1	Amoxicillin, 0.1-50	[81]
2	3-Arylcoumarin	6,8-Diprenyl-3-arylcoumarin ^e	<i>D. longgeracemosa</i>	<i>S. aureus</i>	0.75	Chloramphenicol, 0.5	[82]
3	3-Arylcoumarin	Indicanine B	<i>E. indica</i>	<i>S. aureus</i>	9.7	Streptomycin, 5.5	[83]
4	Flavanone	Kenusanone D	<i>Ec. koreensis</i>	MRSA	3.1-12.5		[84]
5	Flavonol	Papyriflavonol A	<i>B. papyrifera</i>	<i>S. epidermis</i>	10	Ampicillin, 20	[69]
4	Flavone	Topazolin	<i>G. iconica</i>	<i>S. Typhimurium</i>	2.0	Erythromycin, 1.2	[80]
7	Isoflavan	Eryzerin C	<i>E. zayheri</i>	MRSA	3.1-6.2	Ampicillin, >62	[85]
8	Isoflavan	Licoricidin	<i>G. uralensis</i>	<i>E. faecium</i>	8.1	Clarithromycin, 8	[78]
9	Isoflavanone	Diphysolone	<i>U. picta</i>	<i>E. faecalis</i>	8.1	Vancomycin, >100	[86]
10	Isoflavanone	Eriothichin B	<i>E. eriofricha</i>	<i>E. coli</i>	12.5	Linezolid, 2.5	[87]
11	Isoflavone	8-Prenylwighteone	<i>G. uralensis</i>	<i>S. aureus</i>	8.3	Amoxicillin, 12.5	[88]
12	Isoflavone	Licoisoflavone B	<i>G. uralensis</i>	MRSA	8.0	Penicillin, 6	[89]
13	Pterocarpan	Erybraedin A	<i>E. zayheri</i>	<i>H. pylori</i>	3.1-6.2	Oxacillin, 64-512	[90]
14	Pterocarpan	Erythrabyssin II	<i>E. subumbrans</i>	VRE	1.6-3.1	Vancomycin, 12.5-100	[91]
				<i>Streptococcus</i> ssp.	0.8-1.6	Vancomycin, 0.02-256	
				<i>S. aureus</i>	1.6-3.1	Oxacillin, <0.02- >256	
15	Pterocarpane	Eryvarin W	<i>E. variegata</i>	MRSA	0.8-3.1		[61]
				MRSA	1.56-3.13	Vancomycin, 0.8-1.6	

^aNo. refers to the number of the compound given in Figure 1.8. ^b Plant genus: *Broussonetia* (B), *Dequelia* (D), *Erythrina* (E), *Echinosophora* (Ec), *Glycyrrhiza* (G), *Uraria* (U). ^c *B. subtilis*, *Bacillus subtilis*; *E. faecium*, *Enterococcus faecium*; *E. faecalis*, *Enterococcus faecalis*; *E. coli*, *Escherichia coli*; *H. pylori*, *Helicobacter pylori*; *M. luteus*, *Micrococcus luteus*; *S. aureus*, *Staphylococcus aureus*; MRSA, methicillin-resistant *S. aureus*; *S. Typhimurium*, *Salmonella Typhimurium*; VRE, vancomycin-resistant *Enterococcus*. ^d MIC values determined by broth (micro) dilution assay and given in microgram per millilitre ($\mu\text{g}/\text{mL}$). ^e No trivial name given, 4-hydroxy-5-methoxy-6-(3,3-dimethylallyl)-8-(2'',2''-dimethylpyrano)-3-arylcoumarin.

Structure-activity relationships (SAR) of prenylated phenolic compounds as antibacterials

Antibacterial research on prenylated phenolic compounds from legumes has been focused mainly on screening of extracts from different parts of the plant, mainly from the root, but also the stem bark, leaves and seeds. Potentially antibacterial compounds were purified and antibacterial properties were characterized via measurement of MIC values. Systematic SAR studies, considering different subclasses of phenolic compounds and different configurations and positions of prenylation, are scarce. In addition, the vast majority of SAR studies available refrained from correlating the main findings with antibacterial mode of action.

Nevertheless, some structure-antibacterial activity relationships of prenylated phenolic compounds can be defined (**Figure 1.9**). Prenyl groups bearing substituents, such as hydroxyl groups, do not have antibacterial activity, whereas unsubstituted prenyl groups (i.e. 3,3-dimethylallyl, 2,2-dimethylpyran) have been most commonly related to very good (i.e. MIC $\leq 15 \mu\text{g/mL}$) antibacterial activity.^[79,92,93] In contrast, few examples of furan prenylated compounds with antibacterial activity are available.^[68] Regarding the number of prenyl groups, some of the most potent antibacterial prenylated phenolic compounds, especially against Gram positive bacteria, were double prenylated with two chains or with one chain and one pyran ring.^[61,94] Regarding other substituents, C4' and/or C7 hydroxylation are common substitutions in good antibacterial (iso)flavonoids.^[84] Methylation has been found detrimental for antibacterial activity,^[67,86,95] although some methylated prenylated phenolic compounds have shown very good antibacterial activity.^[91,96] With regard to the position of the prenyl group within the phenolic skeleton, no clear SAR can be made, as studies have shown different trends depending on the subclass. For example, flavanones with a prenyl group at position α have shown better antibacterial activity than those with a prenyl group at position β .^[97] For isoflavones, the opposite behavior has been observed.^[98]

In general, SAR cannot be made easily for all prenylated phenolic compounds based on current research reports. Antibacterial activity has proven to be dependent on the overall configuration of the molecule, rather than only on prenylation. Therefore, systematic SAR studies covering the extensive structural diversity of prenylated phenolic compounds are needed to fully understand their activity. Furthermore, application of *in silico* techniques, such as quantitative SAR (QSAR) and pharmacophore modelling, can accelerate the process of antibacterial design from prenylated phenolic compounds. QSAR studies provide mathematical models relating the observed biological activity of molecules to their structural properties.^[10] Pharmacophores are molecular models that contain the essential features responsible for a biological activity of a drug.^[99] Hence, in this thesis, besides investigating the SAR of prenylated phenolic compounds *in vitro*, *in silico* techniques are used to extend the understanding of molecular requirements of these compounds as antibacterials. Furthermore, correlation between main (Q)SAR and

the potential mode of action of prenylated compounds is investigated, as an effort to close the gap between (Q)SAR and mode of action research.

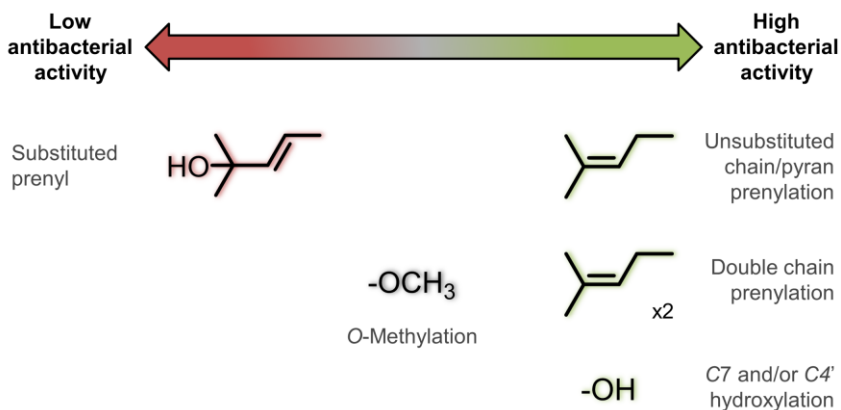


Figure 1.9. SAR for antibacterial activity of prenylated phenolic compounds.

Mode of action of prenylated phenolic compounds

The mechanism of action (MOA) of prenylated phenolic compounds with respect to antibacterial activity is not well understood.^[9] Prenylation increases the hydrophobicity of molecules, which results in an increased affinity to biological targets, such as membranes and proteins.^[100,101] However, many prenylated phenolic compounds have shown to lack antibacterial activity,^[90,102] thereby demonstrating that hydrophobicity is not the only requirement for activity.

Very few studies have investigated the MOA of prenylated phenolic compounds as antibacterials. The main MOAs described for these molecules are: (i) disruption of cell membrane integrity by interacting with the membrane,^[103-105] (ii) inhibition of the respiratory chain (by inhibiting NADH oxidase and NADH-cytochrome c reductase),^[106] (iii) inhibition of efflux pumps systems,^[107] and (iv) inhibition of MurE ligase (cytoplasmic ATPase involved in cell wall synthesis).^[107]

Prenylated phenolic compounds are hydrophobic molecules and the cytoplasmic membrane is one of the first hydrophobic targets encountered by antibacterials. Therefore, in this thesis the effect of prenylated phenolic compounds on the cytoplasmic membrane integrity of the bacterial cell is studied. Unlike for non-prenylated flavonoids,^[108-110] studies reporting the effects of prenylated compounds on membranes are scarce and limited to model systems (liposomes). The main effects of prenylated phenolic compounds on model membranes were alteration of membrane fluidity,^[103] destabilization of membrane organization,^[104] and modification of the thermotropic properties (i.e. phase transition) of lipid bilayers.^[105] These studies confirmed that prenylated compounds can intercalate into lipid membranes. However, such membrane preparations do not necessarily reflect the intrinsic properties of

biological membranes.^[109] Effects of prenylated phenolic compounds on complex bacterial cell membranes, and correlation with antibacterial activity, have not been established.

Therefore, in this thesis, membrane integrity of bacteria will be investigated by measuring the membrane permeability after exposure to different types of prenylated phenolic compounds. Additionally, the relation between antibacterial activity and membrane integrity in both Gram positive and negative bacteria will be investigated.

Prenylated phenolic compounds have shown better antibacterial activity against Gram positive than against Gram negative bacteria. The main cause of the intrinsic resistance of Gram negatives towards prenylated phenolic compounds has not been defined yet. Therefore, in this thesis, the role of the efflux pump systems on the intrinsic resistance of Gram negatives towards different types of prenylated compounds will be studied as well.

METHODS TO PRODUCE PRENYLATED COMPOUNDS

In order to understand SAR and MOA of prenylated phenolic compounds with respect to antibacterial activity, it is necessary to have good coverage of the extensive structural diversity of prenylated phenolic compounds. Currently, availability of such compounds is one of the main limiting factors to perform systematic QSAR studies and, in the long run, to apply prenylated phenolic compounds as antibacterials. Production of double prenylated molecules is, in particular, of great interest, as those have shown potent antibacterial activities (**Figure 1.8**).^[46] Different ways to produce prenylated compounds should be considered. In this thesis, two different methods to produce prenylated phenolic compounds were studied: *in vivo* by stimulating the plant's secondary metabolism and *in vitro* using microbial prenyltransferases.

***In vivo* production of prenylated phenolic compounds**

Legume seedlings are rich sources of phenolic compounds,^[111] such as isoflavones in soybeans with a content ranging from 0.2-3.5 mg/g DW.^[112-114] Several strategies have been investigated towards further enrichment of phenolic compound in legume seedlings.^[115] Because prenylated phenolic compounds are defense metabolites in legumes, the biosynthesis of these types of compounds can be stimulated by application of abiotic or biotic stress factors. These induce production and release of greater amounts of defense metabolites in the plant.^[116] Microbial (pathogen infection), physical (e.g. tissue damage, UV light exposure) or chemical stimuli (e.g. saline stress, exposure to metal ions) can be used as elicitors for the biosynthesis of prenylated phenolic compounds.^[117] The nature of the elicitor, the conditions of the treatment, as well as the characteristics of the plant (i.e. species, cultivar) influence the type and concentration of the defense compounds released.^[118]

Regarding the elicitor, the fungus *Rhizopus oryzae* has been reported to be a more effective elicitor than light and wounding to alter the isoflavonoid content and composition of soybean seedlings.^[119] Germination in combination with fungal elicitation increased the total content of phenolic compounds in legumes 2-30 fold, and stimulated *de novo* synthesis of prenylated phenolic compounds.^[119-121] Some of the main fungi reported to be effective elicitors of legume seedlings are those from the genus *Rhizopus* and *Aspergillus*.^[122-127] The species of fungus can strongly affect the content and composition of prenylated compounds in elicited seedlings. In peanut seedlings, *Aspergillus oryzae* induced a higher content of prenylated stilbenoids than *Rhizopus oryzae*. However, the former fungus was also more efficient in detoxification by chemically modifying the prenylated compounds formed by the plant.^[122]

The phenolic compound (sub)class, as well as position and configuration of prenylation of the compounds produced, is dependent on the legume species.^[128] In **Table 1.2** the main prenylated phenolic compounds produced by fungal elicitation of different legume seedlings are shown. All main prenylated compounds produced were single prenylated. Double prenylated phenolic compounds have been rarely found in fungus-elicited legume seedlings. If so, they are only present in very low concentrations. Examples of these include 8-prenyl-luteone, lupichromone and angustone A/B in blue lupine,^[121] and arahypins in peanut.^[129]

Besides the content and composition of prenylated phenolic compounds, germination in combination with (fungal) elicitation has been shown to boost the bioactivity profile (e.g. antimicrobial, estrogenic, antioxidant activity) of plants.^[118] Elicitation of soybean seedlings with fungi increased the estrogenic activity of extracts by more than 10-fold,^[120] and the radical scavenging activity 2-3 fold.^[130] Glyceollins I-III isolated from *Aspergillus sojae* elicited soybean seeds demonstrated antifungal activity (MIC 25-75 $\mu\text{g}/\text{mL}$) against different fungal species.^[126] Nevertheless, studies on extracts with prenylated phenolic compounds from different elicited legume seedlings and their antibacterial potential against human pathogenic bacteria are lacking.

In this thesis, we applied germination and fungal elicitation to seeds of different legume species in order to obtain different types of potentially antibacterial prenylated phenolic compounds. For this, we used *Rhizopus oryzae* and *Rhizopus oligosporus* (two food grade fungi used in the production of tempeh) as elicitors and the seeds of seven different species of legumes. The composition of legume seedling extracts with regard to the main classes of secondary metabolites, (prenyated) phenolic compounds and saponins, and their contribution to the antibacterial activity of the seedling extracts, were studied.

***In vitro* production of prenylated phenolic compounds using prenyltransferases**

Attempts have been made to isolate the enzymes responsible for prenylation of natural compounds (i.e. prenyltransferases) to use them for the *in vitro* production of prenylated compounds. Some characterization studies of prenyltransferases from legumes, such as soybean,^[131,132] kidney bean^[133] and lupine,^[134,135] and non-legume plants, such as hops,^[136] white mulberry and cudrang,^[137] have demonstrated that plant prenyltransferases are difficult to isolate because they are membrane-bound. Additionally, most plant prenyltransferases studied have shown strict substrate specificity. For example, the prenyltransferase from kidney bean responsible for the production of the prenylated pterocarpan phaseollin showed little activity when similar compounds, such as the pterocarpan medicarpin or the coumestan coumestrol, were used as acceptor substrates.^[133] This strict substrate specificity limits the applications of plant prenyltransferases for the production of known compounds. Consequently, most plant prenyltransferases are not a good option for the *in vitro* production of novel or double prenylated phenolic compounds.

Contrary to plant prenyltransferases, microbial prenyltransferases appear to be an attractive biotechnological tool as most of them are not membrane-bound^[138] and can be used for the *in vitro* production of novel prenylated compounds as they are known to have broad acceptor substrate specificity.^[139] In the last decade, a new superfamily of soluble aromatic prenyltransferases, isolated mainly from *Streptomyces* sp., was discovered.^[140] This so-called ABBA prenyltransferase superfamily has been considered for enhancement of molecular diversity and bioactivity of natural compounds. Different ABBA enzymes have been reported to use different donor substrates, i.e. prenyl, geranyl or farnesyl, and showed promiscuity for non-genuine acceptor substrates, including phenolic compounds.^[141,142]

CloQ from *Streptomyces roseochromogenus* was one of the first ABBA prenyltransferases discovered.^[143] SrCloQ is involved in the biosynthesis of the prenylated aminocoumarin antibiotic clorobiocin. SrCloQ uses the pyrophosphate-activated prenyl group as donor substrate, but its non-genuine acceptor substrate specificity has not been investigated yet. Therefore, in this thesis SrCloQ was investigated as a potential tool to produce novel and double prenylated phenolic compounds, from the flavonoid, isoflavonoid and stilbenoid classes.

Table 1.2. Overview of prenylated phenolic compounds induced by fungal elicitation of legume seedlings.

Plant	Elicitor	Increase in phenolic content (DW)	Most abundant prenylated phenolics produced	Prenyl configuration/position	Subclass	Ref.
Soybean (<i>Glycine max</i>)	<i>Aspergillus sojae</i>	0.24 to 0.50 mg/g total phenolics	Glyceollin I-II	Ring-closed/ α and β	6 α -OH-Pterocarpan	[120]
	<i>Rhizopus oryzae</i>	0.4 to 4.5 mg/g isoflavonoid content	Glyceollin I-IV Glyceollidin II Glyceofuran Prenyl genistein Phaseol Arachidin 1 and 3 IPD ^a	Ring-closed/ α and β Chain/ α and β	6 α -OH-Pterocarpan Isoflavone Coumestan	[120]
Peanut (<i>Arachis hypogaea</i>)	<i>R. oryzae</i>	0.8 to 5 mg/g stilbenoid content	Arachidin 1 and 3 IPD ^a	Chain/ β and δ	Stilbenoid	[122]
	<i>A. oryzae</i>	0.8 to 6.4 mg/g stilbenoid content	Arachidin 1 and 3 Stilbene-1 ^b	Chain/ β	Stilbenoid	[122]
Lupine (<i>Lupinus albus</i> , <i>L. angustifolius</i> , <i>L. luteus</i>)	<i>R. oryzae</i>	0.3-0.5 to 6.0-8.8 mg/g isoflavonoid content	Luteone Licoisoflavone A	Chain/ α , β and δ	Isoflavone	[121]
	<i>R. oryzae</i>	1.0 to 2.5 mg/g isoflavonoid content	2,3-Dehydrokivitone Kevitone	Chain/ α and δ	Isoflavanone Isoflavone	[128]
Kidney bean (<i>Phaseolus vulgaris</i>) Winged bean (<i>Psophocarpus tetragonolobus</i>)	<i>R. oryzae</i>	0.1 to 1.2 mg/g isoflavonoid content	Phaseollin Phaseollidin	Ring-closed/ δ Chain/ δ	Pterocarpan	[128]

^a *Trans*-3',5,4'-trihydroxystilbene. ^b Product of fungal metabolism.

AIM AND OUTLINE OF THESIS

From the above it is clear that there are key issues that still need to be addressed to move forward towards successfully applying prenylated phenolic compounds as antibacterial agents: (i) detailed quantitative SAR (QSAR) need to be established to understand the key molecular properties responsible for the antibacterial activity of prenylated phenolic compounds; (ii) the mode of action (MOA) of prenylated phenolic compounds; (iii) different ways of production of novel and double prenylated phenolic compounds should be further explored, due to their limited availability.

To investigate these key issues, in this thesis, prenylated phenolic compounds, specifically isoflavonoids, flavonoids and stilbenoids, from legumes were studied as antibacterial agents against Gram positive and negative bacteria. Systematic (Q)SAR were linked with the MOA of the compounds. The main hypothesis of this thesis is that, besides hydrophobicity, other molecular characteristics are required to understand the antibacterial action of prenylated phenolic compounds.

In **Chapter 2** fungal elicitation of seedlings from 7 different legume species was performed in order to increase the molecular diversity of the plant's spectrum of secondary metabolites. Liquid chromatography coupled with mass spectrometry allowed an extensive characterization of the main components in the seedling extracts. Correlation between composition of extracts, including phenolics and saponins, and antibacterial activity against Gram positive bacteria was studied. In **Chapter 3**, pools enriched in prenylated phenolic compounds from legume seedling extracts were made and antibacterial activity against Gram positive and Gram negative bacteria was determined. SAR regarding the skeleton and the configuration of prenylation were established. Additionally, the effects of antibacterial prenylated compounds on cell membrane integrity were determined, as well as the role of efflux pump systems on intrinsic Gram negative resistance. In **Chapter 4**, QSAR and pharmacophore modelling were used to investigate the antibacterial activity of purified prenylated (iso)flavonoids. Models using molecular descriptors to explain the antibacterial activity against Gram positive and Gram negative bacteria were defined in this chapter and correlated with the MOA. In **Chapter 5**, the enzymatic *in vitro* production of prenylated phenolic compounds was evaluated. For this, the phenolic acceptor substrate specificity of microbial prenyltransferase SrCloQ was investigated. Mass spectrometric tools to annotate the reaction products and molecular docking to explain the acceptor substrate specificity observed *in vitro* were used. The most important findings of this PhD research and the prospects of prenylated phenolic compounds as antibacterials are discussed in **Chapter 6**.

REFERENCES

- [1] Dastidar, S.G.; Manna, A.; Kumar, K.A.; Mazumdar, K.; Dutta, N.K.; Chakrabarty, A.N.; Motohashi, N.; Shirataki, Y. Studies on the antibacterial potentiality of isoflavones. *International Journal of Antimicrobial Agents*, 2004, **23**, 99-102.
- [2] Lewis, K. Platforms for antibiotic discovery. *Nature Reviews Drug Discovery*, 2013, **12**, 371-387.
- [3] Walsh, C.T.; Wenczewicz, T.A. Prospects for new antibiotics: a molecule-centered perspective. *The Journal of Antibiotics*, 2014, **67**, 7-22.
- [4] Gibbons, S. Plants as a source of bacterial resistance modulators and anti-infective agents. *Phytochemistry Reviews*, 2005, **4**, 63-78.
- [5] Pawlowski, A.C.; Johnson, J.W.; Wright, G.D. Evolving medicinal chemistry strategies in antibiotic discovery. *Current Opinion in Biotechnology*, 2016, **42**, 108-117.
- [6] Ventola, C.L. The antibiotic resistance crisis: Part 1: causes and threats. *Pharmacy and Therapeutics*, 2015, **40**, 277-283.
- [7] WHO. Antimicrobial resistance: global report on surveillance 2014. 2014. World Health Organization: Geneva, Switzerland. p. 257.
- [8] Brown, E.D.; Wright, G.D. Antibacterial drug discovery in the resistance era. *Nature Reviews*, 2016, **529**, 336-343.
- [9] Simoes, M.; Bennett, R.N.; Rosa, E.A.S. Understanding antimicrobial activities of phytochemicals against multidrug resistant bacteria and biofilms. *Natural Product Reports*, 2009, **26**, 746-757.
- [10] Kar, S.; Roy, K. QSAR of phytochemicals for the design of better drugs. *Expert Opinion on Drug Discovery*, 2012, **7**, 877-902.
- [11] Denyer, S.P.; Maillard, J.Y. Cellular impermeability and uptake of biocides and antibiotics in Gram-negative bacteria. *Journal of Applied Microbiology*, 2002, **92**, 35S-45S.
- [12] Delcour, A.H. Outer membrane permeability and antibiotic resistance. *Biochimica et Biophysica Acta*, 2009, **1794**, 808-816.
- [13] Zgurskaya, H.I.; López, C.A.; Gnanakaran, S. Permeability barrier of Gram-Negative cell envelopes and approaches to bypass it. *ACS Infectious Diseases*, 2015, **1**, 512-522.
- [14] Silhavy, T.J.; Kahne, D.; Walker, S. The bacterial cell envelope. *Cold Spring Harbor Perspectives in Biology*, 2010, **2**, 1-16.
- [15] Lambert, P.A. Cellular impermeability and uptake of biocides and antibiotics in Gram-positive bacteria and mycobacteria. *Journal of Applied Microbiology*, 2002, **92**, 46S-54S.
- [16] Chopra, I. Molecular mechanisms involved in the transport of antibiotics into bacteria. *Parasitology*, 1988, **96**, 25-44.
- [17] Li, X.-Z.; Plésiat, P.; Nikaido, H. The challenge of efflux-mediated antibiotic resistance in Gram-negative bacteria. *Clinical Microbiology Reviews*, 2015, **28**, 337-418.
- [18] Blair, J.M.A.; Webber, M.A.; Baylay, A.J.; Ogbolu, D.O.; Piddock, L.J.V. Molecular mechanisms of antibiotic resistance. *Nature Reviews: Microbiology*, 2015, **13**, 42-51.
- [19] Randall, C.P.; Mariner, K.R.; Chopra, I.; O'Neill, A.J. The target of daptomycin is absent from *Escherichia coli* and other Gram-negative pathogens. *Antimicrobial Agents and Chemotherapy*, 2013, **57**, 637-639.
- [20] Nikaido, H. Multidrug efflux pumps of Gram-negative bacteria. *Journal of Bacteriology*, 1996, **178**, 5853-5859.
- [21] Nikaido, H.; Pagès, J.M. Broad-specificity efflux pumps and their role in multidrug resistance of Gram-negative bacteria. *FEMS Microbiology Reviews*, 2012, **36**, 340-363.
- [22] McChesney, J.D.; Venkataraman, S.K.; Henri, J.T. Plant natural products: Back to the future or into extinction? *Phytochemistry*, 2007, **68**, 2015-2022.
- [23] Newman, D.J.; Cragg, G.M. Natural products as sources of new drugs over the 30 years from 1981 to 2010. *Journal of Natural Products*, 2012, **75**, 311-335.
- [24] Nwachukwu, I.D.; Luciano, F.B.; Udenigwe, C.C. The inducible soybean glyceollin phytoalexins with multifunctional health-promoting properties. *Food Research International*, 2013, **54**, 1208-1216.
- [25] Upadhyay, A.; Upadhyaya, I.; Kollanoor-Johny, A.; Venkitanarayanan, K. Combating pathogenic microorganisms using plant-derived antimicrobials: A minireview of the mechanistic basis. *BioMed Research International*, 2014, **2014**, 1-18.
- [26] Cowan, M.M. Plant products as antimicrobial agents. *Clinical Microbiology Reviews*, 1999, **12**, 564-582.
- [27] Gao, T.; Yao, H.; Song, J.; Liu, C.; Zhu, Y.; Ma, X.; Pang, X.; Xu, H.; Chen, S. Identification of medicinal plants in the family Fabaceae using a potential DNA barcode ITS2. *Journal of Ethnopharmacology*, 2010, **130**, 116-121.

- [28] Sharma, V.; Sarkar, I.N. Leveraging biodiversity knowledge for potential phyto-therapeutic applications. *Journal of the American Medical Informatics Association*, 2013, **20**, 668-679.
- [29] Veitch, N.C. Isoflavonoids of the Leguminosae. *Natural Product Reports*, 2007, **24**, 417-464.
- [30] Shi, J.; Arunasalam, K.; Yeung, D.; Kakuda, Y.; Mittal, G.; Jiang, Y. Saponins from edible legumes: Chemistry, processing, and health benefits. *Journal of Medicinal Food*, 2004, **7**, 67-78.
- [31] Liu, J.; Henkel, T. Traditional Chinese medicine (TCM): Are polyphenols and saponins the key ingredients triggering biological activities? *Current Medicinal Chemistry*, 2002, **9**, 1483-1485.
- [32] Güçlü-Üstündağ, Ö.; Mazza, G. Saponins: Properties, applications and processing. *Critical Reviews in Food Science and Nutrition*, 2007, **47**, 231-258.
- [33] Qiao, X.; Song, W.; Ji, S.; Wang, Q.; Guo, D.-a.; Ye, M. Separation and characterization of phenolic compounds and triterpenoid saponins in licorice (*Glycyrrhiza uralensis*) using mobile phase-dependent reversed-phase \times reversed-phase comprehensive two-dimensional liquid chromatography coupled with mass spectrometry. *Journal of Chromatography A*, 2015, **1402**, 36-45.
- [34] Simons, R.; Vincken, J.-P.; Mol, L.A.M.; The, S.A.M.; Bovee, T.F.H.; Luijendijk, T.J.C.; Verbruggen, M.A.; Gruppen, H. Agonistic and antagonistic estrogens in licorice root (*Glycyrrhiza glabra*). *Analytical and Bioanalytical Chemistry*, 2011, **401**, 305-313.
- [35] van de Schans, M.G.M.; Vincken, J.-P.; de Waard, P.; Hamers, A.R.M.; Bovee, T.F.H.; Gruppen, H. Glyceollins and dehydroglyceollins isolated from soybean act as SERMs and ER subtype-selective phytoestrogens. *The Journal of Steroid Biochemistry and Molecular Biology*, 2016, **156**, 53-63.
- [36] Hassan, S.M.; Byrd, J.A.; Cartwright, A.L.; Bailey, C.A. Hemolytic and antimicrobial activities differ among saponin-rich extracts from guar, quillaja, yucca, and soybean. *Applied Biochemistry and Biotechnology*, 2010, **162**, 1008-1017.
- [37] Kim, H.J.; Sung, M.-K.; Kim, J.-S. Anti-inflammatory effects of glyceollins derived from soybean by elicitation with *Aspergillus sojae*. *Inflammation Research*, 2011, **60**, 909-917.
- [38] Avato, P.; Buccini, R.; Tava, A.; Vitali, C.; Rosato, A.; Bialy, Z.; Jurzysta, M. Antimicrobial activity of saponins from *Medicago* sp.: structure-activity relationship. *Phytotherapy Research*, 2006, **20**, 454-457.
- [39] Messier, C.; Epifano, F.; Genovese, S.; Grenier, D. Licorice and its potential beneficial effects in common oro-dental diseases. *Oral Diseases*, 2012, **18**, 32-39.
- [40] Osbourn, A.; Goss, R.J.M.; Field, R.A. The saponins - polar isoprenoids with important and diverse biological activities. *Natural Product Research*, 2011, **28**, 1261-1268.
- [41] Vincken, J.-P.; Heng, L.; de Groot, A.; Gruppen, H. Saponins, classification and occurrence in the plant kingdom. *Phytochemistry*, 2007, **68**, 275-297.
- [42] Guang, C.; Chen, J.; Sang, S.; Cheng, S. Biological functionality of soyasaponins and soyasapogenols. *Journal of Agricultural and Food Chemistry*, 2014, **62**, 8247-8255.
- [43] Decroos, K.; Vincken, J.-P.; Heng, L.; Bakker, R.; Gruppen, H.; Verstraete, W. Simultaneous quantification of differently glycosylated, acetylated, and 2,3-dihydro-2,5-dihydroxy-6-methyl-4H-pyran-4-one-conjugated soyasaponins using reversed-phase high-performance liquid chromatography with evaporative light scattering detection. *Journal of Chromatography A*, 2005, **1072**, 185-193.
- [44] Ahuja, I.; Kissen, R.; Bones, A.M. Phytoalexins in defense against pathogens. *Trends in Plant Science*, 2012, **17**, 73-90.
- [45] Yazaki, K.; Sasaki, K.; Tsurumaru, Y. Prenylation of aromatic compounds, a key diversification of plant secondary metabolites. *Phytochemistry*, 2009, **70**, 1739-1745.
- [46] Botta, B.; Menendez, P.; Zappia, G.; de Lima, R.A.; Torge, R.; Delle Monache, G. Prenylated isoflavonoids: Botanical distribution, structures, biological activities and biotechnological studies. An update (1995-2006). *Current Medicinal Chemistry*, 2009, **16**, 3414-3468.
- [47] Veitch, N.C. Isoflavonoids of the Leguminosae. *Natural Product Reports*, 2013, **30**, 988-1027.
- [48] Vogt, T. Phenylpropanoid biosynthesis. *Molecular Plant*, 2010, **3**, 2-20.
- [49] Jäger, A.; Saaby, L. Flavonoids and the CNS. *Molecules*, 2011, **16**, 1471-1485.
- [50] Ververidis, F.; Trantas, E.; Douglas, C.; Vollmer, G.; Kretzschmar, G.; Panopoulos, N. Biotechnology of flavonoids and other phenylpropanoid-derived natural products. Part I: Chemical diversity, impacts on plant biology and human health. *Biotechnology Journal*, 2007, **2**, 1214-1234.
- [51] Veitch, N.C.; Grayer, R.J. Flavonoids and their glycosides, including anthocyanins. *Natural Product Reports*, 2011, **28**, 1626-1695.
- [52] Kodan, A.; Kuroda, H.; Sakai, F. A stilbene synthase from Japanese red pine (*Pinus densiflora*): Implications for phytoalexin accumulation and down-regulation of flavonoid biosynthesis. *Proceedings of the National Academy of Sciences*, 2002, **99**, 3335-3339.
- [53] Veitch, N.C. Isoflavonoids of the Leguminosae. *Natural Product Reports*, 2009, **26**, 776-802.

- [54] Simons, R.; Gruppen, H.; Bovee, T.F.H.; Verbruggen, M.A.; Vincken, J.-P. Prenylated isoflavonoids from plants as selective estrogen receptor modulators (phytoSERMs). *Food & Function*, 2012, **3**, 810-827.
- [55] Hammerbacher, A.; Ralph, S.G.; Bohlmann, J.; Fenning, T.M.; Gershenzon, J.; Schmidt, A. Biosynthesis of the major tetrahydroxystilbenes in spruce, astringin and isorhapontin, proceeds via resveratrol and is enhanced by fungal infection. *Plant Physiology*, 2011, **157**, 876-890.
- [56] Shen, T.; Wang, X.-N.; Lou, H.-X. Natural stilbenes: an overview. *Natural Product Reports*, 2009, **26**, 916-935.
- [57] Šmejkal, K. Cytotoxic potential of C-prenylated flavonoids. *Phytochemistry Reviews*, 2014, **13**, 245-275.
- [58] Tahara, S.; Ibrahim, R.K. Prenylated isoflavonoids—An update. *Phytochemistry*, 1995, **38**, 1073-1094.
- [59] Yang, X.; Jiang, Y.; Yang, J.; He, J.; Sun, J.; Chen, F.; Zhang, M.; Yang, B. Prenylated flavonoids, promising nutraceuticals with impressive biological activities. *Trends in Food Science & Technology*, 2015, **44**, 93-104.
- [60] Ibrahim, R.K. A forty-year journey in plant research: Original contributions to flavonoid biochemistry. *Canadian Journal of Botany*, 2005, **83**, 433-450.
- [61] Tanaka, H.; Atsumi, I.; Shirota, O.; Sekita, S.; Sakai, E.; Sato, M.; Murata, J.; Murata, H.; Darnaedi, D.; Chen, I.S. Three new constituents from the roots of *Erythrina variegata* and their antibacterial activity against methicillin-resistant *Staphylococcus aureus*. *Chemistry & Biodiversity*, 2011, **8**, 476-482.
- [62] Su, X.; Howell, A.B.; D'Souza, D.H. Antibacterial effects of plant-derived extracts on methicillin-resistant *Staphylococcus aureus*. *Foodborne Pathogens and Disease*, 2012, **9**, 573-578.
- [63] Gupta, V.K.; Fatima, A.; Faridi, U.; Negi, A.S.; Shanker, K.; Kumar, J.K.; Rahuja, N.; Luqman, S.; Sisodia, B.S.; Saikia, D.; Darokar, M.P.; Khanuja, S.P.S. Antimicrobial potential of *Glycyrrhiza glabra* roots. *Journal of Ethnopharmacology*, 2008, **116**, 377-380.
- [64] McCue, P.; Lin, Y.T.; Labbe, R.G.; Shetty, K. Characterization of the effect of sprouting or solid-state bioprocessing by dietary fungus on the antibacterial activity of soybean extracts against *Listeria monocytogenes*. *Food Biotechnology*, 2005, **19**, 121-136.
- [65] Vattem, D.A.; Lin, Y.T.; Labbe, R.G.; Shetty, K. Phenolic antioxidant mobilization in cranberry pomace by solid-state bioprocessing using food grade fungus *Lentinus edodes* and effect on antimicrobial activity against select food borne pathogens. *Innovative Food Science and Emerging Technologies*, 2004, **5**, 81-91.
- [66] Dastidar, S.G.; Mahapatra, S.K.; Ganguly, K.; Chakrabarty, A.N.; Shirataki, Y.; Motohashi, N. Antimicrobial activity of prenylflavanones. *In Vivo*, 2001, **15**, 519-523.
- [67] Hufford, C.D.; Jia, Y.; Croom, E.M.; Muhammed, I.; Okunade, A.L.; Clark, A.M.; Rogers, R.D. Antimicrobial compounds from *Petalostemum purpureum*. *Journal of Natural Products*, 1993, **56**, 1878-1889.
- [68] Rao, S.A.; Merugu, R.; Rao, M.J. Antibacterial and antifungal studies of prenylated isoflavones and prenylated 3-aryl coumarins isolated from *Derris scandens* BENTH. *Journal of Pharmacognosy*, 2012, **3**, 51-54.
- [69] Sohn, H.Y.; Kwon, C.S.; Son, K.H. Fungicidal effect of prenylated flavonol, papyriflavonol A, isolated from *Broussonetia papyrifera* (L.) Vent. against *Candida albicans*. *Journal of Microbiology and Biotechnology*, 2010, **20**, 1397-1402.
- [70] Reller, L.B.; Weinstein, M.; Jorgensen, J.H.; Ferraro, M.J. Antimicrobial susceptibility testing: A review of general principles and contemporary practices. *Clinical Infectious Diseases*, 2009, **49**, 1749-1755.
- [71] Balouiri, M.; Sadiki, M.; Ibsouda, S.K. Methods for *in vitro* evaluating antimicrobial activity: A review. *Journal of Pharmaceutical Analysis*, 2016, **6**, 71-79.
- [72] Aryani, D.C.; den Besten, H.M.W.; Hazeleger, W.C.; Zwietering, M.H. Quantifying strain variability in modeling growth of *Listeria monocytogenes*. *International Journal of Food Microbiology*, 2015, **208**, 19-29.
- [73] CLSI. Methods for dilution antimicrobial susceptibility test for bacteria that grow aerobically; approved standard-ninth edition. 2012. Clinical and Laboratory Standards Institute: Wayne, PA, USA.
- [74] Tan, J.B.L.; Lim, Y.Y. Critical analysis of current methods for assessing the *in vitro* antioxidant and antibacterial activity of plant extracts. *Food Chemistry*, 2015, **172**, 814-822.
- [75] Andrews, J.M. Determination of minimum inhibitory concentrations. *Journal of Antimicrobial Chemotherapy*, 2001, **48**, 5-16.
- [76] Biesta-Peters, E.G.; Reij, M.W.; Joosten, H.; Gorris, L.G.M.; Zwietering, M.H. Comparison of two optical-density-based methods and a plate count method for estimation of growth

- parameters of *Bacillus cereus*. *Applied and Environmental Microbiology*, 2010, **76**, 1399-1405.
- [77] Gibbons, S. Anti-staphylococcal plant natural products. *Natural Product Reports*, 2004, **21**, 263-277.
- [78] Eerdunbayaer; Mohamed A. A. Orabi; Hiroe Aoyama; Kuroda, T.; Hatano, T. Structures of new phenolics isolated from licorice, and the effectiveness of licorice phenolics on vancomycin-resistant *Enterococci*. *Molecules*, 2014, **19**, 13027-13041.
- [79] Fukai, T.; Kaitou, K.; Terada, S. Antimicrobial activity of 2-arylbenzofurans from *Morus* species against methicillin-resistant *Staphylococcus aureus*. *Fitoterapia*, 2005, **76**, 708-711.
- [80] Kirmizibekmez, H.; Uysal, G.B.; Masullo, M.; Demirci, F.; Bağcı, Y.; Kan, Y.; Piacente, S. Prenylated polyphenolic compounds from *Glycyrrhiza ionicica* and their antimicrobial and antioxidant activities. *Fitoterapia*, 2015, **103**, 289-293.
- [81] Fukai, T.; Marumo, A.; Kaitou, K.; Kanda, T.; Terada, S.; Nomura, T. Antimicrobial activity of licorice flavonoids against methicillin-resistant *Staphylococcus aureus*. *Fitoterapia*, 2002, **73**, 536-539.
- [82] Magalhaes, A.F.; Tozzi, A.; Magalhaes, E.G.; Souza-Neta, L.C. New prenylated metabolites of *Deguelia longeracemosa* and evaluation of their antimicrobial potential. *Planta Medica*, 2006, **72**, 358-363.
- [83] Waffo, A.K.; Azebaze, G.A.; Nkengfack, A.E.; Fomum, Z.T.; Meyer, M.; Bodo, B.; van Heerden, F.R. Indicanines B and C, two isoflavonoid derivatives from the root bark of *Erythrina indica*. *Phytochemistry*, 2000, **53**, 981-985.
- [84] Tsuchiya, H.; Sato, M.; Miyazaki, T.; Fujiwara, S.; Tanigaki, S.; Ohyama, M.; Tanaka, T.; Iinuma, M. Comparative study on the antibacterial activity of phytochemical flavanones against methicillin-resistant *Staphylococcus aureus*. *Journal of Ethnopharmacology*, 1996, **50**, 27-34.
- [85] Tanaka, H.; Oh-Uchi, T.; Etoh, H.; Sako, M.; Asai, F.; Fukai, T.; Sato, M.; Murata, J.; Tateishi, Y. Isoflavonoids from roots of *Erythrina zeyheri*. *Phytochemistry*, 2003, **64**, 753-758.
- [86] Rahman, M.M.; Gibbons, S.; Gray, A.I. Isoflavanones from *Uraria picta* and their antimicrobial activity. *Phytochemistry*, 2007, **68**, 1692-1697.
- [87] Nkengfack, A.E.; Vardamides, J.C.; Fomum, Z.T.; Meyer, M. Prenylated isoflavanone from *Erythrina eriotricha*. *Phytochemistry*, 1995, **40**, 1803-1808.
- [88] Hatano, T.; Shintani, Y.; Aga, Y.; Shiota, S.; Tsuchiya, T.; Yoshida, T. Phenolic constituents of licorice. VIII. Structures of glycofenone and glicoisoflavanone, and effects of licorice phenolics on methicillin-resistant *Staphylococcus aureus*. *Chemical & Pharmaceutical Bulletin*, 2000, **48**, 1286-1292.
- [89] Fukai, T.; Marumo, A.; Kaitou, K.; Kanda, T.; Terada, S.; Nomura, T. Anti-*Helicobacter pylori* flavonoids from licorice extract. *Life Sciences*, 2002, **71**, 1449-1463.
- [90] Sato, M.; Tanaka, H.; Oh-Uchi, T.; Fukai, T.; Etoh, H.; Yamaguchi, R. Antibacterial activity of phytochemicals isolated from *Erythrina zeyheri* against vancomycin-resistant enterococci and their combinations with vancomycin. *Phytotherapy Research*, 2004, **18**, 906-910.
- [91] Rukachaisirikul, T.; Innok, P.; Aroonrerk, N.; Boonamnuaylap, W.; Limrangsun, S.; Boonyon, C.; Woonjina, U.; Suksamrarn, A. Antibacterial pterocarpans from *Erythrina subumbrans*. *Journal of Ethnopharmacology*, 2007, **110**, 171-175.
- [92] Innok, P.; Rukachaisirikul, T.; Phongpaichit, S.; Suksamrarn, A. Fuscacarpans A-C, new pterocarpans from the stems of *Erythrina fusca*. *Fitoterapia*, 2010, **81**, 518-523.
- [93] Yin, S.; Fan, C.-Q.; Wang, Y.; Dong, L.; Yue, J.-M. Antibacterial prenylflavone derivatives from *Psoralea corylifolia*, and their structure-activity relationship study. *Biorganic & Medicinal Chemistry*, 2004, **12**, 4387-4392.
- [94] Nanayakkara, N.P.D.; Burandt, C.L.; Jacob, M.R. Flavonoids with activity against methicillin-resistant *Staphylococcus aureus* from *Dalea scandens* var. *paucifolia*. *Planta Medica*, 2002, **68**, 519-522.
- [95] Osawa, K.; Yasuda, H.; Maruyama, T.; Morita, H.; Takeya, K.; Itokawa, H. Isoflavanones from the heartwood of *Swartzia polyphylla* and their antibacterial activity against cariogenic bacteria. *Chemical & Pharmaceutical Bulletin*, 1992, **40**, 2970-2974.
- [96] He, J.; Chen, L.; Heber, D.; Shi, W.Y.; Lu, Q.Y. Antibacterial compounds from *Glycyrrhiza uralensis*. *Journal of Natural Products*, 2006, **69**, 121-124.
- [97] Tahara, S.; Katagiri, Y.; Ingham, J.L.; Mizutani, J. Prenylated flavonoids in the roots of yellow lupin. *Phytochemistry*, 1994, **36**, 1261-1271.
- [98] Sato, M.; Tanaka, H.; Tani, N.; Nagayama, M.; Yamaguchi, R. Different antibacterial actions of isoflavones isolated from *Erythrina poeppigiana* against methicillin-resistant *Staphylococcus aureus*. *Letters in Applied Microbiology*, 2006, **43**, 243-248.
- [99] Yang, S.-Y. Pharmacophore modeling and applications in drug discovery: challenges and recent advances. *Drug Discovery Today*, 2010, **15**, 444-450.

- [100] Botta, B.; Vitali, A.; Menendez, P.; Misiti, D.; Delle Monache, G. Prenylated flavonoids: Pharmacology and biotechnology. *Current Medicinal Chemistry*, 2005, **12**, 713-739.
- [101] Botta, B.; Monache, G.D.; Menendez, P.; Boffi, A. Novel prenyltransferase enzymes as a tool for flavonoid prenylation. *Trends in Pharmacological Sciences*, 2005, **26**, 606-608.
- [102] Tanaka, H.; Sato, M.; Fujiwara, S.; Hirata, M.; Etoh, H.; Takeuchi, H. Antibacterial activity of isoflavonoids isolated from *Erythrina variegata* against methicillin-resistant *Staphylococcus aureus*. *Letters in Applied Microbiology*, 2002, **35**, 494-498.
- [103] Tsuchiya, H.; Iinuma, M. Reduction of membrane fluidity by antibacterial sophoraflavanone G isolated from *Sophora exigua*. *Phytomedicine*, 2000, **7**, 161-165.
- [104] Hendrich, A.B.; Malon, R.; Pola, A.; Shirataki, Y.; Motohashi, N.; Michalak, K. Differential interaction of *Sophora* isoflavonoids with lipid bilayers. *European Journal of Pharmaceutical Sciences*, 2002, **16**, 201-208.
- [105] Wesołowska, O.; Gąsiorowska, J.; Petrus, J.; Czarnik-Matusewicz, B.; Michalak, K. Interaction of prenylated chalcones and flavanones from common hop with phosphatidylcholine model membranes. *Biochimica et Biophysica Acta (BBA) - Biomembranes*, 2014, **1838**, 173-184.
- [106] Haraguchi, H.; Tanimoto, K.; Tamura, Y.; Mizutani, K.; Kinoshita, T. Mode of antibacterial action of retrochalcones from *Glycyrrhiza inflata*. *Phytochemistry*, 1998, **48**, 125-129.
- [107] Shiu, W.K.P.; Malkinson, J.P.; Rahman, M.M.; Curry, J.; Stapleton, P.; Gunaratnam, M.; Neidle, S.; Mushtaq, S.; Warner, M.; Livermore, D.M.; Evangelopoulos, D.; Basavannacharya, C.; Bhakta, S.; Schindler, B.D.; Seo, S.M.; Coleman, D.; Kaatz, G.W.; Gibbons, S. A new plant-derived antibacterial is an inhibitor of efflux pumps in *Staphylococcus aureus*. *International Journal of Antimicrobial Agents*, 2013, **42**, 513-518.
- [108] Hendrich, A.B. Flavonoid-membrane interactions: possible consequences for biological effects of some polyphenolic compounds. 2006, **27**, 27-40.
- [109] Tsuchiya, H. Structure-dependent membrane interaction of flavonoids associated with their bioactivity. *Food Chemistry*, 2010, **120**, 1089-1096.
- [110] Selvaraj, S.; Krishnaswamy, S.; Devashya, V.; Sethuraman, S.; Krishnan, U.M. Influence of membrane lipid composition on flavonoid-membrane interactions: Implications on their biological activity. *Progress in Lipid Research*, 2015, **58**, 1-13.
- [111] Cevallos-Casals, B.A.; Cisneros-Zevallos, L. Impact of germination on phenolic content and antioxidant activity of 13 edible seed species. *Food Chemistry*, 2010, **119**, 1485-1490.
- [112] Tsukamoto, C.; Shimada, S.; Igita, K.; Kudou, S.; Kokubun, M.; Okubo, K.; Kitamura, K. Factors affecting isoflavone content in soybean seeds: changes in isoflavones, saponins, and composition of fatty acids at different temperatures during seed development. *Journal of Agricultural and Food Chemistry*, 1995, **43**, 1184-1192.
- [113] Kaufman, P.B.; Duke, J.A.; Briemann, H.; Boik, J.; Hoyt, J.E. A comparative survey of leguminous plants as sources of the isoflavones, genistein and daidzein: Implications for human nutrition and health. *The Journal of Alternative and Complementary Medicine*, 1997, **3**, 7-12.
- [114] Lee, S.-J.; Ahn, J.-K.; Khanh, T.-D.; Chun, S.-C.; Kim, S.-L.; Ro, H.-M.; Song, H.-K.; Chung, I.-M. Comparison of isoflavone concentrations in soybean (*Glycine max* (L.) Merrill) sprouts grown under two different light conditions. *Journal of Agricultural and Food Chemistry*, 2007, **55**, 9415-9421.
- [115] McCue, P.; Shetty, K. Health benefits of soy isoflavonoids and strategies for enhancement: A review. *Critical Reviews in Food Science and Nutrition*, 2004, **44**, 361-367.
- [116] Boue, S.M.; Cleveland, T.E.; Carter-Wientjes, C.; Shih, B.Y.; Bhatnagar, D.; McLachlan, J.M.; Burow, M.E. Phytoalexin-enriched functional foods. *Journal of Agricultural and Food Chemistry*, 2009, **57**, 2614-2622.
- [117] Hammerschmidt, R. Phytoalexins: What have we learned after 60 years? *Annual Review of Phytopathology*, 1999, **37**, 285-306.
- [118] Baenas, N.; García-Viguera, C.; Moreno, D. Elicitation: A tool for enriching the bioactive composition of foods. *Molecules*, 2014, **19**, 13541-13563.
- [119] Aisyah, S.; Gruppen, H.; Madzora, B.; Vincken, J.-P. Modulation of isoflavonoid composition of *Rhizopus oryzae* elicited soybean (*Glycine max*) seedlings by light and wounding. *Journal of Agricultural and Food Chemistry*, 2013, **61**, 8657-8667.
- [120] Simons, R.; Vincken, J.-P.; Roidos, N.; Bovee, T.F.H.; van Iersel, M.; Verbruggen, M.A.; Gruppen, H. Increasing soy isoflavonoid content and diversity by simultaneous malting and challenging by a fungus to modulate estrogenicity. *Journal of Agricultural and Food Chemistry*, 2011, **59**, 6748-6758.
- [121] Aisyah, S.; Vincken, J.-P.; Andini, S.; Mardiah, Z.; Gruppen, H. Compositional changes in (iso)flavonoids and estrogenic activity of three edible *Lupinus* species by germination and *Rhizopus*-elicitation. *Phytochemistry*, 2016, **122**, 65-75.

- [122] Aisyah, S.; Gruppen, H.; Slager, M.; Helmink, B.; Vincken, J.-P. Modification of prenylated stilbenoids in peanut (*Arachis hypogaea*) seedlings by the same fungi that elicited them: The fungus strikes back. *Journal of Agricultural and Food Chemistry*, 2015, **63**, 9260-9268.
- [123] Eromosele, O.; Bo, S.; Huija, J.; Ping, L. Preparative isolation and purification of glyceollins from soybean elicited with *Aspergillus sojae* by high-speed countercurrent chromatography. *Journal of Chromatography and Separation Techniques*, 2012, **3**, 1-7.
- [124] Sobolev, V.S.; Neff, S.A.; Gloer, J.B. New stilbenoids from peanut (*Arachis hypogaea*) seeds challenged by an *Aspergillus caelatus* strain. *Journal of Agricultural and Food Chemistry*, 2009, **57**, 62-68.
- [125] Sobolev, V.S.; Neff, S.A.; Gloer, J.B.; Khan, S.I.; Tabanca, N.; De Lucca, A.J.; Wedge, D.E. Pterocarpenes elicited by *Aspergillus caelatus* in peanut (*Arachis hypogaea*) seeds. *Phytochemistry*, 2010, **71**, 2099-2107.
- [126] Kim, H.J.; Suh, H.-J.; Lee, C.H.; Kim, J.H.; Kang, S.C.; Park, S.; Kim, J.-S. Antifungal activity of glyceollins isolated from soybean elicited with *Aspergillus sojae*. *Journal of Agricultural and Food Chemistry*, 2010, **58**, 9483-9487.
- [127] Wu, Z.; Song, L.; Huang, D. Food grade fungal stress on germinating peanut seeds induced phytoalexins and enhanced polyphenolic antioxidants. *Journal of Agricultural and Food Chemistry*, 2011, **59**, 5993-6003.
- [128] Aisyah, S.; Gruppen, H.; Andini, S.; Bettonvil, M.; Severing, E.; Vincken, J.-P. Variation in accumulation of isoflavonoids in *Phaseoleae* seedlings elicited by *Rhizopus*. *Food Chemistry*, 2016, **196**, 694-701.
- [129] Sobolev, V.S.; Neff, S.A.; Gloer, J.B. New dimeric stilbenoids from fungal-challenged peanut (*Arachis hypogaea*) seeds. *Journal of Agricultural and Food Chemistry*, 2010, **58**, 875-881.
- [130] John, K.M.M.; Jung, E.S.; Lee, S.; Kim, J.-S.; Lee, C.H. Primary and secondary metabolites variation of soybean contaminated with *Aspergillus sojae*. *Food Research International*, 2013, **54**, 487-494.
- [131] Akashi, T.; Sasaki, K.; Aoki, T.; Ayabe, S.I.; Yazaki, K. Molecular cloning and characterization of a cDNA for pterocarpan 4-dimethylallyltransferase catalyzing the key prenylation step in the biosynthesis of glyceollin, a soybean phytoalexin. *Plant Physiology*, 2009, **149**, 683-693.
- [132] Biggs, D.R.; Welle, R.; Grisebach, H. Intracellular localization of prenyltransferases of isoflavonoid phytoalexin biosynthesis in bean and soybean. *Planta*, 1990, **181**, 244-248.
- [133] Biggs, D.R.; Welle, R.; Visser, F.R.; Grisebach, H. Dimethylallylpyrophosphate: 3,9-dihydroxypterocarpan-10-dimethylallyl transferase from *Phaseolus vulgaris* - Identification of the reaction product and properties of the enzyme. *FEBS Letters*, 1987, **220**, 223-226.
- [134] Laflamme, P.; Khouri, H.; Gulick, P.; Ibrahim, R. Enzymatic prenylation of isoflavones in white lupin. *Phytochemistry*, 1993, **34**, 147-151.
- [135] Sasaki, K.; Tsurumaru, Y.; Yamamoto, H.; Yazaki, K. Molecular characterization of a membrane-bound prenyltransferase specific for isoflavone from *Sophora flavescens*. *Journal of Biological Chemistry*, 2011, **286**, 24125-24134.
- [136] Li, H.; Ban, Z.; Qin, H.; Ma, L.; King, A.J.; Wang, G. A heteromeric membrane-bound prenyltransferase complex from hop catalyzes three sequential aromatic prenylations in the bitter acid pathway. *Plant Physiology*, 2015, **167**, 650-659.
- [137] Wang, R.; Chen, R.; Li, J.; Liu, X.; Xie, K.; Chen, D.; Yin, Y.; Tao, X.; Xie, D.; Zou, J.; Yang, L.; Dai, J. Molecular characterization and phylogenetic analysis of two novel regio-specific flavonoid prenyltransferases from *Morus alba* and *Cudrania tricuspidata*. *Journal of Biological Chemistry*, 2014, **289**, 35815-35825.
- [138] Winkelblech, J.; Fan, A.; Li, S.-M. Prenyltransferases as key enzymes in primary and secondary metabolism. *Applied Microbiology and Biotechnology*, 2015, **99**, 7379-7397.
- [139] Saleh, O.; Haagen, Y.; Seeger, K.; Heide, L. Prenyl transfer to aromatic substrates in the biosynthesis of aminocoumarins, meroterpenoids and phenazines: The ABBA prenyltransferase family. *Phytochemistry*, 2009, **70**, 1728-1738.
- [140] Tello, M.; Kuzuyama, T.; Heide, L.; Noel, J.P.; Richard, S.B. The ABBA family of aromatic prenyltransferases: broadening natural product diversity. *Cellular and Molecular Life Sciences*, 2008, **65**, 1459-1463.
- [141] Bonitz, T.; Alva, V.; Saleh, O.; Lupas, A.N.; Heide, L. Evolutionary relationships of microbial aromatic prenyltransferases. *Plos One*, 2011, **6**, 1-8.
- [142] Kumano, T.; Richard, S.B.; Noel, J.P.; Nishiyama, M.; Kuzuyama, T. Chemoenzymatic syntheses of prenylated aromatic small molecules using *Streptomyces* prenyltransferases with relaxed substrate specificities. *Bioorganic & Medicinal Chemistry*, 2008, **16**, 8117-8126.
- [143] Pojer, F.; Wemakor, E.; Kammerer, B.; Chen, H.; Walsh, C.T.; Li, S.-M.; Heide, L. CloQ, a prenyltransferase involved in clorobiocin biosynthesis. *Proceedings of the National Academy of Sciences*, 2003, **100**, 2316-2321.

The position of prenylation of isoflavonoids and stilbenoids from legumes (Fabaceae) modulates the antimicrobial activity against Gram positive pathogens

The legume plant family (Fabaceae) is a potential source of antimicrobial phytochemicals. Molecular diversity in phytochemicals of legume extracts was enhanced by germination and fungal elicitation of seven legume species, as established by RP-UHPLC-UV-MS. The relationship between phytochemical composition, including different types of skeletons and substitutions, and antibacterial properties of extracts was investigated. Extracts rich in prenylated isoflavonoids and stilbenoids showed potent antibacterial activity against *Listeria monocytogenes* and methicillin-resistant *Staphylococcus aureus* at concentrations between 0.05-0.1% (w/v). Prenylated phenolic compounds were significantly ($p < 0.01$) correlated with the antibacterial properties of the extracts. Furthermore, the position of the prenyl group within the phenolic skeleton also influenced the antibacterial activity. Overall, prenylated phenolics from legume seedlings can serve multiple purposes, e.g. as phytoestrogens they can provide health benefits and as natural antimicrobials they offer preservation of foods.

Keywords: Fabaceae, fungal elicitation, prenylation, phytochemical, antimicrobial activity, RP-UHPLC-UV-MS/MS

INTRODUCTION

Natural plant extracts have been shown to exert a wide range of biological activities, such as anti-oncogenic, anti-inflammatory and antimicrobial activity.^[1] These properties of plant extracts have been associated with phytochemicals, secondary metabolites involved in the adaptation of plants to their environment.^[2]

The Fabaceae or legume family is an important source of bioactive phytochemicals, including saponins and phenolic compounds.^[3,4] Saponins are triterpenoid glycosides.^[5] Their amphiphilic structure enables them to complex with triterpenes or sterols in biological membranes (such as cholesterol in animal cells, ergosterols in fungi and hopanoids in bacteria), and thereby alter membrane permeability.^[6] The membranolytic activity of saponins depends on both the structure of the saponin itself (e.g. number of saccharide chains, aglycone skeleton), and on the type of sterol-like components present in the membrane to complex with.^[7] In nature, saponins act as pre-formed barriers against pathogens.^[6] Legumes mainly contain oleanane-class soyasaponins,^[5] with members of the A, B, E and DDMP-conjugated groups.^[4]

Phenolic compounds from the isoflavonoid and stilbenoid classes have been described as main phytoalexins in legumes, i.e. secondary metabolites synthesized *de novo* in response to (microbial) stress.^[3] Phenolic compounds have high structural diversity derived from the number of (aromatic) rings (defining their skeleton), modifications of the skeleton by oxygenation of the (aromatic) carbons, C- or O-glycosylation, C- or O-alk(en)ylation (e.g. methylation or prenylation), and modification of the substituents (e.g. oxygenation of prenyl groups, cyclization with a phenolic hydroxyl group).^[8] The presence of a prenyl group (5-carbon isoprene substituent) attached to a phenolic skeleton is a special chemical feature of many legume phytoalexins.

Prenylated compounds have been reported to have interesting biological and pharmacological properties. For example, the pterocarpan *glyceollins* from soybean (*Glycine max*), have shown strong antioxidant, anti-inflammatory and anti-estrogenic activities.^[9,10] The isoflavone *warangalone* from *Erythrina addisoniae* has shown promising anti-inflammatory activity^[11] and inhibitory activity against enzymes involved in type 2 diabetes and obesity.^[12] It has been hypothesized that prenylated molecules have better partitioning to membranes and better interaction with target proteins than non-prenylated molecules, due to the increase in the compound's hydrophobicity by the addition of the prenyl group.^[13]

The content of saponins and phenolic compounds, isoflavonoids in particular, increases during germination of legume seeds.^[14,15] The combination of germination with fungal elicitation can further increase the structural diversity of these bioactive compounds, including induction of new subclasses and induction of prenylation.^[16] The effect of fungal elicitation of legume seedlings on the antibacterial properties of extracts

against human pathogens has not been systematically studied. Furthermore, the contribution of different types of phenolics (e.g. (iso)flavonoids, stilbenoids and phenolic acids), different types of substitutions (e.g. sugar units, prenyl groups) or other phytochemicals present (e.g. saponins) to the antibacterial activity of seedling extracts needs to be investigated.

In this study, the occurrence of phenolic compounds and saponins in legume seedling extracts was correlated with their antibacterial properties. In order to obtain large structural diversity in phytochemicals, seeds from seven different legume species (mung bean, kidney bean, soybean, peanut, white, yellow and blue lupine) were used, and each species was subjected to germination alone or in combination with fungal elicitation. The antibacterial properties of the extracts were tested using *Listeria monocytogenes* and methicillin-resistant *Staphylococcus aureus* (MRSA) as target bacteria. *L. monocytogenes* is a foodborne pathogen known to be resistant to acid, disinfection, high salt concentrations and, in recent years, to clinically relevant antibiotics.^[17] MRSA is a major cause of community and healthcare-associated infections worldwide and has been the most important antibiotic resistant bacterium in humans and livestock for the last 50 years.^[18]

We hypothesize that prenylated phenolics can increase the antibacterial activity of extracts from legume seedlings against human pathogenic bacteria, considering that prenylation of phenolic compounds is a response to microbial attack in legume seeds.^[16] We also hypothesize that saponins, having membranolytic activity,^[7] contribute to the activity of the extracts.

MATERIALS AND METHODS

Materials

Seeds of mung bean (*Vigna radiata*), kidney bean (*Phaseolus vulgaris*), soybean (*Glycine max*), white lupine (*Lupinus albus*), blue lupine (*L. angustifolius*), yellow lupine (*L. luteus*) and peanut (*Arachis hypogaea*) were purchased from Vreeken's Zaden (Dordrecht, The Netherlands). Daidzein, genistein, *trans*-resveratrol and soyasaponin Bb were purchased from Sigma Aldrich (St. Louis, MO, USA). Acetonitrile (ACN; ULC/MS grade), water acidified with 0.1% (v/v) acetic acid (HOAc) or 0.1% (v/v) formic acid (FA) (ULC/MS grade), and methanol (MeOH) (ULC/MS grade) were purchased from Biosolve (Valkenswaard, The Netherlands). Water for purposes other than UHPLC was prepared using a Milli-Q water purification system (Millipore, Molsheim, France). Growth media, Bacto brain heart infusion (BHI) broth was purchased from BD (Franklin Lakes, NJ, USA); tryptone soya broth (TSB) and agar bacteriological from Oxoid Ltd (Basingstoke, UK) and peptone physiological salt solution (PPS) from Tritium Microbiologie (Eindhoven, The Netherlands). All other chemicals were purchased from Merck (Darmstadt, Germany) and Sigma-Aldrich.

Microorganisms

Food grade fungi *Rhizopus oryzae* (LU 581) and *Rhizopus oligosporus* (LU 575) (Laboratory of Food Microbiology, Wageningen University, Wageningen, The Netherlands), were used to elicit the legume seeds during germination. *L. monocytogenes* EGD-e and methicillin-resistant *Staphylococcus aureus* 18HN (MRSA, kindly provided by RIVM, Bilthoven, The Netherlands) were used to test the antimicrobial properties of the extracts from legume seedlings. Glycerol stocks (50% (v/v)) of these microorganisms were kept at -80 °C.

Elicitation and extraction of legume seedlings

Legume seeds were germinated in the presence of *Rhizopus* sp. as previously described.^[16] Briefly, legume seeds were soaked in water for 1 day, germinated for 2 days at 25 °C (100% RH), and subsequently elicited with the fungus (approx. 1.5×10^7 CFU/g seed) for 5 days at 30 °C (55-85% RH). After the elicitation period, seedlings were freeze-dried, milled, defatted with hexane and extracted with 80% (v/v) aqueous MeOH, as described elsewhere.^[16] The MeOH extract obtained from the seedling meal was cleaned from the presence of sugars and other water-soluble components by solid-phase extraction (SPE) with Sep-Pak Vac C18 cartridges (Waters, Milford, MA, USA), following the protocol of the manufacturer. The final SPE-cleaned seedling extract was dried with a flow of nitrogen gas, solubilized in *tert*-butanol and freeze-dried to obtain a powder. All extracts were kept at -20 °C until further analysis.

Compositional analysis by RP-UHPLC-PDA-ESI-MS

Compositional analysis was performed on an Accela ultra high performance liquid chromatography (RP-UHPLC) system (Thermo Scientific, San Jose, CA, USA) equipped with a pump, autosampler, photodiode array (PDA) detector and ESI-ion trap mass spectrometer (MS).

For flavonoid, isoflavonoid and saponin analysis, seedling extracts (2 μ L; 5 mg/mL in MeOH) were injected onto an Acquity UPLC BEH Shield RP18 column (2.1 mm i.d. x 150 mm, 1.7 μ m particle size) with an Acquity UPLC Shield RP18 Vanguard guard-column (2.1 mm i.d. x 5 mm, 1.7 μ m particle size; Waters, Milford, MA, USA). Water containing 0.1% (v/v) HOAc and 1% (v/v) ACN, eluent A, and ACN containing 0.1% (v/v) HOAc, eluent B, were used as solvents at a flow rate of 300 μ L/min. The following elution gradient was used: 0-1 min isocratic on 9% (v/v) B; 1-2.5 min, linear gradient from 9 to 25% B; 2.5-9.5 min, linear gradient from 25 to 50% B; 9.5-12.5 min isocratic at 50% B; 12.5-22.5 min, linear gradient from 50 to 100% B; 22.5-24.5 min isocratic at 100% B; 24.5-25 min, linear gradient from 100 to 9% B; 25-30 min, isocratic at 9% B. Column temperature was set at 35 °C and the PDA detector was set to measure from 200-600 nm.

For stilbenoid analysis, seedling extracts (2 μL , 5 mg/mL in MeOH) were injected onto a Hypersil Gold C18 column (2.1 mm i.d. x 150 mm, 1.9 μm particle size, Thermo Scientific, San Jose, CA, USA). Water containing 0.1% (v/v) FA + 1% (v/v) ACN, eluent A, and MeOH containing 0.1% (v/v) FA, eluent B, were used as solvents at a flow rate of 300 $\mu\text{L}/\text{min}$. The following elution gradient was used: 0-1 min isocratic on 0% B; 1-2 min linear gradient from 0 to 30% B; 2-18 min linear gradient from 30 to 80% B; 18-23 min linear gradient from 80 to 95% B; 23-24 min linear gradient 95 to 100% B; 24-26 min, linear gradient from 100 to 0% B; 26-31 min, isocratic on 0% B. Column temperature was set at 40 $^{\circ}\text{C}$ and PDA detector was set to measure from 200-600 nm.

MS analysis was performed on a LTQ Velos (Thermo Scientific, San Jose, CA, USA) equipped with a heated ESI-MS probe coupled to RP-UHPLC. Spectra were acquired over an m/z (mass to charge ratio) range of 150–1500 Da in both positive (PI) and negative (NI) mode. Data-dependent MSⁿ analysis was performed on the most intense (product) ion with normalized collision energy of 35%. A dynamic mass exclusion approach was used, in which a compound detected five times as most intense was subsequently excluded for the following 10 s, allowing data dependent MS² of less intense co-eluting compounds. The system was tuned with genistein and resveratrol in PI and NI mode via automatic tuning using Tune Plus (Xcalibur v.2.2, Thermo Scientific). Nitrogen was used as sheath and auxiliary gas. The ITT temperature was 400 $^{\circ}\text{C}$ and the source voltage was 3.50 kV (NI) or 4.50 kV (PI).

Tentative annotation of phytochemicals

Compounds were tentatively annotated based on UV-Vis and MS spectral data, obtained by means of Xcalibur (v.2.2, Thermo Scientific), using the approach reported earlier on legume seeds. A summary of the different diagnostic UV-Vis absorption and MS fragmentation patterns is provided in **Table S2.1** (supplementary data). Briefly, UV-Vis absorption spectra and *retro*-Diels-Alders (RDA) fragmentation patterns were used to indicate the subclass of phenolic compound (isoflavonoid, flavonoid, stilbenoid, phenolic acid).^[19,20] Full MS and tandem MS scans provided information regarding molecular weight and substitutions of the phenolic skeleton by means of characteristic neutral losses. The configuration of the prenyl group (chain or ring-closed) attached to the skeleton was determined by typical neutral losses in MS² PI: a neutral loss of 56 Da (C₄H₈) was used to distinguish a prenyl chain, whereas a ring-closed prenyl typically showed neutral losses of 42 Da (C₃H₆), 54 Da (C₄H₆), 60 Da (C₃H₆ + H₂O) and 15 Da (CH₃).^[21,22] The position of the prenyl group within the phenolic skeleton (i.e. A- or B-ring) was elucidated by analysis of the *retro*-Diels-Alders (RDA) fragments^[23] in PI: when the C-ring of (iso)flavonoids was cleaved in MS³, one of the remaining fragments still contained one carbon reminiscent of the prenyl chain (split in MS²), which can be used to diagnose the ring at which the prenyl was attached.^[22] The position of the prenyl group within the A-ring was established based on a study using authentic standards to distinguish between C₆ and C₈ chain prenylated isoflavone isomers by MS fragmentation pattern.^[22] The fragment ion in MS³ PI [M+H-C₄H₈-C₂H₂O]⁺ was

diagnostic for C8 prenylation, whereas the fragment ion in MS³ PI [M+H- C₄H₈-CO]⁺ was diagnostic for C6 prenylation. Furthermore, previous tentative MS annotation of prenylated pterocarpan^[24] was confirmed by means of NMR spectroscopy of the purified molecules.^[10]

Saponins were distinguished from phenolic compounds in the seedling extracts during the same UHPLC run as saponins (i) do not show any or little UV absorbance contrary to phenolics, except for DDMP-conjugated saponins, which have maximum UV absorption at 295 nm, (ii) have higher molecular weights than most phenolics due to their larger carbon skeleton and more extensive glycosylation (2-5 sugar units; mass range 800-1500 Da), and (iii) are usually more apolar than phenolics due to their triterpenoid backbone. For the tentative annotation of saponins the presence of *m/z* values of the triterpenoid aglycones, such as sapogenol B (*m/z* 457), sapogenol A (*m/z* 473) and sapogenol E (*m/z* 455) in MS² or MS³, was used as a diagnostic tool.^[25] Furthermore, commonly observed neutral losses were those of H₂O, CO₂ and individual sugars (132 Da for a pentosyl unit, 146 Da for a deoxyhexosyl unit, 162 Da for hexosyl unit, 176 Da for a hexuronyl unit) resulting from cleavage of the glycosidic linkages.^[26]

Quantification of phytochemicals

Quantification of phenolics was based on the UV absorption at 260 nm (white, yellow and blue lupine), 280 nm (mung bean, kidney bean and soybean) and 315 nm (peanut). In case of co-elution, the UV peak area was divided over the co-eluting compounds in a ratio based on the MS intensity. Quantification of phenolic compounds was performed using the following equation (Eq. 2.1),^[27] derived from the Lambert-Beer's law:

$$C [M] = \frac{\text{area} \times Q}{\varepsilon \times l \times V_{inj} \times k_{cell}} \quad (\text{Eq. 2.1})$$

in which C (M) is concentration, *area* is the integrated area of the UV peak at the specific wavelength (AU·s), Q is the flow rate (5 μL/s), ε (AU/M·cm) is the molar extinction coefficient, *l* is the path length of the UV cell provided by the manufacturer (5 cm), *V_{inj}* is the injected volume of sample (2 μL), and *k_{cell}* is a constant related to the cell geometry of the UV detector^[27]. This equation relates the duration of absorbance given by the UHPLC system (AU·s) to an actual absorbance value (AU) for the Lambert-Beer's equation. The *k_{cell}* represents the correction factor for the absorption of light by the coating material of the flow cell. The *k_{cell}* (0.82 ± 0.09) was determined with standard solutions of daidzein (248 nm), genistein (263 nm) and resveratrol (310 nm) (with five concentrations each, in the range of 0.001-0.1 mg/mL).

Because the ε of most tentatively annotated compounds were unavailable, for each subclass of phenolics (e.g. flavanone, flavone, flavonol, isoflavanone, isoflavone, coumestan, coumaronochromones, pterocarpan, stilbenoid, phenolic acid) a

representative compound was chosen and its ϵ reported in literature was used (corrected for the wavelength used in this work) (Table S2.2).

Because most saponins have little UV absorption, quantification of saponins was based on MS, using an external standard solution of soyasaponin Bb (0.001-0.1 mg/mL). Results are reported as soyasaponin Bb equivalents per gram of extract (Bb eq./g DW extract).

Antibacterial activity assay

Bacteria (*L. monocytogenes* EGD-e and MRSA 18HN) were streaked from a glycerol stock to a BHI agar plate and incubated 24 h at 37 °C, after which one colony was transferred to BHI broth (10 mL) and further incubated for 18 h at 37 °C. These overnight cultures were diluted 100,000 times with fresh TSB (final inoculum concentration $3.6 \pm 0.5 \text{ Log}_{10}\text{CFU/mL}$). Stock solutions of the different seedling extracts were prepared in 70% (v/v) aqueous ethanol (EtOH). Equal volumes (100 μL) of bacteria and a series of 2-fold dilutions of seedling extracts (final concentrations tested 0.25-1.0 mg/mL) in TSB were mixed into a 96-well plate (maximum concentration of EtOH in test was 2% (v/v)). The 96-well plate was incubated in a SpectraMax PLUS 384 (Molecular Devices, Sunnyvale, CA, USA), at 37 °C with constant shaking, and the optical density (OD) at 600 nm was measured every 5 min for 24 h. Positive controls (ampicillin at 3.1 $\mu\text{g/mL}$ in water for *L. monocytogenes* and vancomycin at 2.0 $\mu\text{g/mL}$ in water for MRSA), negative controls (TSB suspension of bacteria with 2% (v/v) EtOH), and blanks (extracts and TSB medium with no bacteria) were considered for optical comparison and sterility control. The time to detection (TTD) was defined as the time to have a change in OD of 0.05 units.^[28] Extracts were tested in two independent biological duplicates.

When no change in OD was observed after the 24 h of the antimicrobial susceptibility test, cell viability was verified by plate counting. Briefly, 100 μL of the well with no change in OD was decimally diluted in PPS solution and 100 μL of each dilution was spread onto BHI agar plates. Plates were incubated for 24 h at 37 °C. The MBC was defined as the lowest concentration of seedling extract that resulted in >99% bacterial inactivation from the initial bacterial inoculum.

Time-dependent inhibition

An overnight bacterial culture was diluted to 10^4 CFU/mL and mixed with the seedling extracts (final concentration 1.0 mg/mL), and incubated at 37 °C, 125 rpm. At different time points (0-6 h), 100 μL of culture medium were taken and decimally diluted in PPS. Dilutions were spread on BHI agar plates and incubated overnight at 37 °C, after which colonies were counted.

Linear regression analysis

To investigate the relationship between phytochemical composition and antimicrobial activity of the seedling extracts, multiple linear regression (MLR) was used (Eq. 2.2):

$$y = \hat{y} + \beta_1 x_1 + \beta_2 x_2 + \dots + \beta_i x_i \quad (\text{Eq. 2.2})$$

where y is the measured TTD of growth (indicative of their antibacterial activity) for the seedling extracts (extracts that showed TTD beyond the 24 h of the test cannot be included in the statistical analysis), \hat{y} is the TTD of the control experiment (TSB suspension of bacteria with 2% (v/v) EtOH), β is the coefficient of each independent variable x , and x is the concentration of each phytochemical class analysed (phenolic compounds and saponins) in the legume seedling extracts. Significance of the model and of the coefficients was evaluated by the t -test. Analysis was performed using IBM SPSS Statistic v.22 software (SPSS Inc., Chicago, IL, USA).

Prediction of chemical properties

$\text{Log}P$ values were predicted using the *weighted* method (default settings) from the software Marvin (version 6.0.5, 2013, ChemAxon, Budapest, Hungary).

RESULTS

Content and composition of phenolic compounds in extracts

The tentative annotation of the peaks was performed based on a comparison of spectral data from LC-MS/MS (including retention time, UV spectra and fragmentation pattern) to those from literature (Table S2.1).^[16,19,20,25,29-32] Overall, 177 different phenolic compounds were tentatively annotated in the legume seedling extracts. Table S2.3 shows the list of compounds with their respective MS fragmentation pattern in NI and PI mode. The majority of phenolic compounds belonged to the isoflavonoid class, including 62 isoflavones, 23 isoflavanones, 9 pterocarpanes, 5 coumestans, 4 coumaronochromones, 3 pterocarpenes, and 1 isoflavan. From the flavonoid class, 24 flavones, 10 flavanols and 5 flavanones were tentatively annotated. Furthermore, 25 stilbenoids, as well as 4 phenolic acids, were exclusively present in peanut. Lastly, 2 chromones were found exclusively in lupine species. In total, 57 phenolic compounds were prenylated and belonged to the isoflavonoid, stilbenoid and chromone classes.

The contents of phenolic compounds per extract of legume seedlings (G) and fungus-elicited seedlings (GF), grouped as non-prenylated glycosides (with glycosyl residues attached), non-prenylated aglycones (only hydroxyl or methoxyl groups attached), prenylated glycosides and prenylated aglycones (prenyl group attached), is given in Figure 2.1. The concentration of each individual component is given in Table S2.4. The total content of phenolics ranged from 35 to 212 mg/g DW extract. Blue and

yellow lupine (G and GF) were the legume extracts with the highest overall content of phenolic compounds. The peanut seedling extracts had the highest content of prenylated aglycone compounds (52 ± 3.6 mg/g DW G extract and 93 ± 2.9 mg/g DW GF extract), followed by soybean (30.1 ± 0.3 mg/g DW GF extract), kidney bean (25 ± 2.1 mg/g DW GF extract) and yellow lupine (19 ± 0.9 mg/g DW GF extract).

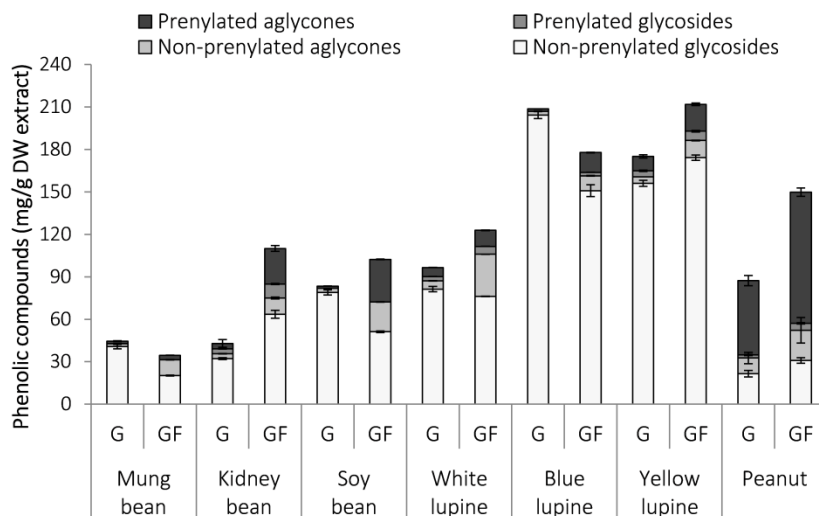


Figure 2.1. Content (mg/g DW extract) of non-prenylated glycosides, non-prenylated aglycones, prenylated glycosides and prenylated aglycone phenolic compounds in extracts from germinated legume seeds (G) and fungus-elicited (GF) legume seedlings.

The normalized weight distribution of the subclasses of the phenolics present in the legume seedling extracts is shown in **Figure 2.2A**. Except for peanut, 50 to 90% (w/w) of the phenolic content belonged to the isoflavonoid class, and 5 to 50% (w/w) to the flavonoid class. With respect to the subclasses, the lupine species showed similar profiles among each other (mainly isoflavone and flavone). Mung bean and kidney bean also showed similarities in the subclasses of phenolics produced (e.g. isoflavanone and flavonol), as expected by the phylogenetic relation between these two species.^[19] Soybean was the only seed containing high abundance of pterocarpan (when elicited), whereas peanut contained around 70% (w/w) stilbenoids. **Figure 2.2B** shows the normalized weight distribution of the subclasses concerning the prenylated compounds. No prenylated flavonoids were present in the legume seedlings. Mung bean and kidney bean mainly contained prenylated isoflavanones; soybean mainly contained prenylated pterocarpan; the lupine species mainly contained prenylated isoflavones and peanut mainly contained prenylated stilbenoids.

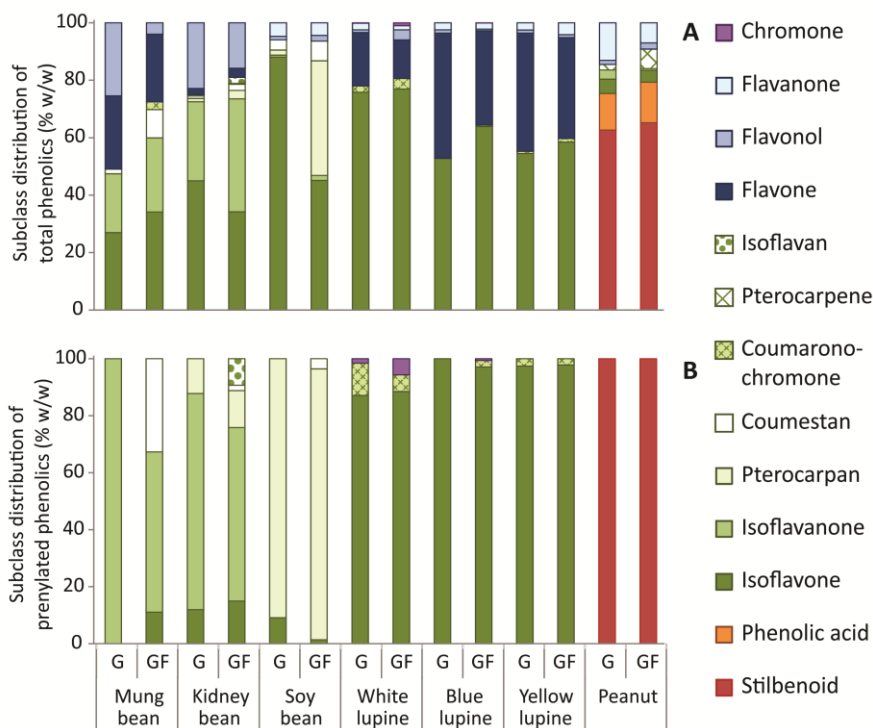


Figure 2.2. Normalized weight distribution of phenolic (sub)classes for all compounds (**A**) and for prenylated compounds (**B**) found in the extracts of legume seedlings, belonging to the isoflavonoid class (green), flavonoid class (blue), stilbenoid class (red), phenolic acid class (orange) and chromone class (purple).

Further analysis of these prenylated compounds showed that chain prenylation (e.g. 3, 3-dimethylallyl) was the most abundant type of prenylation (**Figure 2.3A**). The mung bean and lupine extracts almost exclusively contained chain-prenylated molecules, whereas soybean contained around 80-90% (w/w) ring-closed prenylated molecules (e.g. 2, 2-dimethylpyran or 2''-isopropenyl furan). Double chain-prenylated aglycones were found in white lupine GF seedling extract (lupichromone), blue lupine GF seedling extract (angustone A) and peanut G and GF seedling extracts (arahypin-6 and arahypin-7) (**Table S2.3**). Regarding the mono-prenylated compounds (both chain and ring-closed prenylated), **Figure 2.3B** shows the normalized weight distribution of the different tentatively annotated prenylated positions in the main phenolic skeletons. For this, ring and atom numbering was adapted to facilitate comparison of different (sub)classes of phenolics.^[33] The position of the prenyl group can be tentatively annotated by means of diagnostic MS fragmentation patterns, as described in the section 2.5.^[22] Using these tools we found that prenylated compounds from mung and kidney bean were predominantly prenylated at the A-ring α position (α), whereas A-ring β position (β) was more predominant in the other legume species.

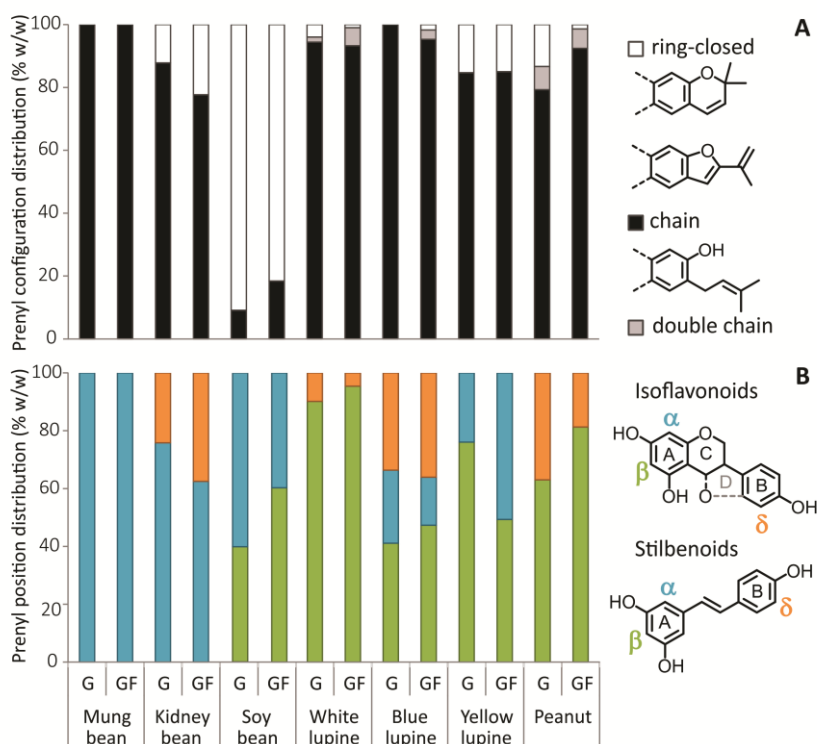


Figure 2.3. Type of prenylation (chain, double chain or ring-closed) (A) and tentative position of the prenyl group (B) of the prenylated phenolic compounds found in extracts from germinated seeds (G) and fungus-elicited (GF) legume seedlings.

Content and composition of saponins in extracts

The saponin content in legume seedlings ranged from 8-101 mg Bb eq./g DW extract (Figure 2.4). Tentatively annotated saponins are listed in Table S2.5 and individual contents are present in Table S2.6. In general, white lupine and peanut seedling extracts had the lowest contents of saponins, whereas soybean and blue lupine G extracts had the highest contents of saponins. Most abundant saponins found in all legume seedling extracts were from the oleanane class.^[5] More specifically, we found high abundance of sapogenol B-type saponins, such as soyasaponin Bb (also known as soyasaponin I, MW 942 Da), soyasaponin β g (DDMP-conjugated soyasaponin Bb, MW 1068 Da) and soyasaponin Be (MW 940 Da). In addition the soybean extracts also contained sapogenol A-type saponins, such as soyasaponin Aa (MW 1364 Da), soyasaponin Ab (MW 1436) and soyasaponin Ae (MW 1202). This result was consistent with a previous saponin screening in legume seeds.^[34]

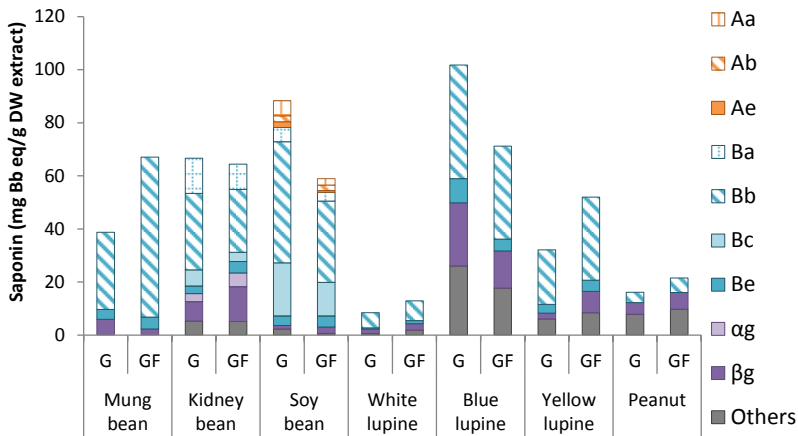


Figure 2.4. Content (mg/g DW extract) of soyasaponins in extracts from untreated legume seeds (U), germinated seeds (G) and fungus-elicited (GF) legume seedlings. The quantified saponins (MW 800-1500 Da) represent $\geq 80\%$ of all saponins present in the extracts.

Antibacterial activity of extracts

All seedling extracts were tested in the antimicrobial susceptibility test using foodborne *L. monocytogenes* as target pathogen. The TTD of growth was determined for all G and GF seedling extracts at different concentrations (**Figure 2.5A**). The TTD increased with increasing concentration of the seedling extracts. The G seedling extracts delayed the growth of *L. monocytogenes* by 1 h (kidney bean) up to 7 h (yellow lupine) at the highest extract concentration tested (1.0 mg/mL), except for the peanut G, which delayed the growth for more than the period of the test (TTD > 24 h). The GF seedling extracts were more effective inhibitors than the G extracts. The most antimicrobial GF seedling extracts were those from peanut, mung bean, soybean and yellow lupine. For MRSA, the same type of assay was performed with the GF extracts, as these were the most active ones (**Figure 2.5B**). Only the peanut GF extract was active against MRSA at 0.5 and 1.0 mg/mL.

Verification of viability on plates revealed that 1.0 mg/mL of peanut G extract and 0.5 mg/mL of peanut GF extract were minimum bactericidal concentrations (MBC) against *L. monocytogenes* (**Figure 2.5C**), and 1.0 mg/mL of peanut GF extracts was bactericidal (MBC) against MRSA (**Figure 2.5D**).

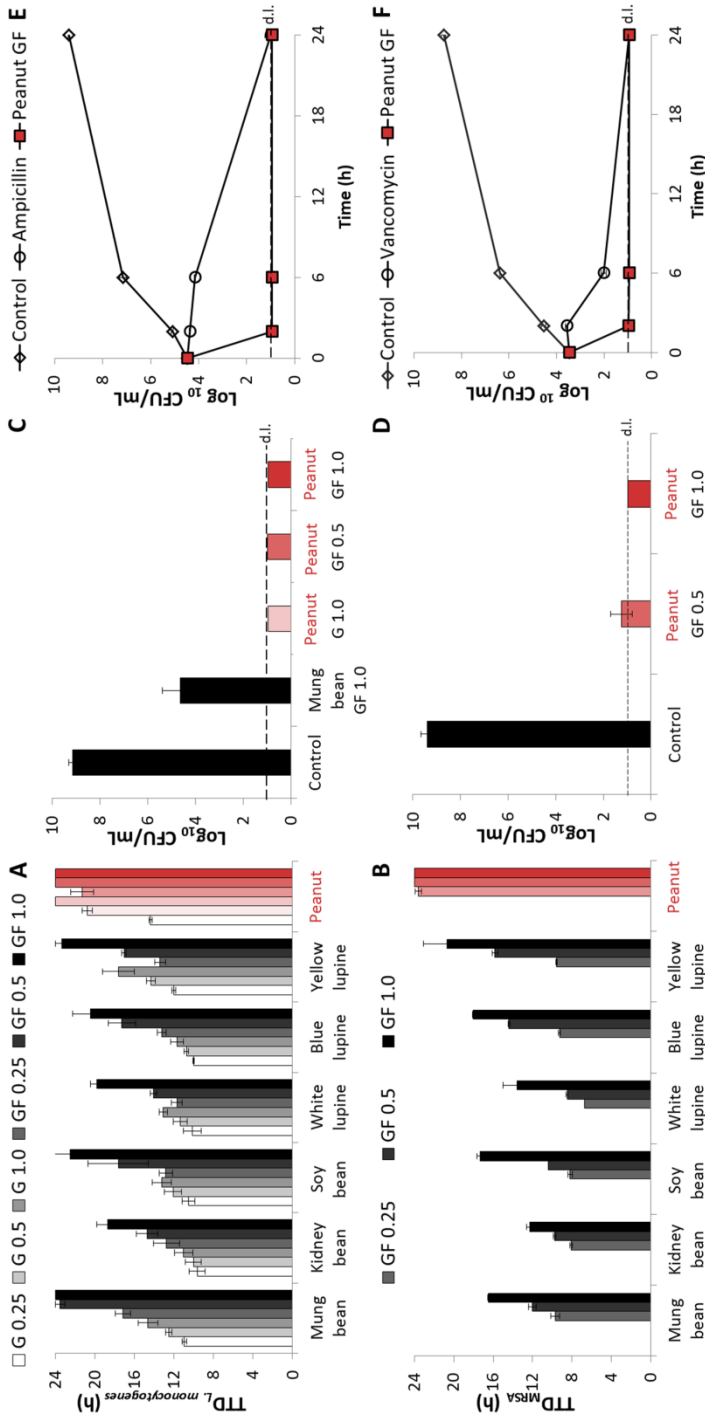


Figure 2.5. Time to detection (TTD) of growth of (A) *L. monocytogenes* and (B) MRSA 18HN in the presence of different seedling extracts at increasing concentrations (0.25, 0.50 and 1.0 mg/mL). Seedling extract (G, light grey), extract from funguselicited seedlings (GF, dark grey). The most active seedling extracts are shown in red colour. TTD of the control experiment for *L. monocytogenes* was 9.7 ± 0.8 h (inoculum $3.2 \pm 0.4 \text{ Log}_{10}$ CFU/mL) and for MRSA was 5.7 ± 0.2 h (inoculum $3.9 \pm 0.3 \text{ Log}_{10}$ CFU/mL). (C) *L. monocytogenes* and (D) MRSA cell counts after the 24 h of incubation with the most active seedling extracts. Dotted line represents the cell count detection limit (d.l.) (E) *L. monocytogenes* and (F) MRSA killing kinetics in the presence of the active peanut GF extract (1.0 mg/mL) in comparison with the negative control (TSB broth) and control antibiotics. Data are means of two independent biological duplicates with standard error bars.

To further study the rate of inhibition of the most antibacterial legume extracts during the first hours of exposure, the growth of *L. monocytogenes* and MRSA was monitored with the active GF extracts at 1.0 mg/mL (Figure 2.5E and 2.5F). Regardless the pathogen, the extract of peanut GF reduced the levels of bacteria to below detection limit (i.e. reduction > 99% from initial inoculum) at already 2 h of incubation. The control antibiotics, however, did not show a significant reduction in cell counts at 2 h. At 24 h, no cell colonies were detected for both the peanut GF extract and the control antibiotics.

Correlation between phytochemical composition and antibacterial properties of extracts

To study the effect of the different phytochemicals analysed on the antibacterial activity of the extracts, multiple linear regression was performed using the $TTD_{L. monocytogenes}$ as response variable. After considering the total content of saponins or phenolic compounds, and subsequently the content of the different types within these compound classes, as predictor variables (Table S2.7), the main phytochemical group determining the TTD of bacterial growth of the extracts from legume seedlings were the prenylated aglycones ($p < 0.001$, Figure 2.6A). The content of non-prenylated aglycones was the second variable influencing the TTD, but to a lesser extent.

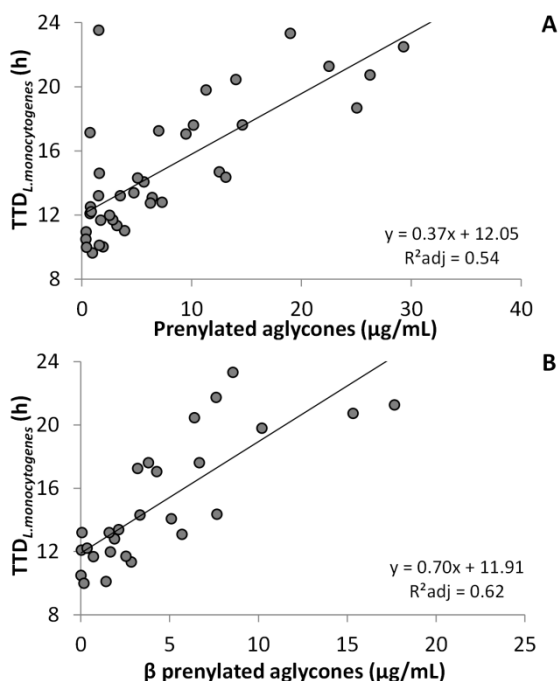


Figure 2.6. Relation between the content of total prenylated aglycones (A) and β prenylated aglycones (B) with the time to detection of *L. monocytogenes* growth (n = 42).

Regarding the position of the prenyl group, the content of compounds prenylated at position β was highly correlated with antibacterial activity (**Figure 2.6B**, $p < 10^{-6}$ and $R^2_{\text{adj}} 0.62$), in comparison with the content of compounds prenylated at position α ($R^2_{\text{adj}} 0.27$) and δ ($R^2_{\text{adj}} 0.48$). For MRSA the content of prenylated aglycones significantly affected ($p < 0.01$) the TTD of bacterial growth and only prenylation at position β was significantly ($p < 0.005$) related to the antibacterial activity of the legume seedling extracts (**Figure S2.1** and **Table S2.7**).

DISCUSSION

Prenylated phenolic aglycones significantly correlate with the antibacterial activity of extracts from legume seedlings

In this study, we performed an extensive characterization of phytochemicals of seven major crop and forage legumes, after germination of the seeds alone, and after subsequent elicitation by fungus. We tentatively annotated 177 compounds distributed over 13 phenolic subclasses. Taken into consideration this large structural variety, we found that the antibacterial activity of the extracts was significantly correlated with the content of prenylated phenolic aglycones (for *L. monocytogenes* and MRSA) and to a lesser extent (only for *L. monocytogenes*) to the non-prenylated aglycones (**Figure 2.6A**). In accordance with our results, the antimicrobial activity of non-prenylated aglycones, such as daidzein and genistein, is known to be lower (MIC values between 100-1000 $\mu\text{g/mL}$)^[35] than those of prenylated analogues (MIC values below 100 $\mu\text{g/mL}$).^[13] Prenylated phenolic glycosides and non-prenylated glycosides were not significantly correlated ($p > 0.05$) with the antimicrobial properties of the legume seedling extracts, as glycosylation is a strategy commonly used by plants to inactivate natural products for storage purposes.^[6]

Among the prenylated phenolic compounds, differences in the type of prenyl group (i.e. chain or ring-closed prenylation), position (i.e. on the A- or B-ring), as well as in configuration of skeletons (e.g. rigid as pterocarpanes or flexible as stilbenoids), can influence their antibacterial activity. After considering all these factors, we found that prenylation at the β position in particular was highly correlated with the antibacterial activity of the legume seedling extracts ($p < 10^{-6}$, $R^2_{\text{adj}} 0.62$, **Figure 2.6B**), in comparison with the position δ ($p < 0.001$, $R^2_{\text{adj}} 0.48$) and α ($p < 0.01$, $R^2_{\text{adj}} 0.27$). This correlation might explain the unexpected low antibacterial activity of the kidney bean GF extract. This extract had one of the highest contents of prenylated phenolic compounds (25 ± 2 mg/g DW) of which 61% (w/w) were α prenylated molecules (e.g. kievitone) and no β prenylated molecules were present in this extract. Studies with pure compounds prenylated at the aforementioned positions need to be done to confirm our correlation analysis.

The unexpectedly high activity of the mung bean GF extract, which had one of the lowest contents of prenylated compounds (3.2 ± 0.1 mg/g DW), of which 100%

were α , indicates that other compounds not yet identified in these extracts might also contribute to the antibacterial activity observed.

The structures of the most abundant prenylated compounds found in the active extracts, with their respective $\log P$ values (indicative of the compound's overall lipophilicity), are shown in **Figure 2.7**. The majority of these prenylated compounds are chain-prenylated at the A-ring, and have $\log P$ values in the range of currently used antimicrobials.^[36] Prenylation increases lipophilicity, which is important for the interaction with lipid bilayers, as in bacterial membranes. Therefore, prenylated molecules have higher antibacterial activity than non-prenylated ones. However, the mechanism involves other factors than lipophilicity, as the position of the prenyl group influenced the antibacterial activity without altering the lipophilicity of the compound, as observed for compounds with same skeleton in **Figure 2.7**.

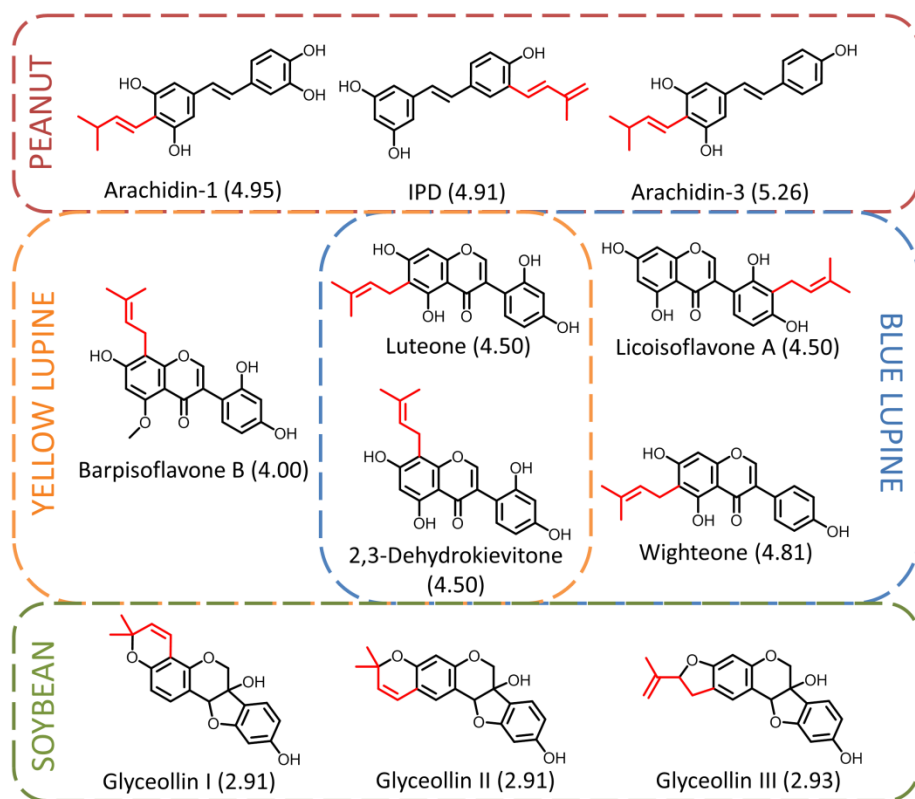


Figure 2.7. Structure and $\log P$ of the most abundant prenylated phenolic compounds tentatively annotated in the extracts of peanut (red square), yellow lupine (yellow square), blue lupine (blue square) and soybean (green square) GF seedlings. These compounds represent $\geq 70\%$ (w/w) of the total prenylated compound content.

The content of saponins does not correlate with antibacterial activity of extracts

Saponins are considered constitutive antimicrobials in plants and antibacterial activity has been shown with phyto(pathogenic) bacteria, especially from *Bacillus* sp.^[7] Saponins in the legume seedling extracts were in the same range of concentration as that of the phenolic compounds. In our study, no correlation was found between the saponin content of legume seedling extracts and the antibacterial activity against *L. monocytogenes* and MRSA. The antibacterial activity of a saponin-rich extract (95% pure) from soybean was previously tested against human pathogens (*S. aureus*, *Salmonella* Typhimurium and *Escherichia coli*) and no antibacterial activity was found (MIC > 12.5 mg/mL).^[37] Sensitivity of a microbe to saponins is determined by both the saponin structure and the presence of triterpenoids in the cell membrane to complex with. In bacteria, hopanoids are the main triterpenoids found in the membrane,^[38] and analysis of different food-related bacteria revealed absence of hopanoids in *L. monocytogenes* and *S. aureus*.^[39] Taken together, the lack of correlation of the saponins with the antibacterial activity of the legume seedling extracts might be explained by the absence of hopanoids in the pathogens tested and probably by the structure of the soyasaponins.

Fungal elicitation enhances antibacterial activity of seedling extracts

The combination of germination with fungal elicitation clearly increased the antibacterial properties of the extracts from legume seedlings, in comparison with those from control seedlings. The TTD of bacterial growth increased 10 to 90% when the seedlings were challenged with fungus. The peanut extracts, containing mainly chain-prenylated stilbenoids, were the most antibacterial of all seedling extracts tested, with a MBC between 0.5-1.0 mg/mL against *L. monocytogenes* and MRSA. When compared with other studies, the antibacterial activity of our extracts from fungus-elicited legume seedlings is notably promising. A concentrated methanolic extract of licorice roots (obtained after sequential extraction with petroleum ether and dichloromethane) inhibited the growth of *S. aureus* at 2.5 mg/mL,^[40] whereas a soybean ethanolic extract (obtained after NaOH/HOAc treatment of the crude extract) inhibited *L. monocytogenes* and *S. aureus* at concentrations above 6 mg/mL.^[41] The fungal elicitation process (followed by SPE cleaning) seems to be a good technique to enhance the chemical diversity and the antimicrobial properties of legume seedlings by increasing the content of prenylated aglycone phenolic compounds.

Prenylated phenolics as multi-purpose bioactive food ingredients.

In this study, we have demonstrated that prenylated phenolic compounds have potent antibacterial properties. With this, we have further substantiated the range of bioactivities that these compounds are able to exert. Previously, these compounds were correlated with the estrogenic activity of extracts from legumes, suggesting that they might have potential as nutraceuticals to ameliorate hormone-related discomforts.^[10,33,42] Besides,

prenylated phenolic compounds have also been shown to inhibit metabolically important enzymes contributing to development of type 2 diabetes, obesity and cancer,^[12,43] and to display immunomodulatory properties.^[43] With their palette of bioactivities, prenylated phenolics hold a promise for formulating novel functional foods, not only with specific health benefits, but also with naturally improved preservation.

ACKNOWLEDGMENTS

The authors would like to thank Dr. Peter A. Wierenga and Yuxi Deng from the Laboratory of Food Chemistry (Wageningen University) for their help on the k_{cell} calculation for the quantification of phenolic compounds.

REFERENCES

- [1] Ververidis, F.; Trantas, E.; Douglas, C.; Vollmer, G.; Kretzschmar, G.; Panopoulos, N. Biotechnology of flavonoids and other phenylpropanoid-derived natural products. Part I: Chemical diversity, impacts on plant biology and human health. *Biotechnology Journal*, 2007, **2**, 1214-1234.
- [2] Cowan, M.M. Plant products as antimicrobial agents. *Clinical Microbiology Reviews*, 1999, **12**, 564-582.
- [3] Ahuja, I.; Kissen, R.; Bones, A.M. Phytoalexins in defense against pathogens. *Trends in Plant Science*, 2012, **17**, 73-90.
- [4] Güçlü-Üstündağ, Ö.; Mazza, G. Saponins: Properties, applications and processing. *Critical Reviews in Food Science and Nutrition*, 2007, **47**, 231-258.
- [5] Vincken, J.-P.; Heng, L.; de Groot, A.; Gruppen, H. Saponins, classification and occurrence in the plant kingdom. *Phytochemistry*, 2007, **68**, 275-297.
- [6] Osbourn, A.; Goss, R.J.M.; Field, R.A. The saponins - polar isoprenoids with important and diverse biological activities. *Natural Product Research*, 2011, **28**, 1261-1268.
- [7] Oleszek, W.A., *Saponins*, in *Natural food antimicrobial systems*, A.S. Naidu, Editor. 2000, CRC Press: Boca Raton, FL, USA. p. 295-324.
- [8] Tahara, S.; Ibrahim, R.K. Prenylated isoflavonoids—An update. *Phytochemistry*, 1995, **38**, 1073-1094.
- [9] Kim, H.J.; Lim, J.-S.; Kim, W.-K.; Kim, J.-S. Soyabean glyceollins: biological effects and relevance to human health. *Proceedings of the Nutrition Society*, 2012, **71**, 166-174.
- [10] van de Schans, M.G.M.; Vincken, J.-P.; de Waard, P.; Hamers, A.R.M.; Bovee, T.F.H.; Gruppen, H. Glyceollins and dehydroglyceollins isolated from soybean act as SERMs and ER subtype-selective phytoestrogens. *The Journal of Steroid Biochemistry and Molecular Biology*, 2016, **156**, 53-63.
- [11] Talla, E.; Njamen, D.; Mbafor, J.T.; Fomum, Z.T.; Kamanyi, A.; Mbanya, J.-C.; Giner, R.M.; Recio, M.C.; Máñez, S.; Ríos, J.L. Warangalone, the isoflavonoid anti-inflammatory principle of *Erythrina addisoniae* stem bark. *Journal of Natural Products*, 2003, **66**, 891-893.
- [12] Bae, E.Y.; Na, M.; Njamen, D.; Mbafor, J.T.; Fomum, Z.T.; Cui, L.; Choung, D.H.; Kim, B.Y.; Oh, W.K.; Ahn, J.S. Inhibition of protein tyrosine phosphatase 1B by prenylated isoflavonoids isolated from the stem bark of *Erythrina addisoniae*. *Planta Medica*, 2006, **72**, 945-948.
- [13] Botta, B.; Menendez, P.; Zappia, G.; de Lima, R.A.; Torge, R.; Delle Monache, G. Prenylated isoflavonoids: Botanical distribution, structures, biological activities and biotechnological studies. An update (1995-2006). *Current Medicinal Chemistry*, 2009, **16**, 3414-3468.
- [14] Ayet, G.; Burbano, C.; Cuadrado, C.; Pedrosa, M.M.; Robredo, L.M.; Muzquiz, M.; de la Cuadra, C.; Castaño, A.; Osagie, A. Effect of germination, under different environmental conditions, on saponins, phytic acid and tannins in lentils (*Lens culinaris*). *Journal of the Science of Food and Agriculture*, 1997, **74**, 273-279.
- [15] Wang, F.; Wang, H.; Wang, D.; Fang, F.; Lai, J.; Wu, T.; Tsao, R. Isoflavone, γ -aminobutyric acid contents and antioxidant activities are significantly increased during germination of three Chinese soybean cultivars. *Journal of Functional Foods*, 2015, **14**, 596-604.

- [16] Aisyah, S.; Gruppen, H.; Madzora, B.; Vincken, J.-P. Modulation of isoflavonoid composition of *Rhizopus oryzae* elicited soybean (*Glycine max*) seedlings by light and wounding. *Journal of Agricultural and Food Chemistry*, 2013, **61**, 8657–8667.
- [17] Obaidat, M.M.; Bani Salman, A.E.; Lafi, S.Q.; Al-Abboodi, A.R. Characterization of *Listeria monocytogenes* from three countries and antibiotic resistance differences among countries and *Listeria monocytogenes* serogroups. *Letters in Applied Microbiology*, 2015, **60**, 609–614.
- [18] Moellering, R.C. MRSA: the first half century. *Journal of Antimicrobial Chemotherapy*, 2012, **67**, 4–11.
- [19] Aisyah, S.; Gruppen, H.; Andini, S.; Bettonvil, M.; Severing, E.; Vincken, J.-P. Variation in accumulation of isoflavonoids in *Phaseoleae* seedlings elicited by *Rhizopus*. *Food Chemistry*, 2016, **196**, 694–701.
- [20] Aisyah, S.; Gruppen, H.; Slager, M.; Helmink, B.; Vincken, J.-P. Modification of prenylated stilbenoids in peanut (*Arachis hypogaea*) seedlings by the same fungi that elicited them: The fungus strikes back. *Journal of Agricultural and Food Chemistry*, 2015, **63**, 9260–9268.
- [21] Xu, M.-J.; Wu, B.; Ding, T.; Chu, J.-H.; Li, C.-Y.; Zhang, J.; Wu, T.; Wu, J.; Liu, S.-J.; Liu, S.-L.; Ju, W.-Z.; Li, P. Simultaneous characterization of prenylated flavonoids and isoflavonoids in *Psoralea corylifolia* L. by liquid chromatography with diode-array detection and quadrupole time-of-flight mass spectrometry. *Rapid Communications in Mass Spectrometry*, 2012, **26**, 2343–2358.
- [22] Aisyah, S.; Vincken, J.-P.; Andini, S.; Mardiah, Z.; Gruppen, H. Compositional changes in (iso)flavonoids and estrogenic activity of three edible *Lupinus* species by germination and *Rhizopus*-elicitation. *Phytochemistry*, 2016, **122**, 65–75.
- [23] Cuyckens, F.; Claeys, M. Mass spectrometry in the structural analysis of flavonoids. *Journal of Mass Spectrometry*, 2004, **39**, 1–15.
- [24] van de Schans, M.G.M.; Vincken, J.-P.; Bovee, T.F.H.; David Cervantes, A.; Logtenberg, M.J.; Gruppen, H. Structural changes of 6a-hydroxy-pterocarpanes upon heating modulate their estrogenicity. *Journal of Agricultural and Food Chemistry*, 2014, **62**, 10475–10484.
- [25] Decroos, K.; Vincken, J.-P.; Heng, L.; Bakker, R.; Gruppen, H.; Verstraete, W. Simultaneous quantification of differently glycosylated, acetylated, and 2,3-dihydro-2,5-dihydroxy-6-methyl-4H-pyran-4-one-conjugated soyasaponins using reversed-phase high-performance liquid chromatography with evaporative light scattering detection. *Journal of Chromatography A*, 2005, **1072**, 185–193.
- [26] West, P.R.; Waller, G.R.; Geno, P.W.; Oleszek, W.; Jurzysta, M., Liquid secondary ion mass spectrometry and linked scanning at constant B/E LSIMS/MS for struture confirmation of saponins in *Medicago sativa* (alfalfa), in *Saponins used in food and agriculture*, G.R. Waller and K. Yamasaki, Editors. 1995, Plenum Press: New York, USA. p. 339–352.
- [27] Kosters, H.A.; Wierenga, P.A.; de Vries, R.; Gruppen, H. Characteristics and effects of specific peptides on heat-induced aggregation of β -lactoglobulin. *Biomacromolecules*, 2011, **12**, 2159–2170.
- [28] Aryani, D.C.; den Besten, H.M.W.; Hazeleger, W.C.; Zwietering, M.H. Quantifying strain variability in modeling growth of *Listeria monocytogenes*. *International Journal of Food Microbiology*, 2015, **208**, 19–29.
- [29] Simons, R.; Vincken, J.P.; Bohin, M.C.; Kuijpers, T.F.M.; Verbruggen, M.A.; Gruppen, H. Identification of prenylated pterocarpanes and other isoflavonoids in *Rhizopus* spp. elicited soya bean seedlings by electrospray ionisation mass spectrometry. *Rapid Communications in Mass Spectrometry*, 2011, **25**, 55–65.
- [30] Sobolev, V.S.; Neff, S.A.; Gloer, J.B.; Khan, S.I.; Tabanca, N.; De Lucca, A.J.; Wedge, D.E. Pterocarpenes elicited by *Aspergillus caelatus* in peanut (*Arachis hypogaea*) seeds. *Phytochemistry*, 2010, **71**, 2099–2107.
- [31] Sobolev, V.S.; Neff, S.A.; Gloer, J.B. New dimeric stilbenoids from fungal-challenged peanut (*Arachis hypogaea*) seeds. *Journal of Agricultural and Food Chemistry*, 2010, **58**, 875–881.
- [32] Sobolev, V.S.; Potter, T.L.; Horn, B.W. Prenylated stilbenes from peanut root mucilage. *Phytochemical Analysis*, 2006, **17**, 312–322.
- [33] Simons, R.; Gruppen, H.; Bovee, T.F.H.; Verbruggen, M.A.; Vincken, J.-P. Prenylated isoflavonoids from plants as selective estrogen receptor modulators (phytoSERMs). *Food & Function*, 2012, **3**, 810–827.
- [34] Price, K.R.; Eagles, J.; Fenwick, G.R. Saponin composition of 13 varieties of legume seed using fast atom bombardment mass spectrometry. *Journal of the Science of Food and Agriculture*, 1988, **42**, 183–193.
- [35] Parkar, S.G.; Stevenson, D.E.; Skinner, M.A. The potential influence of fruit polyphenols on colonic microflora and human gut health. *International Journal of Food Microbiology*, 2008, **124**, 295–298.
- [36] Payne, D.J.; Gwynn, M.N.; Holmes, D.J.; Pompliano, D.L. Drugs for bad bugs: confronting the challenges of antibacterial discovery. *Nature Reviews Drug Discovery*, 2007, **6**, 29–40.

- [37] Hassan, S.M.; Byrd, J.A.; Cartwright, A.L.; Bailey, C.A. Hemolytic and antimicrobial activities differ among saponin-rich extracts from guar, quillaja, yucca, and soybean. *Applied Biochemistry and Biotechnology*, 2010, **162**, 1008-1017.
- [38] Taylor, R.F. Bacterial triterpenoids. *Microbiological Reviews*, 1984, **48**, 181-198.
- [39] Kuchta, T.; Kubinec, R.; Farkaš, P. Analysis of hopanoids in bacteria involved in food technology and food contamination. *FEMS Microbiology Letters*, 1998, **159**, 221-225.
- [40] Nand, P.; Drabu, S.; Gupta, R.K. Phytochemical and antimicrobial screening of medicinal plants for the treatment of acne. *Indian Journal of Natural Products and Resources*, 2012, **3**, 28-32.
- [41] Zhao, D.; Shah, N.P. Tea and soybean extracts in combination with milk fermentation inhibit growth and enterocyte adherence of selected foodborne pathogens. *Food Chemistry*, 2015, **180**, 306-316.
- [42] van de Schans, M.G.M.; Ritschel, T.; Bovee, T.F.H.; Sanders, M.G.; de Waard, P.; Gruppen, H.; Vincken, J.-P. Involvement of a hydrophobic pocket and helix 11 in determining the modes of action of prenylated flavonoids and isoflavonoids in the human estrogen receptor. *ChemBioChem*, 2015, **16**, 2668-2677.
- [43] Chen, X.; Mukwaya, E.; Wong, M.-S.; Zhang, Y. A systematic review on biological activities of prenylated flavonoids. *Pharmaceutical Biology*, 2014, **52**, 655-660.
- [44] Simons, R. Prenylated isoflavonoids from soya and licorice. Analysis, induction and *in vitro* estrogenicity. 2011. Wageningen University: Wageningen, The Netherlands.
- [45] Weast, R.C., CRC Handbook of Chemistry and Physics. 58th ed. 1977, Boca Raton, FL, USA: CRC Press.
- [46] Tahara, S.; Ingham, J.L.; Mizutani, J. New coumaronochromones from white lupine, *Lupinus albus* L. (Leguminosae). *Agricultural and Biological Chemistry*, 1985, **49**, 1775-1783.
- [47] Lee, Y.J.; Notides, A.C.; Tsay, Y.G.; Kende, A.S. Coumestrol, NBD-norhexestrol, and dansyl-norhexestrol, fluorescent probes of estrogen-binding proteins. *Biochemistry*, 1977, **16**, 2896-2901.
- [48] Farkas, L.; Gottsegen, A.; Nógrádi, M. Synthesis of the natural isoflavanones ferreirin, dalbergioidin, and ougenin. *Journal of Chemical Society C*, 1971, 1994-2000.
- [49] Buckingham, J.; Munasinghe, V.R.N., Dictionary of Flavonoids. 2015, Boca Raton, FL, USA: CRC Press. 843.
- [50] Cheynier, V.F.; Trousdale, E.K.; Singleton, V.L.; Salgues, M.J.; Wylde, R. Characterization of 2-S-glutathionylcaftaric acid and its hydrolysis in relation to grape wines. *Journal of Agricultural and Food Chemistry*, 1986, **34**, 217-221.
- [51] Moesta, P.; M.G., H.; Grisebach, H. Development of a radioimmunoassay for the soybean phytoalexin glyceollin I. *Plant Physiology*, 1983, **73**, 233-237.
- [52] Trela, B.C.; Waterhouse, A.L. Resveratrol: isomeric molar absorptivities and stability. *Journal of Agricultural and Food Chemistry*, 1996, **44**, 1253-1257.
- [53] Takasugi, M.; Muñoz, L.; Masamune, T.; Shirata, A.; Takahashi, K. Stilbene phytoalexins from diseased mulberry. *Chemistry Letters*, 1978, **7**, 1241-1242.
- [54] Varshney, I.P.; Jain, D.C.; Srivastava, H.C. Saponins from *Trigonella foenum-graecum* leaves. *Journal of Natural Products*, 1984, **47**, 44-46.
- [55] Decroos, K.; Vincken, J.-P.; van Koningsveld, G.A.; Gruppen, H.; Verstraete, W. Preparative chromatographic purification and surfactant properties of individual soyasaponins from soy hypocotyls. *Food Chemistry*, 2007, **101**, 324-333.

SUPPLEMENTARY INFORMATION

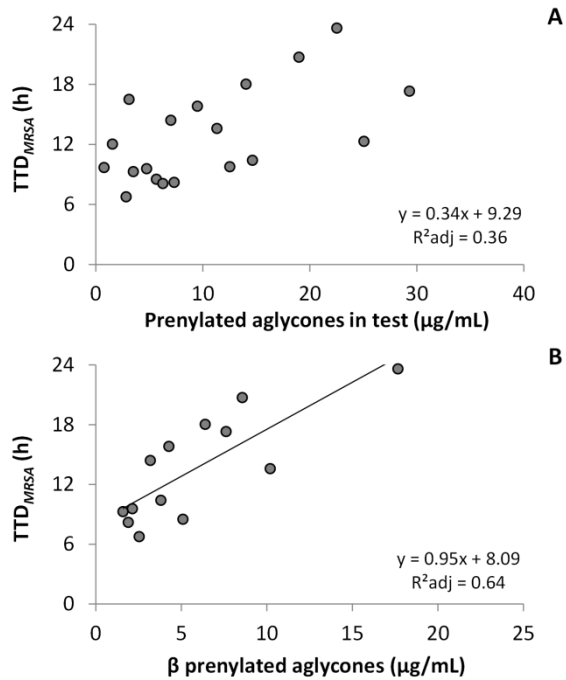


Figure S2.1. Relation between the content of total prenylated aglycones (A) and β prenylated aglycones (B) with the time to detection of MRSA growth (n = 19).

Table S2.1. Summary of diagnostic UV_{max} (nm) and MS neutral losses for different phytochemical skeletons and substitutions.

Structure annotation of phytochemicals	UV _{max} (±5 nm)	Diagnostic fragmentation *	
		NI	PI
SKELETON			
Flavonoid			
Flavone	270, 325-340		^{1,3} A/B, ^{0,2} B, ^{0,4} B
Flavanone	280-290		^{1,3} A, ^{1,3} [B-2H], ^{0,4} [B-H ₂ O]
Flavonol	250-280, 300-350		^{1,3} A, ^{1,3} [B-2H], ^{0,2} A/B, ^{1,4} [B+2H]
Flavanonol	275-280, 310-315		^{1,4} B, ^{0,2} B
Isoflavonoid			
Isoflavones	250-260		^{1,3} A/B, ^{1,4} A/B
Isoflavanone	270-295		^{1,3} A/B, ^{0,4} B, ^{2,3} B
Isoflavan	270-285		^{1,3} A/B, ^{1,4} A/B, ^{2,3} A/B
Pterocarpan	280-310		^{2,4} A/B, -H ₂ O ^{1,4} A/B, ^{5,6} A/B, -H ₂ O ^{6,7} A
Pterocarpene	280-310, 330-365		-
Coumestans	340-350		-
Coumaronochromone	260, 280, 330-350		-
Phenolic acid			
Coumaric acid derivatives	313		
Coumaroyl/caffeoyl/sinapoyl/feruloyl/ nicotinoyl conjugates		146/162/206/176/105	
Stilbenoid			
Resveratrol/piceatannol derivatives	280-340		
Saponin			
Triterpenoid saponin	205		
DDMP-conjugated	295		
SUBSTITUTION			
O-glucoside/rhamnoside/xyloside		162/146/132	
O-xylosyl/rhamnosyl/glucosyl C-glucoside		150/164/180	
O-glucuronide		176	
C-glucoside		90, 120	
Tartaric acid		132	
Malonyl		44	86

ANTIMICROBIAL ACTIVITY OF PRENYLATED PHENOLICS FROM ELICITED LEGUMES SEEDLINGS

Structure annotation of phytochemicals	UV _{max} (±5 nm)	Diagnostic fragmentation *	
		NI	PI
Methyl		16	
Methoxyl		32	
Carboxyl		44	46
Acetyl		42	
Prenyl chain (3,3-dimethylallyl)			56 (MS ²)
C6-prenyl chain			28, 56 (MS ³)
C8-prenyl chain			42 (MS ³)
Prenyl ring (2,2-dimethylpyran or 2-isopropenyl dihydrofuran)			42, 70, 54, 15 (MS ²)
Hydroxylated prenyl ring (e.g. 2,2-dimethyl-3-hydroxy dihydropyran)			18, 60, 72 (MS ²)

* ^{x,y}A/B refers to retro-Diels-Alder fragments (RDA) resulting from the cleavage of the C or D-ring of (iso)flavonoids. A-ring and B-ring fragments are indicated by either ^{x,y}A and ^{x,y}B. The superscripts x,y represent the bonds that are cleaved in the C- or D-ring. Pterocarpenes, coumestans, and coumaronochromones do not show typical RDA fragmentation due to their relatively larger conjugated system and, therefore, low C/D-ring cleavage.^[24,44]

Table S2.2. Molar extinction coefficient of representative phenolics used for the quantification of compounds in the legume seedling extracts.

Subclass	Compound	Molar extinction coefficient					
		Reported			Estimated ^a		
		ϵ (AU/M·cm)	λ (nm)	Ref.	260 nm	280 nm	315 nm
Chromone	Chromone	15849	275	[45]	31236	17474	8021
Coumaronochromone	Lupinalbin	36600	257	[46]	29891	11084	6988
Coumestan	Coumestrol	24800	345	[47]	15345	5412	10138
Flavanone	Eriodictyol	17378	292	[46]	6766	14221	7898
Flavone	Apigenin	19953	269	[46]	19391	14253	18223
Flavonol	Kaempferol	15849	273	[46]	21271	11888	14760
Isoflavanone	Dalbergioidin	20417	288	[48]	9079	19432	5779
Isoflavone (2 hydroxyl groups)	Daidzein	26915	250	[46]	24222	13782	8128
Isoflavone (3 hydroxyl groups)	Genistein	31623	263	[46]	33231	11961	3697
Isoflavone (≥ 4 hydroxyl groups)	3'-OH-genistein	27500	263	[49]	30843	12938	5729
Phenolic acid	<i>trans</i> -Caftaric acid	20600	320	[50]	3619	11012	20614
Pterocarpan	Glycinol	5870	287	[51]	5112	6532	868
Pterocarpan (prenylated)	Glyceollin I	10300	285	[51]	4152	10226	1714
Pterocarpene	Aracarpene-1	18621	330	[30]	8634	8095	16461
Stilbene	<i>trans</i> -Resveratrol	28972	320	[52]	3779	15713	29404
Stilbene (prenylated)	4-Prenyl-2'-OH-resveratrol	33100	330	[53]	8100	7150	23517

^a Estimation of the molar extinction coefficient was based on the UV spectrum of the compound found in the seedling extracts, considering that no co-elution of other UV absorbing compounds occurred.

Table S2.3. Phenolic compounds tentatively annotated by RP-UHPLC-UV-MS present in the legume seedling extracts.

No.	Rt (min)	UV _{max} (nm)	[W-H] ⁻ (m/z)	MS ² NI mode ^a	[W-H] ⁺ (m/z)	MS ² PI mode ^a	MS ² PI mode ^a	Tentatively annotated compound
Chromone								
1	8.54	285	475	313	298	nd	nd	Lupichromone O-glucoside
2	13.34	256, 284, 336	313	298	242, 270, 281	283, 287, 300	255	Lupichromone
Coumarochromone								
3	13.51	256, 281, 333	283	255, 239, 265	227, 211, 237	257, 258, 213	229, 230	Lupinalbin A
4	19.61	nd	351	323, 295, 307	295	297, 285, 269	269, 241, 255	Lupinalbin B/D
5	19.70	257, 336	351	296, 323, 307	295, 279, 268	297	269, 241, 213	Lupinalbin B/D
6	19.93	nd	349	294, 320, 306	266, 294, 182	297, 309, 323	269, 241, 213	Lupinalbin H
Coumestan								
7	8.23	340	515	267	239, 211, 223	269	254, 241, 213	Coumestrol malonyl O-glucoside
8	10.82	349	297	282, 281	254, 253	271, 284, 267	243, 256	Isotrifolol
9	11.57	343	267	239, 211, 223	211, 212	241, 225, 197	213, 214	Coumestrol
10	18.15	344	335	280, 279	252, 251, 224	269, 281, 253	241, 225, 197	Phaseol/psoraleidin/isosojagol
11	18.39	346	335	280, 279, 291	251, 252, 224	281	253, 225	Phaseol/psoraleidin/isosojagol
Flavanone								
12	4.54	278	433	313, 343	285, 269	417, 389	389, 297	Naringenin C-glucoside
13	4.76	291	449	287, 269, 259	259, 243	nd	nd	Eriodictyol O-glucoside
14	5.41	283	435, 563 ^b	255, 329, 315	135, 149, 199	nd	nd	Liquiritigenin O-rhamnosyl glucoside
15	5.63	284	491, 535	287, 463, 259	259, 243	519, 289, 401	271, 501	Eriodictyol O-(6''-O-malonyl) glucoside
16	5.75	279	433	227, 271, 253	185, 183, 159	273, 255	255	Naringenin O-glucoside
Flavone								
17	4.38	238, 335	739	473, 503	311, 353	nd	nd	Apigenin C-glucoside C-(2''-O-rhamnosyl) glucoside
18	4.40	271, 333	593	473, 431, 269	353, 445, 310	271, 433	153, 215, 243	Apigenin 7-O-glucosyl-glucoside
19	4.46	271, 333	725	605, 575, 455	455, 335, 473	577, 595, 457	457, 559, 499	Apigenin C-(2''-O-xylosyl) glucoside-C-glucoside
20	4.63	283, 330	739	619, 575, 455	455, 335, 499	577, 723, 457	457, 559, 499	Apigenin 6-C-glucoside 8-C-(2''-O-rhamnosyl) glucoside
21	4.66	277, 321	431, 575	269	225, 149, 201	271	153, 243, 215	Apigenin O-glucoside
22	5.13	256, 323	431, 563	268, 269, 311	224, 239, 240	433	415, 397, 313	Apigenin 7-O-xylosylglucoside
23	5.40	270, 326	431	311, 341	283	415, 397, 313	397, 367, 337	Apigenin C-glucoside
24	5.53	270, 334	577	311, 341, 395	283	433, 415	415, 367, 313	Apigenin C-glucoside O-rhamnoside
25	5.54	268, 330	841	635, 797, 593	299, 593, 284	681, 549, 463	301, 549	Chrysoeriol O-xylosyl-(6''-O-malonyl) diglucoside
26	5.96	260, 322	653	491, 609, 551	347, 329, 473	nd	nd	Unknown flavone diglycoside
27	6.15	266, 336	577	269	225, 269, 149	271, 433	153, 225, 229	Apigenin 7-O-(2''-O-rhamnosyl) glucoside
28	6.15	259, 332	593	299, 284, 341	284	301, 463	286	Chrysoeriol O-xylosylglucoside
29	6.16	259, 332	765	473, 515	268, 269, 311	519, 271, 681	271, 433	Apigenin O-diglycoside dimalonylated
30	6.41	268, 328	517	473	311, 413, 341	501, 313, 475	295, 457, 483	Apigenin C-glucoside malonylated
31	6.77	267, 324	431	269, 311	225, 149, 201	271	153, 229, 225	Apigenin O-glycoside
32	7.27	265, 333	663	619, 580, 631	577, 559, 269	271, 519, 579	153, 225, 229	Apigenin O-rhamnosyl glucoside malonylated

No.	RT (min)	UV _{max} (nm)	[M ⁺ -H] ⁻ (m/z)	MS ² -NI mode ^a	[M ⁺ -H] ⁺ (m/z)	MS ² -PI mode ^a	MS ² -PI mode ^a	Tentatively annotated compound
33	7.31	254, 342	679	635	299, 593, 284	681	301, 549, 595	Chrysoeriol 3-O-xylosyl-(6''-O-malonyl) glucoside
34	7.32	254, 334	445	282	254, 238, 255	447	285	Acacetin O-glucoside
35	7.82	342, 257	547	503, 299	299	549	301, 463, 505	Chrysoeriol 3-O-(6''-O-malonyl) glucoside
36	7.83	265, 325	473, 517	269, 268, 311	225, 227, 149	519	271, 433	Apigenin malonyl glucoside
37	8.33	262, 327	473	269, 311	225, 149, 201	519	271, 475	Apigenin malonyl glucoside isomer
38	8.61	258, 334	503, 547	299, 487, 443	284	549	301	Chrysoeriol 3-O-(6''-O-malonyl) glucoside isomer
39	10.82	259, 320	299	284	256, 255, 212	301	286, 287, 269	Chrysoeriol
40	11.21	266, 336	269	225, 149, 201	181, 197, 183	271	153, 229, 243	Apigenin
Flavonol								
41	4.85	258, 283, 330	447, 695	379, 284, 217	217	697	535, 287, 449	Kaempferol O-digluconide malonylated isomer
42	4.89	279	755	609, 447	301, 300, 343	757	449, 303, 611	Quercetin O-dirhamnoside O-glucoside
43	4.90	nd	651, 695	489, 447, 285	285, 421	697	535, 287, 449	Kaempferol O-digluconide malonylated
44	5.00	267, 328	695	533, 651, 447	209, 371	697	287, 449, 535	Kaempferol O-digluconide malonylated isomer
45	5.50	269, 320	609	285, 429, 257	257, 255, 151	611	nd	Kaempferol O-digluconide
46	5.63	255, 303, 352	609	301, 300, 343	179, 151, 272	611	303, 465	Quercetin O-rhamnosyl glucoside
47	6.11	265, 292, 347	593	285	257, 267, 241	595	287, 449, 301	Kaempferol O-rhamnosyl glucoside
48	6.54	264, 284, 320	447	285, 284, 327	255, 257, 267	449	nd	Kaempferol O-glucoside
49	7.66	284	489, 533	285	257, 229, 267	535	287	Kaempferol O-glucoside malonylated
50	7.75	320	623	315, 314, 300	300	625	317, 479	isorhamnetin O-rhamnosylglucoside
Isoflavan								
51	15.41	280	323	135, 147, 213	91, 93, 107	325	189, 123, 203	Phaseollinisoflavan
Isoflavanone								
52	3.82	283	611	449, 431, 491	421, 287, 405	613	nd	Dalbergioidin O-digluconide
53	4.32	283	611	449	161, 287, 285	613	nd	Dalbergioidin O-digluconide isomer
54	4.61	283	611	449, 287, 431	287, 161, 281	433, 613	nd	Dalbergioidin O-digluconide isomer
55	4.77	290	449	287, 269, 259	259, 243, 201	451	nd	Dalbergioidin C-glucoside
56	4.95	283	625	463, 301	301	465, 627	303	Isoterreirin O-digluconide
57	5.35	283	449	287, 161, 329	161, 125	451	nd	Dalbergioidin O-glucoside isomer
58	5.75	286	841	517, 355	193, 355, 161	843	441	Kievitone O-trigluconide
59	5.80	286	841	517, 679, 355	193, 355, 161	843	441	Kievitone O-trigluconide isomer
60	6.00	283	449	287, 161	125, 161	451	nd	Dalbergioidin O-glucoside
61	6.02	252, 284	679	517	193, 355, 161	519, 681	357, 339	Kievitone O-digluconide
62	8.07	283	549	505	301, 165, 343	551	nd	Isoterreirin O-glucoside malonylated
63	8.28	285	517	355, 397, 379	193, 161	519	nd	Kievitone O-glucoside
64	8.35	286	517	355, 397, 379	193, 161	519	nd	Kievitone O-glucoside isomer
65	8.54	286	287	161, 125, 255	133	289	271, 179, 151	Dalbergioidin
66	9.12	290	371	209, 161, 179	179, 123, 141	373	355	Kievitol ^c
67	9.45	290	371	209, 161, 191	191, 167, 83	373	355, 337, 301	Kievitol isomer
68	9.74	290	371	209, 161, 191	191, 167, 83	373	355, 337, 301	Kievitol isomer

ANTIMICROBIAL ACTIVITY OF PRENYLATED PHENOLICS FROM ELICITED LEGUMES SEEDLINGS

No.	RT (min)	UV _{max} (nm)	[M-H] ⁻ (m/z)	MS ² NI mode ^a	MS ³ NI mode ^a	[M-H] ⁻ (m/z)	MS ² PI mode ^a	MS ³ PI mode ^a	Tentatively annotated compound
69	9.95	290	517	193, 355, 161	124, 149, 125	519	357, 463, 501	339, 301, 283	Kievitone O-glucoside isomer
70	10.43	286	301	165	137, 93, 121	303	137, 151, 179	107, 109	Isoferreirin
71	12.03	291	559, 603	193, 355	149, 124, 125	605	587, 357, 531	531, 513, 339	Kievitone O-glucoside malonylated
72	12.24	284	339	161, 177	133	341	285, 231, 323	123, 267, 175	5-deoxykievitone ^c
73	13.28	288	355	229, 125	174, 214	357	289, 301, 339	271, 179, 151	Dihydrolicoisoflavone A
74	13.78	290	355	193, 161	124, 125, 149	357	339, 301, 283	283, 284	Kievitone ^c
Isoflavone									
75	3.68	247	431, 593	269, 268	135, 225, 241	595	433, 271	271	Genistein 4',7-O-diglucoside
76	3.89	261	443	237, 361, 425	219, 201, 189	nd	nd	nd	Unknown isoflavone
77	4.00	249	637	415	253, 252, 295	579	417, 255	255	Daidzein O-diglucoside acetylated
78	4.11	257	609	447, 285, 471	285, 379, 217	611	287, 449	217, 153, 259	2'-Hydroxygenistein 4',7-O-diglucoside
79	4.19	260	593	473, 474	445, 310, 282	595	433, 415	415, 313, 367	Genistein-8-C-7-O-diglucoside
80	4.39	257	653	431, 593	268, 269, 311	nd	nd	nd	Genistein O-diglucoside acetylated
81	4.67	260	447	327, 357	299, 259, 283	449	nd	nd	2'-Hydroxygenistein-8-C-glucoside
82	4.73	260	447	327, 357	299, 259, 283	449	431, 329, 413	413, 383, 353	2-Hydroxygenistein glycoside
83	5.00	258	431, 679	268, 269, 311	224, 239, 240	681	271, 519, 433	153, 215, 243	Genistein-4'-O-glucoside-7-O-(6''-O-malonyl)-glucoside
84	5.15	257	475	253, 415	225, 253, 209	417	255	199, 137, 227	Daidzein O-glucoside
85	5.18	269	517	471, 449, 193	309, 291	473	311, 455	175, 293, 283	Genistein-C(6''-O-malonyl)-glucoside
86	5.21	258	447	285, 327, 309	217, 241, 199	449	287	217, 153, 259	2'-Hydroxygenistein-7-O-glucoside
87	5.35	261	431	311	283	433	415, 397, 367	397, 367, 337	Genistein-8-C-glucoside
88	5.75	260	531	487	427, 325, 459	nd	nd	nd	Unknown glycosylated malonylated isoflavone
89	5.85	260	563	269	225, 181, 197	565	nd	nd	Genistein-7-O-xylosylglucoside
90	6.08	261	677	515, 557, 353	353	679	517, 461	461, 355, 299	Luteone-4',7-O-diglucoside
91	6.12	259	447	379, 285, 217	217	449	nd	nd	2',4',7,8-Tetrahydroxyisoflavone-O-glucoside
92	6.20	258	431, 491	268, 269, 311	224, 240, 239	433	271	153, 215, 243	Genistein-7-O-glucoside
93	6.38	255	501	457, 253	253, 252, 295	503	255	199, 137, 227	Daidzein glycosylated malonylated
94	6.39	258	489, 533	285, 309, 327	217, 151, 241	535	287, 449	153, 269, 217	2'-Hydroxygenistein-7-O-(6''-O-malonyl)-glucoside
95	6.50	261	473, 517	413, 311	311, 353, 323	519	313, 501, 295	284, 195, 295	Genistein-8-C(6''-O-malonyl)-glucoside
96	6.86	249	253, 501	209, 224, 225	122, 180, 159	503	255	199, 137, 227	Daidzein malonylated glycoside
97	6.88	258	489, 533	285, 429, 327	217, 241, 199	535	287	153, 217, 269	2'-Hydroxygenistein-7-O-(6''-O-malonyl)-glucoside isomer
98	6.91	261	473, 517	413, 311	323, 335, 269	519	501, 295, 397	367, 397, 295	Genistein-6-C(6''-O-malonyl)-glucoside isomer
99	6.96	260	431	268, 269, 311	224, 239, 240	433	nd	nd	Genistein-4'-O-glucoside
100	7.11	253	489, 533	285	241, 217, 256	535	287, 449	153, 241, 245	2'-Hydroxygenistein-7-O-(6''-O-malonyl)-glucoside isomer
101	7.22	259	515	447, 353, 285	285	519	nd	nd	Licoisoflavone A glycoside
102	7.48	263	763	719, 557	557, 599, 353	765	603, 559	559, 355, 547	Luteone-4',7-O-diglucoside malonylated
103	7.60	260	269, 517	225, 181, 201	181, 197	519	271, 433	215, 153, 149	Genistein-7-O-(6''-O-malonyl)-glucoside
104	8.24	262	515	353, 395	284, 285, 309	517	nd	nd	Luteone-7-O-glucoside isomer
105	8.37	260	269, 517	225, 201, 181	181, 197, 196	519	271	215, 153, 243	Genistein O-glucoside malonylated
106	8.42	261	515	353, 395, 377	309, 285, 219	517	355, 299	299	Luteone-7-O-glucoside

No.	RT (min)	UV _{max} (nm)	[M-H] ⁻ (m/z)	MS ² NI mode ^a	[M-H] ⁺ (m/z)	MS ² PI mode ^a	MS ² PI mode ^a	Tentatively annotated compound
107	8.48	260	269, 517	225, 227, 241	519	271	153, 215, 243	Genistein O-glucoside malonylated isomer
108	8.65	248	253	225, 224, 209	255	199, 137, 227	181, 171, 153	Daidzein
109	8.79	258	285	217, 199, 241	287	217, 153, 259	189, 190	2-Hydroxygenistein
110	9.80	263	369	311, 235, 325	371	nd	nd	Lupinisoﬂavone B isomer
111	9.85	263	515	447, 285, 353	517	355, 299	299	Licoﬂavone-A glucoside
112	9.95	263	499	337, 336, 379	501	339, 283	283	Wighteone-7-O-glucoside
113	10.02	262	385	367, 355	387	nd	nd	Barpisoﬂavone B derivative
114	10.04	259	513	351	353	219, 335, 299	177, 191, 201	Lupinisoﬂavone A glucoside
115	10.10	262	513	351	353	219, 335, 283	177, 201, 191	Parvisoﬂavone B glucoside
116	10.56	263	499	336, 293, 281	501	nd	nd	Wighteone-7-O-glucoside isomer
117	10.69	263	369	299, 301, 351	353, 371	219, 335, 299	191, 177, 201	Lupinisoﬂavone B
118	10.85	269	299	284, 283	301	nd	nd	3'-O-Methylroborol isomer
119	10.96	260	269	225, 181, 201	271	153, 243, 215	109, 111, 67	Genistein
120	11.57	260	557	353, 377, 395	nd	nd	nd	Licoﬂavone A glucoside derivative
121	11.68	265	299	284	301	286, 287	258, 240, 188	3'-O-Methylroborol
122	11.75	263	367, 529	323, 298, 324	369	313, 314	179, 295, 271	Barpisoﬂavone B glucoside
123	11.85	264	365	231, 337, 350	367	337, 349, 352	203, 319, 309	Parvisoﬂavone B methoxylated
124	14.72	nd	321	266, 267	323	267	195, 239, 249	6-Prenyldaidzein
125	14.81	263	353	285, 284, 267	355	299, 300	165, 281, 257	2,3-Dehydrokivitone
126	15.26	261	351	217, 307, 323	353	219, 335, 299	177, 191, 201	Lupinisoﬂavone A
127	15.50	264	353	309, 219, 201	355	299	165, 281	Luteone ^c
128	16.55	261	351	283, 265, 307	353	311, 325, 299	283, 255, 153	Licoﬂavone B
129	16.72	262	353	285, 284, 267	355	299	271, 147, 243	Licoﬂavone A
130	17.42	263	337	282, 283, 309	339	283, 284	241, 242, 213	Lupiwighteone
131	17.60	261	337	281, 282, 294	339	283, 271	255, 153	Isowighteone
132	17.67	262	367	352, 353, 312	369	nd	nd	Lupisoﬂavone isomer
133	17.87	265	337	282, 283	339	283	255, 165, 121	Wighteone
134	18.19	266	367	352, 353, 309	369	313	298, 271	Barpisoﬂavone B
135	19.50	260, 339	351	323, 296, 307	353	297, 285, 298	269, 270, 241	5-Methylwighteone
136	20.58	267	421	352, 353, 377	423	367, 368	311	Angustone A
Phenolic acid								
137	6.95	314	501	337, 277, 203	nd	nd	nd	p-Coumaroyl sinapoyltartaric acid
138	7.05	318	471	307, 277	nd	nd	nd	p-Coumaroyl feruloyltartaric acid
139	7.19	315	501	307, 337, 277	nd	nd	nd	p-Coumaroyl sinapoyltartaric acid isomer
140	7.7	319	471	277, 307, 325	nd	nd	nd	p-Coumaroyl feruloyltartaric acid isomer
Pterocarpan								
141	6.24	278	271	161, 256, 227	255, 273	199, 227, 187	181, 171, 157	Glycinol
142	8.53	257, 290	353	335, 149, 309	337, 355	309, 319, 188	263, 291, 281	Glyceofuran
143	11.35	285	339	161, 270, 324	323, 341	267, 268	239, 211, 225	Glyceollidin II

No.	RT (min)	UV _{max} (nm)	[M-H] ⁻ (m/z)	MS ² NI mode ^a	MS ² NI mode ^a	[M+H] ⁺ (m/z)	MS ² PI mode ^a	MS ² PI mode ^a	Tentatively annotated compound
144	11.77	289	337	319, 149, 293	277, 240, 275	321, 339	279, 306, 251	251, 252	Glyceollin III
145	12.06	283, 307	337	319, 149, 293	277, 240, 275	321, 339	279, 306, 251	251, 220	Glyceollin II
146	12.17	283	337	149, 319, 293	105, 121	321, 339	303, 306, 279	247, 275, 285	Glyceollin I
147	14.14	279, 308	335	317, 149, 291	289, 273, 299	319	263, 291, 319	nd	Glyceollin V
148	14.93	284	353	335, 149	320	337, 355	281, 269, 268	251, 253, 223	Glyceollin IV
149	16.65	279, 313	321	306, 277, 303	291, 289, 277	323	189, 213, 308	147, 171, 161	Phaseollin
Pterocarpene									
150	7.85	325	737	593, 635, 675	431, 179, 299	nd	nd	nd	Aracarpene-2 O-triglycoside
151	8.75	329	781	637, 679, 719	223, 413, 431	301	283, 286, 269	268, 255, 223	Aracarpene-2 O-triglycoside isomer
152	12.28	329	299	284, 271, 231	256, 228, 240	301	283, 273, 245	255, 227	Aracarpene-2
Stilbene									
153	8.82	332	473	311	242, 241, 255	313, 475	257	239, 211, 229	Arachidin-1-O-glucoside isomer
154	9.23	312	473	311	242, 241, 255	313, 475	257	239, 211, 229	Arachidin-1-O-glucoside
155	9.74	326	457	295	239, 240, 226	297, 459	241	223, 195, 213	Arachidin-2-O-glucoside
156	10.01	328	457	295	239, 240, 226	297	241	223, 195, 213	Arachidin-2-O-glucoside isomer
157	11.55	329	311	253, 241, 293	209, 185, 225	313	257, 295, 241	239, 211, 229	Arachidin-1 isomer
158	11.59	331	271	243, 227, 201	225, 201, 199	273	nd	nd	Piceatannol derivative
159	11.64	331	471	309	265, 294, 291	473	nd	nd	IPP glucoside
160	12.14	311	311	242, 241, 255	172, 213, 224	313	257, 295	239, 211, 229	Arachidin-1 isomer
161	12.43	340	311	242, 241, 255	172, 213, 224	313	257	239, 211, 229	trans-Arachidin-1
162	12.79	307, 322	295	239, 226, 240	195, 211, 180	297	241	195, 223, 199	trans-Arachidin-2
163	13.41	302	295	239, 240, 226	195, 211, 145	297	241	223, 195, 213	Arachidin-2 isomer
164	13.59	335	295	239, 240, 226	195, 211, 180	297	241	223, 195, 213	Arachidin-3
165	13.89	298	293	249, 251, 209	194, 180, 234	295	277, 185, 253	262, 249, 259	trans-3'-isopentadienyl-3,5,4'-trihydroxystilbene (IPD)
166	14.18	345	309	265, 294, 291	159, 249, 250	311	201, 283, 135	173, 159, 183	IPP isomer
167	14.45	325	309	265, 294, 291	159, 249, 250	311	201, 283, 135	173, 159, 183	IPP isomer
168	14.74	282	293	249, 251, 209	194, 180, 234	295	277, 185, 253	262, 249, 259	IPD isomer
169	15.37	330	621	243, 511, 377	225, 201, 175	623	379, 567, 501	323, 337, 257	Arahyphin-7 isomer
170	15.71	319, 274	293	236, 221, 278	192, 218	295	201, 267, 277	173, 159, 183	Arahyphin-5 or 10
171	15.90	326	343	311	242, 241, 255	313, 343	257	211, 239, 229	Arachidin-1 derivative
172	16.70	343, 271	621	511	442, 493, 401	623	513, 501, 391	457, 403, 335	Arahyphin-7
173	16.81	329	605	511, 495, 587	493, 442, 401	607	501, 551, 589	445, 323, 391	Arahyphin-6 or 9
174	16.90	326	619	509, 375, 309	491, 440, 465	621	311, 603, 565	283, 201, 269	IPP dimer
175	17.28	328	587	239, 293, 359	211, 195	589	295, 571, 467	287, 201, 253	Arahyphin-8
176	17.49	331	619	309, 509, 375	265, 291, 294	621	311, 514, 565	283, 201, 269	IPP dimer
177	18.10	322	603	309, 363, 243	265, 291, 294	605	311, 445, 587	283, 201, 269	IPP-IPD conjugate

nd, not detected (due to low UV signal, low MS signal or ambiguous λ_{max} due to overlapping signals from different compounds). ^a Product ion in MS² and MS³ are enlisted in order of intensity. ^b The parent ion showed in-source fragmentation and the intensity of the fragment dominated the mass spectrum. The italic m/z is the [M-H]⁻ in NI mode or [M+H]⁺ ion in PI mode. ^c Diagnostic ion used for tentative annotation of prenyl position was not within the three most abundant ions in MS³.

Table S2.4. Quantification of phenolic compounds in the germinated (G) and fungus elicited (GF) legume seedling extracts (mg/g DW extract).

No. ¹	Mung bean		Kidney bean		Soybean		White lupine		Blue lupine		Yellow lupine		Peanut										
	G	GF	G	GF	G	GF	G	GF	G	GF	G	GF	G	GF									
	Conc. std.	Conc. std.	Conc. std.	Conc. std.	Conc. std.	Conc. std.	Conc. std.	Conc. std.	Conc. std.	Conc. std.	Conc. std.	Conc. std.	Conc. std.	Conc. std.									
1								0.59	0.01														
2							0.10	0.01	0.64	0.01	0.09	0.01											
3	0.93	0.04	0.18	0.03	0.36	0.02	1.38	0.05	3.87	0.01	0.58	0.02	1.02	0.03	2.22	0.09							
4											0.21	0.01											
5							0.47	0.02	0.54	0.03	0.12	0.01	0.26	0.08	0.42	0.08							
6							0.26	0.01	0.12	0.01													
7							1.66	0.12															
8							0.61	0.02	1.50	0.03													
9	0.73	0.08	2.36	0.09	0.37		1.87	0.24	0.75	0.02	4.51	0.14											
10			1.04	0.03					1.08	0.02													
11							0.46	0.05															
12																							
13							2.04	0.15	1.64	0.01	2.26	0.09											
14							1.46	0.09	1.85	0.07													
15											1.75	0.07	5.14	0.26	3.74	0.11	4.36	0.46	8.68	0.26			
16							0.39	0.04	0.99	0.01							6.31	1.05	1.35	0.88			
17	1.75	0.15	2.74	0.19																			
18											1.20	1.00	1.11	0.03	2.83	0.84	3.16	0.53	4.27	1.17	4.27	0.94	
19					0.94	0.03	3.48	0.03			13.25	1.22	12.24	0.04	31.10	1.02	34.75	0.65	46.98	1.43	47.00	1.15	
20											2.43	0.11	1.94	0.02									
21	3.18	0.33	1.36	0.02							0.74	0.02	0.98	0.02	6.22	0.35	4.82	0.14	5.70	0.24	5.89	0.20	
22																							
23	3.11	0.52	1.44	0.06																			
24	2.66	0.34	1.82	0.05																			
25											0.81	0.04											
26											0.59	0.05	0.56	0.01									
27																							
28											4.16	0.63	1.42	2.36									
29											12.51	0.81	4.26	3.04									
30	0.69	0.01	0.81	0.10																			
31																							
32																							
33											12.89	0.58	3.24	0.10									
34											0.37	0.02	0.16	0.02									
35																							
											18.11	0.80	4.42	0.13									

ANTIMICROBIAL ACTIVITY OF PRENYLATED PHENOLICS FROM ELICITED LEGUMES SEEDLINGS

No. ¹	Mung bean			Kidney bean			Soybean			White lupine			Blue lupine			Yellow lupine			Peanut			
	G	GF	Conc. std.	G	GF	Conc. std.	G	GF	Conc. std.	G	GF	Conc. std.	G	GF	Conc. std.	G	GF	Conc. std.	G	GF	Conc. std.	
	Conc. ²	std. ³		Conc. std.	Conc. std.		Conc. std.	Conc. std.		Conc. std.	Conc. std.		Conc. std.	Conc. std.		Conc. std.	Conc. std.		Conc. std.	Conc. std.		
36																						
37																						
38																						
39																						
40																						
41				1.06	1.15	1.51	0.31															
42																						
43																						
44				0.79	0.01	6.62	2.15															
45																						
46	8.06	0.73	0.84	0.05	4.88	0.03	5.51	0.33														
47	3.30	0.29	0.52	0.03	2.58	0.02	1.97	0.37														
48				0.55	0.02	1.07	0.32															
49																						
50																						
51																						
52	0.39	0.07	0.33	0.02																		
53	2.43	0.26	2.02	0.09	1.93	0.08	4.54	0.24														
54				0.65	0.32	1.72	0.40															
55	2.84	0.26	2.07	0.04	0.45	0.24	2.66	0.27	0.62	0.12	1.55	0.01										
56				0.74	0.27	1.96																
57	1.02	0.39	0.53	0.03																		
58				0.32	0.06	1.35	0.07															
59				0.98	0.12	3.08	0.20															
60																						
61	0.25	0.04		1.80	0.11	2.06	0.34															
62																						
63																						
64																						
65	0.43	0.04	1.37	0.04	1.51	0.02	4.29	0.47														
66				0.25	0.03	1.61	0.20															
67				0.33	0.08	1.35	0.19															
68				0.25	0.03	0.25	0.12															
69																						
70	0.09	0.01	0.79	0.04	0.20	0.06	1.61	0.18														
71				0.28		2.43	0.27															

No. ¹	Mung bean			Kidney bean			Soybean			White lupine			Blue lupine			Yellow lupine			Peanut					
	G	GF	Conc. std.	G	GF	Conc. std.	G	GF	Conc. std.	G	GF	Conc. std.	G	GF	Conc. std.	G	GF	Conc. std.	G	GF	Conc. std.			
72				0.13	0.03	0.40	0.08																	
73						0.18	0.04																	
74	1.66	0.31	1.80	0.04	2.00	2.67	11.47	1.74																
75	0.34	0.03																						
76																0.05	0.05							
77	1.37	0.18	0.74	0.15	0.29	0.01																		
78	3.36	0.47	1.76	0.17	8.09	0.15	14.34	0.87																
79									1.10	0.08	1.68	0.33	0.84	0.05	1.05	0.02								
80				2.09	0.24	5.02	1.18		3.14	0.15	0.95	0.01	0.66	0.34	1.34	0.12	12.91	0.21	11.99	0.35				
81									0.55	0.07	1.26	0.05	0.79	0.10	0.76	0.03								
82													0.07	0.07	0.16	0.08	1.60	0.06	2.95	0.11				
83																								
84	1.72	0.16							7.78	0.48	4.34	0.06												
85																					4.34	1.60	6.14	1.31
86			0.38	0.02	1.20	0.05	0.80	0.09	14.63	0.57	12.92	0.01	0.80	0.05	2.89	0.08	5.71	0.23	6.91	0.22				
87													7.17	0.37	7.52	0.18	13.79	0.33	19.34	0.29				
88													1.67	0.08	1.06	0.02								
89									0.87	0.06	0.63	0.03												
90									1.35	0.06	1.80	0.02									0.68	0.03	1.23	0.05
91				0.56	0.03	2.13	0.26																	
92	2.43	0.26	0.87	0.03	4.48	0.20	7.36	0.62	24.80	0.56	9.23	0.09	12.66	0.48	12.21	1.19	7.62	0.26	6.02	0.19				
93				0.92					5.38	0.25	9.18	0.13	2.00	0.10	5.11	0.15	4.20	0.09	5.16	0.17				
94													24.10	0.92	15.19	0.24	16.46	0.43	15.94	0.70				
95	0.49	0.14	0.36	0.02																				
96									2.71	0.17	2.05	0.01												
97									0.17	0.01	1.21	0.01												
98													2.20	0.11	1.02	0.03	1.63	0.05	2.62	0.09				
99									0.19	0.01	0.11	0.01					0.66	0.02	1.33	0.01	1.28	0.04		
100													1.31	0.05	1.14	0.03								
101																0.24	0.01							
102																					0.41	0.03	0.88	0.02
103	1.59	0.80	1.63	0.08					25.67	1.33	17.79	0.37	10.98	0.49	18.97	0.05	45.38	0.93	34.08	0.45	6.37	0.22	9.76	0.32
104																							0.12	0.01
105									2.76	0.17	2.09	0.06					6.49	0.36	3.96	0.12				
106									1.58	0.08	2.76	0.01									0.65	0.04	1.78	0.04
107																					0.43	0.01		

ANTIMICROBIAL ACTIVITY OF PRENYLATED PHENOLICS FROM ELICITED LEGUMES SEEDLINGS

No. ¹	Mung bean		Kidney bean		Soybean		White lupine		Blue lupine		Yellow lupine		Peanut																
	G	GF	G	GF	G	GF	G	GF	G	GF	G	GF	G	GF															
	Conc. std.	Conc. std.	Conc. std.	Conc. std.	Conc. std.	Conc. std.	Conc. std.	Conc. std.	Conc. std.	Conc. std.	Conc. std.	Conc. std.	Conc. std.	Conc. std.															
108	0.21	0.01	1.78	0.07																									
109	0.18	0.03	1.98	0.03	0.84	0.07	2.07	0.31	0.91	0.06	1.32	0.03																	
110								2.48	0.11	14.76	0.02	0.77	0.03	2.76	0.10	3.04	0.06	6.14	0.17										
111														1.62	0.07														
112														0.10	0.05	0.04	0.01	0.12	0.03										
113																0.14	0.07	0.47	0.17										
114								0.16	0.01																				
115																0.09	0.09	0.30	0.23										
116										0.20	0.01	2.28	0.50	1.65	0.57														
117																0.89	0.12	0.64	0.13										
118																													
119	0.29	0.10	1.91	0.07	0.36	0.04	0.78	0.06	0.62	0.04	1.22	0.04	2.03	0.11	11.09	0.03	1.35	0.06	5.70	0.21	0.40	0.02	3.57	0.11					
120																0.29	0.01												
121																0.04	0.02	0.11	0.01										
122																		0.56	0.03	4.19	0.18								
123																		0.17	0.03	1.24	0.18								
124																0.05	0.05	0.24	0.01										
125			0.35	0.01			0.30	0.04								0.35	0.01	1.83	0.08	1.15	0.25	2.89	0.34						
126																1.38	0.04	2.92	0.03	0.13	0.01	0.42	0.01	0.70	0.03				
127																3.20	0.09	5.85	0.23	0.22	0.01	2.20	0.07	5.70	1.08	7.10	0.72		
128																				0.12	0.01								
129					0.47	0.20	3.46	0.67								0.63	0.02	0.49	0.03	0.54	0.02	3.73	0.16						
130																0.10	0.10	0.18	0.01	0.09	0.01	0.41	0.02	0.22	0.06	0.49	0.07		
131																				0.05	0.02	0.82	0.04						
132																						0.33	0.01						
133																0.40	0.01	0.45	0.02	0.50	0.03	3.75	0.14	0.63	0.15	0.48	0.08		
134																						0.09	0.01	0.47	0.03				
135																													
136																						0.33	0.02						
137																									5.37	2.68	9.53	4.15	
138																									3.11	2.73	10.27	8.00	
139																									1.38				
140																										1.25	0.97	1.30	0.47
141																													
142																													
143																													

No. ¹	Mung bean		Kidney bean		Soybean		White lupine		Blue lupine		Yellow lupine		Peanut															
	G	GF	G	GF	G	GF	G	GF	G	GF	G	GF	G	GF														
	Conc. ²	std. ³	Conc.	std.	Conc.	std.	Conc.	std.	Conc.	std.	Conc.	std.	Conc.	std.														
144			0.27	0.02	6.54	0.15																						
145			0.07	0.07	3.57	0.09																						
146			0.83	0.05	10.35	0.19																						
147					0.91	0.07																						
148					2.45	0.05																						
149			0.48	0.62	3.25	0.77																						
150													1.69	2.48 0.60														
151														7.61 0.52														
152														0.12 0.08														
153													0.55	2.46 0.26														
154													1.59	0.41 0.59 0.23														
155														0.65 0.17														
156														0.95 0.24														
157														0.29 0.07														
158														0.07 0.03														
159														0.26 0.11														
160													2.70	1.17 4.46 1.19														
161													6.67	2.75 48.16 1.19														
162													5.99	0.08 1.49 0.28														
163													5.89	1.00 0.79														
164													3.43	0.10 7.14 1.51														
165													9.37	1.82 14.95 1.26														
166													2.08	0.44 2.72 0.42														
167													0.89	0.16 0.25 0.17														
168													0.84	0.07 0.04 0.04														
169														1.72 0.05														
170													7.02	0.51 1.32 0.34														
171													1.80	0.18 0.56 0.14														
172													0.76	0.21 3.02 0.88														
173													1.54	0.01														
174													1.20	0.04														
175													0.76															
176														4.59 0.14														
177													1.56	0.08 0.99 0.07														
Total	44.6	1.6	34.5	0.4	43.0	2.8	110.0	3.6	83.5	1.9	102.3	0.7	96.6	1.9	122.8	0.3	208.7	2.5	177.8	4.2	175.1	2.5	211.8	2.2	87.3	5.8	149.8	9.7

¹No., compound number referring to the compound list in Table S3. ²Conc., concentration expressed in mg/g dry weight extract. ³std, standard deviation.

Table S2.5. Saponins (800-1500 Da) annotated by RP-UHPLC-MS in the legume seedling extracts.

No.	RT (min)	[M-H] ⁻	MS ² NI mode	MS ³ NI mode	Tentatively annotated saponin	Ref.
1	5.46	883	577, 619, 659, 721	413, 431, 457, 299	graecunin g	[54]
2	5.90	803	659, 701, 641, 365, 449	365, 407, 449	-	
3	6.51	901	605, 707, 751, 631, 455	455, 335, 383	sapogenol E glycoside	
4	7.36	1235	1173, 1027, 1217, 909, 865	1027, 865, 1011, 751, 571, 457	sapogenol B glycoside	
5	7.62	1035, 1294	991, 473, 743	949, 871, 743, 473	sapogenol A glycoside	
6	8.35	1103	1085, 777, 587, 619, 895, 473	687, 1041, 895, 733, 619, 425	sapogenol A tetraglycoside	
7	9.75	1057	877, 911, 749, 719	815, 749, 731, 719, 601, 469	-	
8	10.32	1057	877, 911, 893, 719, 489	815, 749, 601, 635, 489	-	
9	10.71	1363	1175, 1321, 1157, 1021, 1201	881, 1043, 1013, 719, 473	Aa	[55]
10	11.00	1435	1393, 1187, 1247, 1093, 1205, 877	1333, 1351, 1025, 1187	Ab	[55]
11	11.45	1201	995, 1159, 1013, 1021, 833	883, 719, 605, 863, 749, 473	Ae	[55]
12	11.53	1103	1085, 733, 879, 957, 1041, 457	879, 895, 733, 597, 1041	sapogenol B glycoside	
13	12.15	1103	1085, 879, 733, 751, 1041, 941, 457	879, 1041, 1067, 733, 525	sapogenol B glycoside	
14	13.28	957	939, 525, 895, 733	525, 597, 895, 633, 457	Ba (soyasaponin V)	[55]
15	13.84	941	923, 733, 615, 879	733, 879, 597, 525, 457	Bb (soyasaponin I) isomer	
16	14.05	941	923, 879, 733, 615, 457	879.6, 733.6, 525.3, 597, 457	Bb (soyasaponin I)	[55]
17	14.36	911	893, 615, 849, 703, 457	849, 703, 525, 597, 457	Bc (soyasaponin II)	[55]
18	14.42	1059	983, 997, 717, 835, 1041	821, 965, 659	-	
19	14.52	939	921, 613, 731, 877	877, 731, 595, 523, 455	Be isomer	
20	14.83	939	921, 877, 731, 613	877, 731, 523, 595, 455	Be	[55]
21	15.43	1083	969, 1065, 983, 941, 741, 651, 1039	951, 907, 761, 643	αg	[55]
22	15.88	1067	1049, 967, 733, 879, 921, 651	723, 651, 879	βg isomer	
23	16.15	1067	1049, 879, 967, 741, 733, 651, 583, 457	879, 651, 1005	βg	[55]

Table S2.6. Quantification of saponins in the germinated (G) and fungus elicited (GF) legume seedling extracts.

No. ¹	Content (mg BbE/g DW extract)														
	Mung bean		Kidney bean		Soy bean		White lupine		Blue lupine		Yellow lupine		Peanut		
	G	GF	G	GF	G	GF	G	GF	G	GF	G	GF	G	GF	
1														1.7	1.9
2														2.1	1.8
3										1.7	2.3				
4			5.2	5.0											
5					2.2	0.5	0.5	1.8	15.6	7.0					
6									4.5	4.5					
7														1.2	2.4
8														2.7	3.5
9					5.7	2.4									
10					2.2	2.1									
11					2.1	0.7									
12									1.8	1.6	6.0	8.3			
13									2.17	2.14					
14			13.2	9.4	5.3	3.3									
15	1.5	2.7			5.3	5.3	5.7	7.4	14.9	12.6	20.4	31.0			
16	27.3	57.1	28.6	23.5	40.0	25.1			27.5	22.2				3.9	5.4
17					19.9	12.6									
18			6.1	3.4											
19							0.5	1.2	2.4	1.0	3.3	4.2			
20	3.7	4.5	2.8	4.3	3.5	4.1			6.7	3.3					
21			3.1	5.1											
22			2.1	0.7			1.7	2.4	7.9	4.4	2.2	8.0			
23	5.8	2.2	5.2	12.3	1.3	2.4			15.7	9.5				4.4	6.3
Total	38.7	67.0	66.6	64.3	88.3	58.9	8.4	12.9	101.7	71.1	32.1	51.9	16.1	21.4	

¹Compound number refers to the compound list in **Table S2.5**.

Table S2.7. Coefficients and their respective p-value in parenthesis for the models of the effect of prenylated and non-prenylated aglycones on the TTD of *L. monocytogenes* and MRSA growth. Significance level for all models was $p < 0.001-0.01$.

Variable	<i>L. monocytogenes</i>			MRSA	
	Model A	Model B	Model C	Model A	Model B
Intercept	12.05 (0.000)	11.61 (0.000)	11.91 (0.000)	9.29 (0.000)	8.09 (0.000)
Prenylated aglycones	0.37 (0.000)	0.30 (0.000)	-	0.34 (0.007)	-
Non-prenylated aglycones	-	0.18 (0.045)	-	-	-
β -prenylated aglycones	-	-	0.70 (0.000)	-	0.95 (0.001)
R ² _{adjusted}	0.54	0.58	0.62	0.36	0.64

Rapid membrane permeabilization of *Listeria monocytogenes* and *Escherichia coli* induced by prenylated phenolic compounds: influence of skeleton structure and prenyl configuration

Legumes are the main source of antibacterial prenylated phenolic compounds. Four different pools enriched in prenylated phenolic compounds were made from extracts of lupine, peanut and soybean seedlings. One pool was rich in chain prenylated isoflavones, one in chain prenylated stilbenoids, one in chain prenylated 6 α -OH-pterocarpan, and one in ring-closed prenylated 6 α -OH-pterocarpan. Pools showed high antibacterial activity against *Listeria monocytogenes*, but not against *Escherichia coli*. The isoflavone pool was the most efficient with a minimum inhibitory concentration (MIC) of 10 $\mu\text{g}/\text{mL}$ of chain prenylated isoflavones against *L. monocytogenes*, followed by the chain prenylated pterocarpan pool (MIC 25 $\mu\text{g}/\text{mL}$), and chain prenylated stilbenoid pool (MIC 35 $\mu\text{g}/\text{mL}$). Antibacterial activity against *E. coli* was only observed when the pools were combined with an efflux pump inhibitor (EPI). In this way, *E. coli*'s susceptibility to chain prenylated isoflavones was increased to the same level as that of *L. monocytogenes* (i.e. MIC from > 40 $\mu\text{g}/\text{mL}$ to 10 $\mu\text{g}/\text{mL}$). Chain prenylated isoflavones permeabilized the cytoplasmic membrane of *L. monocytogenes* and *E. coli* (when combined with the EPI) within minutes of exposure, whereas ampicillin did not. Intermediate skeleton flexibility, bent configuration, and chain prenylation, were molecular features of the main prenylated phenolic compounds present in the pools with antibacterial activity. We postulate that the fast membrane permeabilization and high antibacterial activity make these prenylated compounds promising lead structures for the development of new antibacterials.

Keywords: prenylation, phenolics, antibacterial activity, membrane permeabilization, structure-activity relationships

INTRODUCTION

In recent years there has been a significant increase in bacterial resistance to common antimicrobials and a lack of antimicrobial discovery, which represents a threat to public health.^[1] One of the main reasons for the reduced productivity in antimicrobial discovery during the last decades was the unsuccessful generation of lead structures using combinatorial chemistry.^[2] Historically, natural products from plants and animals were the source of virtually all medicinal preparations^[2] and have been the single most productive source of leads for the development of antimicrobials.^[3] Recently, there is a growing interest in developing products that contain standardized mixtures of natural compounds from traditionally used medicines to combat antimicrobial resistance.^[4]

Natural products, either as pure compounds or as standardized extracts, provide unlimited opportunities for control of microbial growth owing to their chemical diversity.^[5] The Fabaceae (Leguminosae) is one of the largest plant families in the world and legume seeds are known to produce a large number of potentially antimicrobial phytochemicals.^[6] Under (a)biotic stress this plant family produces, in particular, prenylated phenolic compounds as a defense mechanism.^[7] These prenylated phenolic compounds have shown very good antibacterial activity, especially against Gram positive pathogens. Low minimum inhibitory concentrations ($<15 \mu\text{g/mL}$) have been found for prenylated phenolic compounds against Gram positives, including strains resistant to current antibiotics.^[8,9] In contrast, it is known that phytochemicals are less effective against Gram negative bacteria.^[10] Intrinsic resistance of Gram negatives is attributed to the interplay between reduced influx and more effective efflux of antimicrobials compared to Gram positives.^[11] Gram negatives have an outer membrane composed of a rigid leaflet consisting of lipopolysaccharide with low permeability and narrow porins facilitating the penetration of hydrophilic solutes up to a certain size exclusion limit.^[12] Active efflux of antimicrobials in Gram negatives is done by double-membrane-spanning efflux systems with unusual broad substrate specificity, allowing extrusion of substrates across the entire cell envelope.^[13]

It is accepted that prenylation increases antibacterial activity (partially) by increasing the hydrophobicity of the molecule.^[14] As a result, the interaction with biological targets, such as bacterial membranes increases.^[15,16] However, other characteristics, such as molecular geometry or charge, can contribute to the affinity of a molecule to a bacterial target site and, consequently, affect the antibacterial activity.^[17] Prenylated phenolic compounds have large structural variety derived from the number and arrangement of the (aromatic) rings defining the main skeleton (i.e. flavonoids, isoflavonoids, stilbenoids, phenolic acids and chromones). Additionally, the number, type and position of substituents decorating that skeleton will increase the structural variety.^[16] Substituents, like prenyl groups, can be attached to the main skeleton at different positions and in different configurations (i.e. chain or ring-closed prenylation).^[16] All these structural differences possibly affect the antibacterial properties of these prenylated phenolic compounds.

We previously investigated the antibacterial properties of crude extracts from (fungus-elicited) legume seedlings against Gram positive pathogens.^[18] Despite the complexity of these extracts, it was found that the content of prenylated aglyconic phenolic compounds correlated with the antibacterial activity of the extracts and that the position of the prenyl group also influenced the activity. Prenylated stilbenoids from peanut, prenylated isoflavones from lupine and prenylated 6 α -OH-pterocarpan from soybean were among the potentially good antibacterials against Gram positive pathogens.

Due to the complexity of plant extracts, it is still difficult to understand the effect of the configuration of prenylation (chain or ring-closed) or the skeleton of the phenolic (sub)class on the antibacterial properties of prenylated phenolic compounds from legumes. Therefore in this study, extracts from fungus-elicited legume seedlings were fractionated using Flash chromatography. Four different pools enriched in prenylated phenolic compounds were obtained: (i) chain prenylated isoflavones (3-ring structure, from lupine); (ii) chain prenylated stilbenoids (2-ring structure, from peanut), (iii) chain prenylated 6 α -OH-pterocarpan, and (iv) ring-closed prenylated 6 α -OH-pterocarpan (both 4-ring structures, from soybean). Structure-antibacterial activity relationships were made by using *Listeria monocytogenes* (Gram positive) and *Escherichia coli* (Gram negative) as target bacteria. The effects on the permeability of the bacterial membrane were studied, as well as the role of the efflux pump systems on *E. coli*'s intrinsic resistance.

We hypothesize that, due to higher hydrophobicity, chain prenylated phenolic compounds have higher antibacterial activity than ring-closed prenylated phenolic compounds. The distribution coefficient ($\log D$), indicator of molecular hydrophobicity and affinity of compounds for biological membranes,^[19] describes the distribution of a molecule between two immiscible phases considering the charge state of the molecule. Chain prenylation (i.e. 3,3-dimethylallyl) causes a larger increment in the $\log D$ (i.e. 1.7-unit increment) than ring-closed prenylation (i.e. 2,2-dimethylchromeno; 1.3-unit increment).^[20] Flexibility has been previously reported to be determinant for activity of membrane-disrupting antibacterials, as the interaction with membranes requires conformational changes.^[21] With 2 rotatable bonds, the skeleton of stilbenoids is more flexible than that of isoflavones (1 rotatable bond) or 6 α -OH-pterocarpan (no rotatable bonds).^[20] Therefore, we hypothesize that the stilbenoid skeleton has more freedom to adopt the right conformation to bind to potential target sites in membranes and thus has higher antimicrobial activity than isoflavones and 6 α -OH-pterocarpan.

MATERIALS AND METHODS

Materials

Lupine (*Lupinus angustifolius*) and peanut (*Arachis hypogaea*) seeds were obtained from Vreeken's Zaden (Dordrecht, The Netherlands). Soybeans (*Glycine max*) were provided by Frutarom (Londerzeel, Belgium). Acetonitrile (ACN; ULC/MS grade), water acidified with 0.1% (v/v) formic acid (FA; ULC/MS grade), methanol (MeOH; ULC/MS grade) and silica gel (60Å, 70-230 mesh) were purchased from Biosolve (Valkenswaard, The Netherlands). Ethanol absolute (EtOH) and *n*-hexane were purchased from VWR International (Radnor, PA, USA). Water for purposes other than UHPLC was prepared using a Milli-Q water purification system (Millipore, Molsheim, France). Growth media, Bacto brain heart infusion (BHI) broth were purchased from BD (Franklin Lakes, NJ, USA), tryptone soya broth (TSB) and bacteriological agar from Oxoid Ltd (Basingstoke, UK), and peptone physiological salt solution (PPS) from Tritium Microbiologie (Eindhoven, The Netherlands). Pure prenylated isoflavones 2,3-dehydrokievitone, licoisoflavone A, luteone and wighteone were purchase from Plantech UK (Reading, UK). All other chemicals were purchased from Merck (Darmstadt, Germany) or Sigma-Aldrich (St. Louis, MO, USA).

Elicitation and extraction of legume seedlings

Legume seeds were germinated and elicited with the fungus *Rhizopus oryzae* (LU581) as described elsewhere.^[22-24] In short, the process consisted of three main steps: soaking in water for 1 day at room temperature, germination for 2 days at 22-25 °C, 90-100% relative humidity (RH) and fungal exposure for 7 days at 25-30 °C, 70-90% RH. After this, the elicited seedlings were freeze-dried, milled (Ultra Centrifugal Mill ZM 200, Retsch, Haan, Germany) and extracted, under influence of sonication (40 °C / 30 min), with hexane followed by aqueous EtOH (80% v/v).^[23,24] EtOH was removed under reduced pressure and the remaining extracts were freeze-dried.

Preparative enrichment of prenylated phenolic compounds

A Reveleris® Flash chromatography system (Grace Davison Discovery Science, Columbia, MD, USA) was used to obtain pools enriched in prenylated phenolics from extracts of the elicited legume seedlings. The crude seedling extracts (250-400 mg) were mixed thoroughly with 3 g of silica gel, and dry-loaded in 5 g cartridges (Grace) on the Flash system with a solid loader plunger. The fractionation was performed at room temperature using a 12 g Reveleris C18 RP column (particle size 38.6 µm, Grace). Water acidified with 0.1% (v/v) FA, eluent A, and ACN (soybean and lupine) or MeOH (peanut) acidified with 0.1% (v/v) FA, eluent B, were used as eluents. The flow rate was 30 mL/min and UV detection was set at 280 nm (soybean and lupine) and 315 nm (peanut). For soybean the following elution profile was performed: 0-10 min, linear gradient from 0-10% (v/v) B; 10-20 min, linear gradient from 10-40% B; 20-24 min,

linear gradient from 40-50%; 24-28 min, isocratic on 50% B; 28-33 min, linear gradient from 50-60% B; 33-34 min, linear gradient from 60-70% B; 34-37 min, linear gradient from 70-80% B; 37-38 min, linear gradient from 80-100% B. For lupine the following elution profile was performed: 0-2 min, isocratic at 0% (v/v) B; 2-24 min, linear gradient from 0-100% B. For peanut the following elution gradient was performed: 0-2 min, isocratic at 0% (v/v) B; 2-16 min, linear gradient from 0-100% B.

Flash fractions (10-15 mL) were collected in glass tubes and subsequently analysed by RP-UHPLC-UV-MS. Fractions containing similar prenylated compounds were pooled. Fractionation of crude extracts and pooling was performed several times until enough material was collected for further experiments. The final pools enriched in prenylated phenolics were evaporated under vacuum, solubilized in *tert*-butanol and freeze-dried. Stock solutions in aqueous EtOH (70% v/v) were made for compositional analysis.

RP-UHPLC-UV-MS analysis

Phenolic compound analysis was performed on an Accela ultra high performance liquid chromatography (RP-UHPLC) system (Thermo Scientific, San Jose, CA, USA) equipped with a pump, autosampler and photodiode array (PDA) detector.

Pools (1 μ L, 2-5 mg/mL) were injected onto an Acquity UPLC BEH RP18 column (2.1 mm i.d. x 150 mm, 1.7 μ m particle size) with an Acquity UPLC RP18 Vanguard guard-column (2.1 mm i.d. x 5 mm, 1.7 μ m particle size; Waters, Milford, MA, USA). Water containing 0.1% (v/v) FA and 1% (v/v) ACN, eluent A, and ACN containing 0.1% (v/v) FA, eluent B, were used as solvents at a flow rate of 300 μ L/min. Column temperature was set at 35 °C and the PDA detector was set to measure from 200-600 nm.

For the lupine and soybean pools the following elution profile was used: 0-1 min, isocratic on 9% (v/v) B; 1-3 min, linear gradient from 9-25% B; 3-10 min, linear gradient from 25-50% B; 10-13 min, isocratic on 50% B; 13-23 min, linear gradient from 50-100% B. For the peanut pool the following elution gradient was used: 0-1 min, isocratic on 10% (v/v) B; 1-10 min, linear gradient from 10-34% B; 10-11 min, linear gradient from 34-42% B; 11-21 min, linear gradient from 42-50% B; 21-23 min, linear gradient from 50-100% B.

Mass spectrometric (MS) analysis was performed on a LTQ Velos (Thermo Scientific) equipped with a heated ESI probe coupled to the RP-UHPLC. Spectra were acquired over an *m/z* (mass to charge ratio) range of 150-1500 Da in negative (NI) and positive (PI) mode. Data-dependent MSⁿ analysis was performed on the most intense (product) ion with a normalized collision energy of 35%. A dynamic mass exclusion approach was used, in which a compound detected five times within 10 s as most intense was subsequently excluded for the following 10 s, allowing data dependent MS² of less abundant co-eluting compounds. The system was tuned with genistein and resveratrol in both PI and NI mode via automatic tuning using Tune Plus (Xcalibur 2.1,

Thermo Scientific). Nitrogen was used as sheath and auxiliary gas. The ITT temperature was 400 °C and the source voltage was 3.50 kV (NI) or 4.50 kV (PI).

Annotation and quantification of phenolic compounds

Compounds were tentatively annotated based on UV-Vis and MS spectral data, obtained by means of Xcalibur (v.2.2, Thermo Scientific), using the approach reported earlier on the same legume seeds.^[24-28] In brief, different subclasses of phenolic compounds have characteristic UV spectra and (*retro*-Diels-Alder) fragmentation patterns in MS.^[22] Furthermore, prenyl configurations were confirmed by characteristic neutral losses in MS² PI mode. A loss of 56 Da (C₄H₈) was used to distinguish chain prenylation from ring-closed prenylation.^[29] Major neutral losses of 42 (C₃H₆) and, to a lesser extent, 60 Da (C₃H₆ + H₂O), 54 Da (C₄H₆) and 15 Da (CH₃•) were used to annotate both 2,2-dimethylpyran and 2''-isopropenyl-dihydrofuran rings.^[30] Isomers were tentatively annotated based on literature,^[24,25,31] considering their elution behaviour and their abundance. The position of the prenyl group within the A-ring of isoflavones was tentatively annotated based on diagnostic tools, previously developed with authentic standards.^[24] A high abundance in MS³ of the ion corresponding to a neutral loss of 42 Da (C₂H₂O) was diagnostic for C8 prenylation, whereas the C6 prenylated isomer showed a neutral loss of 28 Da (CO) instead. These diagnostic tools have been previously used for the annotation of prenylated compounds in soybean and confirmed by NMR.^[32] A summary of the diagnostic UV absorption and MS neutral losses is shown in **Table S3.1** (supplementary information).

Quantification was based on the UV absorption at 260 nm (isoflavones), 280 nm (6*α*-OH-pterocarpan) and 315 nm (stilbenoids), using the following equation (Eq. 3.1),^[33] derived from the Lambert-Beer's law:

$$C = \frac{\text{area} \times Q}{\epsilon \times l \times V_{inj} \times k_{cell}} \quad (\text{Eq. 3.1})$$

in which C is concentration (M), *area* is the integrated area of the UV peak at the specific wavelength (AU·s), Q is the flow rate (5 μL/s), ε is the molar extinction coefficient (AU/M·cm), *l* is the path length of the UV cell provided by the manufacturer (5 cm), *V_{inj}* is the injected volume of sample (1 μL), and *k_{cell}* is a constant related to the cell geometry of the UV detector.^[33] This equation relates the duration of absorbance given by the UHPLC system (AU·s) to an actual absorbance value (AU) for the Lambert-Beer's equation. The *k_{cell}* represents the correction factor for the absorption of light by the coating material of the flow cell. The *k_{cell}* (0.82 ± 0.09) was determined with solutions of daidzein (248 nm), genistein (263 nm) and resveratrol (310 nm) (with five concentrations each, in the range of 0.001-0.1 mg/mL). Because the ε of most annotated compounds were unavailable, for each subclass of phenolics (e.g. isoflavone, coumestan, coumaronochromones, pterocarpan, stilbenoid) a representative compound was chosen and its previously reported ε was used, corrected for the wavelength used in

this study (Table S3.2). In case of co-elution, the UV peak area was divided over the co-eluting compounds in a ratio based on the MS intensities.

Antibacterial activity assay

Pools enriched in prenylated phenolics were tested for their antimicrobial activity against Gram positive *Listeria monocytogenes* EGD-e and Gram negative *Escherichia coli* K12. Bacteria were streaked from a -80 °C glycerol stock onto a BHI agar plate and incubated 24 h at 37 °C, after which one colony was transferred to BHI broth (10 mL) and further incubated for 18 h at 37 °C. These overnight cultures were diluted 100,000 times with TSB (final inoculum concentration $3.0 \pm 0.2 \log_{10}$ CFU/mL for *L. monocytogenes* and $3.7 \pm 0.1 \log_{10}$ CFU/mL for *E. coli*). Equal volumes (100 μ L) of bacteria and a series of 2-fold dilutions of each pool in TSB (final concentrations tested 5-40 μ g/mL of prenylated phenolic compounds with a maximum concentration of 1% (v/v) EtOH) were mixed into a 96-well plate. The 96-well plate was incubated in a SpectraMax M2e (Molecular Devices, Sunnyvale, CA, USA), at 37 °C with constant linear shaking. The optical density (OD) at 600 nm was measured every 5 min for 24 h.

Positive controls (ampicillin at 10 μ g/mL in TSB), negative controls (TSB suspension of bacteria with 1% (v/v) EtOH), and blanks (extracts and TSB medium with no bacteria) were considered for optical comparison and sterility control. The time to detection (TTD) of growth was defined as the time to have a change in OD of 0.05 units above the detection limit.^[34] Pools enriched in prenylated phenolics were tested in two independent biological reproductions, each performed in triplicate.

When no change in OD was observed after the 24 h of the antibacterial susceptibility test, cell viability was verified by plate counting. Briefly, 100 μ L of the well with no change in OD was decimally diluted in PPS solution and 100 μ L of each dilution was spread onto BHI agar plates. Colonies were counted after 24 h incubation at 37 °C. The minimum inhibitory concentration (MIC) was defined as the lowest concentration of pool that resulted in a bacterial count equal or lower than the initial inoculum (i.e. ≤ 3.0 - $3.7 \log_{10}$ CFU/mL depending on the bacterium). The minimum bactericidal concentration (MBC) was defined as the lowest concentration of pool that resulted in no growth after plating^[35], i.e. >99% bacterial inactivation from the initial bacterial inoculum.

To determine the role of the efflux pump systems in the resistance of *E. coli* towards the prenylated phenolic compounds, the efflux pump inhibitor phenylalanine-arginine β -naphthylamide dihydrochloride (PA β N) was used in combination with the pools during the antibacterial susceptibility test. PA β N is able to inhibit the most prominent efflux pump in *E. coli*, the proton-dependent AcrAB-TolC efflux pump system,^[36] and thus increase its susceptibility towards antibacterials. PA β N was added in the medium to a concentration of 25 μ g/mL (48 μ M).^[37]

Cell membrane permeability

To determine the effect on the membrane permeability, the fluorescent probe propidium iodide (PI) was used. Bacteria (-80 °C glycerol stock) were streaked onto a BHI agar plate and incubated overnight at 37 °C, after which one colony was transferred to BHI broth (50 mL) and incubated for 13 h at 25 °C. Cells were harvested by centrifugation (4696 g, 4 °C, 20 min) and washed twice with PPS solution (pH 7.2). The final cell pellet was dispersed in 5 mL of PPS to obtain an inoculum of $10.2 \pm 0.3 \log_{10}$ CFU/mL. Stocks of PI and pools were diluted in PPS to concentrations of 60 μ M and 20-120 μ g/mL, respectively. A volume of 50 μ L of each solution (final concentration in test of PI 15 μ M and pools 5-30 μ g/mL, 1% (v/v) EtOH max.) was added to a black (with clear bottom) 96-well plate (Greiner Bio One, Kremsmünster, Austria). Inoculum (100 μ L) was added to each well and the plate was incubated at room temperature in a Spectramax M2e. Emission of fluorescence was measured every 30 s at 620 nm (bottom read mode), while exciting the sample at 520 nm. For the positive control, cells were treated for 10 min at 95 °C in a Thermomixer (Eppendorf, Hamburg, Germany) and added as inoculum, whereas the blank control contained 100 μ L of PPS instead of inoculum. Intrinsic fluorescence or quenching effects of the legume seedling pools were considered by the use of sample blanks (pool with PI, without cells; PI without cells).

Fluorescence microscopy

Inoculum (250 μ L, prepared as described above) was mixed with the pool stocks (250 μ L) in an eppendorf. Samples (60 μ L) were taken at different time points and mixed with PI (final concentration 15 μ M). After 5 min incubation, cells were visualized with an Olympus BX41 microscope (Olympus, Tokyo, Japan), equipped with a PlanC N 100x/1.25 oil Ph3 objective lens and a red fluorescent protein (RFP) filter. Excitation was performed at 540 nm with a X-Cite® 120Q lamp (Excelitas, Waltham, MA, USA). Images were acquired by Cell^b software version 3.4 (Olympus) using an Olympus XC30 camera.

Prediction of molecular properties

The software Marvin (version 6.0.5, 2013, ChemAxon, Budapest, Hungary) was used to predict the distribution coefficient ($\log D$) of prenylated compounds at pH 7.2 (pH of growth media used in our study), using the software's default settings. Molecular structures and dihedral angles were evaluated using Chem3D (v15.0, CambridgeSoft, Waltham, MA, USA) after MM2 energy minimization. The lead-likeness^[38] of prenylated phenolic compounds was defined based on the following criteria: mass \leq 450 Da, $\log D$ (at pH 7.2) \geq -4 and \leq 4, ring count \leq 4, rotatable bond count \leq 10, hydrogen bond donor count \leq 5, and hydrogen bond acceptor count \leq 8, using the properties viewer of chemicalize.org (ChemAxon, Budapest, Hungary).^[20]

RESULTS

Phenolic content and composition of Flash pools

Four different Flash pools enriched in prenylated phenolics were prepared from legume seedling extracts: chain prenylated isoflavones (clsf) from lupine, chain prenylated stilbenoids (cSti) from peanut, chain prenylated (cPta) and ring-closed prenylated 6a-OH-pterocarpan (rPta) from soybean. **Table S3.3** shows the list of compounds tentatively annotated by means of UV and MSⁿ in the different pools. In total, 57 different phenolic compounds were tentatively annotated, 39 of which were prenylated. In **Figure 3.1A** the overall contents of prenylated and non-prenylated phenolic compounds is shown (the individual amounts of each annotated compound are presented in **Table S3.4**). The pools contained between 165 to 350 mg phenolics/g DW pool. The clsf, cSti, and rPta pools contained more than 90% (w/w) prenylated phenolic compounds, whereas the cPta pool contained 60% (w/w) prenylated phenolic compounds. No glycosylated phenolic compounds were present in any of the pools.

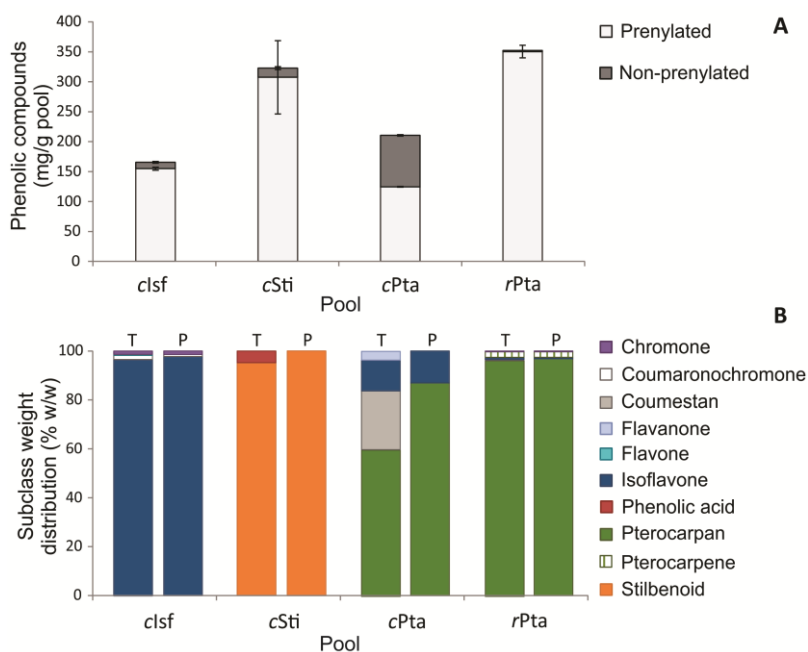


Figure 3.1. Composition (mg/g DW pool) of the pools (A) and normalized subclass weight distribution (% w/w) (B) of the total (T) and prenylated (P) aglyconic phenolic compounds. Chain prenylated isoflavones (clsf), chain prenylated stilbenoids (cSti), chain prenylated 6a-OH-pterocarpan (cPta), ring-closed prenylated 6a-OH-pterocarpan (rPta).

Compounds from the isoflavonoid, flavonoid, stilbenoid, phenolic acid and chromone (sub)classes were identified in the different pools. **Figure 3.1B** shows the subclass weight distribution of the total and the prenylated phenolic compounds in the pools. The distribution of (sub)classes of the total phenolic content was highly specific, with the clsf pool containing more than 95% (w/w) isoflavones, the cSti pool 95% (w/w) stilbenoids and the rPta pool 95% (w/w) 6 α -OH-pterocarpanes. Only the cPta pool had a more diverse composition with 60% (w/w) 6 α -OH-pterocarpanes, 25% (w/w) coumestans and 10% (w/w) isoflavones. Considering only the prenylated phenolic compounds, the clsf, cSti and rPta pools were composed of 96-100% (w/w) isoflavones, stilbenoids or 6 α -OH-pterocarpanes, respectively. The cPta pool was composed of 86% (w/w) prenylated 6 α -OH-pterocarpanes and 14% (w/w) prenylated isoflavones.

Regarding the weight distribution of the configuration of prenyl group (**Figure 3.2A**), the clsf, cSti and cPta pools contained 90-95% (w/w) chain prenylated compounds, whereas rPta contained 95% (w/w) ring-closed prenylated phenolic compounds, 64% (w/w) of which were pyran-prenylated and 36% (w/w) were furan-prenylated. **Figure 3.2B** shows the weight distribution of the different prenyl positions within the phenolic skeletons. To compare the three main (sub)classes of phenolic compounds (isoflavones, stilbenoids and 6 α -OH-pterocarpanes), the IUPAC atom numbering was adapted according to the structures inserted next to the bar diagram. Prenylation at position β was the most abundant in all pools, especially in the cSti and cPta pools (90-100% (w/w) β prenylated compounds). The clsf and rPta pools also contained 20-30% (w/w) compounds prenylated at the α position, whereas clsf and cSti contained 10-30% (w/w) δ prenylated compounds.

Antibacterial activity of Flash pools against *L. monocytogenes* and *E. coli*

In **Figure 3.3**, the time to detection (TTD) of bacterial growth is shown at different concentrations of prenylated compounds. The longer the TTD, the stronger is the inhibition of bacterial growth.

The clsf pool was the most active against *L. monocytogenes* by inhibiting the growth (TTD > 24 h), at already 10 μ g/mL of prenylated compounds (**Figure 3.3A**). Pool rPta was the least active of all; it inhibited the growth of *L. monocytogenes* at 40 μ g/mL of prenylated compounds.

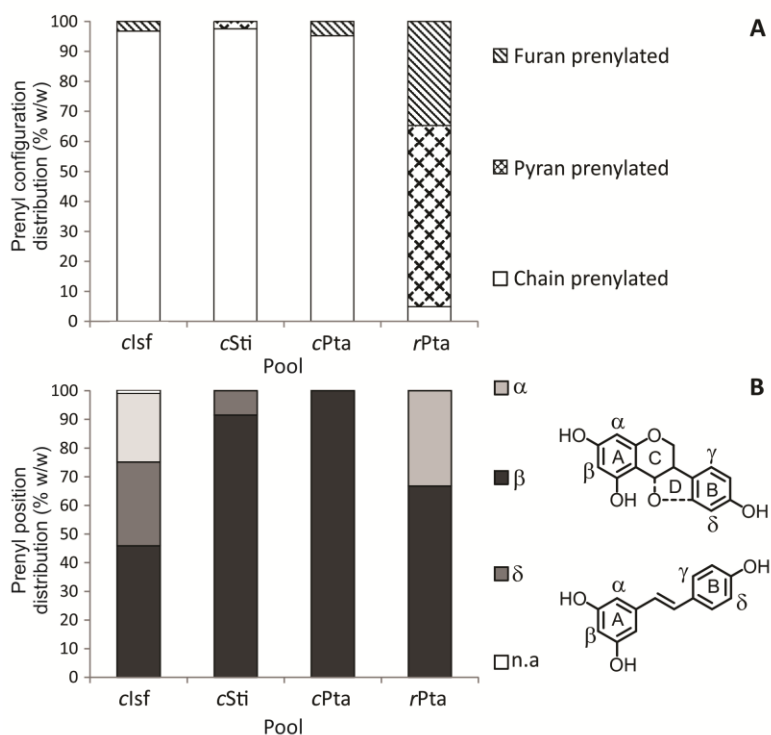


Figure 3.2. Normalized weight distribution (% w/w) of the configuration of prenyl group (**A**) and prenyl position (**B**) in prenylated phenolics present in the legume seedling pools. Positions of prenylation within isoflavonoids and stilbenoids are indicated by the Greek letters α , β , γ and δ in the structures next to the bar diagram. *n.a.* Not annotated.

Regarding the activity against *E. coli*, none of the pools studied inhibited the growth of this bacterium up to the highest tested concentration (40 $\mu\text{g/mL}$, **Table S3.5**). Therefore, the activity of the pools was measured in the presence of the efflux pump inhibitor PA β N. This compound did not considerably affect the growth of *E. coli* by itself. The TTD of cells in the presence of PA β N was delayed by only 1 h and the total cell count after 24 h of incubation was not significantly different in comparison with the cells without PA β N (**Table S3.5**). Furthermore, as PA β N was previously reported to destabilize the outer membrane of *E. coli* and increase its susceptibility towards vancomycin,^[39] susceptibility of *E. coli* towards vancomycin was checked in the presence of PA β N. Vancomycin is normally excluded from entering Gram negatives, but if the outer membrane is compromised this antimicrobial is able to enter the Gram negative cell.^[39] No susceptibility of *E. coli* towards vancomycin (10–50 $\mu\text{g/mL}$) in the presence of PA β N was observed. Growth was comparable to that of the control cells (**Table S3.5**, no further data shown). This led us to conclude that, under our experimental conditions, the main activity of PA β N was to inhibit the efflux pumps and not to destabilize the outer membrane of *E. coli*.

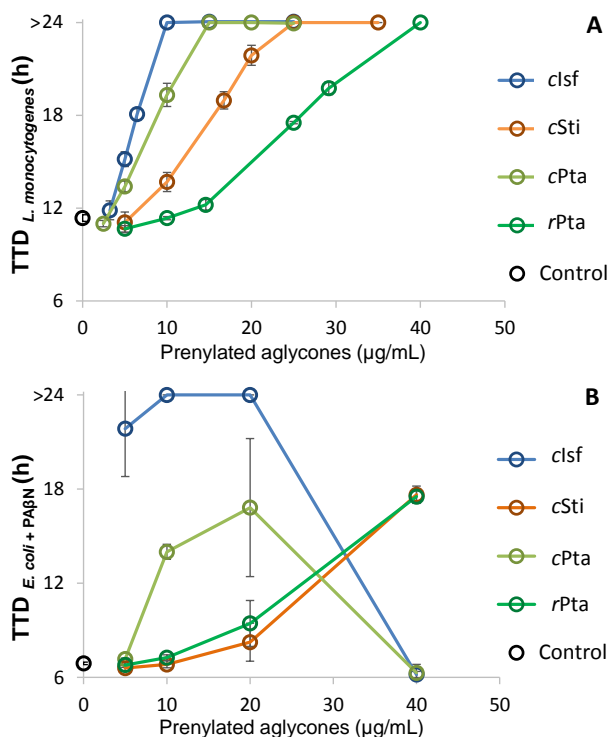


Figure 3.3. Time to detection of *L. monocytogenes* (A) and *E. coli* (+ 25 µg/mL PAβN) (B) growth after incubation with the different pools. Data are means of two independent biological reproductions with standard deviation as error bars. Inoculum was $3.0 \pm 0.2 \log_{10}$ CFU/mL for *L. monocytogenes* and $3.7 \pm 0.1 \log_{10}$ CFU/mL for *E. coli*. Control refers to untreated cells.

In **Figure 3.3B** the TTD of *E. coli* after exposure to all pools in combination with PAβN is shown. The clsf pool at 10 and 20 µg/mL inhibited the growth of *E. coli* (TTD > 24 h). Unexpectedly, the inhibition of bacterial growth by this pool, as well as that of the cPta pool, was cancelled at 40 µg/mL (TTD equal to that of the control cells). The cSti and rPta pools did not inhibit the growth of *E. coli* (TTD < 24 h) up to 40 µg/mL prenylated compounds.

After the 24 h incubation with the different pools, viability of cells was verified by plate counting and the MIC and MBC were determined (**Table 3.1**). The MBC of the clsf pool was the lowest at 15 µg/mL for *L. monocytogenes* and at 10 µg/mL of prenylated phenolic compounds for *E. coli* in combination with PAβN. For the rPta no MIC or MBC against both target microorganisms was found at the highest concentration tested.

Table 3.1. Minimum inhibitory (MIC) and bactericidal (MBC) concentration of prenylated phenolic compounds from the legume seedling pools.

Bacteria		Concentration of prenylated aglycones ($\mu\text{g}/\text{mL}$)			
		clsf	cSti	cPta	rPta
<i>L. monocytogenes</i>	MIC	10	35	25	>40
	MBC	15	>40	>40	-
<i>E. coli</i>	MIC	>40	>40	>40	>40
<i>E. coli</i> (+ PA β N)	MIC	10 ^a	>40	>20 ^a	>40
	MBC	10	-	-	-

^a The results of activity for these pools at 40 $\mu\text{g}/\text{mL}$ prenylated compounds were not considered due to the lack of activity of PA β N under those conditions.

Prenylated phenolic compounds were found previously to correlate with the antibacterial activity of legume seedling extracts.^[18] Therefore, we assumed that the prenylated compounds in the pools were responsible for the antibacterial activity observed. To validate this assumption, a reconstituted clsf pool was created using pure prenylated isoflavones. The main prenylated compounds annotated in the clsf pool (i.e. luteone, licoisoflavone A, 2,3-dehydrokiefvitone and wighteone, **Table S3.3** and **S3.4**) were mixed at the same concentration ratio as in the clsf pool. This reconstituted clsf pool was tested for its antibacterial activity (**Table S3.6**) and MIC and MBC values were similar to those of the Flash pool. Therefore, it can be stated that the annotated prenylated compounds in the pools are the main contributors to the antibacterial activity of the pools. Because other pure prenylated compounds annotated in the pools were unavailable, the validation was performed only for the clsf pool.

Bacterial membrane permeabilization

The fluorescent probe propidium iodide (PI), capable of binding to DNA only after crossing a permeable membrane^[40], was utilized to measure the permeabilization capacity of the different pools. **Figure 3.4A** shows the increment in time of PI fluorescence when *L. monocytogenes* was exposed to the pools (15 $\mu\text{g}/\text{mL}$ prenylated compounds), after intrinsic fluorescence of samples was subtracted from the signal. The clsf pool increased the PI fluorescence very rapidly, indicating cytoplasmic membrane permeabilization of *L. monocytogenes*. In contrast, the cPta, cSti and rPta pools showed a very small permeabilization effect within the time of measurement. **Figure 3.4B** shows the fluorescence intensity of PI when *E. coli* is exposed to the pools in combination with PA β N (without PA β N the pools did not permeabilize *E. coli*, **Figure S3.1**). The clsf pool in combination with the efflux pump inhibitor increased the uptake of PI by *E. coli* very quickly. The cPta pool caused the second highest permeabilization of *E. coli*; the cSti pool caused only a small permeabilization, whereas the rPta pool showed the same

fluorescence as the control cells. Interestingly, the permeabilization of *E. coli* was comparable to that of *L. monocytogenes* when using the efflux pump inhibitor, and the control antimicrobial ampicillin showed little effect on the membrane permeabilization for any of the bacteria, during the time of measurement.

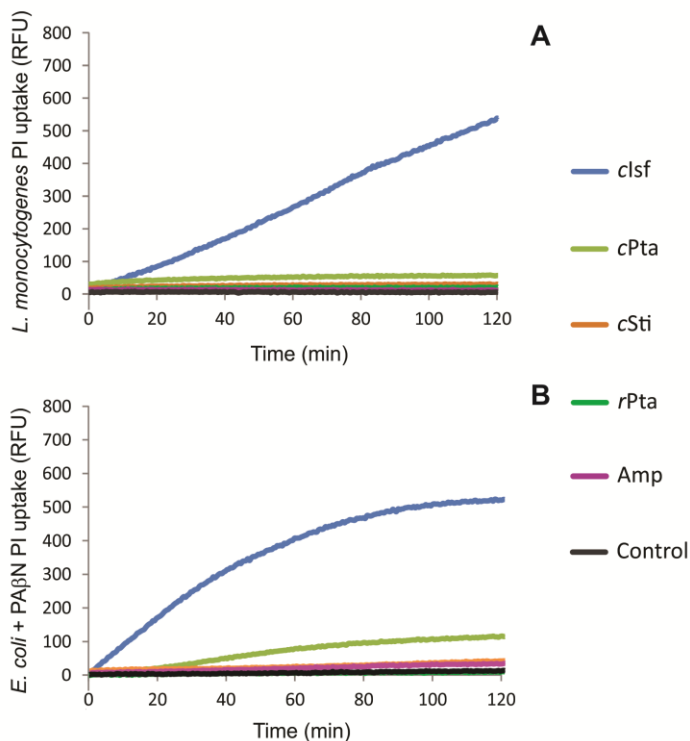


Figure 3.4. PI uptake by *L. monocytogenes* (A) and *E. coli* with PAβN (B) when exposed to the pools at a concentration of 15 μg/mL of prenylated aglycones. Control refers to the untreated cells of *L. monocytogenes* or *E. coli* with PAβN. Ampicillin was tested at 10 μg/mL.

Figure 3.5A shows the net fluorescence of PI after 2 h of treatment of *L. monocytogenes* with increasing concentrations of prenylated compounds. The clsf pool caused a remarkably high permeabilization of *L. monocytogenes* from 10 μg/mL onwards. The second most effective permeabilizing pool was the cPta pool. The cSti and the rPta had the least permeabilizing capacity of all pools. **Figure 3.5B** shows the PI uptake by *E. coli* at increasing concentrations of the pools, in combination with PAβN. Again, the clsf pool showed the most efficient permeabilization, although there was a decrease at 30 μg/mL of prenylated compounds. For the other pools, the permeabilization of cells increased with increasing concentration of prenylated compounds, with the rPta pool being the least efficient one.

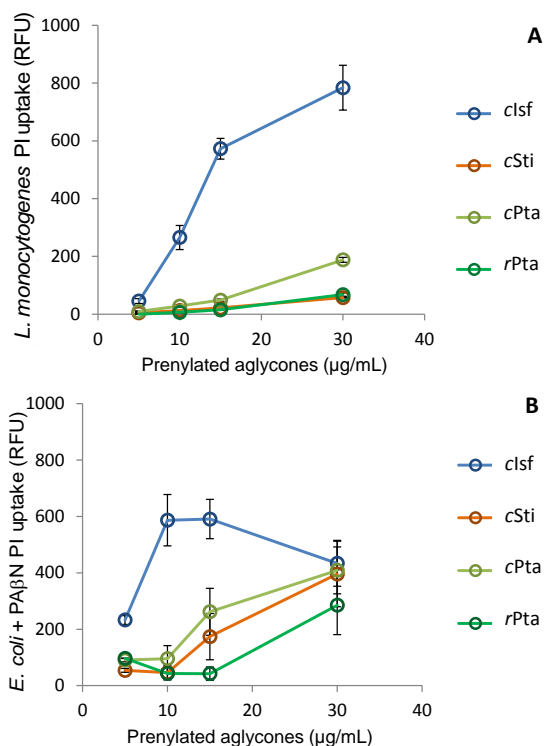


Figure 3.5. PI uptake of *L. monocytogenes* (A) and *E. coli* with PAβN (B) after 2 h of being exposed to different concentrations of the pools. Data are means of two independent biological reproductions; standard deviation is shown as error bars.

In **Figure 3.6**, the fluorescence microscopy images of *L. monocytogenes* and *E. coli* cells after exposure to the clsf pool are shown. Within 30 min all cells of *L. monocytogenes* and *E. coli* (the latter in the presence of the efflux pump inhibitor) were stained red. No substantial staining was observed for the control cells.

DISCUSSION

Fast permeabilization of cytoplasmic membrane by prenylated phenolic compounds

Using propidium iodide, a hydrophilic and thus membrane impermeable, nucleic acid-binding fluorescent probe,^[41] we found that the clsf pool in particular was very fast at permeabilizing the membrane of *L. monocytogenes* and *E. coli*, albeit for the latter the presence of the efflux pump inhibitor was necessary. The influx of PI increased within a few minutes of exposure at concentrations as low as 10 μg/mL of chain prenylated isoflavones (**Figure 3.5**).

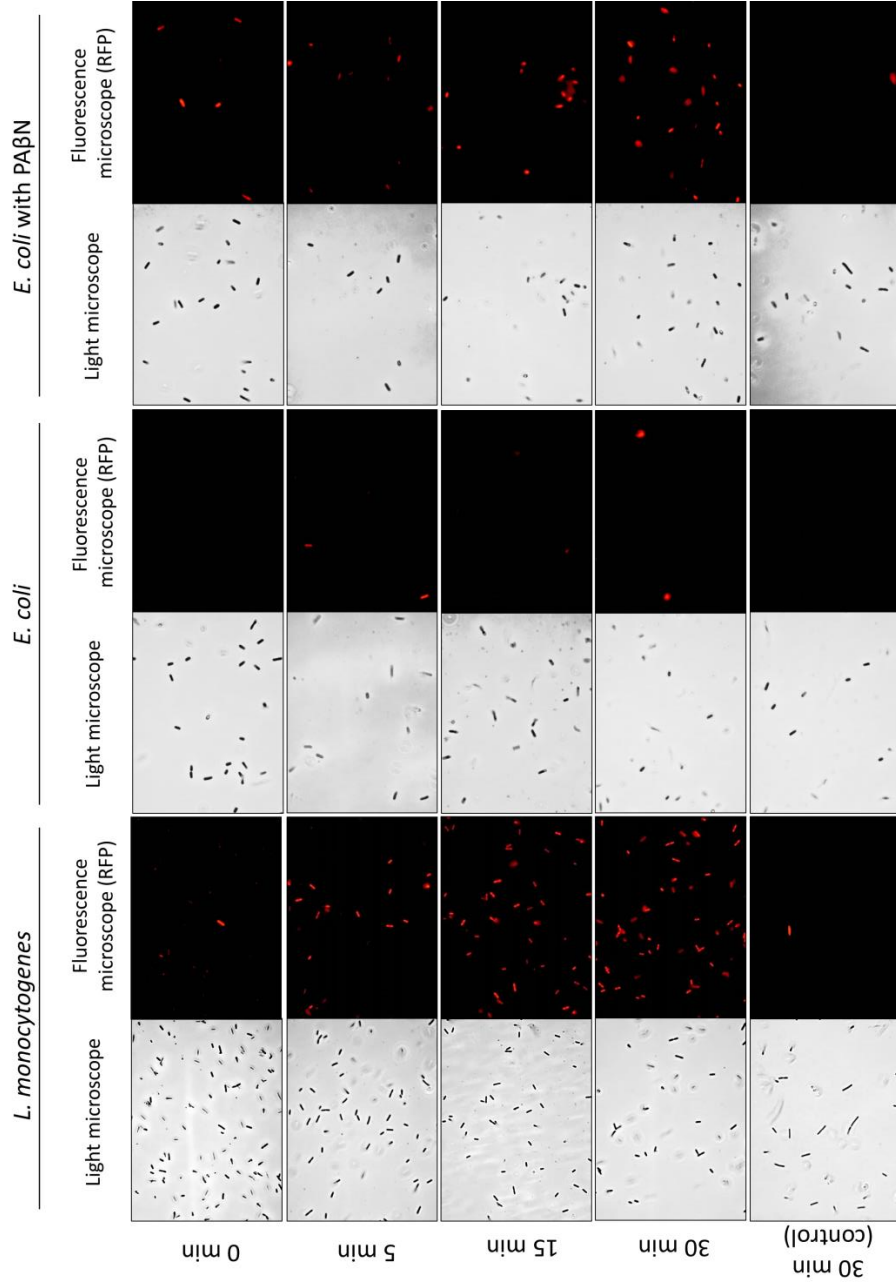


Figure 3.6. Light and fluorescence microscopy images of *L. monocytogenes* (10^9 CFU/mL) and *E. coli* (10^8 CFU/mL) after 5, 15 and 30 min exposure to clsf pool (25 μ g/mL prenylated aglycones).

This efficient permeabilization with the clsf pool is in accordance with the MIC and MBC obtained (**Table 3.1**). Our permeabilization results are in line with effects of (prenylated) phenolic compounds reported on model liposomal systems.^[14,42,43] Prenylated compounds have been reported to penetrate into the hydrophobic part of the lipid bilayer and perturb its organization, including a reduced density of phospholipid packing in the bilayer. Reduced packing density of the lipids might result in a permeable membrane as observed in our study.

The control antimicrobial ampicillin did not cause a significant increase in PI fluorescence after 2 h of exposure of the cells (**Figure 3.4A**), even though counts after this period demonstrated 70-90% cell inactivation for both samples (i.e. clso and ampicillin) in comparison to the control (no further data shown). Ampicillin inactivates actively growing cells by inhibiting the penicillin-binding proteins (PBP) located at the outer surface of the cytoplasmic membrane, resulting in the inhibition of cell wall synthesis and ultimately in cell lysis.^[44] We hypothesize that, as cells in buffer are not as actively dividing as in growth media, exposure to ampicillin might not have caused significant lysis and thus, uptake of PI by cells. In contrast, the clsf permeabilization seemed to be independent of cell division, as PI uptake was immediate. Differences between the number of cells with a permeable membrane and the number of non-viable cells have been reported.^[45] On the one hand, non-viable cells may still have a PI impermeable membrane^[46], as is suspected for the ampicillin-treated cells in our study. On the other hand, in some cases viable cells were able to repair their membrane after uptake of PI.^[47,48]

Overall, the immediate cytoplasmic membrane permeabilization observed with prenylated compounds suggests that the site of action of prenylated phenolic compounds is the cytoplasmic membrane of bacteria rather than a cytosolic target, as some studies have suggested.^[49,50] Further studies are needed to elucidate the exact mode of action of prenylated phenolic compounds.

Prenylated phenolic compounds are effective antibacterials against Gram negative *E. coli* in the presence of an efflux pump inhibitor

Prenylated phenolic compounds have shown very good antibacterial activity against Gram positive pathogens, but not against Gram negative.^[51] Given the contribution of efflux mechanisms to antibiotic resistance, inhibitors of efflux pump systems are currently being researched as adjuvants to potentiate the activities of conventional antibiotics.^[39] In the present study we used a wild-type *E. coli* and a low PA β N concentration (25 μ g/mL).^[52] We found that *E. coli* became equally susceptible to the prenylated phenolic compounds as the Gram positive *L. monocytogenes*. In the presence of the efflux pump inhibitor, the MIC and MBC of the clsf pool against *E. coli* were reduced from > 40 μ g/mL to 10 μ g/mL, which is in the same order of magnitude as some clinically-relevant antibacterials (e.g. 5-12.5 μ g/mL for ampicillin, chloramphenicol and rifampicin against *E. coli*).^[36] These results demonstrated that prenylated phenolic compounds can enter the outer membrane of *E. coli*. Hence, the intrinsic resistance of *E. coli* towards the

compounds used in this study was mainly because of the active efflux rather than the limited influx. Entrance to the periplasmic space might occur via diffusion through porins or through the outer lipid bilayer membrane.^[53] After crossing the OM, compounds can be taken out from the periplasmic space by the efflux pump system^[13], before effectively reaching the inner membrane.

Susceptibility of *E. coli* in the presence of PA β N towards the clsf and cPta pools increased with increasing concentration of prenylated compounds until a certain point. After that susceptibility decreased again, approximately above 20-30 $\mu\text{g/mL}$ of prenylated compounds (**Figures 3.3B** and **3.5**). This might be explained by the fact that PA β N inhibits the efflux pumps in a competitive manner, by displacing other pump substrates^[54], such as the prenylated phenolic compounds. Therefore, we hypothesize that prenylated compounds around the aforementioned concentrations outcompete PA β N in binding to the efflux pump, thereby cancelling the inhibition of the efflux system. As a consequence, at high concentrations the antibacterial action of the prenylated compounds against *E. coli* is lost.

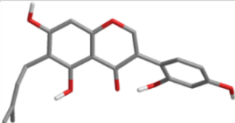
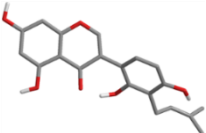
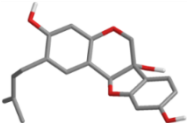
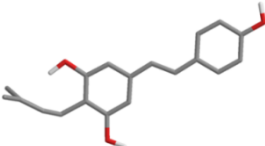
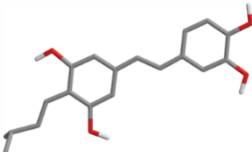
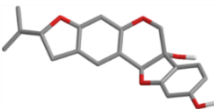
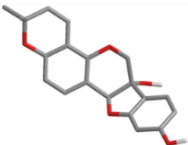
Intermediate skeletal flexibility and chain prenylation as good structural features for antibacterial activity

The pool rich in chain prenylated isoflavones was the most active antibacterial pool towards both bacteria, followed by the chain prenylated 6 α -OH-pterocarpan and chain prenylated stilbenoids. The pool rich in ring-closed prenylated 6 α -OH-pterocarpan was the least active of all.

In **Table 3.2** molecular properties of the most abundant prenylated compounds (representing more than 60% (w/w) of the total prenylated phenolic content) in the different pools are shown. Hydrophobicity has been proposed to be the main molecular contributor to the antibacterial activity of prenylated phenolic compounds.^[55] The chain prenylated stilbenoids are the most hydrophobic compounds ($\log D$ 4.9-5.1, **Table 3.2**), followed by the chain prenylated isoflavones. In contrast, the ring-closed prenylated 6 α -OH-pterocarpan were the least hydrophobic. As observed in **Table 3.2**, the trend in hydrophobicity does not follow the trend observed in antibacterial activity. Therefore, other molecular properties such as conformation and flexibility are thought to contribute to the antibacterial properties of these compounds.

Regarding the configuration of the energy minimized structures, the isoflavone and pterocarpan skeletons are naturally bent (i.e. dihedral angle between two main planes $< 180^\circ$), whereas the stilbenoid skeleton can have both rings aligned in a single plane. Regarding flexibility, the chain prenylated stilbenoids have the highest number of rotatable bonds, whereas the ring-closed prenylated 6 α -OH-pterocarpan have the least. Hence, chain prenylated stilbenoids are the most flexible compounds of this set.

Table 3.2. Molecular properties of the most abundant prenylated compounds present in the legume seedling pools.

Pool (Rel. activity)	Most abundant prenylated compound (% w/w) ^a	Molecular structure ^b	logD ^c	Dihedral angle ^d	Rotatable single bonds	Lead-likeness ^e
clsf (+++)	Luteone (33%)		3.65	135°	3	Yes
	Licoisoflavone A (28%)		3.79	137°	3	Yes
cPta (++)	Glyceollidin II (82%)		3.43	138°	2	Yes
cSti (+)	<i>trans</i> -Arachidin-2 (35%)		5.12	180°	4	No
	<i>trans</i> -Arachidin-1 (26%)		4.94	180°	4	No
rPta (-)	Glyceollin III (34%)		2.93	137°	1	No
	Glyceollin I (32%)		2.91	138	0	No

^a Weight percentage from the total prenylated phenolic content of the legume seedling Flash pool. ^b After MM2 energy minimization (0.01 RMS gradient, Chem3D). ^c Calculated at pH 7.2 (Marvin 6.0.5, ChemAxon). ^d Angle between the A-C ring plane and the B-ring plane, calculated with Chem3D. ^e Criteria for lead-likeness: molecular mass \leq 450 Da; logD (at pH 7.2) between -4.0 and 4.0; ring count \leq 4; rotatable bond count \leq 10; hydrogen bond donor count \leq 5; and hydrogen bond acceptor count \leq 8.^[20]

The lowest antibacterial activity of the ring-closed prenylated compounds might be explained by both their low flexibility and low hydrophobicity. First, these molecules will partition less to hydrophobic regions than any of the other prenylated compounds in **Table 3.2**, as they have the lowest *logD* values. Second, their low flexibility (0-1 rotatable bonds) might limit their effective partitioning and interaction with the cytoplasmic membrane. Flexibility has been shown to be an important structural determinant for antimicrobial peptides, as it improves their insertion and binding to membranes.^[21,56]

Comparing only the chain prenylated compounds, chain prenylated stilbenoids had the lowest antibacterial activity. This might be explained by their combined high flexibility and planar molecular configuration. Chain prenylated stilbenoids may insert fast into membranes, as their hydrophobicity and flexibility are high. However, this high flexibility may also contribute to the ease with which chain prenylated stilbenoids adopt a planar configuration (dihedral angle of 180 °). It is speculated that a planar molecular conformation is less effective at disrupting the membrane integrity than a bent conformation. In contrast, the limited flexibility and bent conformation of the chain prenylated isoflavones and 6a-OH-pterocarpan might make them better skeletons than the stilbenoid to disrupt the bacterial cell membrane integrity and exert antibacterial activity. It has been proposed that prenylated compounds that could adopt a planar or rod shape would diffuse easier and deeper into model phospholipid bilayers, in comparison with compounds with an “elbow” shape, which would interact more at the polar-apolar region of the phospholipids.^[57] This might explain the lack of membrane permeabilization by the stilbenoid pool. Additionally, another study correlated low molecular flexibility to the good activity of 4-aminodiphenyl sulfone antibacterials, i.e. as intramolecular conformational entropy increased (as in the more flexible molecules), the inhibitory potency decreased.^[58] This was explained by the weak binding to the bacterial target due to the conformational fluctuations of the flexible molecules.

The concept of lead-likeness^[38] refers to a set of guidelines that defines whether a compound is suitable as a lead molecule in drug development. A lead molecule is one that has possibilities enough within its molecular properties to improve its binding affinity, solubility and pharmacokinetic profile by modulating properties like hydrophobicity and molecular weight. Usually a lead structure will go through cycles of “lead optimization” until an antimicrobial candidate is obtained.^[38] In **Table 3.2**, the lead-likeness of the main prenylated compounds in each pool are shown. Interestingly, the compounds in the most active pools, i.e. luteone, licoisoflavone A and glyceollidin II, complied with the lead-likeness concept. The other prenylated compounds had higher hydrophobicity (i.e. stilbenoids) or higher number of rings than desired (i.e. pyran-prenylated 6a-OH-pterocarpan).

In conclusion, this is the first report relating the antibacterial properties of prenylated phenolic compounds from legume seedlings to the structure of the phenolic skeleton and to the configuration of prenylation. Bent conformation, intermediate skeleton flexibility, and chain prenylation were identified as potential molecular features defining the activity of prenylated phenolic compounds, besides hydrophobicity.

Experiments with purified prenylated compounds from different phenolic subclasses are necessary to confirm these structural effects on the antibacterial activity. Chain prenylated isoflavones were the most efficient permeabilizers and antibacterials. Such compounds might serve as lead structures for the design and development of novel antibacterial compounds.

ACKNOWLEDGMENTS

The authors would like to thank prof. Dr Tjakko Abee of the Laboratory of Food Microbiology, Wageningen University for his valuable feedback during discussions, as well as the students Tom Somers and Pieter-Paul Thijssen for their contribution to part of the experiments.

REFERENCES

- [1] WHO. Antimicrobial resistance: global report on surveillance 2014. 2014. World Health Organization: Geneva, Switzerland. p. 257.
- [2] Harvey, A.L.; Edrada-Ebel, R.; Quinn, R.J. The re-emergence of natural products for drug discovery in the genomics era. *Nature Reviews: Drug Discovery*, 2015, **14**, 111-129.
- [3] Harvey, A.L. Natural products in drug discovery. *Drug Discovery Today*, 2008, **13**, 894-901.
- [4] Newman, D.J.; Cragg, G.M. Natural products as sources of new drugs over the 30 years from 1981 to 2010. *Journal of Natural Products*, 2012, **75**, 311-335.
- [5] Negi, P.S. Plant extracts for the control of bacterial growth: efficacy, stability and safety issues for food application. *International Journal of Food Microbiology*, 2012, **156**, 7-17.
- [6] Muzquiz, M.; Varela, A.; Burbano, C.; Cuadrado, C.; Guillamón, E.; Pedrosa, M. Bioactive compounds in legumes: pronutritive and antinutritive actions. Implications for nutrition and health. *Phytochemistry Reviews*, 2012, **11**, 227-244.
- [7] Veitch, N.C. Isoflavonoids of the Leguminosae. *Natural Product Reports*, 2007, **24**, 417-464.
- [8] Tanaka, H.; Atsumi, I.; Shirota, O.; Sekita, S.; Sakai, E.; Sato, M.; Murata, J.; Murata, H.; Darnaedi, D.; Chen, I.S. Three new constituents from the roots of *Erythrina variegata* and their antibacterial activity against methicillin-resistant *Staphylococcus aureus*. *Chemistry & Biodiversity*, 2011, **8**, 476-482.
- [9] Eerdunbayaer; Mohamed A. A. Orabi; Hiroe Aoyama; Kuroda, T.; Hatano, T. Structures of new phenolics isolated from licorice, and the effectiveness of licorice phenolics on vancomycin-resistant *Enterococci*. *Molecules*, 2014, **19**, 13027-13041.
- [10] Upadhyay, A.; Upadhyaya, I.; Kollanoor-Johny, A.; Venkitanarayanan, K. Combating pathogenic microorganisms using plant-derived antimicrobials: A minireview of the mechanistic basis. *BioMed Research International*, 2014, **2014**, 1-18.
- [11] Kumar, A.; Schweizer, H.P. Bacterial resistance to antibiotics: Active efflux and reduced uptake. *Advanced Drug Delivery Reviews*, 2005, **57**, 1486-1513.
- [12] Fernández, L.; Hancock, R.E.W. Adaptive and mutational resistance: role of porins and efflux pumps in drug resistance. *Clinical Microbiology Reviews*, 2012, **25**, 661-681.
- [13] Blair, J.M.A.; Webber, M.A.; Baylay, A.J.; Ogbolu, D.O.; Piddock, L.J.V. Molecular mechanisms of antibiotic resistance. *Nature Reviews: Microbiology*, 2015, **13**, 42-51.
- [14] Hendrich, A.B.; Malon, R.; Pola, A.; Shirataki, Y.; Motohashi, N.; Michalak, K. Differential interaction of *Sophora* isoflavonoids with lipid bilayers. *European Journal of Pharmaceutical Sciences*, 2002, **16**, 201-208.
- [15] Terao, J.; Mukai, R. Prenylation modulates the bioavailability and bioaccumulation of dietary flavonoids. *Archives of Biochemistry and Biophysics*, 2014, **559**, 12-16.
- [16] Yazaki, K.; Sasaki, K.; Tsurumaru, Y. Prenylation of aromatic compounds, a key diversification of plant secondary metabolites. *Phytochemistry*, 2009, **70**, 1739-1745.
- [17] Aptula, A.O.; Kühne, R.; Ebert, R.-U.; Cronin, M.T.D.; Netzeva, T.I.; Schüürmann, G. Modeling discrimination between antibacterial and non-antibacterial activity based on 3D molecular descriptors. *QSAR & Combinatorial Science*, 2003, **22**, 113-128.

- [18] Araya-Cloutier, C.; den Besten, H.M.W.; Aisyah, S.; Gruppen, H.; Vincken, J.-P., The position of prenylation of isoflavonoids and stilbenoids from legumes modulates the antimicrobial activity against Gram positive pathogens. (This thesis, Chapter 2).
- [19] Gulyaeva, N.; Zaslavsky, A.; Lechner, P.; Chlenov, M.; McConnell, O.; Chait, A.; Kipnis, V.; Zaslavsky, B. Relative hydrophobicity and lipophilicity of drugs measured by aqueous two-phase partitioning, octanol-buffer partitioning and HPLC. A simple model for predicting blood-brain distribution. *European Journal of Medicinal Chemistry*, 2003, **38**, 391-396.
- [20] ChemAxon. *Chemicalize properties viewer* 2016 [cited 2016; Properties viewer]. Available from: (www.chemicalize.org).
- [21] Liu, L.; Fang, Y.; Wu, J. Flexibility is a mechanical determinant of antimicrobial activity for amphipathic cationic α -helical antimicrobial peptides. *Biochimica et Biophysica Acta (BBA) - Biomembranes*, 2013, **1828**, 2479-2486.
- [22] Aisyah, S.; Gruppen, H.; Andini, S.; Bettonvil, M.; Severing, E.; Vincken, J.-P. Variation in accumulation of isoflavonoids in *Phaseoleae* seedlings elicited by *Rhizopus*. *Food Chemistry*, 2016, **196**, 694-701.
- [23] Simons, R.; Vincken, J.-P.; Roidos, N.; Bovee, T.F.H.; van Iersel, M.; Verbruggen, M.A.; Gruppen, H. Increasing soy isoflavonoid content and diversity by simultaneous malting and challenging by a fungus to modulate estrogenicity. *Journal of Agricultural and Food Chemistry*, 2011, **59**, 6748-6758.
- [24] Aisyah, S.; Vincken, J.-P.; Andini, S.; Mardiah, Z.; Gruppen, H. Compositional changes in (iso)flavonoids and estrogenic activity of three edible *Lupinus* species by germination and *Rhizopus*-elicitation. *Phytochemistry*, 2016, **122**, 65-75.
- [25] Aisyah, S.; Gruppen, H.; Slager, M.; Helmink, B.; Vincken, J.-P. Modification of prenylated stilbenoids in peanut (*Arachis hypogaea*) seedlings by the same fungi that elicited them: The fungus strikes back. *Journal of Agricultural and Food Chemistry*, 2015, **63**, 9260-9268.
- [26] Aisyah, S.; Gruppen, H.; Madzora, B.; Vincken, J.-P. Modulation of isoflavonoid composition of *Rhizopus oryzae* elicited soybean (*Glycine max*) seedlings by light and wounding. *Journal of Agricultural and Food Chemistry*, 2013, **61**, 8657-8667.
- [27] Sobolev, V.S.; Neff, S.A.; Gloer, J.B. New dimeric stilbenoids from fungal-challenged peanut (*Arachis hypogaea*) seeds. *Journal of Agricultural and Food Chemistry*, 2010, **58**, 875-881.
- [28] Sobolev, V.S.; Deyrup, S.T.; Gloer, J.B. New peanut (*Arachis hypogaea*) phytoalexin with prenylated benzenoid and but-2-enolide moieties. *Journal of Agricultural and Food Chemistry*, 2006, **54**, 2111-2115.
- [29] Simons, R.; Vincken, J.-P.; Bakx, E.J.; Verbruggen, M.A.; Gruppen, H. A rapid screening method for prenylated flavonoids with ultra-high-performance liquid chromatography/electrospray ionisation mass spectrometry in licorice root extracts. *Rapid Communications in Mass Spectrometry*, 2009, **23**, 3083-3093.
- [30] Xu, M.-J.; Wu, B.; Ding, T.; Chu, J.-H.; Li, C.-Y.; Zhang, J.; Wu, J.; Liu, S.-J.; Liu, S.-L.; Ju, W.-Z.; Li, P. Simultaneous characterization of prenylated flavonoids and isoflavonoids in *Psoralea corylifolia* L. by liquid chromatography with diode-array detection and quadrupole time-of-flight mass spectrometry. *Rapid Communications in Mass Spectrometry*, 2012, **26**, 2343-2358.
- [31] van de Schans, M.G.M.; Vincken, J.-P.; Bovee, T.F.H.; David Cervantes, A.; Logtenberg, M.J.; Gruppen, H. Structural changes of 6a-hydroxy-pterocarpanes upon heating modulate their estrogenicity. *Journal of Agricultural and Food Chemistry*, 2014, **62**, 10475-10484.
- [32] van de Schans, M.G.M.; Vincken, J.-P.; de Waard, P.; Hamers, A.R.M.; Bovee, T.F.H.; Gruppen, H. Glyceollins and dehydroglyceollins isolated from soybean act as SERMs and ER subtype-selective phytoestrogens. *The Journal of Steroid Biochemistry and Molecular Biology*, 2016, **156**, 53-63.
- [33] Kusters, H.A.; Wierenga, P.A.; de Vries, R.; Gruppen, H. Characteristics and effects of specific peptides on heat-induced aggregation of β -lactoglobulin. *Biomacromolecules*, 2011, **12**, 2159-2170.
- [34] Aryani, D.C.; den Besten, H.M.W.; Hazeleger, W.C.; Zwietering, M.H. Quantifying strain variability in modeling growth of *Listeria monocytogenes*. *International Journal of Food Microbiology*, 2015, **208**, 19-29.
- [35] Hayrapetyan, H.; Hazeleger, W.C.; Beumer, R.R. Inhibition of *Listeria monocytogenes* by pomegranate (*Punica granatum*) peel extract in meat paté at different temperatures. *Food Control*, 2012, **23**, 66-72.
- [36] Sulavik, M.C.; Houseweart, C.; Cramer, C.; Jiwani, N.; Murgolo, N.; Greene, J.; DiDomenico, B.; Shaw, K.J.; Miller, G.H.; Hare, R.; Shimer, G. Antibiotic susceptibility profiles of *Escherichia coli* strains lacking multidrug efflux pump genes. *Antimicrobial Agents and Chemotherapy*, 2001, **45**, 1126-1136.

- [37] Bohnert, J.A.; Kern, W.V. Selected arylpiperazines are capable of reversing multidrug resistance in *Escherichia coli* overexpressing RND efflux pumps. *Antimicrobial Agents and Chemotherapy*, 2005, **49**, 849-852.
- [38] Teague, S.J.; Davis, A.M.; Leeson, P.D.; Oprea, T. The design of leadlike combinatorial libraries. *Angewandte Chemie, Int. Ed.*, 1999, **38**, 3743-3748.
- [39] Lamers, R.P.; Cavallari, J.F.; Burrows, L.L. The efflux inhibitor phenylalanine-arginine beta-naphthylamide (PAβN) permeabilizes the outer membrane of Gram-negative bacteria. *Plos One*, 2013, **8**, 1-7.
- [40] Stiefel, P.; Schmidt-Emrich, S.; Maniura-Weber, K.; Ren, Q. Critical aspects of using bacterial cell viability assays with the fluorophores SYTO9 and propidium iodide. *BMC Microbiology*, 2015, **15**, 36.
- [41] Sträuber, H.; Müller, S. Viability states of bacteria—Specific mechanisms of selected probes. *Cytometry Part A*, 2010, **77A**, 623-634.
- [42] Tsuchiya, H.; Iinuma, M. Reduction of membrane fluidity by antibacterial sophoraflavanone G isolated from *Sophora exigua*. *Phytomedicine*, 2000, **7**, 161-165.
- [43] Ferreira, J.V.N.; Grecco, S.d.S.; Lago, J.H.G.; Caseli, L. Ultrathin films of lipids to investigate the action of a flavonoid with cell membrane models. *Materials Science and Engineering: C*, 2015, **48**, 112-117.
- [44] Fernandes, R.; Amador, P.; Prudêncio, C. β -Lactams: chemical structure, mode of action and mechanisms of resistance. *Reviews in Medical Microbiology*, 2013, **24**, 7-17.
- [45] Breeuwer, P.; Abee, T. Assessment of viability of microorganisms employing fluorescence techniques. *International Journal of Food Microbiology*, 2000, **55**, 193-200.
- [46] Mortimer, F.C.; Mason, D.J.; Gant, V.A. Flow cytometric monitoring of antibiotic-induced injury in *Escherichia coli* using cell-impermeant fluorescent probes. *Antimicrobial Agents and Chemotherapy*, 2000, **44**, 676-681.
- [47] Davey, H.M.; Hexley, P. Red but not dead? Membranes of stressed *Saccharomyces cerevisiae* are permeable to propidium iodide. *Environmental Microbiology*, 2011, **13**, 163-171.
- [48] Park, I.-K.; Kang, D.-H. Effect of electropermeabilization by ohmic heating for inactivation of *Escherichia coli* O157:H7, *Salmonella enterica* serovar Typhimurium, and *Listeria monocytogenes* in buffered peptone water and apple juice. *Applied and Environmental Microbiology*, 2013, **79**, 7122-7129.
- [49] Shiu, W.K.P.; Malkinson, J.P.; Rahman, M.M.; Curry, J.; Stapleton, P.; Gunaratnam, M.; Neidle, S.; Mushtaq, S.; Warner, M.; Livermore, D.M.; Evangelopoulos, D.; Basavannacharya, C.; Bhakta, S.; Schindler, B.D.; Seo, S.M.; Coleman, D.; Kaatz, G.W.; Gibbons, S. A new plant-derived antibacterial is an inhibitor of efflux pumps in *Staphylococcus aureus*. *International Journal of Antimicrobial Agents*, 2013, **42**, 513-518.
- [50] Cushnie, T.P.T.; Lamb, A.J. Recent advances in understanding the antibacterial properties of flavonoids. *International Journal of Antimicrobial Agents*, 2011, **38**, 99-107.
- [51] Hatano, T.; Shintani, Y.; Aga, Y.; Shiota, S.; Tsuchiya, T.; Yoshida, T. Phenolic constituents of licorice. VIII. Structures of glycofenone and glicoisoflavanone, and effects of licorice phenolics on methicillin-resistant *Staphylococcus aureus*. *Chemical & Pharmaceutical Bulletin*, 2000, **48**, 1286-1292.
- [52] Misra, R.; Morrison, K.D.; Cho, H.J.; Khuu, T. Importance of real-time assays to distinguish multidrug efflux pump-inhibiting and outer membrane-destabilizing activities in *Escherichia coli*. *Journal of Bacteriology*, 2015, **197**, 2479-2488.
- [53] Li, X.-Z.; Plésiat, P.; Nikaïdo, H. The challenge of efflux-mediated antibiotic resistance in Gram-negative bacteria. *Clinical Microbiology Reviews*, 2015, **28**, 337-418.
- [54] Kinana, A.D.; Vargiu, A.V.; May, T.; Nikaïdo, H. Aminoacyl β -naphthylamides as substrates and modulators of AcrB multidrug efflux pump. *Proceedings of the National Academy of Sciences*, 2016, **113**, 1405-1410.
- [55] Botta, B.; Menendez, P.; Zappia, G.; de Lima, R.A.; Torge, R.; Delle Monache, G. Prenylated isoflavonoids: Botanical distribution, structural, biological activities and biotechnological studies. An update (1995-2006). *Current Medicinal Chemistry*, 2009, **16**, 3414-3468.
- [56] Oddo, A.; Thomsen, T.T.; Britt, H.M.; Løbner-Olesen, A.; Thulstrup, P.W.; Sanderson, J.M.; Hansen, P.R. Modulation of backbone flexibility for effective dissociation of antibacterial and hemolytic activity in cyclic peptides. *ACS Medicinal Chemistry Letters*, 2016, **7**, 741-745.
- [57] Wesołowska, O.; Gašiorowska, J.; Petrus, J.; Czarnik-Matusiewicz, B.; Michalak, K. Interaction of prenylated chalcones and flavanones from common hop with phosphatidylcholine model membranes. *Biochimica et Biophysica Acta (BBA) - Biomembranes*, 2014, **1838**, 173-184.
- [58] Decompadre, R.L.L.; Pearlstein, R.A.; Hopfinger, A.J.; Seydel, J.K. A quantitative structure activity relationship analysis of some 4-aminodiphenyl sulfone antibacterial agents using linear free-energy and molecular modelling methods. *Journal of Medicinal Chemistry*, 1987, **30**, 900-906.

- [59] Simons, R. Prenylated isoflavonoids from soya and licorice. Analysis, induction and *in vitro* estrogenicity. 2011. Wageningen University: Wageningen, The Netherlands.
- [60] Weast, R.C., CRC Handbook of Chemistry and Physics. 58th ed. 1977, Boca Raton, FL, USA: CRC Press.
- [61] Tahara, S.; Ingham, J.L.; Mizutani, J. New coumaronochromones from white lupine, *Lupinus albus* L. (Leguminosae). *Agricultural and Biological Chemistry*, 1985, **49**, 1775-1783.
- [62] Hatano, T.; Aga, Y.; Shintani, Y.; Ito, H.; Okuda, T.; Yoshida, T. Minor flavonoids from licorice. *Phytochemistry*, 2000, **55**, 959-963.
- [63] Lee, Y.J.; Notides, A.C.; Tsay, Y.G.; Kende, A.S. Coumestrol, NBD-norhexestrol, and dansyl-norhexestrol, fluorescent probes of estrogen-binding proteins. *Biochemistry*, 1977, **16**, 2896-2901.
- [64] Latunde-Dada, A.O.; Cabello-Hurtado, F.; Czittrich, N.; Didierjean, L.; Schopfer, C.; Hertkorn, N.; Werck-Reichhart, D.; Ebel, J. Flavonoid 6-hydroxylase from soybean (*Glycine max* L.), a novel plant P-450 monooxygenase. *Journal of Biological Chemistry*, 2001, **276**, 1688-1695.
- [65] Buckingham, J.; Munasinghe, V.R.N., Dictionary of Flavonoids. 2015, Boca Raton, FL, USA: CRC Press. 843.
- [66] Kinoshita, T.; Saitoh, T.; Shibata, S. A new isoflavone from licorice root. *Chemical & Pharmaceutical Bulletin*, 1978, **26**, 141-143.
- [67] Cheynier, V.F.; Trousdale, E.K.; Singleton, V.L.; Salgues, M.J.; Wylde, R. Characterization of 2-S-glutathionylcaftaric acid and its hydrolysis in relation to grape wines. *Journal of Agricultural and Food Chemistry*, 1986, **34**, 217-221.
- [68] Moesta, P.; M.G., H.; Grisebach, H. Development of a radioimmunoassay for the soybean phytoalexin glyceollin I. *Plant Physiology*, 1983, **73**, 233-237.
- [69] Ayers, A.R.; Ebel, J.; Valent, B.; Albersheim, P. Host-pathogen interactions: X. Fractionation and biological activity of an elicitor isolated from the mycelial walls of *Phytophthora megasperma* var. *sojae*. *Plant Physiology*, 1976, **57**, 760-765.
- [70] Lyne, R.L.; Mulheirn, L.J.; Leworthy, D.P. New pterocarpinoid phytoalexins of soybean. *Journal of the Chemical Society, Chemical Communications*, 1976, 497-498.
- [71] Trela, B.C.; Waterhouse, A.L. Resveratrol: isomeric molar absorptivities and stability. *Journal of Agricultural and Food Chemistry*, 1996, **44**, 1253-1257.
- [72] Cooksey, C.J.; Garratt, P.J.; Richards, S.E.; Strange, R.N. A dienylyl stilbene phytoalexin from *Arachis hypogaea*. *Phytochemistry*, 1988, **27**, 1015-1016.

SUPPLEMENTARY INFORMATION

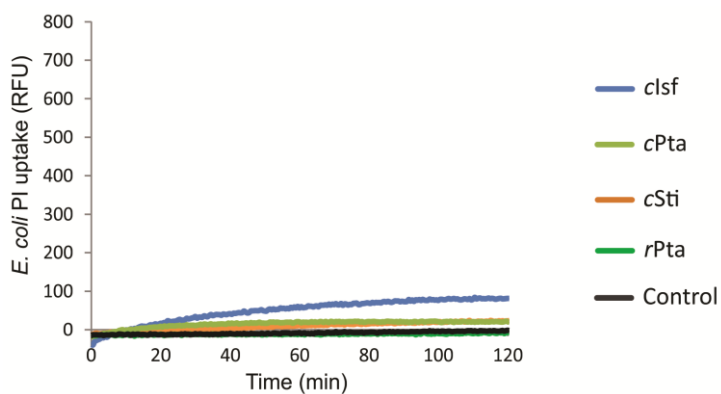


Figure S3.1. PI uptake by *E. coli* when exposed to the pools enriched in prenylated phenolics (15 $\mu\text{g}/\text{mL}$ of prenylated compounds). Intrinsic fluorescence of the probe PI and of the samples have been subtracted. Control refers to untreated *E. coli* cells.

Table S3.1. Summary of diagnostic UV_{max} (nm) and MS neutral losses for different phytochemical skeletons and substitutions.

Structure annotation of phenolic compounds	UV _{max} (±5 nm)	Diagnostic fragmentation ^a	
		NI	PI
SKELETON			
Flavonoids			
Flavone	270, 325-340		^{1,3} A/B, ^{0,2} B, ^{0,4} B
Flavanone	280-290		^{1,3} A, ^{1,3} [B-2H], ^{0,4} [B-H ₂ O]
Isoflavonoids			
Isoflavones	250-260		^{1,3} A/B, ^{1,4} A/B
Pterocarpan	280-310		^{2,4} A/B, -H ₂ O ^{1,4} A/B, ^{5,6} A/B, -H ₂ O ^{6,7} A
Pterocarpene	280-310, 330-365		-
Coumestans	340-350		-
Coumaronochromone	260, 280, 330-350		-
Phenolic acids			
Coutaric acid derivatives	313		
Coumaroyl/caffeoyl/sinapoyl/feruloyl/ nicotinoyl conjugates		146/162/206/179/105	
Stilbenoids			
Resveratrol/piceatannol derivatives	280-340		
SUBSTITUTION			
O-glucoside/rhamnoside/xyloside		162/146/132	
Tartaric acid		132	
Methyl		16	
Methoxyl		32	
Carboxyl		44	46
Prenyl chain (3,3-dimethylallyl)			56 (MS ²)
C6-prenyl chain			28, 56 (MS ³)
C8-prenyl chain			42 (MS ³)
Prenyl ring (2,2-dimethylpyran or 2-isopropenyl dihydrofuran)			42, 70, 54, 15 (MS ²)
Hydroxylated prenyl ring (e.g. 2,2-dimethyl-3-hydroxy dihydropyran)			18, 60, 72 (MS ²)

^a ^{x,y}A/B refers to retro-Diels-Alder fragments (RDA) resulting from the cleavage of the C or D-ring of (iso)flavonoids. A-ring and B-ring fragments are indicated by either ^{x,y}A and ^{x,y}B. The superscripts x,y represent the bonds that are cleaved in the C- or D-ring. Pterocarpenes, coumestans, and coumaronochromones do not show typical RDA fragmentation due to their relatively larger conjugated system and, therefore, low C/D-ring cleavage.^[31,59]

Table S3.2. Molar extinction coefficient of representative phenolics used for the quantification of compounds in the pools enriched in prenylated phenolics.

Subclass	Compound	Molar extinction coefficient					
		Reported		Estimated ^{a,b}			
		ϵ (AU/M·cm)	λ (nm)	Ref.	260 nm	280 nm	315 nm
Chromone	Chromone	15849	275	[60]	31236	17474	-
Coumaronochromone	Lupinalbin	36600	257	[61]	29891	-	-
Coumestan	Isotrifoliol	15135	249	[62]	6894	6043	-
	Coumestrol	24800	345	[63]	15345	5412	-
Flavanone	Liquiritigenin	6500	290	[64]	-	6500	-
Flavone	Apigenin	19953	269	[61]	19391	14253	-
Isoflavone (2 hydroxyl groups)	Daidzein	26915	250	[61]	24222	13782	-
Isoflavone (3 hydroxyl groups)	Genistein	31623	263	[61]	33231	11961	-
Isoflavone (≥ 4 hydroxyl groups)	3'-OH-genistein	27500	263	[65]	30843	12938	-
Isoflavone (prenylated)	Licoisoflavone A	29512	266	[66]	30526	15916	-
Phenolic acid	<i>trans</i> -Cafataric acid	20600	320	[67]	-	-	20614
Pterocarpan	Glycinol	5870	287	[68]	-	6532	-
Pterocarpan (prenylated)	Glyceollin I	10300	285	[69]	-	10300	-
	Glyceollin II	8700	286	[70]	-	8700	-
	Glyceollin III	9600	292	[70]	-	9600	-
	Gyceollidin II	10000	284	[68]	-	10000	-
Pterocarpene (prenylated)	Dehydroglyceollin I	8345	280	[32]	-	8345	-
	Dehydroglyceollin II	8345	280	[32]	-	8345	-
	Dehydroglyceollin III	3103	280	[32]	-	3103	-
Stilbenoid	<i>trans</i> -Resveratrol	28972	320	[71]	-	-	29404
Stilbene (prenylated)	3-Isopentadienyl-4,3',5'-trihydroxystilbene (IPD)	22004	298	[72]	-	-	18535
Stilbene (dimer)	Arahy-pin-7	14791	310	[27]	-	-	16480

^a Estimation of the molar extinction coefficient was based on the UV spectrum of the compound reported in literature or found in the Flash fractions, considering that no co-elution of other UV absorbing compounds occurred. ^b Dash (-) means not relevant.

Table S3.3. Compounds tentatively annotated by RP-UHPLC-UV-MS present in the enriched pools from legume seedlings.

No	Annotated compound	Prenyl type	Prenyl position	RT (min)	UV _{max} (nm)	[M-H] ⁻	MS ² NI mode ^a	[M+H] ⁺	MS ² PI mode	MS ³ PI mode	
Chromone											
1	Lupichromone	chain	C6, C8	13.2	256	313	298	242, 270, 281	315	283, 287	255
2	Lupinalbin A	-	-	13.3	256, 334	283	255, 239, 265	227, 211	285	257, 213	229
Coumaronochromone											
3	Lupinalbin B/D	chain	C6/C3'	19.6	257, 339	351	323, 295, 307	295	353	297, 285, 298	269, 241, 270
4	Lupinalbin B/D	chain	C6/C3'	19.7	257, 339	351	323, 296, 307	279, 295, 268	353	297	269, 241, 213
Coumestan											
5	Isotrifolol isomer	-	-	9.2	308, 351	297	282	254, 226	299	271, 267	243
6	Coumestrol	-	-	9.30	304, 343	267	239, 211	211, 212	269	241, 225, 197	213, 214
7	Isotrifolol	-	-	9.8	348	297	282	254, 253	299	267	239
Flavanone											
8	Liquiritigenin	-	-	10.3	n.d.	255	135, 119	91	257	147, 137, 239	119
Flavone											
9	Chrysoeriol	-	-	11.5	284, 354	299	284	256, 255, 212	301	286, 287	258, 259, 240
Isoflavone											
10	2'-Hydroxygenistein-O-glucoside	-	-	6.2	259	447	285, 327, 309	217, 241, 199	449	287	217, 259, 245
11	Genistein 7-O-glucoside	-	-	7.0	260	269, 431 ^b	201, 225, 181	157, 173, 133	433	n.d.	n.d.
12	Daidzein	-	-	7.7	248	253	225, 209, 253	197, 148, 195	255	199, 227, 137	181, 171, 153
13	Luteone 7-O-glucoside	chain	C6	8.3	n.d	515	353, 395, 377	309, 219, 285	517	n.d.	n.d.
14	2'-Hydroxygenistein	-	-	8.7	258	285	217, 199	173, 175, 189	287	217, 153, 259	189, 190
15	Lupinisoiflavone B	chain	C6	9.7	263	369	299, 301, 351	255, 231, 199	353, 371	219, 335, 299	191, 177, 201
16	Prunetin	-	-	10.2	257	283	255, 239, 265	227, 211	285	257, 258, 213	229, 230
17	6-Prenyl-2'-hydroxydaidzein	chain	C6	10.4	n.d.	337	293, 281, 309	237, 238, 293	339	283, 271	255
18	Genistein	-	-	10.9	259	269	225, 181, 201	181, 197, 169	271	153, 243, 215	109, 111, 67
19	7-Methyluteone	chain	C6	11.6	270	369	351, 325	323, 217, 307	353, 371	297, 285, 231	269, 255, 227
20	2,3-Dihydroklevitone	chain	C8	14.8	263	353	285, 284, 267	267, 216, 230	355	299, 300	165, 281, 257
21	Lupinisoiflavone A	furan	C6	15.0	261	351	217, 307, 323	173, 147, 175	353	219, 335, 299	177, 191, 201
22	Luteone	chain	C6	15.5	264	353	309, 219, 201	265, 293, 267	355	299	165, 281
23	Licoisoflavone A	chain	C3'	16.7	262	353	285, 284, 267	216, 241, 256	355	299	271, 147, 243
24	Lupiwighteone	chain	C8	17.4	263	337	282, 283, 309	253, 254, 238	339	283, 284	241, 242, 213
25	Isowighteone	chain	C3'	17.6	260	337	281, 282, 294	267, 253, 209	339	283, 271	255, 153
26	Wighteone	chain	C6	17.8	265	337	282	254, 253, 238	339	283	255, 165, 121
27	5-Methylwighteone	chain	C6	19.5	256	351	323, 307, 296	279, 305, 149			

No	Annotated compound	Prenyl type	Prenyl position	RT (min)	UV _{max} (nm)	[M-H] ⁻	MS ² NI mode ^a	[M+H] ⁺	MS ² PI mode	MS ³ PI mode	
28	Hydroxycinnamic acid-alkaloid derivative	-	-	8.2	n.d.	680	536, 413, 557	413	682	544	526, 482, 400
29	di-p-Coumaroyltartaric acid	-	-	8.6	314	441	277, 295	203, 233, 259	n.d.		
30	p-Coumaroylsinapoyltartaric acid	-	-	9.1	317	501	337, 277	263, 319, 293	n.d.		
31	p-Coumaroylferuloyltartaric acid	-	-	9.2	318	471	307, 277, 383	233, 263, 289	n.d.		
32	di-p-Coumaroyltartaric acid isomer	-	-	9.4	313	441	277, 295	203, 233, 259	n.d.		
Pterocarpan											
33	Glycinol	-	-	6.3	266, 305	271	241, 243	197, 199, 213	255, 273, 227, 213, 199		199, 209, 157
34	Glycofuran	furan	C6	8.7	256, 291	353	335, 149, 325	317, 307, 277	337, 355, 309, 319, 188		263, 291, 281
35	Glycollidin II	chain	C6	11.4	285	339	161, 270, 324	133, 105	323, 341, 267, 268		239, 211, 225
36	Glycollidin III	furan	C6	11.8	281	337	293, 282, 319	238, 225, 181	321, 339, 306, 279, 251		289, 291, 277
37	Glycollidin II	pyran	C6	12.0	283, 306	337	319, 149, 293	277, 240, 275	321, 339, 279, 306, 251		251, 220
38	Glycollidin I	pyran	C8	12.2	280	337	149, 319, 293	105, 121	321, 339, 306, 303, 293		278, 291
Pterocarpene											
39	Dehydroglycollin III	furan	C6	18.8	343, 359	319	277, 275	n.d.	321	306, 293, 253	278, 291, 289
40	Dehydroglycollin II	pyran	C6	19.2	272, 348, 365	319	277, 291, 304	n.d.	321	293, 306, 279	265, 251, 238
41	Dehydroglycollin I	pyran	C8	19.4	287, 331	319	291, 304, 275	n.d.	321	293, 306, 173	265, 251, 275
Stilbenoid											
42	Hydroxy-IPD	chain	C3'	11.0	323	311	241, 293, 253	197, 157, 185	n.d.		
43	Hydroxy-IPD isomer	chain	C3'	11.7	323	311	253, 241	209, 185, 225	n.d.		
44	Arachidin-1 isomer	chain	C6	12.0	326	311	242, 241, 255	172, 213, 224	313	n.d.	
45	Arachidin-1 isomer	chain	C6	12.6	311	311	242, 241, 255	172, 213, 224	313	257, 295, 241	239, 211, 229
46	trans-Arachidin-1	chain	C6	12.9	339	311	242, 241, 255	172, 213, 224	313	257, 295	239, 211, 229
47	trans-Arachidin-2	chain	C6	13.3	308	295	239, 226, 240	195, 211, 180	297	241	195, 223, 199
48	Arachidin-2 isomer	chain	C6	13.9	301	295	239, 240, 226	195, 211, 145	297	241	223, 195, 213
49	Arachidin-3	chain	C6	14.1	335	295	239, 240, 226	195, 211, 180	297	241	223, 195, 213
50	trans-3'-Isopentadienyl-3,5,4'-trihydroxystilbene (IPD)	chain	C3'	14.4	302	293	249, 251, 209	194, 180, 234	295	277, 185, 253	262, 249, 259
51	4-Isopentadienyl-piceatannol (IPP)	chain	C6	14.7	343	309	265, 294, 291	159, 249, 250	311	201, 283, 135	173, 159, 183
52	IPP isomer	chain	C6	14.9	321	309	265, 294, 291	159, 249, 250	311	201, 283, 135	173, 159, 183
53	Arahypin-5 or 10	pyran	C6	16.2	315	293	236, 221, 278	192, 218	295	201, 267, 277	173, 159, 183
54	Arahypin-6 or 9	chain	C6, C6	16.9	329	605	511, 495, 587	493, 442, 401	607	501, 551, 589	445, 323, 391
55	Arahypin-7	chain	C6, C6	17.0	271, 343	621	511	442, 493, 401	623	513, 501, 391	457, 403, 335
56	IPP-IPD conjugate	chain	C6, C6	17.7	322	603	309, 363, 243	265, 291, 294	605	311, 445, 587	283, 201, 269
57	IPP dimer	chain	C6, C6	18.1	331	619	309, 509, 375	265, 291, 294	621	311, 511, 565	283, 201, 269

^a Product ions in MS² and MS³ are listed in order of intensity, first value is the base peak. ^b The parent ion showed in-source fragmentation and the intensity of the ion dominated the mass spectrum. The italic *m/z* is the [M-H]⁻ in NI mode or [M+H]⁺ in PI mode.

Table S3.4. Content (mg/g DW pool) of tentatively annotated compounds in the pools.

No. ^o	Pools enriched in prenylated phenolics				cPta Value	std.	rPta Value	std.
	clsf Value	std.	cSti Value	std.				
1	2.27	0.46					1.24	0.03
2	1.67	0.26						
3	0.54	0.16						
4	0.74	0.03						
5					5.23	0.48		
6					3.36	0.04		
7					41.78	0.32	1.12	0.16
8					6.68	0.02		
9	0.55	0.16						
10	0.38	0.08						
11	0.11	0.19						
12					0.23	0.00		
13	0.32	0.18						
14	4.62	1.43						
15	0.18	0.31						
16					9.05	0.13	0.57	0.03
17					13.22	0.07	0.57	0.03
18	3.76	0.24			0.89	0.01		
19					3.06	0.02	1.44	0.70
20	35.15	0.21						
21	4.92	0.29						
22	50.26	0.60						
23	42.11	1.89						
24	1.46	0.42						
25	2.06	0.79						
26	13.28	1.04						
27	0.54	0.04						
28			0.59	0.65				
29			4.36	1.86				
30			3.80	0.14				
31			2.85	0.60				
32			3.85	1.40				
33					17.76	0.09		
34					8.54	0.07		
35					102.22	0.34	14.11	2.04
36							119.36	7.66
37							92.82	5.10
38							112.85	4.49
39							2.14	0.56
40							2.59	0.19
41							3.18	0.19
42			2.13	0.76				
43			2.58	1.44				
44			1.33	0.94				
45			2.28	1.34				
46			94.15	30.64				
47			107.87	6.79				
48			23.67	6.38				
49			13.74	6.33				
50			19.84	1.25				
51			10.59	3.23				
52			3.66	2.02				

No. ^a	Pools enriched in prenylated phenolics							
	clsf		cSti		cPta		rPta	
	Value	std.	Value	std.	Value	std.	Value	std.
53			7.54	1.88				
54			6.54	2.05				
55			8.47	2.56				
56			1.34	1.90				
57			3.29	4.65				
Total	164.9	2.9	323.4	33.6	212.0	0.7	352.0	10.5

^a Number refers to compound list in **Table S3.3**.

Table S3.5. Time to detection of *E. coli* growth in the presence of Flash pools (40 µg/mL prenylated phenolic compounds), PAβN (25 µg/mL) or vancomycin (50 µg/mL).

Sample	TTD (h)	24 h count (log ₁₀ CFU/mL)
clsf	5.8 ± 0.08	n.d.
cSti	5.5 ± 0.16	n.d.
cPta	5.7 ± 0.14	n.d.
rPta	5.7 ± 0.11	n.d.
Control	5.8 ± 0.05	9.21 ± 0.16
Control + PAβN	6.9 ± 0.08	9.15 ± 0.12
Vancomycin	5.3 ± 0.60	n.d.
Vancomycin + PAβN	6.7 ± 0.25	n.d.
Control	5.6 ± 0.61	n.d.
Control + PAβN	6.8 ± 0.29	n.d.

n.d., not determined.

Table S3.6. Antibacterial properties of a reconstituted clsf pool.^a

Bacteria	Concentration prenylated aglycones (µg/mL)	
	Reconstituted clsf pool	
<i>L. monocytogenes</i>	TTD > 24 h	15
	MIC	20
	MBC	25
<i>E. coli</i> (+ PAβN)	TTD > 24 h	10
	MIC	10
	MBC	10

^a Data are from one biological reproduction performed in triplicate. Inoculum was $3.2 \pm 0.2 \log_{10}$ CFU/mL for *L. monocytogenes* and $3.9 \pm 0.2 \log_{10}$ CFU/mL for *E. coli*.

QSAR-based molecular signatures of prenylated (iso)flavonoids underlying antimicrobial potency against and membrane-disruption in Gram positive and Gram negative bacteria: *Listeria monocytogenes* and *Escherichia coli*

The antibacterial properties of 30 prenylated (iso)flavonoids, which differed in phenolic skeleton and substitution with hydroxyl and methoxyl groups, as well as configuration, number and position of prenyl substituents, were tested against *Listeria monocytogenes* and *Escherichia coli*. The latter was done in combination with an efflux pump inhibitor. Minimum inhibitory concentrations (MIC) of the most active prenylated compounds ranged between 6.3-12.5 $\mu\text{g}/\text{mL}$ for *L. monocytogenes* and between 10.0-15.0 $\mu\text{g}/\text{mL}$ for *E. coli*. Using quantitative structure-activity relationships, linear and binary classification models were obtained with low number of molecular descriptors. The linear models accounted for 64-82% of the variance observed. The binary models classified compounds as having good or moderate/low antibacterial activity with an accuracy of $\geq 83\%$ accuracy. Hydrophobicity and shape were the most significant molecular characteristics related to antibacterial activity. The molecular shape was illustrated by a 3D pharmacophore model. With this pharmacophore model, differences in activity of compounds from the same subclass, but prenylated at different positions, could be explained. With regard to the mode of action of active prenylated (iso)flavonoids, we found that monoprenylated compounds were better membrane permeabilizers than diprenylated ones, highlighting potential differences in interaction of the mono- and diprenylated molecules with the cytoplasmic membrane. The models developed can be useful for prediction of antibacterial activity of untested molecules and provide valuable information for the design of novel prenylated (iso)flavonoids as antibacterials.

Keywords: QSAR, prenylated isoflavonoids, antibacterial activity, mode of action

Based on: Araya-Cloutier, C.; Vincken, J-P.; van de Schans, M.G.M.; Schaftenaar, G.; Hageman, J.; den Besten, H.M.W.; Gruppen, H. QSAR-based molecular signatures of prenylated (iso)flavonoids underlying antimicrobial potency against and membrane-disruption in Gram positive and Gram negative bacteria: *Listeria monocytogenes* and *Escherichia coli*. To be submitted.

INTRODUCTION

Interest in natural compounds for antimicrobial discovery has increased during the last decade due to the rise in highly resistant bacteria.^[1] Natural products are a potentially rich source of compounds for antimicrobial discovery and development, as they usually have a high degree of stereochemistry with an extensive variety of (ring) scaffolds and generally low toxicity.^[2,3]

In the Fabaceae plant family, prenylated phenolic compounds have been identified as antimicrobials in extracts from elicited seedlings.^[4] These phenolic compounds mainly belong to the flavonoid (2-phenyl benzopyrans), isoflavonoid (3-phenyl benzopyrans) and stilbenoid (1,2-diphenyl ethylene) classes. Besides the skeleton, they differ in configuration and position of prenylation. Prenyl groups can be attached to a phenolic compound as a chain (3,3-dimethylallyl substituent) or as a five- or six-membered ring after undergoing enzymatic cyclisation with an *ortho*-phenolic hydroxyl group.^[5] Prenylation has been shown to increase the antibacterial activity of phenolic compounds,^[6] partly because hydrophobicity increases. Thereby, the partitioning to biological targets, such as membranes, increases.^[7]

Structure-antibacterial activity relationships (SAR) of prenylated (iso)flavonoids have been obtained by comparing the activity data and structures of a few analogues (usually ≤ 10 compounds).^[8,9] Studies have focussed on describing the substituents and positions within a particular phenolic skeleton that provide high or low antibacterial activity.^[10,11] The antibacterial activity of prenylated and non-prenylated (iso)flavonoids from licorice against methicillin-resistant *Staphylococcus aureus* (MRSA) and Gram negative bacteria has been studied.^[12] None of the compounds were active against the Gram negative bacteria (minimum inhibitory concentration (MIC) $> 128 \mu\text{g/mL}$), but some were very active against MRSA, especially diprenylated (iso)flavonoids (MIC $8.0 \mu\text{g/mL}$). It was also observed that the presence of a D-ring in a coumestan was detrimental for the activity, the effect of which was attributed to the rigidity of the skeleton. In contrast, a diprenylated $6\alpha,11\alpha$ -pterocarpene and a monoprenylated pterocarpan, both having rigid skeletons, were the most antibacterial compounds against MRSA (MIC $6.3 \mu\text{g/mL}$ for both).^[13] In another study,^[14] a diprenylated pterocarpan and diprenylated isoflavan were found to be very active (MIC $3.1\text{--}6.3 \mu\text{g/mL}$) against vancomycin-resistant enterococci, whereas a diprenylated isoflavanone was not. Further studies showed that the position of the prenyl groups differently affected the antibacterial activity of different subclasses of (iso)flavonoids.^[15,16] For flavanones, prenylation at C8 provided a higher antibacterial activity (i.e. MIC $12.5\text{--}25 \mu\text{g/mL}$) than prenylation at C6 (MIC $> 100 \mu\text{g/mL}$),^[17] whereas for isoflavones the opposite result was found.^[9] Regarding other substituents, the presence of hydroxyl groups appeared to be essential for antibacterial activity of prenylated (iso)flavonoids.^[6] In contrast, the influence of methoxyl groups was more ambiguous, with reduced activity in some isoflavonoids,^[13,18] and enhanced activity in others.^[11,16,19]

Increase in hydrophobicity by the presence of prenyl groups has been the traditional explanation given for the increase in antibacterial activity observed upon prenylation of (iso)flavonoids.^[7] However, not all prenylated (iso)flavonoids have shown antibacterial activity,^[17,20] highlighting the importance of other, yet to be defined, molecular characteristics for antibacterial activity. Furthermore, it has not been investigated in any large detail how differences in the overall molecular configuration relate to the mode of action. In this context, *in silico* approaches, like quantitative SAR (QSAR)^[21] and pharmacophore modelling,^[22] can help to elucidate the physicochemical properties important for the mode of action and to establish good predictive models for untested compounds. Despite numerous descriptive SAR studies of prenylated (iso)flavonoids, frequently with relatively few compounds, no QSAR analysis of prenylated (iso)flavonoids as antibacterials has been performed so far.

In this study we report on the application of QSAR to elucidate the main molecular characteristics of prenylated (iso)flavonoids as antibacterials. For this, we used the Gram positive *Listeria monocytogenes* and the Gram negative *Escherichia coli* as model organisms. Prenylated (iso)flavonoids are mostly ineffective against Gram negative bacteria.^[12] We previously showed that this intrinsic resistance can be overcome by inhibiting the efflux pump systems in *E. coli*.^[23] Consequently, we here report the antibacterial activity of prenylated (iso)flavonoids against *E. coli* in combination with an efflux pump inhibitor.

In order to perform the QSAR study, we tested 30 prenylated (iso)flavonoids (**Figure 4.1**), belonging to 6 different (iso)flavonoid subclasses, prenylated at different positions of the main skeleton and with chain, pyran or furan prenyl configurations. The majority of these molecules has never been tested before against *L. monocytogenes*, or against *E. coli* in the presence of an efflux pump inhibitor. We determined the minimum inhibitory and bactericidal concentrations of all compounds, and analysed the membrane permeabilization capacity of the antibacterial compounds.

The main goals of this study were (i) to develop a two-state (binary) classification model with high predictive capabilities for the activity of other prenylated (iso)flavonoids by using a QSAR approach, and (ii) to understand the mode of action of prenylated (iso)flavonoids against Gram positive and Gram negative bacteria by linking the QSAR findings to the proposed mode of action of prenylated (iso)flavonoids, i.e. disruption of membrane integrity.^[23-26]

Based on the mode of action proposed, we hypothesize that hydrophobicity (for an effective partitioning to the membrane) together with molecular shape (for an effective disruption of membrane integrity) are important molecular characteristics determining the antibacterial activity of prenylated (iso)flavonoids. In addition, as the cell envelope of Gram negatives contains a highly impermeable outer membrane with narrow water-filled porins,^[27] we expect that the hydrophobicity required to be antibacterially active against *E. coli* will be lower than that of active compounds against *L. monocytogenes*.

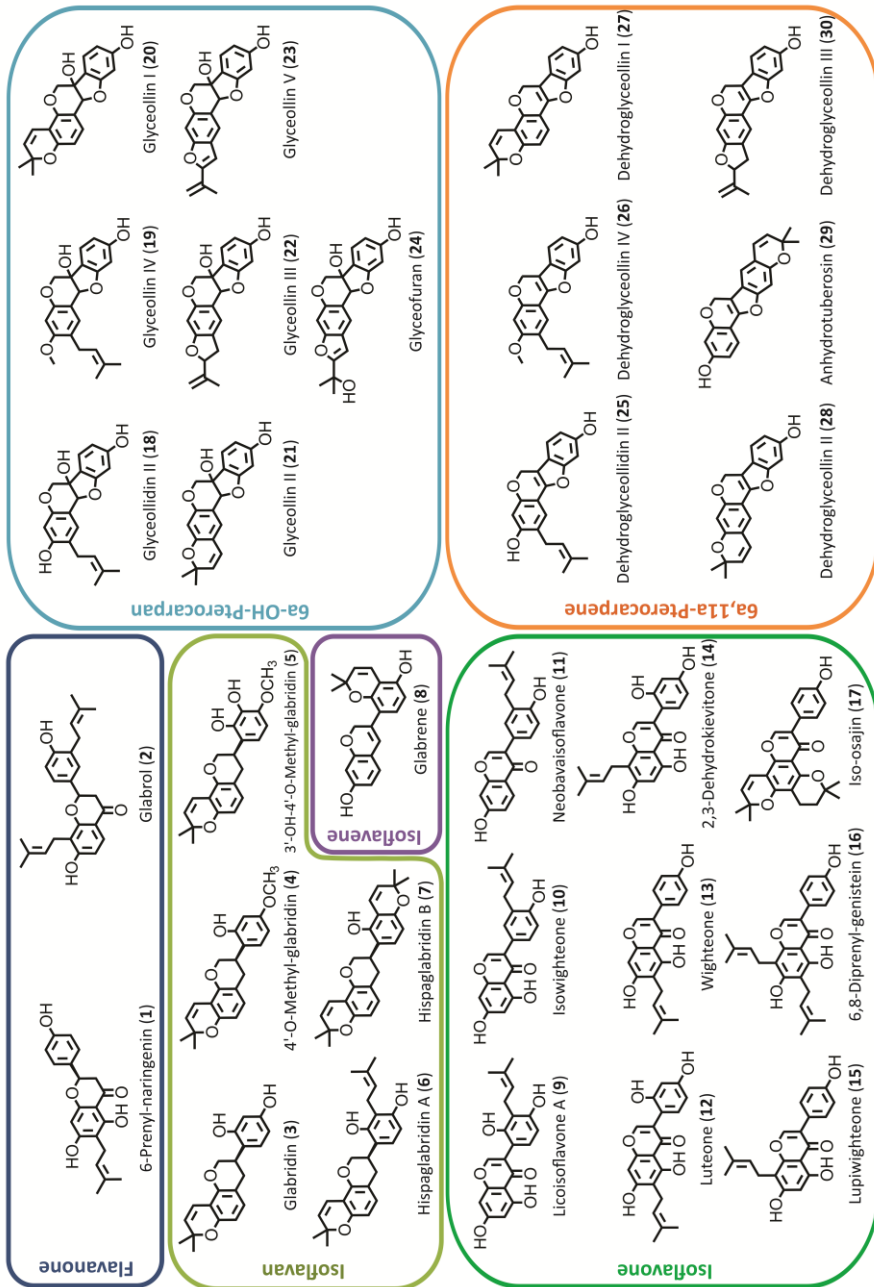


Figure 4.1. Overview of the structures of the prenylated (iso)flavonoids, and subclass to which they belong, tested in this study.

MATERIALS AND METHODS

Materials

Prenylated isoflavonoids (glabrene, 3'-hydroxy-4'-O-methyl-glabridin, 4'-O-methyl-glabridin, hispaglabridin A, hispaglabridin B, glyceofuran, glyceollidin II, glyceollin I, glyceollin II, glyceollin III, glyceollin IV, glyceollin V, dehydroglyceollidin II, dehydroglyceollin I, dehydroglyceollin II, dehydroglyceollin, III, dehydroglyceollin IV) and one prenylated flavone (glabrol) were previously purified and chemically characterized in our laboratory.^[28,29] 6-Prenylnaringenin, propidium iodine (PI), Phe-Arg β -naphthylamide dihydrochloride (Pa β N), ampicillin and ciprofloxacin were purchased from Sigma Aldrich (St. Louis, MO, USA). Isowighteone and anhydrotuberosin were purchased from ChemFaces (Wuhan, Hubei, China). Wighteone, lupiwighteone, isowighteone, luteone, 2,3-dehydrokievitone, licoisoflavone A, neobavaisoflavone, iso-osajin and 6,8-diprenyngenistein were purchased from Plantech UK (Reading, UK). Bacto brain heart infusion (BHI) broth was purchased from BD (Franklin Lakes, NJ, USA), tryptone soya broth (TSB) and bacteriological agar from Oxoid Ltd (Basingstoke, UK), and peptone physiological salt solution (PPS) from Tritium Microbiologie (Eindhoven, The Netherlands). Ethanol absolute (EtOH) was purchased from Biosolve (Valkenswaard, The Netherlands).

Antibacterial activity assay

Compounds were tested for their antimicrobial activity against Gram positive *Listeria monocytogenes* EGD-e and Gram negative *Escherichia coli* K12. For the latter, the experiments were conducted in the presence and absence of the efflux pump inhibitor Pa β N.

Bacteria were streaked from a -80 °C glycerol stock onto a BHI agar plate and incubated 24 h at 37 °C. Next, one colony was transferred to BHI broth (10 mL) and further incubated for 18 h at 37 °C. These overnight cultures were diluted 50,000 times with TSB (final inoculum concentration $3.2 \pm 0.7 \log_{10}$ CFU/mL for *L. monocytogenes* and $4.1 \pm 0.5 \log_{10}$ CFU/mL for *E. coli*). Stock solutions of the different prenylated compounds were prepared in EtOH (96% v/v) and subsequently diluted with TSB. Equal volumes (100 μ L) of bacteria and prenylated compound solutions (final concentrations tested of prenylated (iso)flavonoids 5-50 μ g/mL, 2.5% v/v EtOH max.) in TSB were mixed into a 96-well plate. For *E. coli*, the efflux pump inhibitor (EPI) Pa β N was added in the medium to a concentration of 25 μ g/mL (48 μ M).^[30] The 96-well plate was incubated in a SpectraMax M2e (Molecular Devices, Sunnyvale, CA, USA), at 37 °C with constant linear shaking. The optical density (OD) at 600 nm was measured every 5 min for 24 h.

Positive controls (ampicillin at 10 μ g/mL in water), negative controls (TSB suspension of bacteria with 2.5% (v/v) EtOH) and blanks (extracts and TSB medium with no bacteria) were considered for optical comparison and sterility control. The time to

detection (TTD) was defined as the time to reach a change in OD of 0.05 units.^[31] Prenylated compounds were tested in two independent biological reproductions, each performed in duplicate.

When no change in OD (i.e. $\Delta OD < 0.05$) was observed after the 24 h of incubation, cell viability was verified by plate counting. Briefly, 100 μL of the well with no change in OD was decimally diluted in PPS solution and 100 μL of each dilution was spread onto BHI agar plates. Plates were incubated for 24 h at 37 °C and colonies were counted. The minimum inhibitory concentration (MIC) was defined as the lowest concentration of compound that resulted in a bacterial count equal or lower than that of the initial inoculum. The minimum bactericidal concentration (MBC) was defined as the lowest concentration of compound that resulted in > 99% bacterial inactivation from the initial bacterial inoculum.

Cell membrane permeability

To investigate the effects on the cytoplasmic membrane permeability, the fluorescent probe propidium iodine (PI) was used. Bacteria (-80 °C glycerol stock) were streaked onto a BHI agar plate and incubated overnight at 37 °C. Subsequently, one colony was transferred to 50 mL of BHI broth and incubated for 13 h at 25 °C. Cells were harvested by centrifugation (4696 g, 4 °C, 20 min) and washed twice with PPS (pH 7.2). The final cell pellet was suspended in 5 mL PPS to obtain an inoculum of $9.9 \pm 0.4 \log_{10}$ CFU/mL. Stock solutions of PI and prenylated compounds were diluted in PPS to concentrations of 60 μM and 40-80 $\mu\text{g}/\text{mL}$, respectively. A volume of 50 μL of each solution (final concentration in test of PI 15 μM and of compounds 10-20 $\mu\text{g}/\text{mL}$, 2% (v/v) EtOH max.) and 100 μL of inoculum were added to a black with clear bottom 96-well plate (Greiner Bio One, Kremsmünster, Austria). The plate was incubated in a Spectramax M2e at room temperature, emission of fluorescence was measured every 30 s at 620 nm (bottom read mode), while exciting the sample at 520 nm. For the positive control, cells were treated for 10 min at 95 °C in a Thermomixer (Eppendorf, Hamburg, Germany) and added as inoculum, whereas blank control contained 100 μL of PPS instead of inoculum. Tests with the antimicrobials ciprofloxacin and ampicillin (10-20 $\mu\text{g}/\text{mL}$) were included for comparison. Intrinsic fluorescence or quenching effects of the compounds and of PI were considered by the use of blanks (compounds with PI, without cells; PI without cells). Compounds were tested in two independent biological reproductions, each performed in duplicate.

QSAR model

Molecular Operating Environment (MOE, version 2013.0802, Chemical Computing Group, Montreal, QC, Canada) was used to calculate 159 2D and internal 3D (i3D) molecular descriptors of the prenylated (iso)flavonoids (full list of descriptors is in **Table S4.1**), using the lowest energy conformer (MOPAC energy minimization, gradient 0.05) of all 30 tested (iso)flavonoids. Antibacterial activity, expressed as pMIC

(i.e. $-\log\text{MIC}$),^[32,33] was used as the dependent variable. For those compounds that showed no activity up to the highest concentration tested (i.e. $\text{MIC} > 50 \mu\text{g/mL}$), a MIC value of $100 \mu\text{g/mL}$ (i.e. the next 2-fold higher concentration to be tested) was set for the analysis.

Genetic algorithm-driven variable selection in combination with multiple linear regression (GA-MLR) as implemented in MOE's AutoQuaSAR application (available via MOE svl exchange website) was used. With the GA method different models were built simultaneously using different combinations of descriptors that correlated most with activity (settings: number of generations = 50000, population = auto, mutation probability = 0.05). Quality of fitting was determined by the coefficient of determination (R^2). Cross-validation of the models was performed by the leave-one-out (LOO) method and quality of prediction was assessed with the LOO cross-validated coefficient of determination (Q^2). As GA calculation starts from a random set of descriptors, the outcome (i.e. population of equations) can differ each time the calculation is performed. Therefore, we performed the GA-MLR calculation 5 times^[34] and recorded the top descriptors found. Using this approach, GA-MLR filtered the most relevant molecular descriptors, i.e. those that were constantly chosen and used in the different models obtained (list of top descriptors used is shown in **Figure S4.1**). Using these top descriptors, GA-MLR was performed again to obtain a smaller set of equations. The models were transformed into a binary classification model using MOE's smoothing and condition limit parameters default settings and a cut-off value of $25 \mu\text{g/mL}$ for defining active (1) and inactive (0) compounds. This cut-off value was chosen based on previous reviews on antibacterial activity of natural compounds.^[7,35] Performance of the binary model was assessed by the overall accuracy (proportion of total correct predictions), the accuracies of correctly predicted active and inactive results, and significance (p value). The best model was selected based on the number of descriptors (≤ 5), number of outliers (those with Z score > 2.0), Q^2 of the linear model ($Q^2 > 0.50$) and significance ($p < 0.05$) of both the linear and binary models. Descriptor inter-correlation or multicollinearity was assessed based on the variance inflation factor (VIF). (**Tables S4.2 and S4.3**).

Ligand-based pharmacophore elucidation

The pharmacophore elucidation query module of MOE was used to build a pharmacophore model using the energy minimized 3D conformations of the molecules built as described in the previous section. All compounds were part of the training database and an activity of $\text{MIC } 25 \mu\text{g/mL}$ was set to discriminate good antibacterial activity and moderate/low activity. As the exact interactions and target site of these compounds are unknown, the relevance of each feature (i.e. hydrogen bond acceptor, hydrogen bond donor, hydrophobic atoms and aromatic rings) was considered equal. The different models obtained were ranked based on the accuracy of the pharmacophore in discriminating positive (i.e. good antibacterial activity) and negative (moderate/low activity) compounds, and the significance ($p < 0.05$).

RESULTS

Figure 4.1 shows the structure of the 30 compounds tested, including the (iso)flavonoid subclasses to which they belong. The compounds belonged to the flavone, isoflavan, isoflavone, isoflavone, 6a-hydroxy-pterocarpan and 6a,11a-pterocarpene subclasses. Mono- and diprenylated compounds, encompassing three configurations of prenyl groups (chain, pyran-ring and furan-ring) and different positions of the prenyl group attached, were considered for this study.

Table 4.1 shows the MICs and MBCs determined for each compound. Glabrol (**2**) and diprenylated 6,8-diprenylgenistein (**16**) were very good antibacterials against *L. monocytogenes* with both MIC and MBC values of 6.3 $\mu\text{g}/\text{mL}$. *E. coli* was not susceptible to any of the tested (iso)flavonoids up to 50 $\mu\text{g}/\text{mL}$. When the efflux pumps were inhibited by PA β N, *E. coli* became susceptible to a similar extent as *L. monocytogenes*. Monoprenylated glabridin, luteone and wighteone showed very good antibacterial activity against *E. coli* with MICs of 10 $\mu\text{g}/\text{mL}$ and MBCs of 15.0 $\mu\text{g}/\text{mL}$.

Effect of (iso)flavonoid subclass

In general, isoflavones and isoflavans were among the most active compounds against both *L. monocytogenes* and *E. coli* (**Table 4.1**). Interestingly, most 6a-hydroxy-pterocarpanes did not show antibacterial activity up to the highest concentration tested (MIC > 50 $\mu\text{g}/\text{mL}$) against the two target bacteria, whereas 6a,11a-pterocarpenes were active against *L. monocytogenes*. **Figure 4.2** illustrates the time to detection of growth (the higher the time to detection of growth, the stronger the inhibition with a maximum of 24 h) of *L. monocytogenes*, when exposed to a 6a-hydroxy-pterocarpan (cPta) and a 6a,11a-pterocarpene (cPte). As observed, the presence of the hydroxyl group at position 6a in glyceollidin II (**18**) causes an important reduction of antibacterial activity in comparison with dehydroglyceollidin II (**25**).

Effect of the configuration of prenyl group

The configuration of prenyl group attached to the main skeleton affected the antibacterial activity as well. The chain prenylated dehydroglyceollidin II (**25**, cPte) inhibited the growth of the bacteria at a minimum concentration of 12.5 $\mu\text{g}/\text{mL}$ (**Figure 4.2**). The next most active compound was the pyran prenylated 6a,11a-pterocarpene (pPte) dehydroglyceollidin II (**28**) with a MIC of 15.0 $\mu\text{g}/\text{mL}$. Last, the furan prenylated 6a,11a-pterocarpene (fPte) dehydroglyceollidin III (**30**) did not inhibit the growth at any concentration tested. Also, none of the furan prenylated compounds (**22-24**, **30**) showed antibacterial activity against the target bacteria (**Table 4.1**, MIC > 50 $\mu\text{g}/\text{mL}$).

Table 4.1. Minimum inhibitory concentration (MIC) and minimum bactericidal concentration (MBC) of prenylated (iso)flavonoids against *L. monocytogenes* and against *E. coli*, with and without the presence of PAβN (25 µg/mL).^a

No.	Compound	<i>L. monocytogenes</i>		<i>E. coli</i>	<i>E. coli</i> + EPI	
		MIC	MBC	MIC	MIC	MBC
Flavanone						
1	6-Prenyl-naringenin	> 50		>50	25	25
2	Glabrol	6.3	6.3	>50	>50	
Isoflavan						
3	Glabridin	15	20	>50	10	15
4	4'-O-Methyl-glabridin	10	12.5	>50	25	25
5	3'-OH-4'-O-methyl-glabridin	12.5	15	>50	>50	
6	Hispaglabridin A	12.5	20	>50	>50	
7	Hispaglabridin B	15	25	>50	>50	
Isoflavene						
8	Glabrene	50	50	>50	50	50
Isoflavone						
9	Licoisoflavone A	25	50	>50	15	20
10	Isowighteone	15	20	>50	20	25
11	Neobavaisoflavone	50	50	>50	25	25
12	Luteone	15	20	>50	10	15
13	Wighteone	10	15	>50	10	15
14	2,3-Dehydrokievitone	>50		>50	>50	
15	Lupiwighteone	>50		>50	>50	
16	6,8-Diprenyl-genistein	6.3	6.3	>50	>50	
17	Iso-osajin	>50		>50	>50	
6α-OH-Pterocarpan						
18	Glyceollidin II	>50		>50	>50	
19	Glyceollin IV	50	>50	>50	>50	
20	Glyceollin I	>50		>50	>50	
21	Glyceollin II	>50		>50	>50	
22	Glyceollin III	>50		>50	>50	
23	Glyceollin V	>50		>50	>50	
24	Glyceofuran	>50		>50	>50	
6α,11α-Pterocarpene						
25	Dehydroglyceollidin II	12.5	15	>50	50	>50
26	Dehydroglyceollin IV	25	50	>50	50	>50
27	Dehydroglyceollin I	15	20	>50	>50	
28	Dehydroglyceollin II	15	20	>50	>50	
29	Anhydrotuberosin	>50		n.t. ^b	n.t.	
30	Dehydroglyceollin III	>50		>50	>50	

^a Concentrations in micrograms per milliliter (µg/mL). ^b Not tested (n.t.)

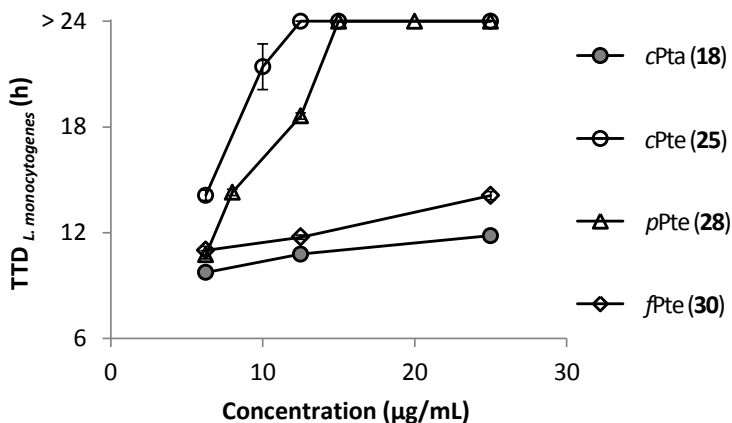


Figure 4.2. Time to detection (TTD) of *L. monocytogenes* growth in the presence of different concentrations of prenylated 6 α -hydroxy-pterocarpanes (glyceollidin II, **18**) and 6 α ,11 α -pterocarpenes (dehydroglyceollidin II, **25**; dehydroglyceollin II, **28**; dehydroglyceollin III, **30**). Error bars represent the standard deviation of two biologically independent reproductions. TTD of control cells (i.e. cells not exposed to prenylated compounds) was 11.7 ± 2.2 h.

Effect of the number of prenyl groups

The growth inhibition of *L. monocytogenes* (solid line) and *E. coli* in the presence of the EPI (dashed line) by mono- and diprenylated isoflavans (Isa) is illustrated in **Figure 4.3**. Except for iso-osajin (**17**), diprenylated (iso)flavonoids, i.e. hispaglabridin A (**6**) and B (**7**), were among the most active ones against the Gram positive bacterium (MICs ≤ 10 $\mu\text{g/mL}$). Opposite results were found for the Gram negative bacterium. The diprenylated (iso)flavonoids were not effective antibacterials against *E. coli* with and without the EPI (**Table 4.1**, MIC > 50 $\mu\text{g/mL}$), whereas monoprenylated compounds, including glabridin (**3**), were active against this bacterium (**Table 4.1**, MIC 10 $\mu\text{g/mL}$).

Effect of the position of the prenyl group

Concerning the (iso)flavonoid skeletons, there are four main positions of C-prenylation: C6, C8, C3' and C5' (or the equivalents C2, C4, C8 and C10 in 6 α -hydroxy-pterocarpanes and 6 α ,11 α -pterocarpenes). In order to compare different subclasses of (iso)flavonoids, the Greek numbering system of Simons et al.^[5] was adopted, which is illustrated by the isoflavonoid skeleton in **Figure 4.4**. The position of the prenyl group clearly affected the antibacterial activity of these compounds. Genistein prenylated at the α position (**15**) showed no inhibition towards *L. monocytogenes*, whereas β -prenylated genistein (**13**) had high antibacterial activity, followed by δ prenylated genistein (**10**). For 6 α ,11 α -pterocarpenes, inhibition was similar for α and β prenylated compounds, i.e. dehydroglyceollin I (**27**) and II (**28**), whereas the δ prenylated 6 α ,11 α -pterocarpene, i.e. anhydrotuberosin (**29**), showed the lowest growth inhibition.

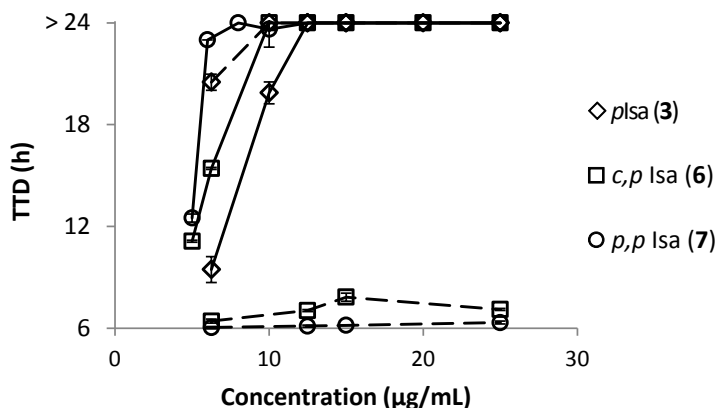


Figure 4.3. Time to detection (TTD) of *L. monocytogenes* (solid line) and *E. coli* (with EPI, dashed line) growth in the presence of different prenylated isoflavans: glabridin (3), hispaglabridin A (6) and hispaglabridin B (7). Error bars represent the standard deviation of two biologically independent reproductions. TTD of control untreated cells was 10.4 ± 1.9 h.

Effect of other substituents

The number of hydroxyl groups influenced the antibacterial activity of prenylated isoflavones. The presence of 3 OH groups in isowighteone (Table 4.1, 10) was almost twice more effective (MIC 15 µg/mL) than the presence of 4 OH groups as in licoisoflavone A (9, MIC 25 µg/mL) and thrice more effective than 2 OH groups as in neobavaisoflavone (11, MIC 50 µg/mL). For *E. coli*, the prenylated isoflavone with 4 OH groups (9) was slightly better (MIC 15 µg/mL) than prenylated isoflavones with 3 OH groups (10, MIC 20 µg/mL) or 2 OH groups (11, 25 µg/mL).

With regard to O-methylation, we found no clear trend in the antibacterial activity of prenylated (iso)flavonoids. In one case, O-methylation was detrimental for activity, as for dehydroglyceollin IV (26) in comparison with dehydroglyceollidin II (25) (Table 4.1). In another case, O-methylation improved the activity, as for 4'-O-methylglabridin (4) in comparison with glabridin (3).

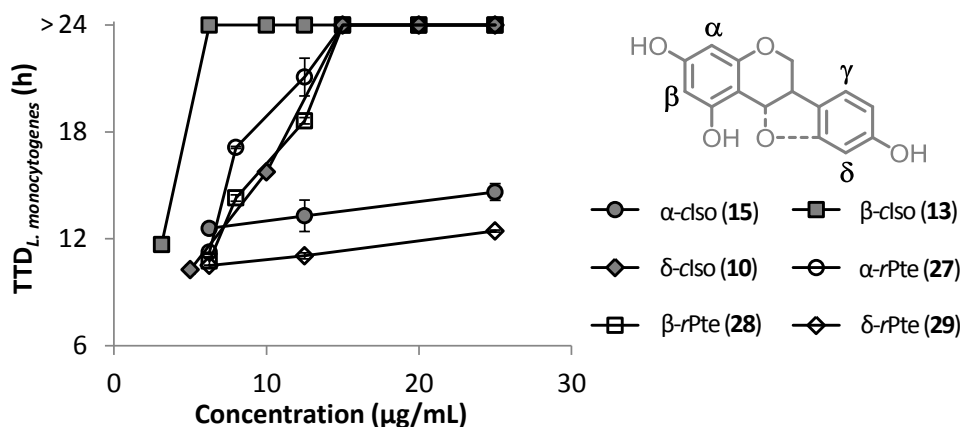


Figure 4.4. Time to detection of *L. monocytogenes* growth in the presence of chain prenylated isoflavonoids (closed symbols): isowighteone (**10**), wighteone (**13**), lupiwighteone (**15**); and ring-closed prenylated pterocarpenes (open symbols): dehydroglyceollin I (**27**), dehydroglyceollin II (**28**), anhydrotuberostin (**29**). Prenyl positions are annotated based on the inset. Error bars represent the standard deviation of two biologically independent reproductions. TTD of control untreated cells was 11.4 ± 2.3 h.

Membrane permeabilization by prenylated (iso)flavonoids

Permeabilization of the cytoplasmic membrane of *L. monocytogenes* and *E. coli*, the latter in the presence and absence of EPI, was assayed by measuring the uptake of the fluorescent probe propidium iodide (PI). We tested very active prenylated (iso)flavonoids (i.e. $MIC \leq 15 \mu\text{g/mL}$, **Table 4.1**) and compared them with the traditional antimicrobials ampicillin (Amp) and ciprofloxacin (Cip). **Figure 4.5A** shows the net PI uptake of *L. monocytogenes* after 2 h of exposure to different prenylated (iso)flavonoids. The monoprenylated isoflavonoids isowighteone (**10**), luteone (**12**) and wighteone (**13**) were good membrane permeabilizers (i.e. PI uptake > 500 RFU). Unexpectedly, other antibacterially active compounds, including some diprenylated compounds, ampicillin and ciprofloxacin, showed little change in fluorescence after 2 h (PI < 100 RFU).

Figure 4.5B shows the uptake of PI by *E. coli* when exposed to the very active prenylated (iso)flavonoids (i.e. $MIC \leq 15 \mu\text{g/mL}$). In this case, glabridin (**3**), licoisoflavone A (**9**), luteone (**12**) and wighteone (**13**) were good in permeabilizing the cytoplasmic membrane of *E. coli* in the presence of the EPI (i.e. PI uptake > 500 RFU). Interestingly, these compounds were able to permeabilize the inner membrane of *E. coli* without the EPI, although to a lesser extent than when EPI was present (i.e. poor permeabilization, PI uptake 100-500 RFU). This indicated that monoprenylated isoflavonoids were able to permeabilize *E. coli* cells (as some PI uptake occurred), but no lethal permeabilization took place as no MIC or MBC were found under those conditions. It cannot be excluded that recovery of PI permeable cells has occurred, as this has been observed previously for other microorganisms.^[36]

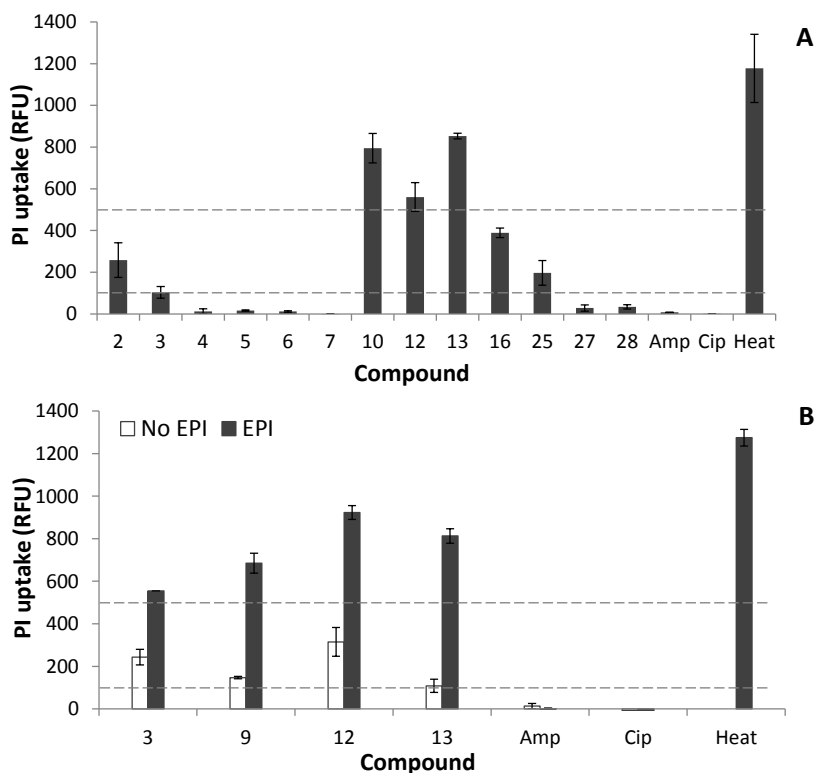


Figure 4.5. PI uptake by *L. monocytogenes* (A) and *E. coli* (B) after 2 h exposure to very good prenylated (iso)flavonoids or antibiotics (20 µg/mL). Dashed lines represent the ranges used to define non-permeabilizers (PI uptake < 100), poor (PI uptake 100-500 RFU) and good permeabilizers (PI uptake > 500 RFU). Data are means of two independent biological reproductions, with standard deviation as error bars. Number of compound refers to those of **Table 4.1**. Ampicillin (Amp), ciprofloxacin (Cip), heat-treated cells (Heat).

QSAR analysis for prediction of antibacterial activity

Using genetic algorithm-driven selection of variables in combination with multiple linear regression (GA-MLR), relevant descriptors from the list of 159 descriptors (**Table S4.1**) were identified for both *L. monocytogenes* and *E. coli* antibacterial activity. With this subset of descriptors identified (**Figure S4.1**), a final population of linear models was obtained by running GA-MLR one more time. The best equations were chosen based on the R^2 , Q^2 , number of descriptors and of outliers, as well as the significance ($p < 0.05$) of the models obtained (**Table S4.2**). The selected QSAR models are shown in **Table 4.2**.

***L. monocytogenes* regression model.** For the antibacterial activity against *L. monocytogenes*, two different sets of equations were observed within the population of final equations obtained: those containing *KierFlex* (i.e. Kier molecular shape flexibility index) and those containing *logD* (distribution coefficient at pH 7.2) as independent

variables. For this reason, we selected the best equations of these two different sets, models A and B, as shown in **Table 4.2**. With a relatively low number of descriptors, the linear models covered $\geq 64\%$ of the experimental variance. The binary classification models had an overall accuracy between 83-86% and a prediction accuracy of 78-79%.

Model A predicted the antibacterial activity against *L. monocytogenes* with only two descriptors: *logD* and *vsurf_ID7* (hydrophobic moment at -1.4 kcal/mol) as explanatory variables. *logD*, indicator of hydrophobicity, describes the distribution of a molecule between two immiscible phases considering the charge state of the molecule. Hence, it is pH dependent. The hydrophobic moment (*vsurf_ID*) describes the location of the hydrophobic region in the molecule, by measuring the length of the vector from the centre of mass of the molecule to the centre of the hydrophobic domain.^[37] As volume and shape are dependent on the energy level of the molecule, the *vsurf_ID* descriptor is calculated at multiple energy levels from 0.0 to -2.0 kcal/mol (i.e. the usual energy range of hydrophobic interactions).^[38] The specific energy level used in the model was the most correlated with activity and chosen by the GA-MLR, as observed in the list of top descriptors (**Figure S4.1**).

Model B predicts the antibacterial activity using four descriptors: *KierFlex* (flexibility index), *PEOE_RPC⁻* (relative negative partial charge), *vsurf_A* (amphiphilic moment) and *vsurf_W7* (hydrophilic volume at -5.0 kcal/mol). The flexibility index (*KierFlex*) describes the flexibility of a molecule and is calculated from the kappa shape indices that characterize the overall molecular shape, including relative cyclicality, branching and spatial density of the molecule.^[39,40] The relative negative partial charge (*PEOE_RPC⁻*) is the ratio between the partial charge of the most negative atom in a molecule and the total negative partial charge of the molecule. The amphiphilic moment (*vsurf_A*) measures the vector between the centre of the hydrophobic domain and the centre of the hydrophilic domain in a molecule.^[38] The hydrophilic volume (at -5.0 kcal/mol, *vsurf_W7*) is defined as the accessible volume that has affinity to water molecules.^[38] This *vsurf_W* descriptor is computed at multiple energy levels, similarly to the *vsurf_ID* mentioned above. According to the GA-MLR performed, the particular energy level chosen was the one mostly correlated with antibacterial activity. Energy levels of -1.0 to -6.0 kcal/mol are related to polar and H-bond donor-acceptor regions.^[38]

Using the level of significance (p value) of each descriptor in the QSAR models (**Table 4.2**), it is possible to determine their relative importance for determining the antibacterial activity of prenylated (iso)flavonoids. For the antibacterial activity against *L. monocytogenes*, the *logD* value (in model A) and the *KierFlex* index (in model B) were the most important descriptors ($p < 0.0001$). *Kierflex* is correlated to a certain extent to *logD* (Fisher's correlation coefficient of 0.67, **Table S4.3**). This might be explained by the role of the prenyl groups, the main contributor to the *logD*, in increasing molecular branching, which is a shape characteristic considered within the *KierFlex* flexibility index. Hence, these two descriptors can cover part of the same experimental variance and, therefore, they were not selected together in one model by the GA-MLR analysis.

Table 4.2. QSAR models calculated for the antibacterial activity of prenylated (iso)flavonoids.

Bacteria	Compounds used	Linear model Variables	Coefficients Value	Std. error	p value	R ²	Q ²	Binary model ^c Total accuracy	Active accuracy	Inactive accuracy
<i>L. monocytogenes</i> A	28 ^a	logD	0.443	0.067	6.3 x10 ⁻⁷	0.64	0.56	0.86 (0.78) ^d	0.87 (0.80)	0.85 (0.77)
		<i>vsurf_ID7</i>	0.311	0.147	0.04					
		intercept	1.987	0.347	5.8 x10 ⁻⁶					
		Kierflex	0.605	0.099	3.0 x10 ⁻⁶	0.67	0.57	0.83 (0.79)	0.67 (0.67)	1.00 (0.93)
<i>E. coli</i> B	29 ^b	PEOE_RPC-	11.388	2.514	0.0001					
		<i>vsurf_A</i>	-0.092	0.035	0.015					
		<i>vsurf_W7</i>	0.290	0.122	0.026					
		intercept	0.212	0.753	0.780					
		α_{acc}	-0.357	0.055	1.0 x10 ⁻⁶	0.82	0.74	0.96 (0.93)	0.88 (0.75)	1.00 (1.00)
<i>E. coli</i> A	29	<i>std_dim3</i>	1.976	0.234	1.2 x10 ⁻⁸					
		<i>vsurf_Wp3</i>	-0.023	0.004	1.8 x10 ⁻⁶					
		PEOE_VSA_FHYD	-7.913	0.858	2.4 x10 ⁻⁹					
<i>E. coli</i> B	29	intercept	11.529	0.933	6.8 x10 ⁻¹²					

^a Excluded compounds (z score > 2.0): iso-osajin and 6-prenylnaringenin. ^b Excluded compound (z score > 2.0): 6-prenylnaringenin. ^c Threshold for binary model was set at 4.1 pMIC, i.e. compounds with a MIC ≤ 25 µg/mL would be consider active (1) and compounds with a MIC > 25 µg/mL inactive (0). ^d Values between brackets indicate the leave-one-out cross-validated accuracies.

***E. coli* regression model.** We obtained a model (Table 4.2) using four descriptors to predict antibacterial activity against *E. coli* in the presence of EPI: fractional hydrophobic surface area (*PEOE_VSA_FHYD*), i.e. the proportion of surface area of hydrophobic atoms (i.e. atoms with a net partial charge of ≤ 0.2); standard dimension (*std_dim3*), i.e. size of the molecule along the z-axis or molecular globularity; the polar volume (*vsurf_Wp3*, at -1.0 kcal/mol), i.e. volume of atoms with a net partial charge > 0.2 ; number of hydrogen bond acceptors in the molecule (*a_acc*). This model explained over 80% of the variance observed and high predictive qualities for both the linear and the binary model were obtained. From the descriptors selected, the fractional hydrophobic surface area (*PEOE_VSA_FHYD*) was the most important descriptor in the regression model ($p \ 2 \times 10^{-9}$). The shape of the compounds, represented by *std_dim3*, was the second most important variable defining activity against *E. coli* ($p \ 1 \times 10^{-8}$).

It is important to note that the number of active ($\text{MIC} \leq 25 \ \mu\text{g/mL}$) compounds against *E. coli* was about one fourth of the complete set of compounds tested, whereas for *L. monocytogenes* this was half. Thus, the model obtained in this study for *E. coli* might be further optimized by including more active compounds during model development.

Pharmacophore elucidation with antibacterial prenylated (iso)flavonoids

To extend the understanding of the effect of the position of prenylation on antibacterial activity we employed the pharmacophore elucidation query in MOE to model the structural requirements of prenylated (iso)flavonoids for antibacterial activity against *L. monocytogenes* (Figure 4.6A) and *E. coli* (Figure 4.6B). The 3D pharmacophore models were similar for both bacteria, consisting of one hydrophobic feature (green in Figures 4.6 and 4.7, at the location of the prenyl group), two aromatic ring features (orange in Figures 4.6 and 4.7, corresponding to the A- and B-ring of isoflavonoids), and one (for *L. monocytogenes*) or two (for *E. coli*) hydrogen bond acceptor projection features (blue in Figures 4.6 and 4.7). A projection feature defines the position of a potential hydrogen bond partner. Using an activity threshold of a MIC value of $25 \ \mu\text{g/mL}$, these two pharmacophore models showed a 72-77% overall accuracy, i.e. proportion of true positives and negatives results (Table S4.6).

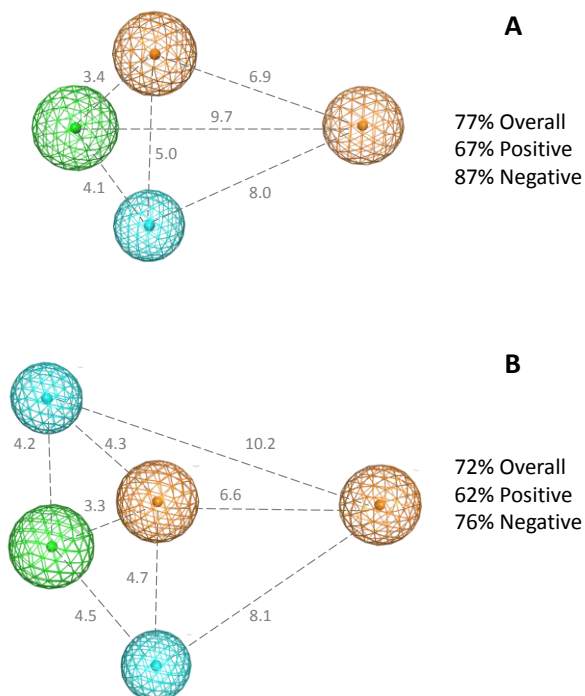


Figure 4.6. Ligand-based pharmacophore model for good antibacterial ($\text{MIC} \leq 25 \mu\text{g/mL}$) prenylated (iso)flavonoids against *L. monocytogenes* (A) and *E. coli* (B). The colour of the spheres represents the following features: blue spheres are hydrogen bond acceptor projection features (i.e. feature that annotates the location of possible hydrogen bond partner), whereas green and orange spheres represent the presence in the ligand of hydrophobic areas or aromatic rings, respectively. The numbers represent the distance between the features in Ångström. The percentage values represent the different prediction accuracies of the model. Overall accuracy, i.e. proportion of correctly predicted compounds (positives and negatives); positive accuracy, i.e. proportion of correctly predicted positive compounds (those with good antibacterial activity); negative accuracy, i.e. proportion of correctly predicted negative compounds (those with moderate to low antibacterial activity).

Figure 4.7 shows examples of isoflavones prenylated at different positions in relation to the *E. coli* pharmacophore model. For all three isoflavones, the aromatic (orange) and hydrogen bond acceptor (blue) features can be mapped. For the α prenylated isoflavone (4.7A) it was not possible to map the hydrophobic (green) feature as the prenyl group points into a different direction. Thus, this compound was correctly predicted by the pharmacophore model as inactive (i.e. it was not recognized as a positive hit, Table S4.6). In contrast, β prenylated isoflavones (4.7B) precisely mapped the hydrophobic feature, in accordance with the very good activity experimentally observed for these compounds. Isoflavones prenylated at the δ position showed good activity as well (Table 4.1). During the pharmacophore search, however, the δ

prenylated isoflavones were not recognized as positive hits (Table S4.6). Nevertheless, by a simple flip of the skeleton of the β prenylated isoflavone (along the short axis), we were able to build the energy minimized δ prenylated isoflavone and map all pharmacophore features, as shown in Figure 4.7C. This lack of recognition of active compounds can mean that the fit of the molecule is not good enough, but does not necessarily mean mismapping of the features.^[41]

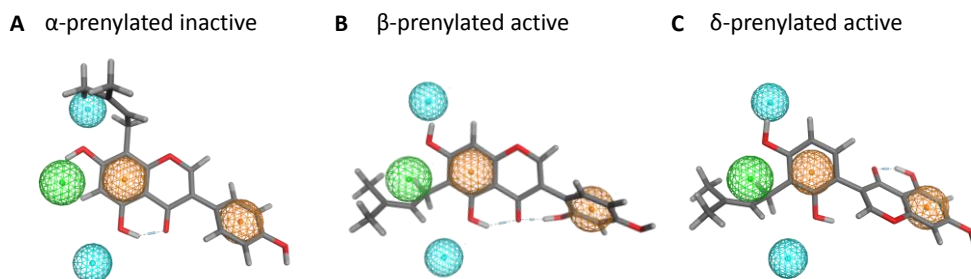


Figure 4.7. Comparison of isoflavones prenylated at different positions with regard to their fit to the pharmacophore and activity against *E. coli*. Lupiwighteone (A), luteone (B) and licoisoflavone A (C). The colour of the spheres represents the following features: blue spheres are hydrogen bond acceptor projection features (i.e. feature that annotates the location of possible hydrogen bond partner), whereas green and orange spheres represent the presence in the ligand of hydrophobic areas or aromatic rings, respectively.

Some compounds were falsely predicted as positive during the pharmacophore search (Table S4.6). The diprenylated isoflavans (prenylated at α and δ position) were able to map *E. coli*'s pharmacophore features and consequently predicted as active, although no MIC value was found against *E. coli*. The same result was observed for the α prenylated 6α -hydroxy-pterocarpan (incorrectly predicted as active). To reach (i.e. permeate) the inner membrane, hydrophobicity is known to be determinant. These false positive results might be explained by an inappropriate hydrophobicity of these molecules: hydrophobicity might be too high for the diprenylated molecules to cross the OM or too low for the 6α -OH-pterocarpan to permeate to the inner membrane.

DISCUSSION

Hydrophobicity and shape were identified as the most important molecular characteristics, highlighted by very significant *p* values in the QSAR analysis, that affect the antibacterial activity of prenylated (iso)flavonoids against both *L. monocytogenes* and *E. coli*. We propose that hydrophobicity mainly defines the efficiency of partitioning of the compounds into the cytoplasmic membrane, whereas the molecular shape defines the antibacterial action inside the membrane.

Effect of hydrophobicity on antibacterial activity of prenylated (iso)flavonoids

Hydrophobicity, in the form of different descriptors (distribution coefficient, hydrophobic moment and hydrophobic surface area), was included in the QSAR models obtained in our study. The effect of hydrophobicity of compounds on antibacterial activity was bacterium-dependent. For Gram positive *L. monocytogenes*, hydrophobicity (in the form of $\log D$) was positively correlated with antibacterial activity, whereas for *E. coli* it (in the form of fractional hydrophobic surface area) was negatively correlated (Table 4.2). According to our results, the minimum hydrophobicity for prenylated (iso)flavonoids to be active against *L. monocytogenes* and *E. coli* corresponds to a $\log D$ of 3.6 and the maximum to be active against *E. coli* corresponds to a $\log D$ of 4.6 (Tables S4.4 and S4.5). With regard to the fractional hydrophobic surface area, the majority (73%) of active compounds against *L. monocytogenes* had a fractional hydrophobic surface area > 0.80 , whereas the majority (71%) of active compounds against *E. coli* had a fractional hydrophobic surface area < 0.80 (Tables S4.4 and S4.5).

As hypothesized, hydrophobicity affects the partitioning of prenylated compounds to the cytoplasmic membrane. The differences in hydrophobicity requirements observed between *L. monocytogenes* and *E. coli* might be explained by the different influx pathways of compounds for entering these bacteria. In *E. coli* the entrance to the periplasmic space of small (MW < 600 -700) and hydrophilic antimicrobials is usually through the nonspecific porins. These are narrow (6-15 Å diameter) hydrophilic channels with exposed negatively charged residues.^[42-44] Because of the porin's charged lining, hydrophobicity of antimicrobials has been shown to strongly reduce their influx rates through porins.^[45] Alternatively, diffusion across the lipid bilayer of the outer membrane (OM), composed of lipopolysaccharides (LPS) highly ordered and packed, is known to be very slow for hydrophobic compounds.^[46] The other known ways of influx through the outer membrane (OM) are substrate-specific (e.g. long chain fatty acid transport)^[47] or active transporters (e.g. iron transport), both of which require substrate recognition.^[44] There are no studies regarding the pathway of influx of prenylated (iso)flavonoids into Gram negative bacterial cells. Nevertheless, based on (i) the high substrate specificity of the specialized OM transporters,^[47,48] (ii) the known porin-mediated entrance of antimicrobials of similar size and hydrophobicity as some of our prenylated (iso)flavonoids,^[46,49] (iii) the observed detrimental effects of hydrophobicity, and (iv) the beneficial effects of extra polar groups of our prenylated (iso)flavonoids regarding *E. coli* antibacterial activity, we postulate that prenylated (iso)flavonoids mainly enter via the unspecific porins. Consequently, the rate of influx through porins decreases as the hydrophobicity of the antibacterials increases, and thus, the efficiency of killing *E. coli*.

In contrast, because of the absence of the OM in Gram positives, prenylated (iso)flavonoids need to cross only the cell wall (peptidoglycan layer) before reaching the inner membrane. The cell wall is known to exert low barrier effects for the passage of

antimicrobials.^[50] Thus, to be antibacterially active against *L. monocytogenes*, (double) prenylated compounds do not suffer from hydrophobicity restrictions, as they do to be active against *E. coli*.

Effect of molecular shape on antibacterial activity of prenylated (iso)flavonoids

The shape of the molecules is hypothesized to be the main factor responsible for disruption of cytoplasmic membrane integrity. Shape is part of the QSAR models in the form of flexibility (*KierFlex* flexibility index, derived from molecular shape, i.e. cyclicity, branching and density) for *L. monocytogenes* and globularity (standard dimension, *std_dim3*) for *E. coli*. Additionally, shape was illustrated by the 3D pharmacophore model (**Figure 4.6**).

The majority (86%) of the good antibacterials against *L. monocytogenes* showed a *KierFlex* index > 2.8. Flexibility has been shown to be a mechanical determinant for membrane-interacting antimicrobial peptides. Peptides require some degree of conformational freedom to partition into membranes as well as to arrange effective intermolecular interactions by rearranging their flexible side chains.^[40,51,52] In line with this, we propose that chain prenylated (iso)flavonoids are able to rearrange more effectively inside the cytoplasmic membrane than ring-closed prenyl groups, as prenyl chains are more flexible than prenyl rings. These rearrangements will improve their intermolecular interactions and, thus, the disruption of membrane integrity.

We postulate that molecular globularity of prenylated (iso)flavonoids influences the disruption of membrane integrity, as well. A globular structure might perturb the bilayer organization when inserted into the membrane to a larger extent than a flat one. Five out of the eight good antibacterials against *E. coli* had a standard dimension (*std_dim3*, indicator of globularity) > 1.1. The positive correlation of globularity with antibacterial activity is in accordance with our previous results^[23], where flatness of prenylated stilbenoids was associated with their relatively low antibacterial activity as opposed to the relatively good antibacterial activity of elbow-shaped prenylated (iso)flavonoids.

Membrane permeabilization is not the only mechanism of integrity disruption of prenylated (iso)flavonoids

We observed that prenylated (iso)flavonoids disrupt the bacterial membrane integrity by permeabilization. This permeabilization was considered to be the main mechanism of membrane disruption and thus, of antibacterial activity. However, among the very good antibacterial (iso)flavonoids against *L. monocytogenes*, some compounds were good permeabilizers and others were not. In **Figure 4.8** the molecular surfaces of some of the very active antibacterial compounds against *L. monocytogenes* are shown, coloured according to hydrophobicity and polarity. Furthermore, the ratio between the hydrophobic and polar surface areas is shown in the figure.

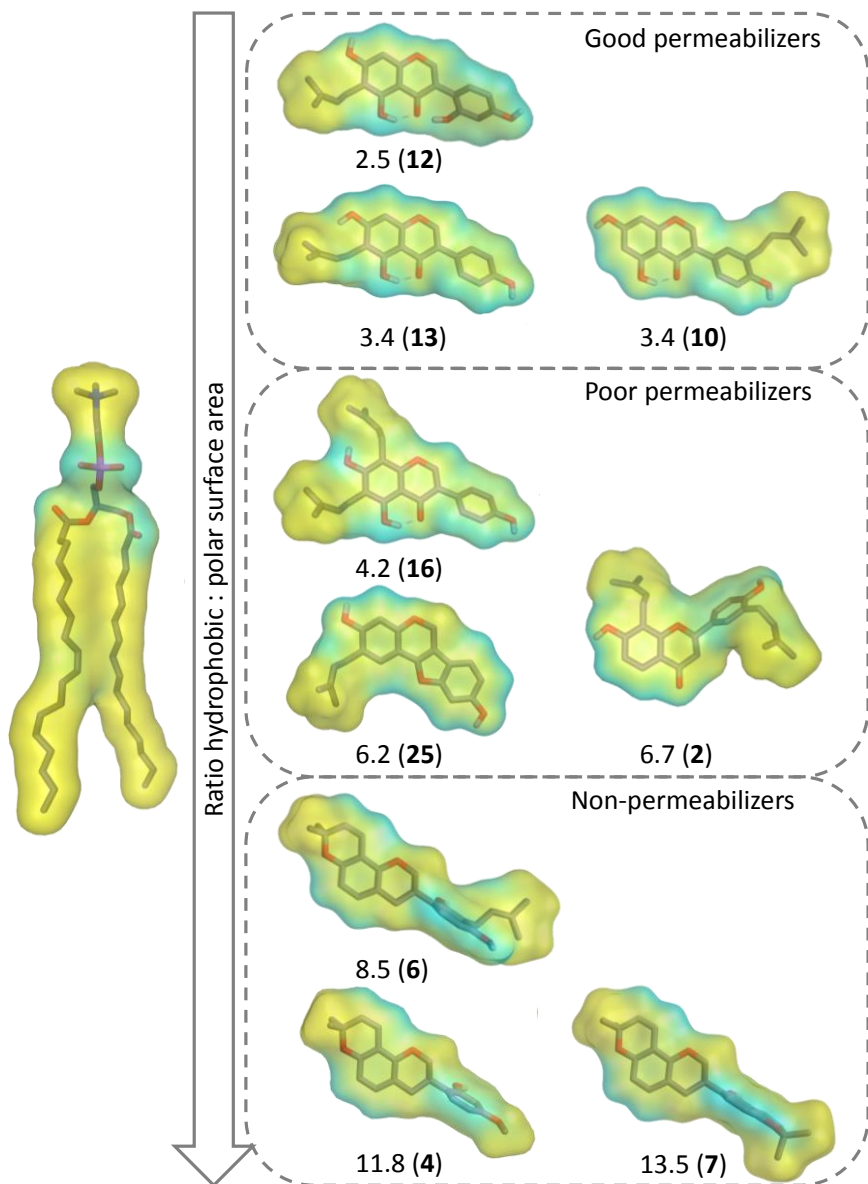


Figure 4.8. Molecular surface of very active antibacterial prenylated (iso)flavonoids against *L. monocytogenes* ($\text{MIC} \leq 15 \mu\text{g/mL}$) with different membrane permeabilization properties. Good permeabilizer (PI uptake > 500 RFU after 2 h exposure), poor permeabilizer (PI uptake 100-500 RFU after 2 h exposure), non-permeabilizer (PI uptake < 100 RFU after 2 h exposure). Model of membrane phospholipid is presented only as a visualization aid (taken from Heller et al.^[53]). Surface colour is yellow for hydrophobic areas and light blue for polar areas. Number below each molecule refers to the ratio between the hydrophobic surface area and the polar surface area, as calculated by MOE.

Besides partitioning, hydrophobicity has been proposed to be determinant for the localization of (prenylated) flavonoids within model membranes (liposomes).^[26,54] Although no strict linear relation was found, the good antibacterial/poor and non-permeabilizing molecules had a relatively larger hydrophobic surface area than the good antibacterial/good permeabilizing molecules. All poor and non-permeabilizers, including those that are not in this figure, had a hydrophobic:polar surface area ratio equal or higher than 4.2. We postulate that (i) prenylated (iso)flavonoids with relatively little hydrophobic surface area interact more with the glycerol region of the phospholipids; (ii) (iso)flavonoids with relatively large hydrophobic surface area will penetrate deeper and interact more with the acyl chains of the phospholipids. The difference in distribution along the phospholipids, and consequently, along the membrane might be responsible for the effectiveness in permeabilization observed in this study. Thus, compounds interacting closer to the surface of the membrane, near the polar head groups, might permeabilize the membrane more efficiently than compounds interacting deeper in the membrane. The latter ones are expected to leave the membrane surface organization intact.

Shape was also expected to contribute to the capacity of the antibacterial prenylated (iso)flavonoids to permeabilize membranes, as shape was highly correlated with antibacterial activity. However, no relationship was found between permeabilization capacity and the shape descriptors considered in this study.

In general, these findings highlight the possibility that different types of interactions of prenylated (iso)flavonoids within the bacterial cytoplasmic membrane might exist. They also indicate that permeabilization is not the sole membrane integrity disrupting effect of these antibacterial compounds. Integrity of cytoplasmic membrane can also be disrupted by alteration of membrane fluidity or elasticity, alteration of hydration of membrane surface, alteration of membrane conductivity, or induction of lipid peroxidation.^[54,55]

Mode of action of prenylated (iso)flavonoids revisited

The proposed effects of hydrophobicity and shape on both partitioning to membranes, and disruption of membrane integrity (which includes permeabilization but also other undefined mechanisms), are summarized in **Figure 4.9**. Main differences regarding the cell architecture include the presence of an outer membrane (composed of a special lipid bilayer) and a thin cell wall in the Gram negative bacterium.

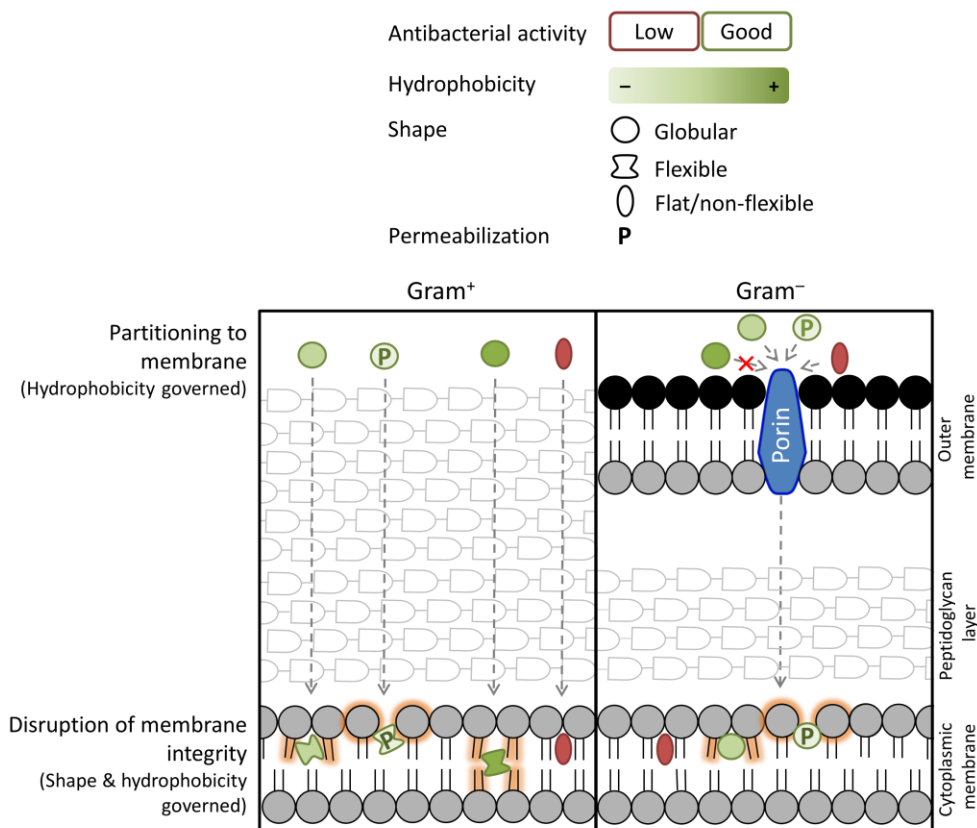


Figure 4.9. Schematic overview of the main molecular characteristics found in this study to influence the antibacterial activity of prenylated (iso)flavonoids against Gram positive and negative bacteria. Compounds with green outline are good antibacterials (i.e. MIC \leq 25 μ g/mL). The intensity of the green shading in the compounds indicates the extent of hydrophobicity. Compound with red outline and red shading indicates a hydrophobic molecule with moderate or low antibacterial activity. Good antibacterials against Gram positives required flexibility (indicated by the deformed shape). Good antibacterials against Gram negatives required globularity (represented by the circles). The compound with moderate/low antibacterial activity is a non-flexible or planar molecule. Orange shading around the phospholipids represents disruption of membrane integrity. P, permeabilizer.

In the Gram positive bacterium, prenylated compounds do not encounter significant barrier effects by the peptidoglycan layer to reach the cytoplasmic membrane where they integrate, provided that the minimum hydrophobicity is met (as is the case for all compounds shown in **Figure 4.9**). Flexibility (positively correlated with Gram positive antibacterial activity) is represented by the deformation of the circles inside the cytoplasmic membrane. Flexible compounds (e.g. chain prenylated isoflavones, such as wighteone or 6,8-diprenyl-genistein) are able to make effective intermolecular interactions with the lipid bilayer and alter its integrity. Less flexible compounds (e.g. pyran prenylated pterocarpenes, such as dehydroglyceollin III) will have less

intermolecular interactions and trigger less membrane disruption (as for the red compound). Consequently, they show less antibacterial activity, despite their hydrophobicity.

Membrane integrity can be disrupted by permeabilization when the antibacterial breaks up the organization of the polar head groups of the phospholipids. When the antibacterial permeates deeper into the membrane other disruption effects (e.g. alteration of membrane fluidity) might occur.

In the Gram negative bacterium, highly hydrophobic compounds (e.g. 6,8-diprenyl-genistein) encounter influx restrictions due to porins, but compounds meeting the hydrophobicity restrictions of porins cross the outer membrane of Gram negatives. Globularity was positively correlated with the antibacterial activity against the Gram negative bacterium. It is proposed that inside the cytoplasmic membrane globular compounds (e.g. those with prenyl chains such as wighteone) can disrupt the membrane integrity more effectively than less globular ones (e.g. those with planar conformation such as dehydroglyceollin III).

It should be noted that flexibility and globularity are not exclusive characteristics. The same compound can be flexible and globular. Due to the lack of knowledge on the exact arrangement and intermolecular interactions between prenylated (iso)flavonoids and the cytoplasmic membrane of bacteria, at this point, we cannot explain the differences in the shape-related descriptors between the Gram positive (flexibility) and Gram negative bacteria (globularity).

This is the first report on the QSAR of prenylated (iso)flavonoids as antibacterials against Gram positive and Gram negative bacteria. Important molecular characteristics identified in this study can be used for the design and development of novel antibacterials from these natural compounds.

REFERENCES

- [1] WHO. Antimicrobial resistance: global report on surveillance 2014. 2014. World Health Organization: Geneva, Switzerland. p. 257.
- [2] Harvey, A.L.; Edrada-Ebel, R.; Quinn, R.J. The re-emergence of natural products for drug discovery in the genomics era. *Nature Reviews: Drug Discovery*, 2015, **14**, 111-129.
- [3] Upadhyay, A.; Upadhyaya, I.; Kollanoor-Johny, A.; Venkitanarayanan, K. Combating pathogenic microorganisms using plant-derived antimicrobials: A minireview of the mechanistic basis. *BioMed Research International*, 2014, **2014**, 1-18.
- [4] Araya-Cloutier, C.; den Besten, H.M.W.; Aisyah, S.; Gruppen, H.; Vincken, J.-P., The position of prenylation of isoflavonoids and stilbenoids from legumes modulates the antimicrobial activity against Gram positive pathogens. (This thesis, Chapter 2).
- [5] Simons, R.; Gruppen, H.; Bovee, T.F.H.; Verbruggen, M.A.; Vincken, J.-P. Prenylated isoflavonoids from plants as selective estrogen receptor modulators (phytoSERMs). *Food & Function*, 2012, **3**, 810-827.
- [6] Tsuchiya, H.; Sato, M.; Miyazaki, T.; Fujiwara, S.; Tanigaki, S.; Ohyama, M.; Tanaka, T.; Iinuma, M. Comparative study on the antibacterial activity of phytochemical flavanones against methicillin-resistant *Staphylococcus aureus*. *Journal of Ethnopharmacology*, 1996, **50**, 27-34.

- [7] Botta, B.; Menendez, P.; Zappia, G.; de Lima, R.A.; Torge, R.; Delle Monache, G. Prenylated isoflavonoids: Botanical distribution, structures, biological activities and biotechnological studies. An update (1995-2006). *Current Medicinal Chemistry*, 2009, **16**, 3414-3468.
- [8] Mbaveng, A.T.; Kuete, V.; Ngameni, B.; Beng, V.P.; Ngadjui, B.T.; Meyer, J.J.M.; Lall, N. Antimicrobial activities of the methanol extract and compounds from the twigs of *Dorstenia mannii* (Moraceae). *BMC Complementary and Alternative Medicine*, 2012, **12**,
- [9] Sato, M.; Tanaka, H.; Tani, N.; Nagayama, M.; Yamaguchi, R. Different antibacterial actions of isoflavones isolated from *Erythrina poeppigiana* against methicillin-resistant *Staphylococcus aureus*. *Letters in Applied Microbiology*, 2006, **43**, 243-248.
- [10] Mukne, A.P.; Viswanathan, V.; Phadatare, A.G. Structure pre-requisites for isoflavones as effective antibacterial agents. *Pharmacognosy Reviews*, 2011, **5**, 13-18.
- [11] Eerdunbayaer; Mohamed A. A. Orabi; Hiroe Aoyama; Kuroda, T.; Hatano, T. Structures of new phenolics isolated from licorice, and the effectiveness of licorice phenolics on vancomycin-resistant *Enterococci*. *Molecules*, 2014, **19**, 13027-13041.
- [12] Hatano, T.; Shintani, Y.; Aga, Y.; Shiota, S.; Tsuchiya, T.; Yoshida, T. Phenolic constituents of licorice. VIII. Structures of glycofenone and glicoisoflavanone, and effects of licorice phenolics on methicillin-resistant *Staphylococcus aureus*. *Chemical & Pharmaceutical Bulletin*, 2000, **48**, 1286-1292.
- [13] Tanaka, H.; Sato, M.; Fujiwara, S.; Hirata, M.; Etoh, H.; Takeuchi, H. Antibacterial activity of isoflavonoids isolated from *Erythrina variegata* against methicillin-resistant *Staphylococcus aureus*. *Letters in Applied Microbiology*, 2002, **35**, 494-498.
- [14] Sato, M.; Tanaka, H.; Oh-Uchi, T.; Fukai, T.; Etoh, H.; Yamaguchi, R. Antibacterial activity of phytochemicals isolated from *Erythrina zeyheri* against vancomycin-resistant enterococci and their combinations with vancomycin. *Phytotherapy Research*, 2004, **18**, 906-910.
- [15] Rao, S.A.; Merugu, R.; Rao, M.J. Antibacterial and antifungal studies of prenylated isoflavones and prenylated 3-aryl coumarins isolated from *Derris scandens* BENTH. *Journal of Pharmacognosy*, 2012, **3**, 51-54.
- [16] Yin, S.; Fan, C.-Q.; Wang, Y.; Dong, L.; Yue, J.-M. Antibacterial prenylflavone derivatives from *Psoralea corylifolia*, and their structure-activity relationship study. *Bioorganic & Medicinal Chemistry*, 2004, **12**, 4387-4392.
- [17] Zhou, B.; Wan, C.-X. Phenolic constituents from the aerial parts of *Glycyrrhiza inflata* and their antibacterial activities. *Journal of Asian Natural Products Research*, 2014, 1-6.
- [18] Nanayakkara, N.P.D.; Burandt, C.L.; Jacob, M.R. Flavonoids with activity against methicillin-resistant *Staphylococcus aureus* from *Dalea scandens* var. *paucifolia*. *Planta Medica*, 2002, **68**, 519-522.
- [19] Wu, T.; Zang, X.; He, M.; Pan, S.; Xu, X. Structure-activity relationship of flavonoids on their anti-*Escherichia coli* activity and inhibition of DNA gyrase. *Journal of Agricultural and Food Chemistry*, 2013, **61**, 8185-8190.
- [20] Villinski, J.R.; Bergeron, C.; Cannistra, J.C.; Gloer, J.B.; Coleman, C.M.; Ferreira, D.; Azelmat, J.; Grenier, D.; Gafner, S. Pyrano-isoflavans from *Glycyrrhiza uralensis* with antibacterial activity against *Streptococcus mutans* and *Porphyromonas gingivalis*. *Journal of Natural Products*, 2014, **77**, 521-526.
- [21] Kar, S.; Roy, K. QSAR of phytochemicals for the design of better drugs. *Expert Opinion on Drug Discovery*, 2012, **7**, 877-902.
- [22] Yang, S.-Y. Pharmacophore modeling and applications in drug discovery: challenges and recent advances. *Drug Discovery Today*, 2010, **15**, 444-450.
- [23] Araya-Cloutier, C.; Vincken, J.-P.; den Besten, H.M.W.; van Ederen, R.; Gruppen, H., Rapid membrane permeabilization of *Listeria monocytogenes* and *Escherichia coli* induced by prenylated phenolic compounds: influence of skeleton structure and prenyl configuration. (This thesis, Chapter 3).
- [24] Hendrich, A.B.; Malon, R.; Pola, A.; Shirataki, Y.; Motohashi, N.; Michalak, K. Differential interaction of *Sophora* isoflavonoids with lipid bilayers. *European Journal of Pharmaceutical Sciences*, 2002, **16**, 201-208.
- [25] Tsuchiya, H.; Iinuma, M. Reduction of membrane fluidity by antibacterial sophoraflavanone G isolated from *Sophora exigua*. *Phytomedicine*, 2000, **7**, 161-165.
- [26] Wesołowska, O.; Gąsiorowska, J.; Petrus, J.; Czarnik-Matusiewicz, B.; Michalak, K. Interaction of prenylated chalcones and flavanones from common hop with phosphatidylcholine model membranes. *Biochimica et Biophysica Acta (BBA) - Biomembranes*, 2014, **1838**, 173-184.
- [27] Silhavy, T.J.; Kahne, D.; Walker, S. The bacterial cell envelope. *Cold Spring Harbor Perspectives in Biology*, 2010, **2**, 1-16.
- [28] van de Schans, M.G.M.; Ritschel, T.; Bovee, T.F.H.; Sanders, M.G.; de Waard, P.; Gruppen, H.; Vincken, J.-P. Involvement of a hydrophobic pocket and helix 11 in determining the

- modes of action of prenylated flavonoids and isoflavonoids in the human estrogen receptor. *ChemBioChem*, 2015, **16**, 2668-2677.
- [29] van de Schans, M.G.M.; Vincken, J.-P.; de Waard, P.; Hamers, A.R.M.; Bovee, T.F.H.; Gruppen, H. Glyceollins and dehydroglyceollins isolated from soybean act as SERMs and ER subtype-selective phytoestrogens. *The Journal of Steroid Biochemistry and Molecular Biology*, 2016, **156**, 53-63.
- [30] Bohnert, J.A.; Kern, W.V. Selected arylpiperazines are capable of reversing multidrug resistance in *Escherichia coli* overexpressing RND efflux pumps. *Antimicrobial Agents and Chemotherapy*, 2005, **49**, 849-852.
- [31] Aryani, D.C.; den Besten, H.M.W.; Hazeleger, W.C.; Zwietering, M.H. Quantifying strain variability in modeling growth of *Listeria monocytogenes*. *International Journal of Food Microbiology*, 2015, **208**, 19-29.
- [32] Dolezal, R.; Soukup, O.; Malinak, D.; Savedra, R.M.L.; Marek, J.; Dolezalova, M.; Pasdiorova, M.; Salajkova, S.; Korabecny, J.; Honegr, J.; Ramalho, T.C.; Kuca, K. Towards understanding the mechanism of action of antibacterial N-alkyl-3-hydroxypyridinium salts: Biological activities, molecular modeling and QSAR studies. *European Journal of Medicinal Chemistry*, 2016, **121**, 699-711.
- [33] Khazaei, A.; Sarmasti, N.; Seyf, J.Y. Quantitative structure-activity relationship of the curcumin-related compounds using various regression methods. *Journal of Molecular Structure*, 2016, **1108**, 168-178.
- [34] Saccenti, E.; Westerhuis, J.A.; Smilde, A.K.; van der Werf, M.J.; Hageman, J.A.; Hendriks, M.M.W.B. Simplivariate models: uncovering the underlying biology in functional genomics data. *Plos One*, 2011, **6**, e20747.
- [35] Gibbons, S. Anti-staphylococcal plant natural products. *Natural Product Reports*, 2004, **21**, 263-277.
- [36] Davey, H.M.; Hexley, P. Red but not dead? Membranes of stressed *Saccharomyces cerevisiae* are permeable to propidium iodide. *Environmental Microbiology*, 2011, **13**, 163-171.
- [37] Cruciani, G.; Pastor, M.; Guba, W. VolSurf: a new tool for the pharmacokinetic optimization of lead compounds. *European Journal of Pharmaceutical Sciences*, 2000, **11**, Supplement 2, S29-S39.
- [38] Cruciani, G.; Crivori, P.; Carrupt, P.A.; Testa, B. Molecular fields in quantitative structure-permeation relationships: the VolSurf approach. *Journal of Molecular Structure*, 2000, **503**, 17-30.
- [39] Hall, L.H.; Mohney, B.; Kier, L.B. The electrotopological state: structure information at the atomic level for molecular graphs. *Journal of Chemical Information and Computer Sciences*, 1991, **31**, 76-82.
- [40] Kier, L.B. An index of molecular flexibility from kappa shape attributes. *Quantitative Structure-Activity Relationships*, 1989, **8**, 221-224.
- [41] Roland, W.S.U.; van Buren, L.; Gruppen, H.; Driesse, M.; Gouka, R.J.; Smit, G.; Vincken, J.-P. Bitter taste receptor activation by flavonoids and isoflavonoids: Modeled structural requirements for activation of hTAS2R14 and hTAS2R39. *Journal of Agricultural and Food Chemistry*, 2013, **61**, 10454-10466.
- [42] Li, X.-Z.; Plésiat, P.; Nikaido, H. The challenge of efflux-mediated antibiotic resistance in Gram-negative bacteria. *Clinical Microbiology Reviews*, 2015, **28**, 337-418.
- [43] Galdiero, S.; Falanga, A.; Cantisani, M.; Tarallo, R.; Pepa, M.E.; D'Orlando, V.; Galdiero, M. Microbe-host interactions: structure and role of Gram-negative bacterial porins. *Current Protein & Peptide Science*, 2012, **13**, 843-854.
- [44] Braun, V.; Bös, C.; Braun, M.; Killmann, H. Outer membrane channels and active transporters for the uptake of antibiotics. *Journal of Infectious Diseases*, 2001, **183**, S12-S16.
- [45] Nikaido, H.; Rosenberg, E.Y. Porin channels in *Escherichia coli*: studies with liposomes reconstituted from purified proteins. *Journal of Bacteriology*, 1983, **153**, 241-252.
- [46] Nikaido, H. Molecular basis of bacterial outer membrane permeability revisited. *Microbiology and Molecular Biology Reviews*, 2003, **67**, 593-656.
- [47] Black, P.N.; Zhang, Q. Evidence that His'10 of the protein FadL in the outer membrane of *Escherichia coli* is involved in the binding and uptake of long-chain fatty acids: possible role of this residue in carboxylate binding. *Biochemical Journal*, 1995, **310**, 389-394.
- [48] van den Berg, B. The FadL family: unusual transporters for unusual substrates. *Current Opinion in Structural Biology*, 2005, **15**, 401-407.
- [49] Hirai, K.; Aoyama, H.; Irikura, T.; Iyobe, S.; Mitsuhashi, S. Differences in susceptibility to quinolones of outer membrane mutants of *Salmonella Typhimurium* and *Escherichia coli*. *Antimicrobial Agents and Chemotherapy*, 1986, **29**, 535-538.
- [50] Lambert, P.A. Cellular impermeability and uptake of biocides and antibiotics in Gram-positive bacteria and mycobacteria. *Journal of Applied Microbiology*, 2002, **92**, 46S-54S.

- [51] Liu, L.; Fang, Y.; Wu, J. Flexibility is a mechanical determinant of antimicrobial activity for amphipathic cationic α -helical antimicrobial peptides. *Biochimica et Biophysica Acta (BBA) - Biomembranes*, 2013, **1828**, 2479-2486.
- [52] Reißer, S.; Strandberg, E.; Steinbrecher, T.; Ulrich, Anne S. 3D Hydrophobic moment vectors as a tool to characterize the surface polarity of amphiphilic peptides. *Biophysical Journal*, 2014, **106**, 2385-2394.
- [53] Heller, H.; Schaefer, M.; Schulten, K. Molecular dynamics simulation of a bilayer of 200 lipids in the gel and in the liquid crystal phase. *The Journal of Physical Chemistry*, 1993, **97**, 8343-8360.
- [54] Selvaraj, S.; Krishnaswamy, S.; Devashya, V.; Sethuraman, S.; Krishnan, U.M. Influence of membrane lipid composition on flavonoid-membrane interactions: Implications on their biological activity. *Progress in Lipid Research*, 2015, **58**, 1-13.
- [55] Hendrich, A.B. Flavonoid-membrane interactions: possible consequences for biological effects of some polyphenolic compounds. *Acta Pharmacologica Sinica*, 2006, **27**, 27-40.

SUPPLEMENTARY INFORMATION

Table S4.1. List of molecular descriptors calculated with MOE for the QSAR analysis.

No.	Name	Description
1	<i>a_acc</i>	Number of hydrogen bond acceptor atoms
2	<i>a_don</i>	Number of hydrogen bond donor atoms
3	<i>a_nO</i>	Number of oxygen atoms
4	<i>AM1_dipole</i>	The dipole moment calculated using the AM1 Hamiltonian [MOPAC]
5	<i>AM1_HF</i>	The heat of formation (kcal/mol) calculated using the AM1 Hamiltonian
6	<i>AM1_HOMO</i>	The energy (eV) of the Highest Occupied Molecular Orbital calculated using the AM1 Hamiltonian
7	<i>AM1_LUMO</i>	The energy (eV) of the Lowest Unoccupied Molecular Orbital calculated using the AM1 Hamiltonian
8	<i>ASA</i>	Water accessible surface area calculated using a radius of 1.4 Å for the water molecule
9	<i>ASA⁻</i>	Water accessible surface area of all atoms with negative partial charge
10	<i>ASA_H</i>	Water accessible surface area of all hydrophobic ($ q_i < 0.2$) atoms
11	<i>ASA_P</i>	Water accessible surface area of all polar ($ q_i \geq 0.2$) atoms
12	<i>ASA⁺</i>	Water accessible surface area of all atoms with positive partial charge
13	<i>b_rotN</i>	Number of rotatable single bonds
14	<i>b_ar</i>	Number of aromatic bonds
15	<i>b_Cont_Rot</i>	Number of contiguous rotatable bonds
16	<i>b_double</i>	Number of double bonds
17	<i>bpol</i>	Sum of the absolute value of the difference between atomic polarizabilities of all bonded atoms in the molecule
18	<i>CASA⁻</i>	Negative charge weighted surface area, ASA^- times $\max\{q_i < 0\}$
19	<i>CASA⁺</i>	Positive charge weighted surface area, ASA^+ times $\max\{q_i > 0\}$
20	<i>chiral</i>	The number of chiral centers
21	<i>LogD^o</i>	Distribution coefficient at pH 7.2
22	<i>DASA</i>	Absolute value of the difference between ASA^+ and ASA^-
23	<i>dens</i>	Mass density: molecular weight divided by van der Waals volume
24	<i>diameter</i>	Largest value in the distance matrix
25	<i>dipole</i>	Dipole moment calculated from the partial charges of the molecule
26	<i>directional_hyd_sa</i>	Directional atomic hydrophobic surface area
27	<i>directional_pol_sa</i>	Directional atomic polar surface area
28	<i>FASA⁻</i>	Fractional ASA^- calculated as ASA^- / ASA
29	<i>FASA_H</i>	Fractional ASA_H calculated as ASA_H / ASA
30	<i>FASA_P</i>	Fractional ASA_P calculated as ASA_P / ASA
31	<i>FASA⁺</i>	Fractional ASA^+ calculated as ASA^+ / ASA
32	<i>FCASA⁻</i>	Fractional $CASA^-$ calculated as $CASA^- / ASA$

QSAR AND MODE OF ACTION OF PRENYLATED (ISO)FLAVONOIDS AS ANTIBACTERIALS

No.	Name	Description
33	FCASA ⁺	Fractional CASA+ calculated as CASA+ / ASA
34	glob	Globularity, or inverse condition number (smallest eigenvalue divided by the largest eigenvalue) of the covariance matrix of atomic coordinates.
35	KierFlex	Kier molecular flexibility index: (KierA1) (KierA2) / n
36	logS	Log of the aqueous solubility (mol/L)
37	MNDO_dipole	The dipole moment calculated using the MNDO Hamiltonian
38	MNDO_HF	The heat of formation (kcal/mol) calculated using the MNDO Hamiltonian
39	MNDO_HOMO	The energy (eV) of the Highest Occupied Molecular Orbital calculated using the MNDO Hamiltonian
40	MNDO_LUMO	The energy (eV) of the Lowest Unoccupied Molecular Orbital calculated using the MNDO Hamiltonian
41	mr	Molecular refractivity
42	npr1	Normalized PMI ratio pmi1/pmi3
43	npr2	Normalized PMI ratio pmi2/pmi3
44	opr_nring	The number of ring bonds
45	PBF	Plane of best fit
46	PC ⁻	Total negative partial charge
47	PC ⁺	Total positive partial charge
48	PEOE_RPC ⁻	Relative negative partial charge: the smallest negative q _i divided by the sum of the negative q _i
49	PEOE_RPC ⁺	Relative positive partial charge: the largest positive q _i divided by the sum of the positive q _i .
50	PEOE_VSA_FHYD	Fractional hydrophobic van der Waals surface area. This is the sum of the v _i such that q _i is less than or equal to 0.2 divided by the total surface area.
51	PEOE_VSA_FNEG	Fractional negative van der Waals surface area. This is the sum of the v _i such that q _i is negative divided by the total surface area
52	PEOE_VSA_FPNEG	Fractional negative polar van der Waals surface area. This is the sum of the v _i such that q _i is less than -0.2 divided by the total surface area.
53	PEOE_VSA_FPOL	Fractional polar van der Waals surface area. This is the sum of the v _i such that q _i is greater than 0.2 divided by the total surface area
54	PEOE_VSA_FPOS	Fractional positive van der Waals surface area. This is the sum of the v _i such that q _i is non-negative divided by the total surface area
55	PEOE_VSA_FPPOS	Fractional positive polar van der Waals surface area. This is the sum of the v _i such that q _i is greater than 0.2 divided by the total surface area
56	PEOE_VSA_HYD	Total hydrophobic van der Waals surface area. This is the sum of the v _i such that q _i is less than or equal to 0.2
57	PEOE_VSA_NEG	Total negative van der Waals surface area. This is the sum of the v _i such that q _i is negative.
58	PEOE_VSA_PNEG	Total negative polar van der Waals surface area. This is the sum of the v _i such that q _i is less than -0.2.
59	PEOE_VSA_POL	Total polar van der Waals surface area. This is the sum of the v _i such that q _i is greater than 0.2.
60	PEOE_VSA_POS	Total positive van der Waals surface area. This is the sum of the v _i such that q _i is non-negative.
61	PEOE_VSA_PPOS	Total positive polar van der Waals surface area. This is the sum of the v _i such that q _i is greater than 0.2.
62	PEOE_VSA+0	Sum of v _i where q _i is in the range [0.00,0.05)
63	PEOE_VSA+1	Sum of v _i where q _i is in the range [0.05,0.10)
64	PEOE_VSA+2	Sum of v _i where q _i is in the range [0.10,0.15)
65	PEOE_VSA+4	Sum of v _i where q _i is in the range [0.20,0.25)

No.	Name	Description
66	PEOE_VSA-0	Sum of v_i where q_i is in the range [-0.05,0.00]
67	PEOE_VSA-1	Sum of v_i where q_i is in the range [-0.10,-0.05]
68	PEOE_VSA-6	Sum of v_i where q_i is less than -0.30
69	petitjeanSC	Petitjean graph Shape Coefficient: (diameter - radius) / radius
70	PM3_dipole	The dipole moment calculated using the PM3 Hamiltonian
71	PM3_HF	The heat of formation (kcal/mol) calculated using the PM3 Hamiltonian
72	PM3_HOMO	The energy (eV) of the Highest Occupied Molecular Orbital calculated using the PM3 Hamiltonian
73	PM3_LUMO	The energy (eV) of the Lowest Unoccupied Molecular Orbital calculated using the PM3 Hamiltonian
74	radius	If r_i is the largest matrix entry in row i of the distance matrix D , then the radius is defined as the smallest of the r_i
75	rgyr	Radius of gyration
76	rings	The number of rings
77	RPC ⁻	Relative negative partial charge
78	RPC ⁺	Relative positive partial charge
79	SlogP_VSA0	Sum of v_i such that $L_i \leq -0.4$
80	SlogP_VSA4	Sum of v_i such that L_i is in (0.1,0.15]
81	SlogP_VSA5	Sum of v_i such that L_i is in (0.15,0.20]
82	SlogP_VSA7	Sum of v_i such that L_i is in (0.25,0.30]
83	SlogP_VSA8	Sum of v_i such that L_i is in (0.30,0.40]
84	SMR	Molecular refractivity
85	SMR_VSA0	Sum of v_i such that R_i is in [0,0.11]
86	SMR_VSA1	Sum of v_i such that R_i is in (0.11,0.26]
87	SMR_VSA3	Sum of v_i such that R_i is in (0.35,0.39]
88	SMR_VSA4	Sum of v_i such that R_i is in (0.39,0.44]
89	SMR_VSA5	Sum of v_i such that R_i is in (0.44,0.485]
90	SMR_VSA6	Sum of v_i such that R_i is in (0.485,0.56]
91	SMR_VSA7	Sum of v_i such that $R_i > 0.56$
92	std_dim1	Standard dimension 1: the square root of the largest eigenvalue of the covariance matrix of the atomic coordinates
93	std_dim2	Standard dimension 2: the square root of the second largest eigenvalue of the covariance matrix of the atomic coordinates.
94	std_dim3	Standard dimension 3: the square root of the third largest eigenvalue of the covariance matrix of the atomic coordinates.
95	TPSA	Polar surface area (\AA^2) calculated using group contributions to approximate the polar surface area from connection table information only.
96	vdw_area	Area of van der Waals surface (\AA^2) calculated using a connection table approximation
97	vdw_vol	van der Waals volume (\AA^3) calculated using a connection table approximation.
98	vol	van der Waals volume calculated using a grid approximation (spacing 0.75 A)
99	VSA	van der Waals surface area.

QSAR AND MODE OF ACTION OF PRENYLATED (ISO)FLAVONOIDS AS ANTIBACTERIALS

No.	Name	Description
100	<i>vsa_acc</i>	Approximation to the sum of VDW surface areas (\AA^2) of pure hydrogen bond acceptors
101	<i>vsa_hyd</i>	Approximation to the sum of VDW surface areas of hydrophobic atoms (\AA^2)
102	<i>vsa_other</i>	Approximation to the sum of VDW surface areas (\AA^2) of atoms typed as <i>other</i>
103	<i>vsa_pol</i>	Approximation to the sum of VDW surface areas (\AA^2) of polar atoms (atoms that are both hydrogen bond donors and acceptors), such as -OH
104	<i>vsurf_A</i>	Amphiphilic moment
105	<i>vsurf_D1</i>	Hydrophobic volume at -0.2
106	<i>vsurf_D2</i>	Hydrophobic volume at -0.4
107	<i>vsurf_D3</i>	Hydrophobic volume at -0.6
108	<i>vsurf_D4</i>	Hydrophobic volume at -0.8
109	<i>vsurf_D5</i>	Hydrophobic volume at -1.0
110	<i>vsurf_D6</i>	Hydrophobic volume at -1.2
111	<i>vsurf_D7</i>	Hydrophobic volume at -1.4
112	<i>vsurf_D8</i>	Hydrophobic volume at -1.6
113	<i>vsurf_EDmin1</i>	Lowest hydrophobic energy
114	<i>vsurf_EDmin2</i>	Second lowest hydrophobic energy
115	<i>vsurf_EDmin3</i>	Third lowest hydrophobic energy
116	<i>vsurf_EWmin1</i>	Lowest hydrophilic energy
117	<i>vsurf_EWmin2</i>	Second lowest hydrophilic energy
118	<i>vsurf_EWmin3</i>	Third lowest hydrophilic energy
119	<i>vsurf_G</i>	Surface globularity
120	<i>vsurf_HB1</i>	H-bond donor capacity at -0.2
121	<i>vsurf_HB2</i>	H-bond donor capacity at -0.5
122	<i>vsurf_HB3</i>	H-bond donor capacity at -1.0
123	<i>vsurf_HB4</i>	H-bond donor capacity at -2.0
124	<i>vsurf_HB5</i>	H-bond donor capacity at -3.0
125	<i>vsurf_HB6</i>	H-bond donor capacity at -4.0
126	<i>vsurf_HB7</i>	H-bond donor capacity at -5.0
127	<i>vsurf_HL1</i>	First hydrophilic-lipophilic balance
128	<i>vsurf_HL2</i>	Second hydrophilic-lipophilic balance
129	<i>vsurf_ID1</i>	Hydrophobic integy moment at -0.2
130	<i>vsurf_ID2</i>	Hydrophobic integy moment at -0.4
131	<i>vsurf_ID3</i>	Hydrophobic integy moment at -0.6
132	<i>vsurf_ID4</i>	Hydrophobic integy moment at -0.8
133	<i>vsurf_ID5</i>	Hydrophobic integy moment at -1.0
134	<i>vsurf_ID6</i>	Hydrophobic integy moment at -1.2

CHAPTER 4

No.	Name	Description
135	<i>vsurf_ID7</i>	Hydrophobic integy moment at -1.4
136	<i>vsurf_ID8</i>	Hydrophobic integy moment at -1.8
137	<i>vsurf_IW1</i>	Hydrophilic integy moment at -0.2
138	<i>vsurf_IW2</i>	Hydrophilic integy moment at -0.5
139	<i>vsurf_IW3</i>	Hydrophilic integy moment at -1.0
140	<i>vsurf_IW4</i>	Hydrophilic integy moment at -2.0
141	<i>vsurf_IW5</i>	Hydrophilic integy moment at -3.0
142	<i>vsurf_IW6</i>	Hydrophilic integy moment at -4.0
143	<i>vsurf_IW7</i>	Hydrophilic integy moment at -5.0
144	<i>vsurf_R</i>	Surface rugosity
145	<i>vsurf_S</i>	Interaction field surface area
146	<i>vsurf_V</i>	Interaction field volume
147	<i>vsurf_W1</i>	Hydrophilic volume at -0.2
148	<i>vsurf_W2</i>	Hydrophilic volume at -0.5
149	<i>vsurf_W3</i>	Hydrophilic volume at -1.0
150	<i>vsurf_W4</i>	Hydrophilic volume at -2.0
151	<i>vsurf_W5</i>	Hydrophilic volume at -3.0
152	<i>vsurf_W6</i>	Hydrophilic volume at -4.0
153	<i>vsurf_W7</i>	Hydrophilic volume at -5.0
154	<i>vsurf_Wp1</i>	Polar volume at -0.2
155	<i>vsurf_Wp2</i>	Polar volume at -0.5
156	<i>vsurf_Wp3</i>	Polar volume at -1.0
157	<i>vsurf_Wp4</i>	Polar volume at -2.0
158	<i>vsurf_Wp5</i>	Polar volume at -3.0
159	<i>vsurf_Wp6</i>	Polar volume at -4.0

^a Calculated at pH 7.2 with Marvin software (ChemAxon).

Table S4.2. Criteria for selection of the best QSAR models from the GA MLR population.

Parameter	Criteria
q^2 (continuous model)	> 0.50
Number of outliers (continuous model)	max. 2
Significance linear and binary models	$p < 0.05$
Number of descriptors	≤ 5
Descriptor inter-correlation (r)	≤ 0.70
Multicollinearity variance inflation factor (VIF)	< 4

Table S4.3. Correlation coefficient (r) matrices for the descriptors used in the different QSAR models.

L. monocytogenes

Descriptor ^a	KierFlex	PEOE_RPC ⁻	LogD	vsurf_A	vsurf_ID7	vsurf_W7
KierFlex	1					
PEOE_RPC ⁻	-0.70	1				
LogD	0.67	-0.08	1			
vsurf_A	-0.28	0.28	-0.19	1		
vsurf_ID7	0.05	-0.38	-0.35	-0.25	1	
vsurf_W7	0.18	-0.44	-0.19	-0.02	0.47	1

E. coli

Descriptor	α_{acc}	PEOE_VSA_FHYD	std_dim3	vsurf_Wp3
α_{acc}	1			
PEOE_VSA_FHYD	-0.51	1		
std_dim3	0.39	-0.03	1	
vsurf_Wp3	0.37	-0.70	0.38	1

^a Descriptor definition is in **Table S4.1**.

Table S4.4. Values of descriptors of the prenylated phenolic compounds used in the model for *L. monocytogenes* (sorted from highest to lowest activity).

Name	Activity (pMIC)	KierFlex	PEOE_RPC	vsurf_A	vsurf_W7	LogD	vsurf_ID 7
6,8-Diprenyl-genistein	4.831	4.958	0.152	3.432	0.250	5.540	1.840
Glabrol	4.816	5.029	0.171	2.986	0.000	5.800	0.224
4-O-Me-Glab	4.529	3.282	0.204	3.285	0.000	4.240	0.913
Wighteone	4.529	3.506	0.171	2.263	1.000	3.970	1.203
Hispaglabridin A	4.515	4.255	0.177	1.943	0.125	5.820	1.056
3'-OH-4'-O-Methyl-Glabridin	4.429	3.500	0.169	6.443	0.000	3.930	1.344
Dehydroglyceollidin II	4.416	2.845	0.239	2.117	0.125	4.400	0.749
Hispaglabridin B	4.373	3.409	0.187	2.020	0.875	5.300	0.620
Luteone	4.353	3.729	0.152	4.228	0.250	3.650	1.335
Isowighteone	4.335	3.506	0.172	5.541	0.000	4.110	0.572
Glabridin	4.330	2.918	0.202	5.076	0.000	4.090	0.859
Dehydroglyceollin I	4.330	2.186	0.251	5.020	0.000	3.890	1.057
Dehydroglyceollin II	4.248	2.186	0.256	4.592	2.250	3.890	0.812
Licoisoflavone A	4.152	3.729	0.152	3.181	1.250	3.790	1.234
Dehydroglyceollin IV	4.129	3.207	0.240	7.887	0.000	4.560	0.603
Glabrene	3.964	2.708	0.202	2.137	0.000	3.980	0.796
Glyceollin IV	3.851	3.500	0.175	5.095	0.500	3.580	0.987
Neobavaisoflavone	3.809	3.285	0.199	4.536	0.000	3.670	0.390
Iso-osajin	3.607	3.382	0.172	5.768	0.000	4.950	0.772
2,3-Dehydrokievitone	3.549	3.729	0.152	5.945	0.000	3.650	0.788
Glyceofuran	3.549	2.637	0.187	2.428	0.375	2.020	1.966
6-Prenyl-naringenin	3.532	3.769	0.168	3.238	0.375	4.450	1.242
Glyceollidin II	3.532	3.131	0.174	2.509	0.375	3.430	1.177
Glyceollin I	3.529	2.443	0.182	4.813	0.000	2.910	1.070
Glyceollin II	3.529	2.443	0.185	4.484	0.375	2.910	1.130
Glyceollin III	3.529	2.550	0.182	4.429	0.250	2.930	1.182
Lupiwighteone	3.529	3.506	0.170	4.661	0.375	3.970	0.794
Glyceollin V	3.527	2.375	0.212	5.336	0.250	3.120	1.207
Anhydrotuberosin	3.506	2.186	0.256	6.564	0.000	3.880	0.767
Dehydroglyceollin III	3.506	2.289	0.250	5.613	0.000	3.900	0.355

Table S4.5. Values of descriptors of the prenylated phenolic compounds used in the model for *E. coli* (sorted from highest to lowest activity).

Name	Activity (pMIC)	α_{acc}	PEOE_VSA_FHYD	std_dim3	vsurf_Wp3
Luteone	4.549	5	0.712	1.187	89.125
Wighteone	4.529	4	0.758	0.902	60.875
Glabridin	4.511	4	0.865	1.174	64.125
Licoisoflavone A	4.373	5	0.712	1.163	88.000
Isowighteone	4.228	4	0.758	0.864	78.750
6-Prenyl-naringenin	4.134	5	0.785	1.246	77.000
4-O-Me-Glab	4.131	4	0.922	1.222	47.500
Neobavaisoflavone	4.110	3	0.835	0.835	68.750
Dehydroglyceollin IV	3.828	3	0.920	0.888	54.375
Dehydroglyceollidin II	3.809	3	0.862	0.868	75.875
Glabrene	3.809	4	0.864	1.120	68.250
6,8-Diprenyl-genistein	3.609	4	0.808	0.999	82.125
Iso-osajin	3.607	4	0.873	1.053	78.250
Glabrol	3.594	4	0.870	1.197	94.250
Hispaglabridin A	3.594	4	0.894	1.220	75.625
Hispaglabridin B	3.592	4	0.931	1.215	58.875
3'-OH-4'-O-Methyl-Glabridin	3.549	5	0.871	1.098	66.375
Glyceollin IV	3.549	5	0.870	1.014	59.375
2,3-Dehydrokievitone	3.549	5	0.712	0.841	93.500
Glyceofuran	3.549	5	0.798	0.882	75.250
Glyceollidin II	3.532	5	0.811	1.044	78.125
Glyceollin I	3.529	5	0.852	0.872	55.750
Glyceollin II	3.529	5	0.852	0.872	57.125
Glyceollin III	3.529	5	0.850	0.944	59.125
Lupiwighteone	3.529	4	0.758	0.860	87.250
Glyceollin V	3.527	4	0.849	0.620	53.250
Dehydroglyceollin I	3.506	3	0.908	0.726	49.000
Dehydroglyceollin II	3.506	3	0.908	0.723	45.375
Dehydroglyceollin III	3.506	3	0.906	0.748	47.625

Table S4.6. Compounds matching all features of the pharmacophore models of *L. monocytogenes* and *E. coli* (hits obtained by performing a pharmacophore search in MOE).

<i>L. monocytogenes</i>	RMSD ^a	Result ^b
Luteone	0.432	+
Wighteone	0.339	+
Glabridin	0.514	+
4'-O-methyl-glabridin	0.499	+
Dehydroglyceollidin II	0.445	+
6,8-Diprenyl-genistein	0.440	+
Hispaglabridin A	0.447	+
Hispaglabridin B	0.306	+
3'-OH-4'-O-methyl-glabridin	0.511	+
Glyceollidin II	0.475	-
Glyceollin I	0.564	-
Dehydroglyceollin I	0.538	+
<i>E. coli</i>	RMSD	Result
Luteone	0.287	+
Wighteone	0.317	+
Glabridin	0.347	+
6-Prenyl-naringenin	0.291	+
4'-O-methyl-glabridin	0.340	+
Glabrene	0.343	-
Hispaglabridin A	0.284	-
Hispaglabridin B	0.407	-
3'-OH-4'-methyl-glabridin	0.389	-
Glyceollin I	0.352	-

^a Root mean standard deviation of the molecule from the model. ^b True positive (+), false positive (-).

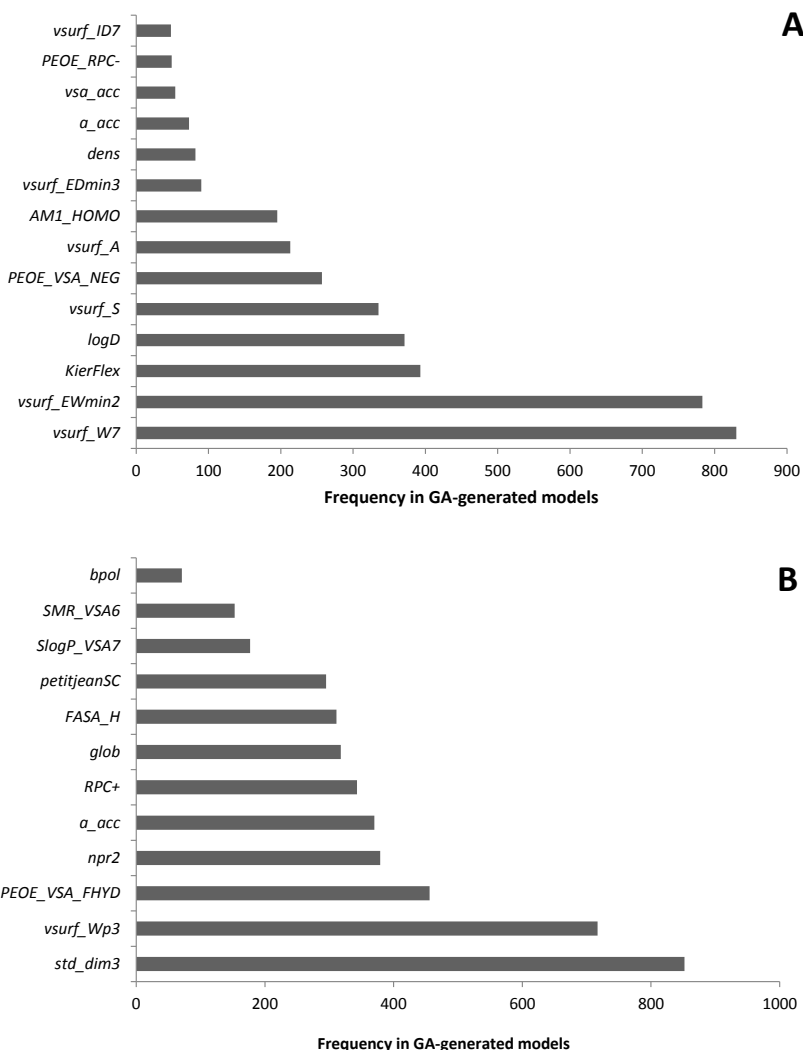


Figure S4.1. Most relevant descriptors selected using GA-driven variable selection method as implemented in MOE for regression models regarding the antibacterial activity against *L. monocytogenes* (A) and *E. coli* (B).

Structural basis for non-genuine phenolic acceptor substrate specificity of *Streptomyces roseochromogenes* prenyltransferase CloQ from the ABBA PT-barrel superfamily

Acceptor substrate specificity of *Streptomyces roseochromogenes* prenyltransferase SrCloQ was investigated using different non-genuine phenolic compounds. RP-UHPLC-UV-MSⁿ was used for the tentative annotation and quantification of the prenylated products. Flavonoids, isoflavonoids and stilbenoids with different types of substitution were prenylated by SrCloQ, although with less efficiency than the genuine substrate 4-hydroxyphenylpyruvate. The isoflavan equol, followed by the flavone 7,4'-dihydroxyflavone, were the best non-genuine acceptor substrates. B-ring C-prenylation was in general preferred over A-ring C-prenylation (ratio 5:1). Docking studies of non-genuine acceptor substrates with the B-ring oriented towards the donor substrate dimethylallyl pyrophosphate, showed that the carbonyl group of the C-ring was able to make stabilizing interactions with the residue Arg160, which might determine the preference observed for B-ring prenylation. No reaction products were formed when the acceptor substrate had no phenolic hydroxyl groups. This preference can be explained by the essential hydrogen bond needed between a phenolic hydroxyl group and the residue Glu281. Acceptor substrates with an additional hydroxyl group at the C3' position (B-ring), were mainly O3'-prenylated (> 80% of the reaction products). This can be explained by the proximity of the C3' hydroxyl group to the donor substrate at the catalytic site. Flavones were preferred over isoflavones by SrCloQ. Docking studies suggested that the orientation of the B ring and of the phenolic hydroxyl group at position C7 (A-ring) of flavones towards the residue Tyr233 plays an important role in this observed preference. Finally, the insights obtained on acceptor substrate specificity and regioselectivity for SrCloQ were extended to other prenyltransferases from the CloQ/NhpB family.

Keywords: aromatic prenyltransferase, enzyme catalysis, flavonoids, mass spectrometry.

Based on: Araya-Cloutier, C.; Martens, B.; Schaftenaar, G.; Leipoldt, F.; Gruppen, H.; Vincken, J-P. Structural basis for non-genuine phenolic acceptor substrate specificity of *Streptomyces roseochromogenes* prenyltransferase CloQ from the ABBA/PT-barrel superfamily. **Manuscript accepted in PLOS ONE.**

INTRODUCTION

Prenylation is one of nature's tools to modulate the bioactivity of primary^[1] and secondary metabolites^[2,3] by increasing their lipophilicity and, thereby, their interactions with biological targets, such as proteins and membranes.^[4] The enzymes responsible for transferring a prenyl group from a donor substrate (e.g. dimethylallyl pyrophosphate) to an acceptor substrate are known as prenyltransferases (PTs).^[5] Aromatic PTs catalyse the transfer reaction of prenyl moieties onto aromatic acceptors, such as phenolic acids, (iso)flavonoids, coumarins, naphthalenes, phenazines, and indole derivatives. These enzymes contribute substantially to the large diversity of secondary metabolites present in plants, fungi, and bacteria.^[6,7]

Plants from the Fabaceae family are well known for their production of prenylated isoflavonoids upon abiotic or biotic stress.^[8] The prenyl group is most often added to a free aromatic carbon (C-prenylation), but also to phenolic oxygens (O-prenylation).^[9] Several reports on legume PTs are available. PTs responsible for the production of glyceollins in soybean (*Glycine max* L.) and phaseollin in kidney bean (*Phaseolus vulgaris* L.) are localized in the membrane of plastids. Solubilisation of these PTs required detergents, which negatively affected enzyme activity and stability.^[10] Furthermore, characterization of *Sophora flavescens* PT revealed donor and acceptor specificity to be confined to the known genuine substrates (i.e. *in vivo* substrates).^[11] An overview of recently characterized plant PTs can be found elsewhere.^[12]

Contrary to plant PTs, microbial PTs appear to be attractive biotechnological tools as most of them are soluble, i.e. not membrane-bound^[4] and can potentially be obtained in significant amounts for the *in vitro* production of (novel) prenylated compounds.^[13] In the last decade, a new superfamily of soluble aromatic PTs isolated from microorganisms was discovered. This superfamily, named ABBA, has been considered for enhancement of molecular diversity and bioactivity of natural compounds due to their promiscuity for different non-genuine acceptor substrates.^[14] The ABBA superfamily is a group of enzymes with a unique type of PT barrel fold comprising a series of 5 repetitive $\alpha\beta\beta$ elements.^[13,15] More specifically, this PT-barrel is formed of 10 antiparallel β strands forming a spacious central solvent-filled cavity, where acceptor and donor substrates bind, surrounded by a ring of 10 α -helices.^[16] Structural analysis of these PTs has revealed that there is a tendency for polar residues to cluster into the top half of the cavity where the pyrophosphate isoprenoid donor substrate binds. Non-polar residues cluster in the lower half of the cavity where the acceptor substrate binds.^[17] Assays with microbial PTs have revealed broad aromatic acceptor substrate specificity, while often preserving donor substrate selectivity.^[18,19]

Phylogenetic analysis of the ABBA PT superfamily revealed two distinct homologous families: one comprises the indole PTs, i.e. the DMATS/CymD family; the other one comprises the phenol/phenazines PTs, i.e. the CloQ/NphB family.^[14,20] Within the CloQ/NphB family there are PTs involved in meroterpenoid and prenylated

phenazine biosynthesis (e.g. NphB, Fnq26, SCO7190, PpzP and Fur7) and PTs involved in novobiocin and clorobiocin biosynthesis (i.e. NovQ and CloQ).^[4,13]

Streptomyces roseochromogenes CloQ (*SrCloQ*) was one of the first members of the ABBA superfamily discovered.^[15,21] *SrCloQ* is an aromatic PT catalysing the C-prenylation (C₅ isoprenoid unit) of 4-hydroxyphenylpyruvate (4-HPP), as part of the biosynthesis of the antibiotic clorobiocin.^[21] More recent crystallization and simulation studies report key residues involved in substrate binding and on the mechanism of action of this enzyme (**Figure 5.1**). *SrCloQ* is thought to perform a Friedel-Crafts type of alkylation of the acceptor 4-HPP via the formation of a carbocation on the prenyl donor. The electropositive nature of the upper cavity of the PT barrel helps to lower the energy barrier to catalysis by facilitating the cleavage of the C–O bond of the isoprenoid donor substrate resulting in the formation of a prenyl cation.^[17] The prenyl cation, stabilized by charge delocalization, performs an electrophilic attack on the C3 of the aromatic ring of the acceptor substrate, resulting in an intermediary positive σ complex. The residue Glu281 is ideally placed in the active site to make a hydrogen bond with the phenolic hydroxyl group of 4-HPP and to neutralize the σ complex by proton abstraction. The residues Arg160 and Arg176 form salt bridges with the carboxyl group of 4-HPP, which is thought to be important for positioning the substrate.^[22] The residues Glu281 and Arg160 proved to be essential for good catalytic activity, while other residues (e.g. Cys215, Cys297) stabilise binding of the aromatic substrates in the active site.^[17,22]

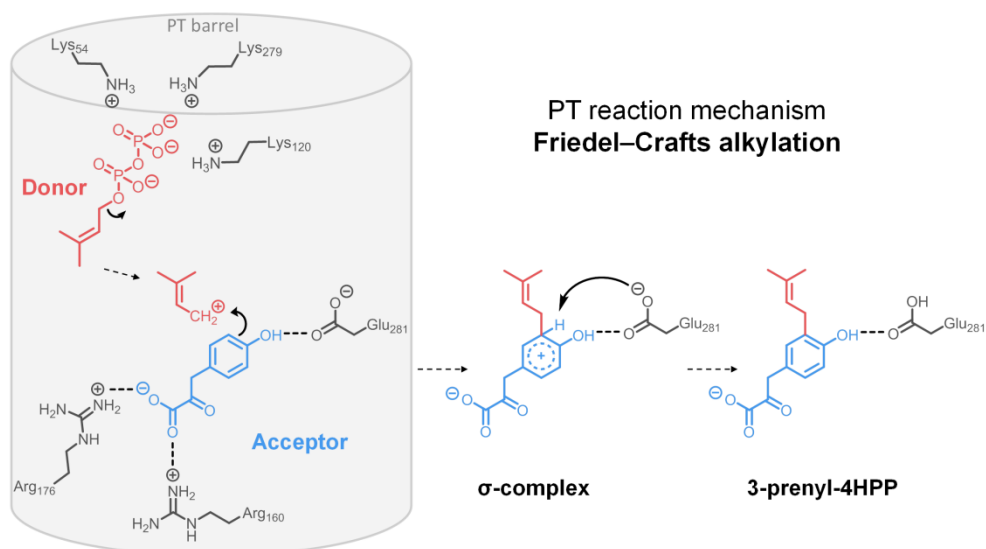


Figure 5.1. Schematic representation of the proposed mechanism of prenylation by *SrCloQ*, adapted from previous work.^[17] Important residues interacting with the donor and acceptor substrate are shown in grey colour. The donor substrate DMAPP is shown in red, whereas the genuine substrate is shown in blue.

To date, there have been no studies on the acceptor substrate specificity of SrCloQ regarding phenolic compounds, such as flavonoids, isoflavonoids and stilbenoids. Other studies with closely related PTs (e.g. *Streptomyces spheroides* NovQ) have reported the substrate specificity with phenolic compounds as acceptor substrates,^[18,19,23] but have not studied in detail the structural basis for non-genuine substrate specificity. In order to provide insight on the structural basis for prenylation of phenolic compounds, (iso)flavonoid and stilbenoid substrate specificities of SrCloQ were determined by *in vitro* enzymatic assays and analysis of reaction products by means of RP-UHPLC-UV-MSⁿ. Furthermore, we analysed *in silico* the interactions between the phenolic acceptors and SrCloQ's active site, and propose the interactions between the phenolic acceptor substrates and the active site residues, governing the substrate specificity experimentally observed. In addition, we compared the phenolic substrate specificity and regioselectivity of SrCloQ with that of other members of the CloQ/NphB family. We hypothesized that (iso)flavonoids will be prenylated by SrCloQ at the B-ring due to the similarities of this ring with the phenolic ring of SrCloQ's genuine substrate 4-HPP.

MATERIALS AND METHODS

Materials

The construction of the plasmid containing SrCloQ has been described elsewhere.^[21] Daidzein, genistein, dimethylallyl pyrophosphate (DMAPP, donor substrate), growth media (lysogeny broth (LB) and terrific broth (TB)) and antibiotics (kanamycin and chloramphenicol) were obtained from Sigma Aldrich (St. Louis, MO, USA). 3'-Hydroxydaidzein was obtained from Alfa Aesar (Ward Hill, MA, USA) and all other pure (iso)flavonoids and resveratrol were obtained from ICC Chemical Corporation (New York, NY, USA). Acetonitrile (ACN; ULC/MS grade), water acidified with 0.1% (v/v) acetic acid (HOAc) (ULC/MS grade), and methanol (MeOH) (ULC/MS grade) were purchased from Biosolve (Valkenswaard, The Netherlands). Water for purposes other than UHPLC was prepared using a Milli-Q water purification system (Millipore, Molsheim, France). Glycerol was purchased from VWR International BV (Radnor, PA, USA). Other chemicals were purchased from Merck (Darmstadt, Germany) or Sigma Aldrich.

Expression and purification of SrCloQ

Production of SrCloQ was based on previous studies.^[16,21] Calcium chloride transformation was performed with cells of *Escherichia coli* Rosetta (DE3) plysS (Promega, Madison, WI, USA). Cells harbouring *Srcloq* were cultured in TB medium supplemented with chloramphenicol (34 $\mu\text{g}/\text{mL}$) and kanamycin (50 $\mu\text{g}/\text{mL}$). Induction with isopropyl thiogalactoside (IPTG, Promega) was performed for 19 h at 20 °C, after an OD_{600nm} of 0.6 was reached. After harvesting the cells, cells were resuspended in lysis buffer (2.5 mL lysis buffer/g cells; 50 mM Tris-HCl pH 8.0, 500 mM NaCl, 10% (v/v)

glycerol, 10 mM β -mercaptoethanol, 1% (v/v) Tween 20, 20 mM imidazole, 0.5 mM phenylmethylsulfonyl fluoride, 0.5 mg/mL lysozyme). Lysis was performed by sonication (Sonifier S-250D, Branson, Danbury, CT, USA) in 9 sets of 30 s at an amplitude of 30% (pulse was alternatively turned on and off for periods of 10 s). The His-tagged *SrCloQ* was purified from the cell lysate by affinity chromatography with an ÄKTA explorer system (GE Healthcare, Little Chalfont, UK), using a 20-250 mM imidazole gradient on a HisTrap HP 5 mL column (GE Healthcare). The fractions containing the His-tagged protein were pooled, concentrated and desalted using Amicon Ultra-15 10K centrifugal filter devices (Merck Millipore, Billerica, MA, USA).

Protein content and composition

Protein content was determined according to Bradford. A calibration curve was made with bovine serum albumin (BSA) in concentrations of 0.25-1.0 mg/mL. Enzyme purity was confirmed by SDS-PAGE under reducing conditions on a Mini-protean II system (Bio-Rad Laboratories, Hercules, CA, USA), according to the manufacturer's instructions. Commercially prepared mini-protean TGX gels (Bio-Rad) were used with Coomassie InstantBlue (Expedion, Cambridge, UK), with the marker Precision Plus Protein™ dual colour standards (Bio-Rad). Samples (8 μ L) were loaded onto a gel, and the separation was done by applying 200 V for 45 min.

Assay for PT activity

The reaction mixture contained 0.5 mM aromatic substrate (4-HPP, flavonoids, isoflavonoids or resveratrol), 0.5 mM DMAPP, 500 mM NaCl, 10% (v/v) glycerol, 100 mM Tris·HCl buffer (pH 7.5), 7 mM Mg^{2+} (in the form of $MgCl_2$, for enhancement of activity) and 30 μ M purified *SrCloQ*. In analogy with previous studies on the *in vitro* prenylation of flavonoids with *Streptomyces* sp. strain CL190 (*ScINphB*, 22% identity with *SrCloQ*),^[15,18] incubation time of *SrCloQ* with the non-genuine substrates was prolonged in comparison with that of the genuine substrate 4-HPP (24-48 h), due to the anticipated lower efficiency in conversion of the (iso)flavonoids. The mixtures were incubated for a maximum of 48 h at 30 °C. The reaction was ended by adding 400 μ L ethyl acetate containing 0.5% (v/v) formic acid. The solution was vortexed and centrifuged (room temperature, 5 min, 10,000 g), after which the organic layer was evaporated and the residue was re-suspended in 100 μ L methanol for analysis on RP-UHPLC-MS. Experiments were performed in duplicate.

Analysis of reaction products

Reaction products were analysed by Ultra High Performance Liquid Chromatography and Mass Spectrometry (UHPLC-MS). An Accela Velos UHPLC system (Thermo Scientific, San Jose, CA, USA) was equipped with a pump, autosampler and photodiode array (PDA) detector. Samples (1 μ L) were loaded onto an Acquity UPLC BEH Shield RP18 column (2.1 i.d. mm x 150 mm, 1.7 μ m particle size; Waters, Milford, MA, USA) with an

Acquity UPLC BEH Shield RP18 VanGuard pre-column (2.1 i.d. mm x 5 mm, 1.7 μ m particle size; Waters).

Water containing 0.1% (v/v) HOAc + 1% (v/v) ACN, eluent A, and ACN containing 0.1% (v/v) HOAc, eluent B, were used as solvents at a flow rate of 300 μ L/min. The following elution profile was used: 1 min isocratic at 9% B; 1.5 min linear gradient from 9-25% B; 7 min linear gradient from 25-50% B; 3 min isocratic on 50% B; 10 min linear gradient from 50-100% B; 2 min isocratic on 100% B, 1 min linear gradient from 100-9% B. Column temperature was set at 40 °C and PDA detector was set to measure from 200-600 nm.

Mass spectrometric (MS) analysis was performed on a LTQ Velos (Thermo Scientific), which was equipped with a heated ESI-MS probe coupled to the RP-UHPLC. Full scan MS was performed in both negative ionisation (NI) and positive ionisation (PI) mode, in which data were acquired in a m/z range of 90-1500 Da. For tentative annotation, data-dependent MS^n analysis on the most intense (product) ion was performed with normalised collision energy of 35%. Prenylated products were monitored by single ion monitoring (SIM) scanning mode followed by single reaction monitoring (SRM) on the most abundant fragment ions. The system was tuned with genistein in PI and NI mode via automatic tuning using Tune Plus (Xcalibur v.2.2, Thermo Scientific). Nitrogen was used as sheath and auxiliary gas. The ITT temperature was 400 °C and the source voltage was 3.50 kV (NI) or 4.50 kV (PI).

The tentative annotation of prenylated reaction products was performed by means of Xcalibur (version 2.2., Thermo Scientific). The position of the prenyl group within the phenolic skeleton (i.e. A- or B-ring) was elucidated by analysis of the *retro*-Diels-Alders (RDA) fragments^[24] in PI: when the C-ring of (iso)flavonoids was cleaved in MS^3 , one of the remaining fragments still contained one carbon reminiscent of the prenyl chain (split in MS^2), which can be used to diagnose the ring at which the prenyl was attached.^[25]

Quantification of phenolic compounds was performed using the following equation (Eq. 5.1),^[26] derived from the Lambert-Beer's law:

$$C = \frac{area \times Q}{\epsilon \times l \times V_{inj} \times k_{cell}} \quad (\text{Eq. 5.1})$$

in which C is concentration (M), *area* is the integrated area of the UV peak at the specific wavelength (AU·s), Q is the flow rate (5 μ L/s), ϵ is the molar extinction coefficient (AU/M·cm), *l* is the path length of the UV cell provided by the manufacturer (5 cm), V_{inj} is the injected volume of sample (1 μ L), and k_{cell} is a constant related to the cell geometry of the UV detector.^[26] This equation relates the duration of absorbance given by the UHPLC system (AU·s) to an actual absorbance value (AU) for the Lambert-Beer's equation. The k_{cell} represents the correction factor for the absorption of light by the coating material of the flow cell. The k_{cell} (0.82 ± 0.09) was determined with standard solutions of daidzein (248 nm), genistein (263 nm) and resveratrol (310 nm) (with five

concentrations each, in the range of 0.001-0.1 mg/mL). The ϵ of the prenylated reaction products was assumed to be the same as that of the non-prenylated substrate, as shown in **Table S5.1**. The percentage of conversion of the different aromatic substrates was calculated as the μ moles of prenylated products formed from 500 μ M of substrate used in the assay, multiplied by 100.

***In silico* modelling**

Molecular Operating Environment (MOE), 2013.08 (Chemical Computing Group, Montreal, QC, Canada) was used to analyse the PT structure and to perform docking studies. The *SrCloQ* model (Protein Database entry 2XLQ) with the substrate 4-hydroxyphenylpyruvate (4-HPP) bound to the active site was used for the docking studies.^[17] The location of the DMAPP substrate inside the *SrCloQ* active site was modelled based on the position of the geranyl pyrophosphate (GPP) inside *ScINphB* (PDB 1ZB6).^[27] The placement of DMAPP was achieved by first creating a 3D alignment of the 2XLQ and 1ZB6 structures and subsequently taking the GPP position and transferring it to the 2XLQ structure, followed by molecular editing to convert GPP into DMAPP. Finally, a local geometry optimization was performed, at which only DMAPP was kept flexible. Further refinement of the DMAPP and 4-HPP position was performed using MMFF94x energy minimization in MOE. The *LigX* module in MOE was used as a guide to confirm that the placement was in line with that of the GPP inside 1ZB6. In accordance with previous literature,^[17,22] our modelled negatively charged donor substrate DMAPP (**Figure S5.1**) made interactions with the positively charged residues Lys54, Arg66, Lys 279, and Lys120, and with the aromatic residues Tyr233 and Tyr174. The genuine substrate 4-HPP made the essential hydrogen bond with the residue Glu281, as well as with Arg160 and Arg176.

The 3D structures of the phenolic compounds were built with MOE and MMFF94x energy minimization (gradient 0.01) was performed for all molecules. Induced fit was used as docking mode.

RESULTS

Enzyme activity of *SrCloQ*

SrCloQ was expressed as His-tagged protein in *E. coli* and purified by Ni²⁺ affinity chromatography (**Figure S5.2**). The purified enzyme showed the expected molecular mass (35 kDa)^[21] and an estimated purity of > 90% according to the SDS-PAGE analysis (**Figure S5.3**). Activity of *SrCloQ* was confirmed in control experiments with its genuine substrate (4-HPP); incubations without *SrCloQ* did not yield prenylated products (**Figure S5.4**).

Figure 5.2 shows the structure of all aromatic acceptor substrates tested, i.e. flavonoids, isoflavonoids and the stilbenoid resveratrol, as well as the percentage of molar conversion by *SrCloQ*. Compounds had different types of substituents, such as

hydroxyl, methoxyl and carbonyl groups, at different positions of the skeleton. For optimal visualization, the structures of compounds are oriented with the B-ring of the phenolics in the same direction as the phenol ring of the genuine substrate 4-HPP. *SrCloQ* showed promiscuity in that it was able to use most phenolics provided as acceptor substrates, i.e. we found reaction products for 10 out of 12 phenolic compounds tested. As expected, conversion of the genuine substrate 4-HPP was more efficient (> 80% conversion) in comparison to those of the other phenolic test substrates (< 10% conversion) under the conditions used. Of all phenolics tested, the isoflavan equol and the flavone 4',7-dihydroxyflavone were the best substrates for prenylation. Daidzein and genistein were converted only in very small amounts, whereas isoflavone (no hydroxyl groups present) and glycitein (methoxyl group at position C6) were not converted at all.

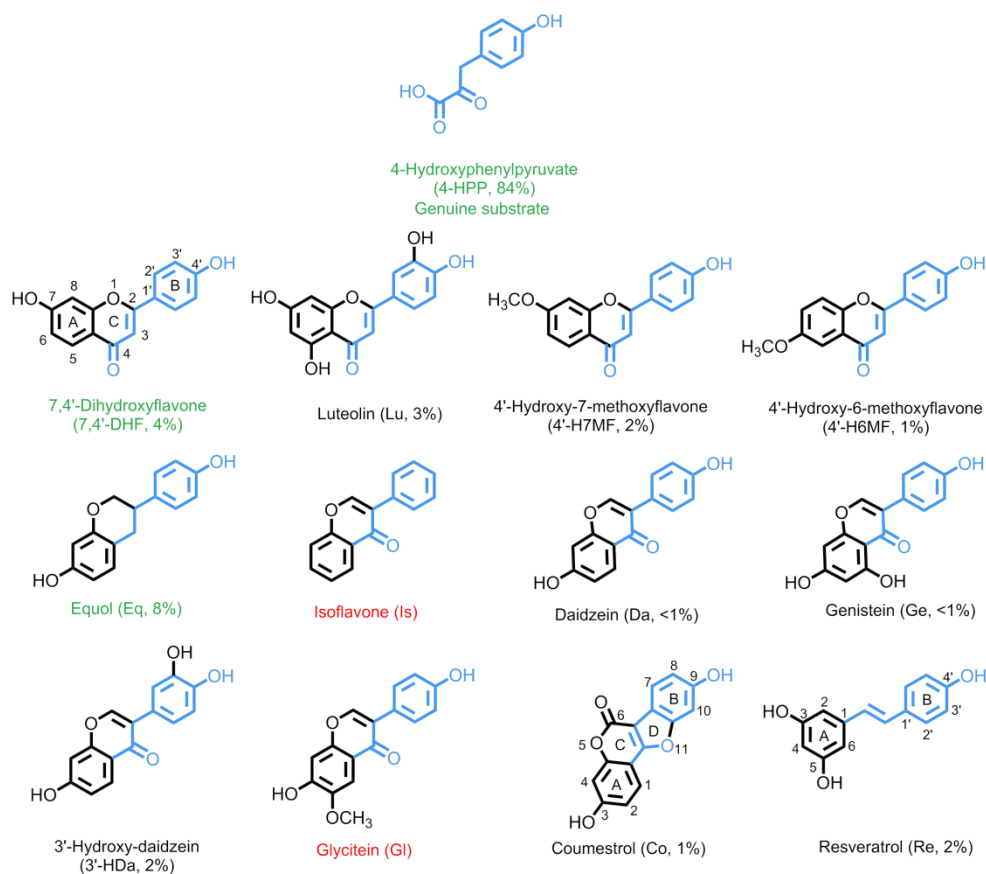


Figure 5.2. Aromatic acceptor substrates and their percentage of conversion (molar %) by *SrCloQ*. The atoms shared with the genuine substrate are highlighted in blue colour. Phenolic substrates with green label represent the best acceptor substrates, whereas those with red labels were not utilized by the enzyme.

Structure elucidation of reaction products

Table 5.1 shows the list of reaction products tentatively annotated by means of UHPLC-UV-MSⁿ. Prenylation of substrates was confirmed by the neutral loss of 56 Da [C₄H₈] or 68 Da [C₅H₉] in NI and/or PI mode.^[28] For more in-depth structural elucidation, tandem MS, single-ion-monitoring and single-reaction-monitoring scan modes were used to tentatively annotate the reaction products with respect to A- or B-ring prenylation and C- or O-prenylation.

A- or B-ring prenylation. Analysis of the *retro*-Diels-Alder (RDA) fragment ions from prenylated isomers in both NI and PI mode was used to determine the position of the prenyl substituents (A- or B-ring). The formation of the RDA fragments upon cleavage of the C-rings of (iso)flavonoids leave (part of) the prenyl group attached to the phenolic ring, which results in diagnostic fragments.^[25] The most common bonds in (iso)flavonoids split, resulting in A-ring and B-ring containing ions, are the 1/3, 2/3, 0/2, 0/3, 0/4 or 2/4 bonds of the C-ring.^[24]

Figures 5.3A and 5.3B show the UV and MS in NI mode chromatograms of the reaction products of equol incubated with SrCloQ. The two main prenylated products formed eluted at 16.9 min (peak **8**) and 17.1 min (peak **9**). **Figures 5.3C and 5.3D** show the MS² spectra of these prenylated equol isomers. Peak **8** showed high abundances of ions with *m/z* 121, 187 and 135. These values matched the RDA fragments of B-ring prenylated equol, i.e. ^{1,3}A⁻, ^{1,3}B⁻ and ^{2,3}A⁻, respectively, as shown by the fragmentation pattern (**Figure 5.3C**). Peak **9** had different main *m/z* values (189, 203 and 119). These ions were formed by the same fragmentation pathways as described before, but now the RDA fragments corresponded with A-ring prenylated equol (**Figure 5.3D**).

C- or O-prenylation. Tandem MS analysis was used to distinguish O- and C-prenylation of the aromatic substrates. **Figures 5.4A and 5.4B** show the UV and MS in PI mode chromatograms of the prenylated products of 4'-hydroxy-7-methoxyflavone produced by SrCloQ. Three main prenylated isomers were found. Two distinct fragmentation patterns could be distinguished for these isomers. Peak **14** and **15** showed [M+1-56]⁺ as main fragment (**Figure 5.4C** for peak **15**; see **Table 5.1** for peak **14** fragmentation). Peak **16** showed [M+1-68]⁺ as the main fragment (**Figure 5.4D**). The prenyl group generates the fragment [M+H-56]⁺ when it is attached to a carbon of an aromatic ring,^[28] as in the MS² of peak **14** and **15**. When it is attached to an oxygen of an aromatic ring, the prenyl group will split off intact ([M+H-68]⁺)^[16], leaving the original aromatic substrate as main daughter ion, as in the MS² spectrum of peak **16**. Moreover, the higher retention time of peak **16** in comparison with peak **14** and **15** on the reversed phase column, reflects that peak **16** is less polar than the other two, supporting our tentative annotation of O-prenylation of this reaction product.

Table 5.1. *SyCloQ* reaction products tentatively annotated by RP-UHPLC-UV-MSⁿ.

Substrate	Conversion (%)	No.	RT (min)	λ_{\max}	[M-H] ⁻	MS ² NI mode (rel. abundance)	[M+H] ⁺	MS ² PI mode (rel. abundance)	MS ³ PI mode (rel. abundance)	Tentative annotation
4-HPP	8.4 ± 1.5	1	7.8	279	189	134 (100), 174 (10)	n.d. ^a			C-prenyl-4-HBAL ^b
		2	8.9	n.d.	189	134 (100), 174 (10)	n.d.			C-prenyl-4-HBAL
		3	9.1	n.d.	189	134 (100), 174 (10)	n.d.			C-prenyl-4-HBAL
		4	9.9	278	219	175 (100), 201 (10)	n.d.			C-prenyl-4-HPA ^b
Eq	7.7 ± 1.4	5	10.1	278	219	175 (100)	n.d.			C-prenyl-4-HPA
		6	11.4	278	189	134 (100), 174 (10)	n.d.			C-prenyl-4-HBAL
Eq	7.7 ± 1.4	7	12.6	285	189	134 (100), 174 (10)	n.d.			C-prenyl-4-HBAL
		8	16.9	n.d.	309	121 (100), 187 (70), 135 92 (100), 77 (25), 65 (15)	311	123 (100), 175 (90), 255 95 (100), 67 (35), 77 (10)	(50), 189 (40), 149 (15), 201 (10)	B _{ring} -C-prenyl-Eq
7,4'-DHF	4.2 ± 1.2	9	17.1	285	309	189 (100), 203 (20), 119 134 (100)	311	191 (100), 205 (50), 255 173 (100), 149 (50), 145	(10), 137 (10), 135 (10)	A _{ring} -C-prenyl-Eq ^f
		10	14.5	334	321	266 (100), 265 (10)	323	267 (100), 268 (15)	239 (100), 213 (80), 240(20), 228(20)	B _{ring} -C-prenyl-7,4'-DHF
Lu	3.2 ± 0.6	11	13.4	n.d.	353	151 (100), 284 (95), 283 n.d.	355	n.d.	n.d.	C-prenyl-Lu
		12	14.4	n.d.	353	(90), 201 (70), 335 (50), 324 (20)	355	n.d.	n.d.	B _{ring} -C-prenyl-Lu
Lu	3.2 ± 0.6	13	16.5	266, 348	353	151(100), 298 (50), 201 107 (100), 83 (10)	355	287(100)	153 (100), 287 (90), 259	O-prenyl-Lu
						(30), 231 (20), 335 (15)			(50), 245 (30), 241 (30), 161 (20)	

Substrate	Conversion (%)	No.	RT (min)	λ_{max}	[M-H] ⁻	MS ² NI mode (rel. abundance)	MS ² NI mode (rel. abundance)	[M+H] ⁺	MS ² PI mode (rel. abundance)	MS ² PI mode (rel. abundance)	Tentative annotation
4'-H-7-MF	1.7 ± 0.3	14	16.6	334	357, 335 ^c , 342 (100), 343 (20), 207 342 (100), 341 (90), 343 (40), 325 (30), 314 (20), 205 (20)	342 (100), 343 (20), 207 342 (100), 341 (90), 343 (40), 325 (30), 314 (20), 205 (20)	342 (100), 343 (20), 207 342 (100), 341 (90), 343 (40), 325 (30), 314 (20), 205 (20)	359, 337 ^c	281 (100), 344 (30), 253 (30), 282 (20)	253 (100), 227 (25), 254 (20)	B _{ring} -C-prenyl-4'-H-7-MF
		15	17.2	335	335	280 (100), 320 (80), 277 n.d.	280 (100), 320 (80), 277 n.d.	337	281 (100), 282 (15)	253 (100), 227 (90), 254 (20), 228 (15)	B _{ring} -C-prenyl-4'-H-7-MF
		16	18.2	327	357, 335 ^c n.d.	n.d.	n.d.	359, 337 ^c	268 (100), 331 (30), 269 (20)	240 (100), 241 (20)	4'-O-prenyl-7-MF
3-HDa	1.7 ± 0.4	17	10.9	n.d.	337	268 (100), 201 (25), 309 n.d.	268 (100), 201 (25), 309 n.d.	339	n.d.	n.d.	B _{ring} -C-prenyl-3-HDa
		18	12.8	n.d.	337	(10), 293 (10), 135 (10)	(10), 293 (10), 135 (10)	339	n.d.	n.d.	prenyl-3-HDa
		19	13.2	260	337	268 (100)	268 (100)	339	271 (100), 283 (10)	137 (100), 243 (90), 253 (85), 215 (80), 225 (80), 161 (20), 181 (15), 201 (10)	O-prenyl-3-HDa
Re	1.6 ± 0.3	20	13.5	n.d.	295	240 (100), 251 (80), 235 n.d.	240 (100), 251 (80), 235 n.d.	n.d.	n.d.	n.d.	A _{ring} -C-prenyl-Re
		21	14.2	323	295	(50), 253 (35), 225 (30)	(50), 253 (35), 225 (30)	n.d.	n.d.	n.d.	B _{ring} -C-prenyl-Re
		22	16.6	320	295	240 (100), 251 (60), 253 195 (100), 212 (75), 170 (30), 225 (30)	240 (100), 251 (60), 253 195 (100), 212 (75), 170 (30), 225 (30)	n.d.	269 (100), 270 (15), 281 (20), 241 (100), 225 (30), 197 (25), 242 (20)	O-prenyl-Re	
Co	0.8 ± 0.3	23	18.5	349	335	279 (100), 280 (25), 292 251 (100), 279 (40), 223 (20)	279 (100), 280 (25), 292 251 (100), 279 (40), 223 (20)	337	269 (100), 270 (15), 281 (20), 241 (100), 225 (30), 197 (25), 242 (20)	269 (100), 270 (15), 281 (20), 241 (100), 225 (30), 197 (25), 242 (20)	C-prenyl-Co
		24	19.6	n.d.	335	266 (100), 279 (10)	266 (100), 279 (10)	337	n.d.	n.d.	O-prenyl-Co
		25	17.2	330	357, 335 ^c	342 (100), 343 (20)	298 (100), 314 (30), 251 (25)	359, 337 ^c	281 (100), 344 (40), 282 (20), 253 (100), 254 (20), 225 (20), 316 (20), 253 (15)	(10), 242 (10)	B _{ring} -C-prenyl-4'-H-6-MF
		26	17.4	n.d.	357, 335 ^c n.d.	n.d.	359, 337 ^c n.d.	n.d.	n.d.	n.d.	MF
		27	18.6	n.d.	357, 335 ^c	342 (100), 343 (20)	357, 335 ^c	359, 337 ^c n.d.	n.d.	n.d.	prenyl-4'-H-6-MF

Substrate	Conversion (%)	No.	RT (min)	λ_{max}	$[\text{M}-\text{H}]^-$	MS^2 NI mode (rel. abundance)	MS^3 NI mode (rel. abundance)	$[\text{M}+\text{H}]^+$	MS^2 PI mode (rel. abundance)	MS^3 PI mode (rel. abundance)	Tentative annotation
Da	0.6 ± 0.2	28	15.0	n.d.	321	265 (100), 266 (60), 278 (15), 252 (10)	n.d.	323	267 (100), 268 (10)	255 239 (100), 240 (15), 211 (15), 137 (10)	$\text{B}_{\text{ring}}-\text{C}-\text{prenyl}-\text{Da}$
Ge	0.4 ± 0.1	29	17.7	263	337	281 (100), 282 (30), 293 (15)	n.d.	n.d.			$\text{B}_{\text{ring}}-\text{C}-\text{prenyl}-\text{Ge}$
Gl	n.p. ^e	30	17.9	266	337	282 (100)	n.d.	n.d.			$\text{A}_{\text{ring}}-\text{C}-\text{prenyl}-\text{Ge}$
Is	n.p.	31	19.0	n.d.	337	268 (100), 255 (10)	n.d.	n.d.			$\text{O}-\text{prenyl}-\text{Ge}$

^a Not determined (n.d.). ^b Under alkaline conditions 4-HPP decomposes to 4-Hydroxybenzaldehyde (4-HBAL) or 4-hydroxyphenylacetic acid (4-HPA).^[21,29] ^c Parent ion formed a sodium adduct. The italic *m/z* represents the $[\text{M}-\text{H}]^-$ or $[\text{M}+\text{H}]^+$ ion. ^d Not annotated (n.a.). ^e No products formed (n.p.). ^f Based on previous studies on the MS fragmentation of standard isoflavones^[25] we proposed this product to be C8-prenyl-euol.

In cases where O-prenylation could occur at both the A- and the B-ring (contrary to 4'-hydroxy-7-methoxyflavone, which has only one OH group available), the annotation of the A- or B-ring position of the prenyl group was not possible, because the prenyl detached completely in MS^2 , leaving no footprints to annotate the ring position.

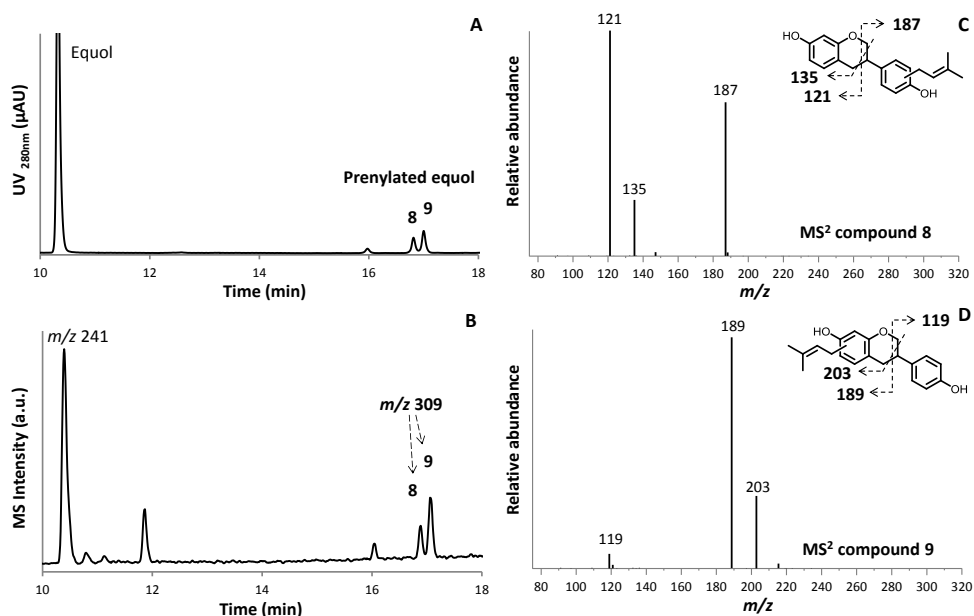


Figure 5.3. RP-UHPLC-UV (A) and MS in NI (B) profiles of equol and prenylated equol products (products **8** and **9** in Table 5.1) after incubation of equol with DMAPP and *SrCloQ*. MS^2 spectra of C-prenylated equol (m/z 309) at retention times 16.9 (**8**, panel C) and 17.1 min (**9**, panel D). The proposed RDA fragmentation pathways are shown as inset.

***SrCloQ* favours B-ring C-prenylation of (iso)flavonoids and stilbenoids**

For all phenolic substrates tested with *SrCloQ*, the prenylated products obtained were tentatively annotated using the above rationale. **Figure 5.5** shows the composition of the mixture of prenylated isomers formed by *SrCloQ*. The enzyme favoured B-ring C-prenylation of substrates in aromatic rings. Considering the regioselectivity of *SsNovQ* (84% sequence identity with *SrCloQ*) towards daidzein and genistein,^[23] we postulate that the C3' (B-ring) is the preferred position for prenylation by *SrCloQ*. The only substrates that were A-ring prenylated were equol and genistein, albeit the latter in minute amounts. It was not possible to annotate the ring position of the prenyl group in coumestrol, as coumestrol does not undergo typical RDA fragmentation.^[30,31] Consequently no apparent A- or B-ring fragment ions were formed in MS^n . Additionally, A-ring and B-ring prenylated coumestrol have been shown to yield the same fragmentation pattern in MS.^[32,33] Resveratrol does not show RDA fragmentation due to the lack of the C-ring. Thus, reaction products of resveratrol were tentatively annotated

based on the fragmentation behaviour of (prenylated) resveratrol previously reported.^[34,35]

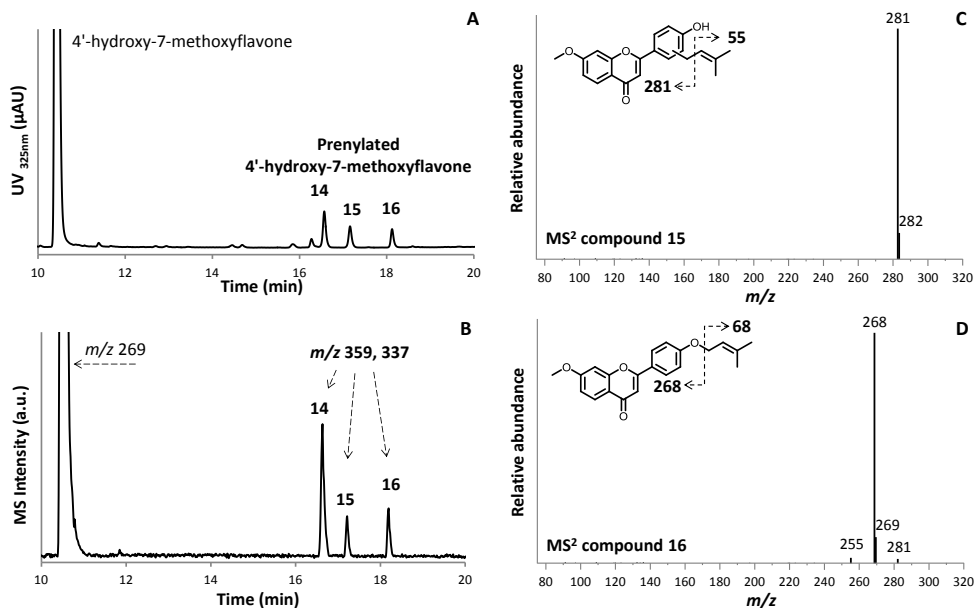


Figure 5.4. RP-UHPLC-UV (A) and MS in PI (B) profiles of 4'-hydroxy-7-methoxyflavone and prenylated products (14, 15 and 16 in Table 5.1) after incubation of 4'-hydroxy-7-methoxyflavone with DMAPP and SrCloQ. MS² spectra of *C*-prenylated isomer (m/z 359, Na adduct) at retention time 17.1 min (15, panel C) and *O*-prenylated isomer at 18.1 min (16, panel D). The proposed RDA fragmentation pathway is shown as inset.

SrCloQ was able to *C*- or *O*-prenylate an acceptor molecule, such as luteolin, 4'-hydroxy-7-methoxyflavone, 3'-hydroxydaidzein, and genistein. Luteolin and 3'-hydroxydaidzein were primarily *O*-prenylated ($\geq 80\%$ of the reaction products). These two substrates were the only ones with an extra phenolic hydroxyl group attached to the B-ring (*meta*-hydroxyl group). The presence of hydroxyl groups proved to be essential for catalysis, as isoflavone (no hydroxyl groups) yielded no reaction products with SrCloQ. Furthermore, the number of hydroxyl groups on (iso)flavonoids proved to have an effect on the enzyme activity. SrCloQ yielded slightly higher quantity of reaction products with 7,4'-dihydroxyflavone (2 hydroxyl groups) compared to luteolin (4 hydroxyl groups). Methoxylated substrates resulted in lower conversion yields than their non-methoxylated derivatives, as for 4'-hydroxy-7-methoxyflavone compared to 4',7-dihydroxyflavone.

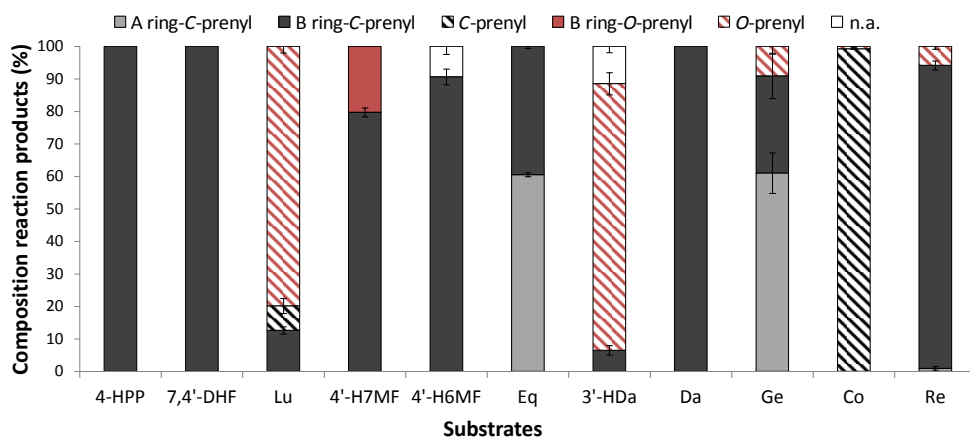


Figure 5.5. Molar composition of the prenylated products obtained with *SrCLOQ*. Error bars represent the standard deviation. 4-Hydroxyphenylpyruvate (4-HPP), 7,4'-dihydroxyflavone (7,4'-DHF), luteolin (Lu), 4'-hydroxy-7-methoxyflavone (4'-H7MF), 4'-hydroxy-6-methoxyflavone (4'-H6MF), equol (Eq), isoflavone (Is), daidzein (Da), genistein (Ge), coumestrol (Co), resveratrol (Re), not annotated (n.a).

DISCUSSION

Mechanism behind non-genuine acceptor substrate specificity of *SrCLOQ*

To verify the interactions of the acceptor substrates tested with the protein, we docked all the molecules, including the genuine substrate 4-HPP, into the active site. Our docked 4-HPP made the essential interactions^[22] with the residues Glu281 and Arg160, as well as with Arg176 and Cys297 (**Figure S5.1**).

Using this model, we docked the different phenolic substrates tested into the active site cavity of *SrCLOQ*. In principle, the active site had room to accommodate all acceptor substrates tested, as no clashes were observed, not even for unreacted compounds such as glycitein. This observation is in accordance with simulation analysis done previously,^[22] which showed that the active site is large enough to accommodate flavonoids.

The best aromatic substrate tested was equol, which was prenylated at the A- or the B-ring. Upon docking of equol into the active site of *SrCLOQ* (**Figure 5.6A**), both the A- and B-ring can orient towards the donor substrate and make the hydrogen bond between the phenolic hydroxyl group and Glu281. Additionally, the aromatic ring can make H- π interactions with Tyr233 and Trp122, whereas the tetrahydropyran (C-ring) can interact with Arg160. These interactions are likely to help stabilizing the binding of equol inside the active site. Finally, this isoflavan is one of the smallest acceptor substrates tested, it is more amenable to torsion than other isoflavonoids due to the lack of the C2-C3 double bond. Also, it has less space limitations inside the active site due to

the absence of the C4 carbonyl group. This might explain the promiscuity of SrCl_oQ to prenylate both the A- and the B-ring of equol.

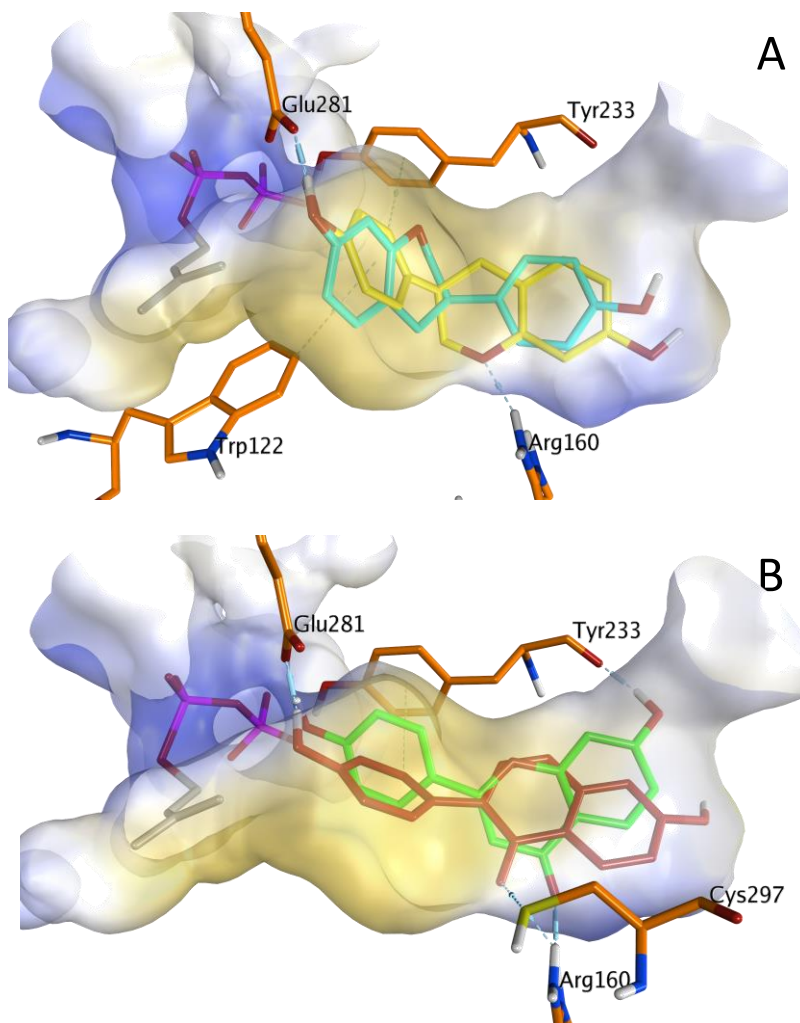


Figure 5.6. Phenolic aromatic substrates docked in the active site of SrCl_oQ (PDB 2XLQ). **A)** Comparison of equol with the A-ring (light blue) and B-ring (yellow) oriented towards the prenyl donor. **B)** 7,4'-Dihydroxyflavone (green) and daidzein (dark red) with their B-ring towards the prenyl donor. Protein surface is coloured according to the lipophilic potential using MOE software default's setting: yellow being lipophilic and blue hydrophilic (cut-off of 2.5). Donor substrate DMAPP is shown in gray with the phosphate group in pink. Residues that interact with the acceptor substrates are shown in orange: Glu281 anchors the substrate by H-bonding with the phenolic hydroxyl group; Arg160 stabilizes binding by H-bonding with the carbonyl or ether groups; Tyr233 aromatic ring can make H- π bonds or π stacking interactions with the aromatic rings of the phenolic substrates, while its carbonyl group can make H-bonding with phenolic hydroxyl groups; Cys297 thiol group can interact with the carbonyl group of the phenolic substrate.

In addition, we studied the interactions of the second best acceptor substrate (7,4'-dihydroxyflavone) with SrCloQ and compared them with those of one of the worst acceptor substrates (daidzein) (**Figure 5.6B**). We found that 7,4'-dihydroxyflavone can form the crucial hydrogen bond between the phenolic hydroxyl group at the B-ring and the residue Glu281. Furthermore, the C4 carbonyl group interacts with the anchoring residue Arg160. Also, the aromatic residue Tyr233 is able to make a hydrogen bond with the C7 hydroxyl group in the A-ring and π stacking interactions with the B-ring of the flavone. Tyr233 has been reported to stabilize the DMAPP substrate by hydrogen bonding and to make van der Waals interactions with 4-HPP.^[17,22]

Daidzein, which is the isoflavone isomer of 7,4'-dihydroxyflavone, also showed the essential interaction between the C4' hydroxyl group and Glu281. Furthermore, the carbonyl group of daidzein makes the interactions with Arg160 and with Cys297. In contrast to the flavone, due to the different orientation of the A- and B-rings, daidzein does not make any interactions with Tyr233.

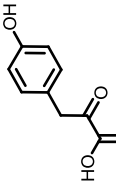
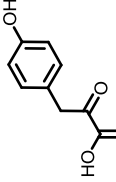
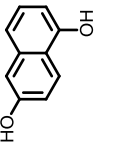
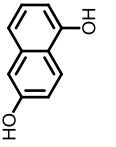
Overall, our results show that Arg160 plays an important role in stabilizing (iso)flavonoids in the active site of SrCloQ via hydrogen bonds with the carbonyl or ring oxygen in the C-ring. Moreover, our docking studies revealed that interactions with Tyr233 might determine the flavone over isoflavone preference observed in this study with SrCloQ, and also in a previous study with SsNovQ.^[23] The C7 hydroxyl group at the A-ring of isoflavones is far away from this residue and the B-ring is oriented in a different direction. This makes daidzein unable to make the relevant contacts with Tyr233, as opposed to the flavone. Mutation studies are needed to confirm the role of Tyr233 in flavonoid over isoflavone preference by SrCloQ and by SsNovQ.

Comparison of non-genuine substrate preferences of different ABBA prenyltransferases

Using the information obtained from the docking studies with SrCloQ, we can extend our knowledge of the non-genuine aromatic substrate preferences of other closely related ABBA PTs.^[4,15]

Acceptor substrate specificity. **Table 5.2** shows an overview of the main acceptor substrate preferences of SrCloQ, as well as of other members of the CloQ/NphB PT family reported in literature. For all enzymes, flavonoids were preferred over isoflavonoids, which supports our hypothesis that the interaction of the C7 hydroxyl group in the A-ring of flavonoids with a tyrosine residue (or equivalent) is determinant for the flavonoid preference of these bacterial PTases.

Table 5.2. Summary of acceptor substrate preferences and regioselectivity of *SrCloQ* and other closely related ABBA prenyltransferases.

	<i>SrCloQ</i>	<i>SsNovQ</i> ^[23]	<i>Sco7190</i> ^[18,19]	<i>ScINphB</i> ^[18]
Genuine acceptor substrate				
	4-HPP ^a	4-HPP	1,6-DHN ^b	1,6-DHN
Genuine donor substrate	DMAPP ^c	DMAPP	DMAPP	GPP ^d
Non-genuine acceptor substrate preferences				
Flavonoids	+	+	+/-	+
Isoflavonoids	+/-	+/-	-	+/-
Substrate with no OH groups	-	n.t.	n.t.	n.t.
Substrate with OCH ₃ groups	-	n.t.	n.t.	-
Regioselectivity				
A-ring prenylation	+/-	-	+	+
B-ring prenylation	+	+	-	-
C-prenylation	++	++	+	+
O-prenylation	+	+	-	++
Double prenylation	-	+ ^e	-	+

^a 4-hydroxyphenylpyruvate. ^b 1,6-dihydroxynaphthalene. ^c dimethylallylpyrophosphate. ^d geranylpyrophosphate. ^e Only with a phenolic acid (i.e. 3,4-O-diprenyl-caffeic acid), but not with any of the (iso)flavonoids or stilbenoids tested in their study.^[23]

The presence of the *para*-hydroxyl group in 4-HPP is essential, as the substrate is anchored with this hydroxyl by a hydrogen bond to Glu281, which additionally facilitates the formation of the prenylated σ -complex.^[17] This explains the lack of reaction products of *SrCloQ* with isoflavone. The addition of methoxyl groups to the A-ring, as in glycitein, decreased or cancelled the activity of *SrCloQ*. The same result was observed for *ScINphB* with the methoxylated substrate pterostilbene.^[18] The increase in molecular size by the addition of this bulky substituent possibly hampers the entrance to the active site of the PTs. The effect of hydroxylation on the activity of *SsNovQ*, *Sco7190* and *ScINphB* and the effect of methoxylation of phenolics on the activity of *SsNovQ* and *Sco7190* has to our knowledge not been tested, but it is tempting to propose a similar trend on activity as observed with *SrCloQ*.

A- or B-ring regioselectivity. *SrCloQ* and *SsNovQ* favour B-ring prenylation, whereas *Streptomyces coelicolor* *SCO7190* (*Sco7190*) and *ScINphB* prefer A-ring prenylation. This preference for either the B- or A-ring prenylation might be explained by the structure of their reported genuine substrates: *SrCloQ* and *SsNovQ* use 4-HPP as the genuine substrate, which contains one phenyl ring thereby resembling the B-ring of (iso)flavonoids. In contrast, *Sco7190* and *ScINphB* use 1,6-dihydroxynaphthalene, which contains two connected rings, resembling the A- and C-ring of (iso)flavonoids.

C- or O-prenylation. *SrCloQ* and *SsNovQ* were able to either C- or O-prenylate the same (iso)flavonoid substrate, although C-prenylation was predominant. *Sco7190* did not O-prenylate any of the (iso)flavonoids substrates tested, whereas *ScINphB* predominantly showed preference for O-prenylation. There are no studies explaining what exactly determines C- versus O- prenylation preference of these microbial prenyltransferases. With regard to *SrCloQ*, O-prenylation was preferred when the aromatic ring contained two neighbouring hydroxyl groups, as with luteolin and 3'-hydroxydaidzein. Previous biochemical studies with *SrCloQ* and *Sco7190* showed only C-prenylation of aromatic substrates,^[17,18,21] however, none of the acceptors tested had the extra *meta* (C3') hydroxyl group. Based on our docking studies, we observed that the *meta* hydroxyl group can be close enough to the donor substrate in the catalytic centre and prone to electrophilic attack by the allyl cation.

In contrast to *SrCloQ*, *SsNovQ* was able to B-ring O-prenylate many (iso)flavonoid substrates without the extra *meta* hydroxyl group. Further (crystallization) studies with *SsNovQ* may provide insight to understand this difference.

With regard to the number of prenyl groups attached to the phenolic substrates used in this study, *SrCloQ* produced only mono prenylated products, similarly to *SsNovQ* and *Sco7190*. In contrast, *ScINphB* has been reported to produce double prenylated stilbenoids, specifically 2,4-digeranyl-resveratrol.^[18] This difference might be explained by the facts that the bottom part of the PT barrel of *SrCloQ* is less accessible and significantly narrower than that of *ScINphB*.^[17]

In this study we demonstrated that: (i) *SrCloQ* can prenylate aromatic substrates belonging to the (iso)flavonoid and stilbenoid classes; (ii) *SrCloQ* is able to either C- or

O-prenylate the same acceptor substrate; (iii) SrCloQ showed a preference for C-prenylation at the B-ring of (iso)flavonoids; (iv) the addition of a meta hydroxyl group at the B-ring changes the preference to O-prenylation. The genuine substrate 4-HPP showed the highest conversion yield, followed by equol and 7,4'-dihydroxyflavone. We propose, using *in silico* modelling, the mechanisms by which the acceptor substrate specificity and regioselectivity observed with SrCloQ, but also of related PTs, can be explained. This information can help to choose the appropriate acceptor substrate for a specific PT when tailoring novel prenylated phenolic compounds.

ACKNOWLEDGMENTS

The authors would like to thank Prof. Dr. Lutz Heide from the Pharmaceutical Institute, Eberhard-Karls-University Tübingen, Germany for kindly providing the *cloq* plasmid and for his input during the writing process of this manuscript.

REFERENCES

- [1] Palsuledesai, C.C.; Distefano, M.D. Protein prenylation: enzymes, therapeutics, and biotechnology applications. *ACS Chemical Biology*, 2015, **10**, 51-62.
- [2] Simons, R.; Gruppen, H.; Bovee, T.F.H.; Verbruggen, M.A.; Vincken, J.-P. Prenylated isoflavonoids from plants as selective estrogen receptor modulators (phytoSERMs). *Food & Function*, 2012, **3**, 810-827.
- [3] van de Schans, M.G.M.; Vincken, J.-P.; de Waard, P.; Hamers, A.R.M.; Bovee, T.F.H.; Gruppen, H. Glyceollins and dehydroglyceollins isolated from soybean act as SERMs and ER subtype-selective phytoestrogens. *The Journal of Steroid Biochemistry and Molecular Biology*, 2016, **156**, 53-63.
- [4] Winkelblech, J.; Fan, A.; Li, S.-M. Prenyltransferases as key enzymes in primary and secondary metabolism. *Applied Microbiology and Biotechnology*, 2015, **99**, 7379-7397.
- [5] Liang, P.H.; Ko, T.P.; Wang, A.H.J. Structure, mechanism and function of prenyltransferases. *European Journal of Biochemistry*, 2002, **269**, 3339-3354.
- [6] Heide, L. Prenyl transfer to aromatic substrates: genetics and enzymology. *Current Opinion in Chemical Biology*, 2009, **13**, 171-179.
- [7] Yazaki, K.; Sasaki, K.; Tsurumaru, Y. Prenylation of aromatic compounds, a key diversification of plant secondary metabolites. *Phytochemistry*, 2009, **70**, 1739-1745.
- [8] Veitch, N.C. Isoflavonoids of the Leguminosae. *Natural Product Reports*, 2013, **30**, 988-1027.
- [9] Khalivulla, S.I.; Reddy, B.A.K.; Gunasekar, D.; Blond, A.; Bodo, B.; Murthy, M.M.; Rao, T.P. A new di-O-prenylated isoflavone from *Tephrosia tinctoria*. *Journal of Asian Natural Products Research*, 2008, **10**, 953-955.
- [10] Welle, R.; Grisebach, H. Properties and solubilization of the prenyltransferase of isoflavonoid phytoalexin biosynthesis in soybean. *Phytochemistry*, 1991, **30**, 479-484.
- [11] Sasaki, K.; Tsurumaru, Y.; Yamamoto, H.; Yazaki, K. Molecular characterization of a membrane-bound prenyltransferase specific for isoflavone from *Sophora flavescens*. *Journal of Biological Chemistry*, 2011, **286**, 24125-24134.
- [12] Yang, X.; Jiang, Y.; Yang, J.; He, J.; Sun, J.; Chen, F.; Zhang, M.; Yang, B. Prenylated flavonoids, promising nutraceuticals with impressive biological activities. *Trends in Food Science & Technology*, 2015, **44**, 93-104.
- [13] Saleh, O.; Haagen, Y.; Seeger, K.; Heide, L. Prenyl transfer to aromatic substrates in the biosynthesis of aminocoumarins, meroterpenoids and phenazines: The ABBA prenyltransferase family. *Phytochemistry*, 2009, **70**, 1728-1738.
- [14] Bonitz, T.; Alva, V.; Saleh, O.; Lupas, A.N.; Heide, L. Evolutionary relationships of microbial aromatic prenyltransferases. *Plos One*, 2011, **6**, 1-8.
- [15] Tello, M.; Kuzuyama, T.; Heide, L.; Noel, J.P.; Richard, S.B. The ABBA family of aromatic prenyltransferases: broadening natural product diversity. *Cellular and Molecular Life Sciences*, 2008, **65**, 1459-1463.

- [16] Haagen, Y.; Unsöld, I.; Westrich, L.; Gust, B.; Richard, S.B.; Noel, J.P.; Heide, L. A soluble, magnesium-independent prenyltransferase catalyzes reverse and regular C-prenylations and O-prenylations of aromatic substrates. *FEBS Letters*, 2007, **581**, 2889-2893.
- [17] Metzger, U.; Keller, S.; Stevenson, C.E.M.; Heide, L.; Lawson, D.M. Structure and mechanism of the magnesium-independent aromatic prenyltransferase CloQ from the clorobiocin biosynthetic pathway. *Journal of Molecular Biology*, 2010, **404**, 611-626.
- [18] Kumano, T.; Richard, S.B.; Noel, J.P.; Nishiyama, M.; Kuzuyama, T. Chemoenzymatic syntheses of prenylated aromatic small molecules using *Streptomyces* prenyltransferases with relaxed substrate specificities. *Bioorganic & Medicinal Chemistry*, 2008, **16**, 8117-8126.
- [19] Kuzuyama, T.; Noel, J.P.; Richard, S.B. Structural basis for the promiscuous biosynthetic prenylation of aromatic natural products. *Nature*, 2005, **435**, 983-987.
- [20] Leipoldt, F.; Zeyhle, P.; Kulik, A.; Kalinowski, J.; Heide, L.; Kaysser, L. Diversity of ABBA prenyltransferases in marine *Streptomyces* sp. CNQ-509: Promiscuous enzymes for the biosynthesis of mixed terpenoid compounds. *PLoS One*, 2015, **10**, 1-15.
- [21] Pojer, F.; Wemakor, E.; Kammerer, B.; Chen, H.; Walsh, C.T.; Li, S.-M.; Heide, L. CloQ, a prenyltransferase involved in clorobiocin biosynthesis. *Proceedings of the National Academy of Sciences*, 2003, **100**, 2316-2321.
- [22] Bayse, C.A.; Merz, K.M. Mechanistic insights into Mg²⁺-independent prenylation by CloQ from classical molecular mechanics and hybrid quantum mechanics/molecular mechanics molecular dynamics simulations. *Biochemistry*, 2014, **53**, 5034-5041.
- [23] Ozaki, T.; Mishima, S.; Nishiyama, M.; Kuzuyama, T. NovQ is a prenyltransferase capable of catalyzing the addition of a dimethylallyl group to both phenylpropanoids and flavonoids. *The Journal of Antibiotics*, 2009, **62**, 385-392.
- [24] Cuyckens, F.; Claeys, M. Mass spectrometry in the structural analysis of flavonoids. *Journal of Mass Spectrometry*, 2004, **39**, 1-15.
- [25] Aisyah, S.; Vincken, J.-P.; Andini, S.; Mardiah, Z.; Gruppen, H. Compositional changes in (iso)flavonoids and estrogenic activity of three edible *Lupinus* species by germination and *Rhizopus*-elicitation. *Phytochemistry*, 2016, **122**, 65-75.
- [26] Kusters, H.A.; Wierenga, P.A.; de Vries, R.; Gruppen, H. Characteristics and effects of specific peptides on heat-induced aggregation of β -lactoglobulin. *Biomacromolecules*, 2011, **12**, 2159-2170.
- [27] Metzger, U.; Schall, C.; Zocher, G.; Unsöld, I.; Stec, E.; Li, S.-M.; Heide, L.; Stehle, T. The structure of dimethylallyl tryptophan synthase reveals a common architecture of aromatic prenyltransferases in fungi and bacteria. *Proceedings of the National Academy of Sciences*, 2009, **106**, 14309-14314.
- [28] Simons, R.; Vincken, J.-P.; Bakx, E.J.; Verbruggen, M.A.; Gruppen, H. A rapid screening method for prenylated flavonoids with ultra-high-performance liquid chromatography/electrospray ionisation mass spectrometry in licorice root extracts. *Rapid Communications in Mass Spectrometry*, 2009, **23**, 3083-3093.
- [29] Doy, C.H. Alkaline conversion of 4-hydroxyphenylpyruvic acid to 4-hydroxybenzaldehyde. *Nature*, 1960, **186**, 529-531.
- [30] van de Schans, M.G.M.; Vincken, J.-P.; Bovee, T.F.H.; David Cervantes, A.; Logtenberg, M.J.; Gruppen, H. Structural changes of 6a-hydroxy-pterocarpanes upon heating modulate their estrogenicity. *Journal of Agricultural and Food Chemistry*, 2014, **62**, 10475-10484.
- [31] Yang, M.; Wang, W.; Sun, J.; Zhao, Y.; Liu, Y.; Liang, H.; Guo, D.-a. Characterization of phenolic compounds in the crude extract of *Hedysarum multijugum* by high-performance liquid chromatography with electrospray ionization tandem mass spectrometry. *Rapid Communications in Mass Spectrometry*, 2007, **21**, 3833-3841.
- [32] Morandi, D.; Le Quere, J.L. Influence of nitrogen on accumulation of isosojagol (a newly detected coumestan in soybean) and associated isoflavonoids in roots and nodules of mycorrhizal and non-mycorrhizal soybean. *New Phytologist*, 1991, **117**, 75-79.
- [33] O'Neill, M.J. Aureol and phaseol, two new coumestans from *Phaseolus aureus* Roxb. *Zeitschrift für Naturforschung C*, 1983, **38**, 698-700.
- [34] Stella, L.; De Rosso, M.; Panighel, A.; Vedova, A.D.; Flamini, R.; Traldi, P. Collisionally induced fragmentation of [M-H]⁻ species of resveratrol and piceatannol investigated by deuterium labelling and accurate mass measurements. *Rapid Communications in Mass Spectrometry*, 2008, **22**, 3867-3872.
- [35] Sobolev, V.S.; Potter, T.L.; Horn, B.W. Prenylated stilbenes from peanut root mycelium. *Phytochemical Analysis*, 2006, **17**, 312-322.
- [36] Lee, Y.J.; Notides, A.C.; Tsay, Y.G.; Kende, A.S. Coumestrol, NBD-norhexestrol, and dansyl-norhexestrol, fluorescent probes of estrogen-binding proteins. *Biochemistry*, 1977, **16**, 2896-2901.
- [37] Weast, R.C., CRC Handbook of Chemistry and Physics. 58th ed. 1977, Boca Raton, FL, USA: CRC Press.

- [38] Franke, A.A.; Lai, J.F.; Halm, B.M. Absorption, distribution, metabolism, and excretion of isoflavonoids after soy intake. *Archives of Biochemistry and Biophysics*, 2014, **559**, 24-28.
- [39] Song, T.T.; Hendrich, S.; Murphy, P.A. Estrogenic activity of glycitein, a soy isoflavone. *Journal of Agricultural and Food Chemistry*, 1999, **47**, 1607-1610.
- [40] Warburton, W.K. The isoflavones. *Chemical Society Reviews*, 1954, **8**, 67-87.
- [41] Trela, B.C.; Waterhouse, A.L. Resveratrol: isomeric molar absorptivities and stability. *Journal of Agricultural and Food Chemistry*, 1996, **44**, 1253-1257.
- [42] Buckingham, J.; Munasinghe, V.R.N., *Dictionary of Flavonoids*. 2015, Boca Raton, FL, USA: CRC Press. 843.
- [43] Johnson-Winters, K.; Purpero, V.M.; Kavana, M.; Nelson, T.; Moran, G.R. (4-Hydroxyphenyl)pyruvate dioxygenase from *Streptomyces avermitilis*: the basis for ordered substrate addition. *Biochemistry*, 2003, **42**, 2072-2080.
- [44] Hartwig, U.A.; Maxwell, C.A.; Joseph, C.M.; Phillips, D.A. Chrysoeriol and luteolin released from alfalfa seeds induce nod genes in *Rhizobium meliloti*. *Plant Physiology*, 1990, **92**, 116-122.

SUPPLEMENTARY INFORMATION

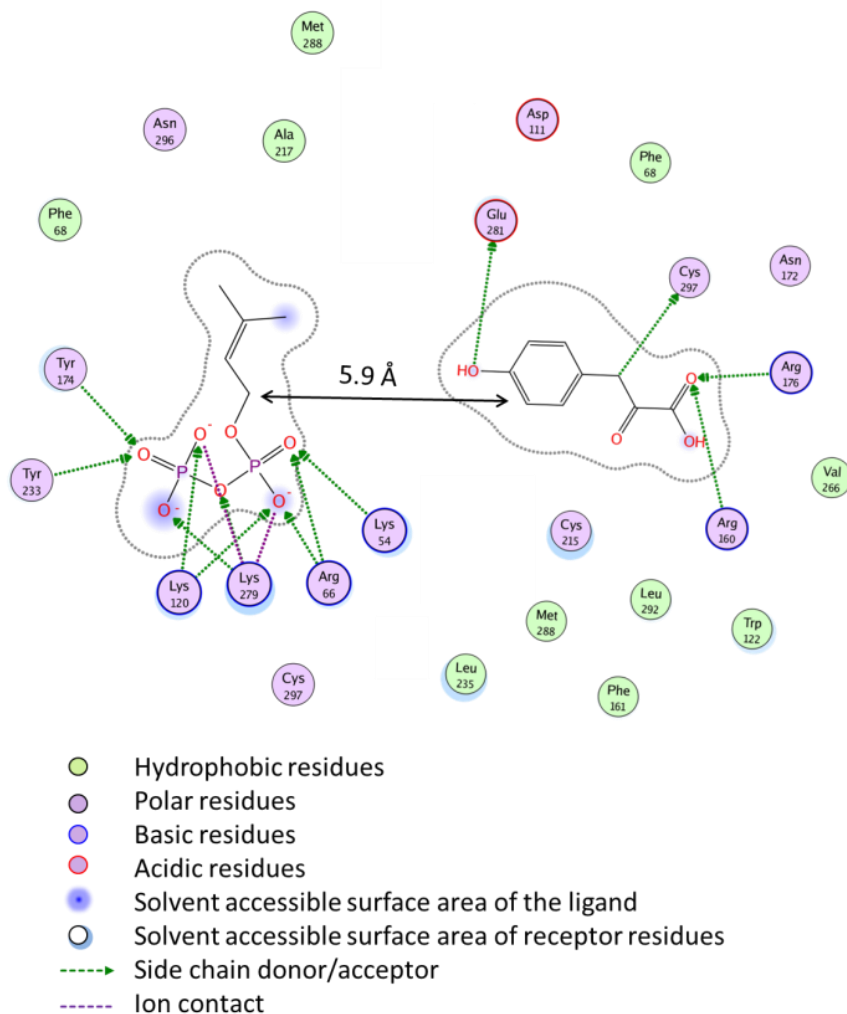


Figure S5.1. Interaction 2D diagram between *SrClOQ* and the genuine ligands 4-HPP (acceptor substrate) and DMAPP (donor substrate) as modelled in this study, using the PDB 2XLQ.

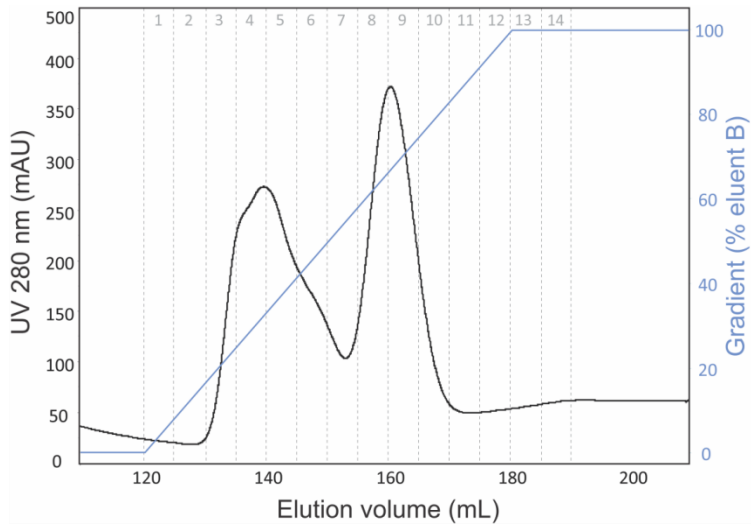


Figure S5.2. Pattern of elution of the lysate for the purification of *SrCloQ* by Ni^{2+} affinity chromatography. Eluent B, imidazole 250 mM in Tris-HCL buffer (pH 8.0). Peak at elution volume of 160 mL represents the His-tagged *SrCloQ* protein. Grey numbers represent the fractions collected during the run. Fractions 8 and 9 were pooled.

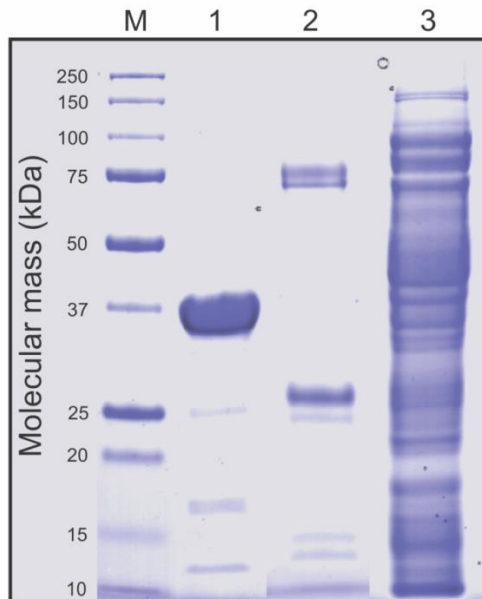


Figure S5.3. SDS-PAGE of *SrCloQ* enzyme. Lanes: M, molecular marker; 1, purified enzyme (35 kDa) after affinity chromatography and concentration (fractions 8-9, **Figure S5.2**); 2, non-*SrCloQ* bound protein (fractions 4-6); 3, unbound protein (i.e. protein eluting before start of gradient).

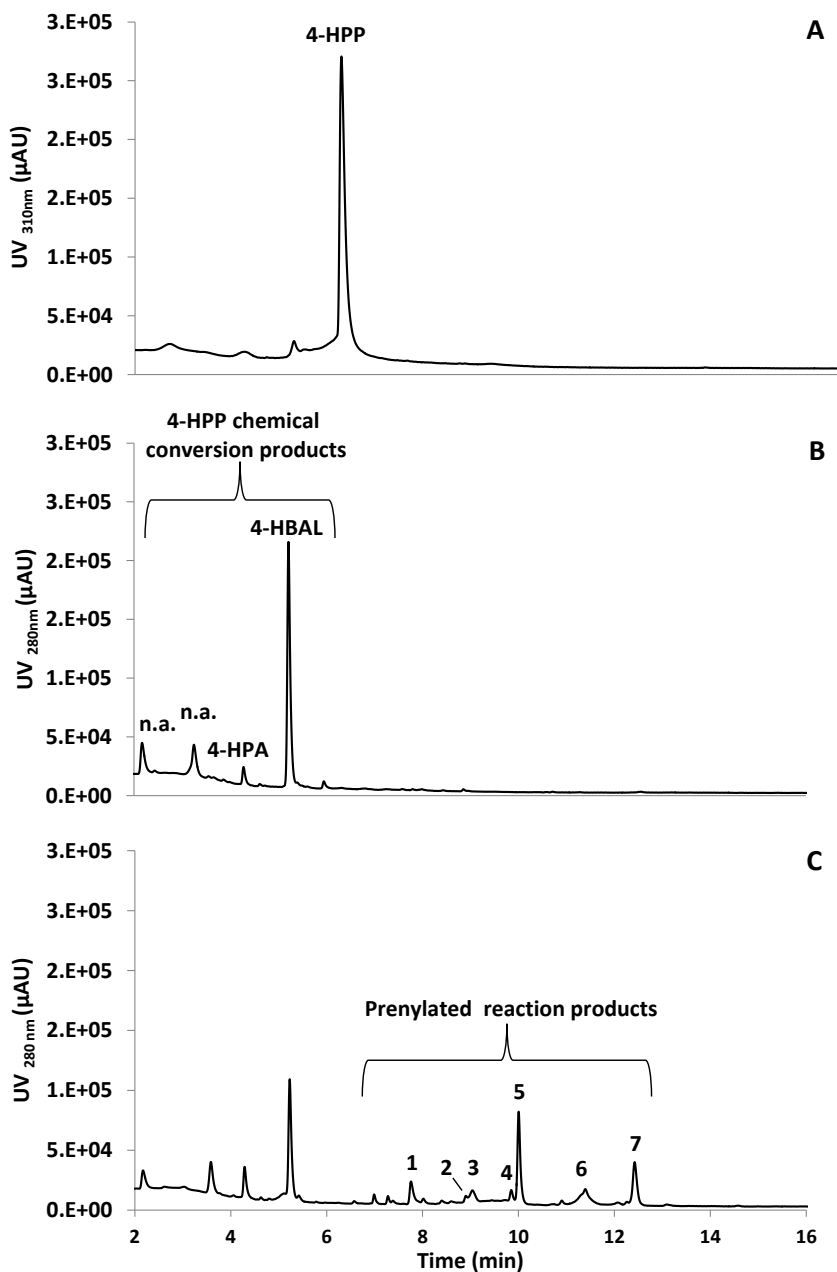


Figure S5.4. UV chromatograms of 4-HPP standard solution (0.5 mM) (A), reaction products formed after incubation of 4-HPP and DMAPP without (B) and with *SrCloQ* (C). Peak numbers refer to those from **Table 5.1**. 4-Hydroxybenzaldehyde (4-HBAL) and 4-hydroxyphenylacetic acid (4-HPA) were annotated using reference compounds. Not annotated (n.a.).

Table S5.1. Molar extinction coefficients used for the quantification of prenylated products from the phenolic acceptor substrates.

Acceptor substrate	λ (nm)	ϵ (AU/M·cm)	Reference
Coumestrol	345	24800	[36]
Daidzein	250	26915	[37]
Equol	281	6761	[38]
Genistein	263	31623	[37]
Glycitein	257	25388	[39]
Isoflavone	245	25704	[40]
Luteolin	256	15849	[37]
Resveratrol	308	29959	[41]
3'-Hydroxy-daidzein	250	15849	[42]
4-Hydroxyphenylpyruvate	276	2800	[43]
7,4'-Dihydroxyflavone	328	33000	[42]
4'-Hydroxy-7-methoxy-flavone	assumed to be similar as 7,4'-dihydroxyflavone ^a		
4'-Hydroxy-6-methoxy-flavone	assumed to be similar as 7,4'-dihydroxyflavone		

^a Methoxylation has been shown not to significantly change the molar extinction coefficient of flavones.^[44]

Chapter 6

General Discussion

As described in the General Introduction of this thesis, prenylated phenolic compounds, especially from the isoflavonoid class, are secondary metabolites involved in the defence against pathogens of plants from the Fabaceae family. These compounds have antimicrobial properties and have the potential to be used as natural antibacterials against human pathogens. Due to contradictory reports in the literature with regard to antibacterial activity of prenylated phenolic compounds, a systematic investigation on their quantitative structure-activity relationships (QSAR) and their mode of action was performed. In this thesis it was hypothesized that prenylation modulated antibacterial activity, not only by increasing the hydrophobicity of the phenolics, but also by providing a specific molecular configuration responsible for disrupting the integrity of the cytoplasmic membrane. The principal aims of this thesis were (i) to define (Q)SAR of prenylated phenolic compounds as antibacterials against Gram positive and Gram negative bacteria, and (ii) to investigate the mechanisms of action of these compounds in the bacterial cell and to correlate it with the main QSAR found. An additional aim was (iii) to investigate the possibility of *in vitro* production of diprenylated phenolic compounds to be used in future QSAR studies, due to their scarce availability. This chapter addresses (i) the different approaches taken in this thesis, (ii) the main findings with regard to the antibacterial activity of prenylated phenolic compounds, and (iii) prospects for the use of these compounds as antibacterials.

MAIN CONSIDERATIONS WITH TECHNIQUES USED IN THIS THESIS

Quantification of phenolic compounds without reference compounds

Plant extracts can contain an enormous array of phytochemicals. For assessing the antibacterial properties of such samples, it is essential to identify and quantify the individual compounds responsible for the properties observed.

After separation of the constituents of a plant extract by liquid chromatography, UV detection allows the quantification of the individual phenolic compounds in crude extracts. This is done by relating their peak area to a calibration curve of the reference compound. However, quantification of individual compounds is a challenging task, as the vast majority of reference compounds are not readily available. As a consequence, indirect methods are used for quantification. These encompass methods with an external (look-alike) reference compound for calibration, which enables expression of the quantities of the compound(s) of interest in equivalents. The main problem with such an approach is that the response signal is considered equal for all compounds within a set of look-alikes, whereas actually it is not. For instance, the isoflavone genistein has been used as reference compound for the quantification of main isoflavonoids in elicited soybean seedlings, i.e. pterocarpanes such as glycinol. The molar extinction coefficients of glycinol and genistein differ by a factor 7 at 260 nm (5112 for glycinol vs 33231 AU/M·cm for genistein). Thus, the presence of glycinol is underestimated using the aforementioned approach. A more accurate approach includes a correction for the differences in response signals between the external reference compound and the compounds being quantified, by including their molar extinction coefficients.

An alternative method, performed in this thesis, involves no calibration with reference compounds. Instead, it is directly derived from the Lambert-Beer's law. This method, used previously to quantify individual peptides, adapts the Lambert-Beer equation for application in a continuous UHPLC system.^[1] For this, the flow rate, the injected sample volume and the effective path length of the UV cell (k_{cell}) are included in the following equation (Eq. 6.1):

$$C [M] = \frac{\text{area} \times Q}{\varepsilon \times l \times V_{inj} \times k_{cell}} \quad (\text{Eq. 6.1})$$

in which C (M) is concentration, *area* is the integrated area of the UV peak at the specific wavelength (AU·s), Q is the flow rate (5 $\mu\text{L/s}$), ε (AU/M·cm) is the molar extinction coefficient, l is the path length of the UV cell provided by the manufacturer (5 cm), V_{inj} is the injected volume of sample (2 μL), and k_{cell} is a constant related to the cell geometry of the UV detector. The k_{cell} depends on the geometry and materials of the flow cell of the detector. It is determined by measuring the absorbance of reference solutions within the detector's linearity range and by rearranging the equation describing Lambert-Beer's law.^[2] As a constant of every UV cell, the k_{cell} needs to be determined once. Nevertheless,

a regular check on the possible contamination of the cell is part of good laboratory practices.

Table 6.1 provides a comparison of the outcome of different quantification methods for a number of representative phenolic compounds: (i) the “ k_{cell} method” used in this thesis, (ii) the “look-alike reference method” using an external compound with additional correction for differences in molar extinction coefficients, and (iii) the method of using the compound itself as reference.

Table 6.1. Comparison of the content of phenolic compounds calculated using different UV-based quantification methods.

Compound (mg/mL)	Quantification method		
	Lambert-Beer based k_{cell} mg/mL	Look-alike method with ϵ correction mg/mL	Using the reference compound mg/mL
Genistein (0.05)	0.053 (6%) ^a	0.050 (0%) ^c	0.050
Daidzein (0.05)	0.050 (4%)	0.045 (6%) ^d	0.048
Glabridin (0.01)	0.010 (0%)	0.006 (39%) ^d	0.010
Wighteone (0.10)	0.112	0.107 ^d	- ^b
Luteone (0.10)	0.123	0.120 ^d	-

^a Absolute error. ^b No calibration curve available for this compound. ^c Using daidzein as look-alike reference. ^d Using genistein as look-alike reference.

In most of the cases, the indirect method of correcting for the molar extinction coefficient after using an external reference compound gave similar results as the more direct k_{cell} method. The main advantage of the k_{cell} method is the straightforwardness of the calculation from the UV area given by the system to absolute quantities of the compound of interest. Having no need for running and processing calibration curves is a clear practical advantage of this method, especially when dealing with many samples containing phenolic compounds belonging to many different subclasses.

Both the k_{cell} and the external reference methods require the molar extinction of the compounds of interest. Even though there is large amount of published data, such as in chemical handbooks, information on molar extinction coefficients determined under similar conditions of many different phenolic compounds is the main limitation of both methods. In case of an unknown molar extinction coefficient, the reported extinction coefficient of a compound that closely matched the structure of the compound being quantified (i.e. same subclass, similar substitution pattern) has been used. Some substitutions, such as glycosyl groups, were assumed not to significantly influence the molar extinction coefficient of a phenolic compound.^[3] In addition, molar extinction coefficients are reported at specific wavelengths in specific solvents. In this thesis, molar extinction coefficients from the literature, measured in organic solvents, such as alcohols (e.g. methanol or ethanol) were used, as most phenolic compounds are readily soluble

under those conditions. For practical reasons, in this thesis all compounds in a plant extract were quantified at the same wavelength (not necessarily at the wavelength of the reported molar extinction coefficient or the wavelength of maximum absorbance of the compound). In order to correct for the differences in reported and used wavelength, the molar extinction coefficient reported in literature was multiplied by the ratio of absorbance at the different wavelengths, as follows (Eq. 6.2):

$$\varepsilon_i = \varepsilon_r \times \frac{A_i}{A_r} \quad (\text{Eq. 6.2})$$

where ε is the molar extinction coefficient, A is the UV absorbance, i is the wavelength at which the compound is being quantified, and r the wavelength reported in literature. It is necessary to take these factors into account to obtain reliable quantification results, when dealing with molar extinction coefficients from literature.

In conclusion, the absolute quantification of phenolic compounds by using the Lambert-Beer based k_{cell} method is a faster and more accurate method than that using external reference calibration curves. It should be emphasized that the utilization of reference compounds should still be part of the routine check for the chromatographic systems.

Quantification of antibacterial activity by broth dilution

Evaluation of antibacterial activity is usually performed by determination of minimum inhibitory concentrations (MIC), according to standard protocols established by clinical authorities (e.g. CLSI, EUCAST) for conventional antimicrobials.^[4] These protocols are meant for routine analysis of antibacterial susceptibility or resistance of isolated strains in patients. Following these official protocols, which are applied throughout the literature for conventional and natural antibacterial research, in this thesis it was decided to use weight basis, not molar, for measuring MIC values. As MIC values are presented in $\mu\text{g}/\text{mL}$, this unit was also used in this thesis.

Nevertheless, in terms of methodology applied these protocols are not specific enough for research purposes, as inoculum size (defined with McFarland turbidity standards), growth of bacteria and MIC determination are based on absorbance measurements. Hence, in this thesis, complementary plate count was performed to report the exact inoculum size, the final levels after exposure to prenylated compounds and to define the MIC of a given compound against a bacterium. In this sense, the MIC determination done here, although it takes more time due to the plate counts, is more specific and has lower detection limits than those based on absorbance measurements.

To measure the MIC of a compound, various concentrations of the antibacterial need to be tested. This is usually done by a dilution assay, which can be performed in broth or agar. In this thesis broth dilution was used as a practical and reliable method for measuring the susceptibility of a bacterium to different concentrations of prenylated compounds. Dilution methods are quantitative (i.e. determination of MIC values), require

low amount of sample (it can be performed in micro-well plate format) and represent no risk for thermally labile samples, as is the case for agar dilution methods. The main limitation of broth in comparison with agar dilution methods, is that highly hydrophobic compounds may not dissolve well (e.g. essential oils).^[5] Nevertheless, prenylated phenolic compounds, being characterized as hydrophobic, were soluble in broth at the concentrations used in this thesis as no precipitation was observed. Moreover, mixing was performed constantly during the assay in order to get appropriate contact between the bacteria and the compound being tested.

In conclusion, quantification of antibacterial activity by broth dilution in combination with plate counts for determination of MIC values can be regarded as accurate and practical for research purposes, without any large difficulties or specialized equipment requirements.

Model development in QSAR studies

The goal of quantitative structure-activity relationship (QSAR) studies is to build a mathematical equation with molecular descriptors that best quantifies an observed biological activity. The type of function (linear or non-linear), as well as the descriptor selection method, affect the final outcome of a QSAR study.

The main goals of the QSAR in this thesis were to (i) develop models with good predictive capabilities, (ii) identify the main molecular characteristics contributing to the antibacterial activity, and (iii) correlate them with the mode of action. Genetic algorithm (GA)-driven selection of variables was performed in this thesis. This technique is considered as an effective tool to tackle optimization problems, such as local optima, when selecting the best regression model from a large descriptor space.^[6,7] GA can extensively explore the descriptor space and, therefore, increases the probabilities of finding global optimum solutions in multivariate analysis. Although dimension reduction techniques (e.g. principal component analysis or principal component regression) are common in multivariate settings, GA in combination with multiple linear regression (MLR) has the advantage of providing more readily interpretable models than those dimension reduction techniques. This is because the measured variables are used directly in the model, i.e. they are not transformed into latent variables.

In this thesis efforts were made to keep the models simple with the least number of significant descriptors still giving a minimum robustness and prediction quality (i.e. $q^2 > 0.5$). Larger and/or more complicated (e.g. non-linear) models run the risk of overfitting the data and are difficult for mechanistic interpretations. Nevertheless, for prediction purposes, binary classification models based on the linear models were built in this thesis. Binary models are more robust as they can be used to predict the probability of a compound of being active or inactive, without predicting a specific value of activity (i.e. MIC value).

In line with our goal of identifying important descriptors that might describe the mode of action of prenylated phenolic compounds, the complete chemical diversity of

the dataset was used for building of the models. Thus, the dataset was not split into a training and a test set, as is sometimes done in QSAR studies. Using less compounds by splitting the set and/or using single subclasses would perhaps have improved the fit (r^2) of the models, but not their applicability to other prenylated phenolic subclasses. Internal validation was performed by using the leave-one-out cross-validation method. External validation with a different set of compounds is necessary to confirm the prediction power of the models.

In conclusion, GA in combination with MLR can reduce the challenge of variable selection in exploratory QSAR studies. This is particularly important when there is lack of knowledge on the requirements for a certain biological activity and when the number of available descriptors is large.

PRENYLATED PHENOLICS AS ANTIBACTERIALS

Structural features defining antibacterial activity of prenylated phenolics

The first aim of this thesis was to systematically define (Q)SAR of prenylated phenolic compounds as antibacterials. In **Chapters 3** and **4** it was shown that prenylation and subsequent increase in hydrophobicity are not the only requirements for prenylated phenolic compounds to be antibacterially active. Activity of prenylated compounds was more specific than previously considered. It depends on the overall molecular shape.

In **Figure 6.1** (Q)SAR of antibacterial prenylated phenolics found in **Chapters 3** and **4**, extended with those from the literature, particularly for methicillin-resistant *S. aureus*, are shown. In general, substituted prenyl groups are detrimental, whereas unsubstituted ones are good for antibacterial activity of phenolic compounds. The presence of hydroxyl groups is essential for activity, whereas the presence of methoxyl groups can be detrimental or beneficial depending on the compound.

As highlighted by the results of **Chapters 3** and **4**, few SAR are generic for prenylated compounds, as most of the SAR are subclass specific, including the position of prenyl groups and hydroxyl groups. For most subclasses studied, monoprenylated compounds can have very good (i.e. $MIC \leq 15 \mu\text{g/mL}$) antibacterial activity when the position requirements for prenyl and hydroxyl substituents are met. For 6 α -OH-pterocarpan, however, one prenyl group was not enough to provide good antibacterial activity. All 6 α -OH-pterocarpan tested had $\log D$ values < 3.6 (glyceollins I-V, glyceofuran and glyceollidin II, **Chapter 4**), whereas all active compounds showed $\log D$ values > 3.6 . Analysing the effect of the particular 6 α hydroxylation position (i.e. between the C- and D-ring), the 6 α -OH group decreases the hydrophobic volume and the $\log D$ of the molecule more than hydroxylation positions at the A- or B-rings. As a result, 6 α hydroxylation is detrimental for partitioning of a pterocarpan to hydrophobic sites. Therefore, to have good activity all 6 α -OH-pterocarpan need to be diprenylated to compensate for the low hydrophobicity of these molecules.

The presence of non-substituted hydroxyl groups is known to be essential for antibacterial activity of prenylated compounds.^[8-11] However, the location of those essential hydroxyl groups is subclass dependent. For example, prenylated isoflavones (e.g. neobavaisoflavone, **Chapter 4**) lacking the OH at C5 did not show good activity.^[12,13] This hydroxyl group has been previously proposed^[14,15] to form a hydrogen bond with the carbonyl group in the C-ring of isoflavones. This hydrogen bond results in an increased hydrophobicity from the increase in electron delocalization in the molecule. This increased hydrophobicity will increase the partitioning to membranes and, thereby, the antibacterial activity.

Some SAR also depend on the type of bacteria targeted. The most antibacterial prenylated phenolics found in this thesis against the Gram positive bacterium were double chain prenylated ones (MIC < 10 µg/mL). For the Gram negative *E. coli*, prenylated phenolic compounds were found active only when the efflux pumps systems were inhibited. However, even under conditions of efflux inhibition, diprenylated phenolic compounds were inactive, highlighting their limited influx into the cell. In **Chapter 4** a maximum effective $\log D$ of 4.6 was proposed for *E. coli* antibacterial prenylated (iso)flavonoids, as all inactive diprenylated compounds tested had higher coefficients. Interestingly, a double chain prenylated flavonol (papyriflavonol A) has shown good activity against *E. coli* (MIC 20 µg/mL).^[16] The $\log D$ value of this compound is relatively low (i.e. 4.62) and it fits with the limit set in this thesis. This flavonol has five hydroxyl groups, including one at C-ring, which is more effective at decreasing hydrophobicity than hydroxylation at the A- or B-ring (similarly as for the pterocarpanes). As a result, we speculate that this particular diprenylated molecule has no influx restrictions through the water-filled porins, and thus, can be effective against *E. coli*. In **Chapter 4**, QSAR were developed to elucidate the main molecular characteristics influencing the antibacterial activity of prenylated (iso)flavonoids. Based on the models obtained, it was concluded that two main molecular characteristics modulate of the antibacterial activity of prenylated (iso)flavonoids: hydrophobicity and shape (mainly flexibility and globularity). More specifically, it was found that the previously mentioned hydrophobicity of $\log D > 3.6$ for both Gram positive and Gram negative combined with a flexible (*KierFlex* index > 2.8) and globular skeleton (*std_dim3* > 1.1), can be considered as good signatures for antibacterial activity of prenylated phenolic compounds. Additionally, a specific arrangement of atoms, as depicted by the 3D-pharmacophore model developed in **Chapter 4**, was found to be necessary to have good (i.e. MIC ≤ 25 µg/mL) antibacterial activity.

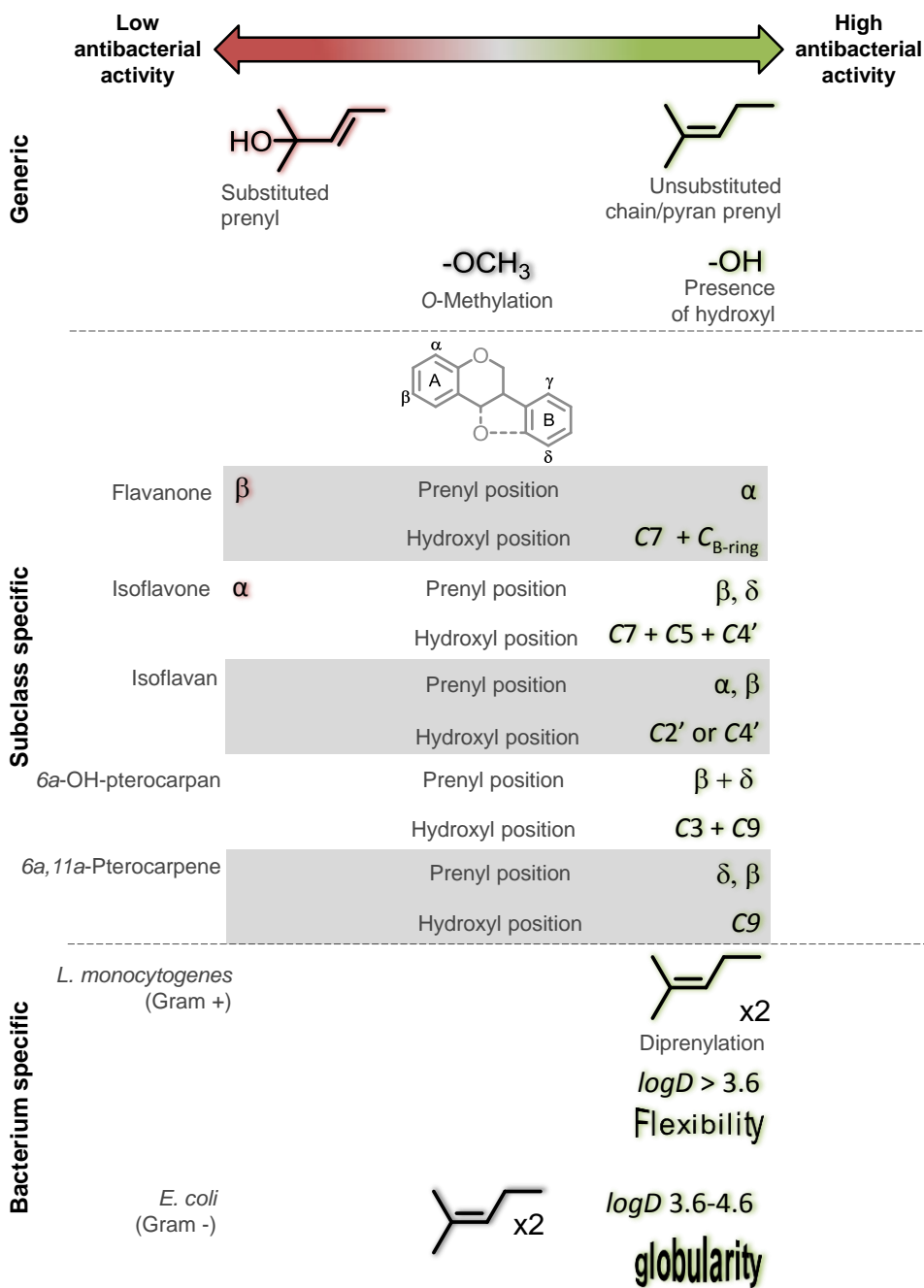


Figure 6.1. Extended quantitative structure-activity relationships of prenylated phenolic compounds as antibacterial agents, according to the main findings of this thesis. Prenyl position is indicated using the Greek numbering system, as illustrated in the isoflavonoid skeleton.

In this thesis, different effects of flexibility of the skeleton and of the substituents were found. In **Chapter 3** it was found that for chain prenylated compounds, flexible skeletons, such as stilbenoids showed lower antibacterial activity than less flexible ones (isoflavones and pterocarpanes). This was explained by the planar configuration adopted by the stilbenoid skeleton, leading to reduced disruption of membrane integrity. In **Chapter 4**, molecular flexibility was positively correlated with antibacterial activity using an index that considers cyclicality, branching and density. It was observed that chain prenylation increased the molecular flexibility by increasing branching, whereas ring-closed prenylation decreases it by increasing cyclicality. It is speculated that the higher flexibility of prenyl chains, compared to ring-closed prenyl groups, improves their intermolecular interactions with the membrane bilayer. Simulation studies of antimicrobial peptides showed that peptides rearrange their flexible sidechains upon embedding in the membrane, thereby enhancing their interactions in the membrane-bound state.^[17]

It should be emphasized that some good antibacterial prenylated compounds had structures that deviate from these conclusions. Pyran prenylated 6a,11a-pterocarpenes (e.g. dehydroglyceollin I with a *KierFlex* index of 2.2 and *std_dim3* of 0.7 **Chapter 4**) have non-flexible skeleton and prenyl groups. Additionally, this skeleton is flat due to the presence of the C6a-C11a double bond. Nevertheless, this compound mapped the *L. monocytogenes* 3D pharmacophore and showed very good antibacterial activity against this bacterium (MIC 15 $\mu\text{g}/\text{mL}$). Thus, these QSAR obtained might be regarded as a starting point for further research to complete the overview of molecular requirements for prenylated phenolic compounds as antibacterial agents.

In conclusion, these QSAR can be used to select prenylated (iso)flavonoid structures for further design and development as good antibacterials. Extrapolation of these QSAR to other phenolic subclasses or other bacteria not used in this thesis should be performed with caution and experimentally confirmed.

Correlation of QSAR with mode of action of prenylated (iso)flavonoids

The second aim of this thesis was to elucidate the mode of action (MOA) of prenylated phenolic compounds. In this thesis, disruption of cytoplasmic membrane integrity was studied as the potential mode of action of these compounds. Hydrophobicity and shape were the predominant molecular features defining antibacterial activity (**Chapter 4**). It was proposed that hydrophobicity defines the effective partitioning to membranes, whereas shape (flexibility and globularity) determine the effective disruption of the membrane integrity. Hydrophobicity and shape have been reported before to play a dominant role in determining the localization of phenolic compounds in model membranes.^[18-21] High hydrophobicity and planar structure were proposed to promote a deep insertion into model membranes. Considering the QSAR findings of this thesis, it is speculated that planar structures diffuse deeper into the membrane, but will not effectively kill the bacterium. More globular molecules might penetrate less deep than planar ones, but will disrupt the integrity of the membrane more efficiently.

One of the mechanisms of disruption of membrane integrity initially proposed was membrane permeabilization. In this thesis it was found that prenylated phenolic compounds can permeabilize the bacterial cytoplasmic membrane, although permeabilization was not directly correlated with antibacterial activity. Some antibacterial prenylated phenolic compounds were able to permeabilize the cytoplasmic membrane of bacteria faster than some traditional antibacterials, whereas other antibacterial prenylated phenolics were unable to permeabilize at all (**Chapters 3 and 4**).

Wighteone, a monoprenylated isoflavone, was one of the most efficient permeabilizers (**Chapter 4**). **Figure 6.2** shows a preliminary experiment in which wighteone permeabilization capacity towards *L. monocytogenes* was tested at its MIC (i.e. 10 $\mu\text{g}/\text{mL}$) and at twice its MIC (2xMIC). Even though cell counts were not available for the 2xMIC experiment, it was clear that wighteone could reduce the number of cells significantly, without effectively permeabilizing them. Therefore, membrane permeabilization does not seem to be the only factor by which certain antibacterial prenylated phenolic compounds can influence membrane integrity. The main mechanism of killing is yet to be determined. Disruption of membrane integrity may be caused by other mechanism, such as rigidification of the membrane.^[18]

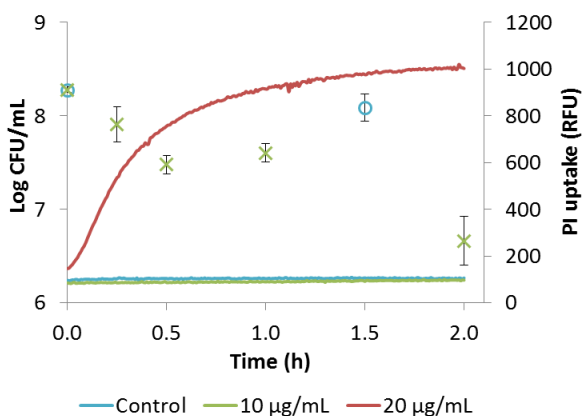


Figure 6.2. PI uptake (lines) and cell counts (symbols) of *L. monocytogenes* when exposed to wighteone. Control refers to the untreated cells.

In **Chapter 4** a negative correlation between the permeabilization capacity of prenylated (iso)flavonoids and their hydrophobic:polar surface area ratio was proposed. Compounds with a relatively large hydrophobic surface area might interact deep in the membrane. In contrast, compounds with a relatively low hydrophobic surface area might interact close to the surface. A scheme illustrating the potential differences in localization in the cytoplasmic membrane between good antibacterial(iso)flavonoids, but with different permeabilization capacity, is depicted in **Figure 6.3**. For both Gram positive and Gram negative microorganism, the cytoplasmic membrane is composed of a phospholipid bilayer.^[22] Poor and non-permeabilizers, such as diprenylated 6,8-

diprenylgenistein, glabrol and hispaglabridin A/B, might interact deep in the membrane with the acyl chains of the phospholipids,^[19] as they have a larger hydrophobic:polar surface area ratio (≥ 4.2 , **Chapter 4**) than permeabilizers. In contrast, permeabilizers, such as monopenylyated wighteone, isowighteone and luteone, might interact more intensively with the phospholipid head groups (e.g. with the carbonyl of the ester groups). When a minimum number of molecules have integrated into the membrane, the packing of the membrane surface might be compromised. This facilitates passage of charged compounds, such as propidium iodine. This is in line with previous work,^[20] reporting that monopenylyated flavonoids interact with both the glycerol and acyl chain regions of the membranes. In that study, the prenylated compounds affected the dipalmitoyl phosphatidyl choline (DPPC) head group packing and increased the hydration of the membrane surface. Furthermore, it has been hypothesized that compounds interacting deep in the membrane may cause rigidification of membranes, whereas compounds penetrating less into the membrane may cause fluidization.^[18] In both cases, membrane integrity is disrupted.

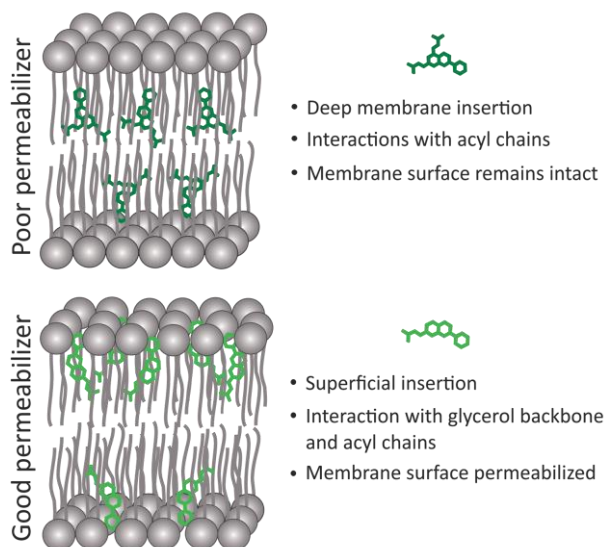


Figure 6.3. Schematic illustration of the proposed membrane localization and effects of two antibacterial prenylated isoflavonoids in the cytoplasmic membrane. The dark green diprenylyated compound represents a poor-permeabilizer, whereas the light green monopenylyated compound represents a good membrane permeabilizer (**Chapter 4**).

Prediction of antibacterial activity of untested prenylated stilbenoids

Prenylyated stilbenoids were correlated with the antibacterial activity of peanut seedling extracts (**Chapters 2 and 3**), however, pure prenylyated stilbenoids were not available for testing. As a subsequent action, the antibacterial activity of the main prenylyated stilbenoids identified in the peanut extract (**Chapter 2 and 3**) were predicted by using the

QSAR models developed in **Chapter 4**. This was performed to obtain an indication of which compound will potentially show good antibacterial activity.

Table 6.2 shows the predicted activities of prenylated stilbenoids against *L. monocytogenes* and *E. coli*. In **Chapter 4** two significant models were proposed for *L. monocytogenes* antibacterial activity (i.e. models A and B), using different sets of molecular descriptors. As observed in **Table 6.2** *L. monocytogenes* models predicted two of the five activities very differently. While model A gave high probability (i.e. ≥ 0.85) to all compounds, except IPD, for being active, model B predicted that only arachidin-2 had high probability (0.87) of having good antibacterial activity against *L. monocytogenes*. Additionally, the pharmacophore model was mapped by all prenylated stilbenoids except for IPD. Only arachidin-2 showed high probabilities of having antibacterial activity against *E. coli* and mapped the features of the pharmacophore model.

Table 6.2. Predicted activity and pharmacophore feature mapping of prenylated stilbenoids found in elicited peanut seedlings, using the binary ^a and pharmacophore models developed in **Chapter 4**.

Compound	Configuration of prenyl	<i>L. monocytogenes</i>			<i>E. coli</i> ^c	
		QSAR-A	QSAR-B	Pharmac. ^b	QSAR	Pharmac.
Arachidin-1	3-methyl-1-butenyl	0.92	0.08	+	0.01	-
Arachidin-2	3-methyl-2-butenyl	0.94	0.87	+	0.97	+
Arachidin-3	3-methyl-1-butenyl	0.99	0.73	+	0.01	-
IPD ^d	3-methyl-1,3-butadienyl	0.51	0.67	-	0.02	-
IPP ^e	3-methyl-1,3-butadienyl	0.89	0.08	+	0.01	-

^a An active (1) and inactive (0) compound is defined using an activity threshold of MIC ≤ 25 $\mu\text{g}/\text{mL}$, expressed as pMIC ($-\log_{10}\text{MIC}$) in molar. ^b +, compounds mapped all pharmacophore model features; - compounds did not map all pharmacophore features. ^c The model for *E. coli* is for *E. coli* under efflux pump inhibition conditions. ^d *trans*-3'-isopentadienyl-3,5,4'-trihydroxystilbene. ^e 4-isopentadienyl-3,5,3',4'-tetrahydroxystilbene/4-iso-pentadienyl piceatannol).

Arachidin-2 was the compound most frequently predicted to have good antibacterial activity. This compound is the only one from the stilbenoids aforementioned with a standard prenyl configuration, i.e. with a dimethylallyl or 3-methyl-2-butenyl substituent. The other stilbenoids have prenyl groups with different positions of double bonds. **Figure 6.4** shows the effect of the prenyl configuration on the molecular properties of these compounds. As observed the shape becomes more flat when changing from 3-methyl-2-butenyl prenyl configuration (as in arachidin-2) via 3-methyl-1-butenyl (as in arachidin-3) to 3-methyl-1,3-butadienyl (as in IPP). The standard prenyl

configuration provides a more globular structure and a relatively larger hydrophobic surface area (yellow colour) in comparison to the non-standard prenyl groups. In contrast, the prenyl chain containing two double bonds as in IPP or IPD induced an almost completely flat shape and low hydrophobic surface area. This might be explained by the long conjugated system of IPP or IPD, as it extends from the stilbenoid skeleton to the end of the prenyl group. In accordance with the main descriptors of the QSAR models and our proposed mode of action, the more globular molecular shape of arachidin-2 will make it more effective at disrupting the membrane integrity than the more flat shapes of the other prenylated stilbenoids in **Table 6.2**. With regard to flexibility, prenylated stilbenoids have similar *KierFlex* indices as those in good antibacterial (iso)flavonoids (**Chapter 4**). Therefore, flexibility is not expected to be a limiting factor for the effective antibacterial action of these molecules.

With regard to permeabilization capacity, making the assumption that prenylated stilbenoids will interact with membranes in a similar way as prenylated (iso)flavonoids, arachidin-2 and arachidin-3 most probably will be poor membrane permeabilizers. Their hydrophobic:polar surface area ratio (**Figure 6.4**) is comparable to those of poor permeabilizing antibacterial prenylated (iso)flavonoids previously tested (roughly between 4.0-7.0, **Chapter 4**). This is in agreement with the low permeabilization capacity found for the peanut Flash pool enriched in prenylated stilbenoids (**Chapter 3**, arachidin-2 was the most abundant compound in this pool). Furthermore, planar compounds have been shown to diffuse deep into model membranes,^[20] which will support a low permeabilization capacity for these compounds.

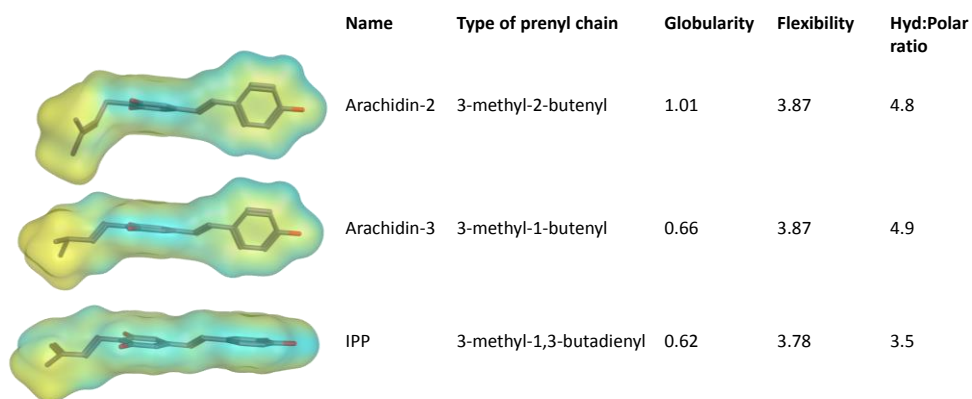


Figure 6.4. Molecular surface and properties of prenylated stilbenoids (MOPAC energy minimization). Surface is coloured by hydrophobicity (yellow) and polarity (light blue). Globularity is indicated by the standard dimension along the z axis (*std_dim3*). Flexibility is indicated by the *KierFlex* index. The permeabilization capacity is indicated by the fractional hydrophobic:polar surface area ratio (Hyd:Polar ratio) as explained in **Chapter 4**. Molecular surfaces and descriptors are calculated using MOE (Chemical Computing Group).

It should be emphasized that these predictions are made under the assumption that the molecular requirements for exerting antibacterial activity and mode of action are the same as those of prenylated (iso)flavonoids. It is worthwhile investigating these prenylated stilbenoids in order to obtain experimental confirmation of these predictions.

Intrinsic bacterial resistance towards prenylated phenolics

Apart from *L. monocytogenes* and *E. coli*, antibacterial activity of glabridin, a pyran prenylated isoflavan, was tested against other bacteria using the same methodology as in **Chapter 4 (Table 6.3)**. *L. monocytogenes* was the most resistant Gram positive; *S. aureus* was the second most resistant, whereas *Bacillus cereus* was the most susceptible Gram positive bacterium. Gram negative bacteria, as expected, showed high intrinsic resistance to glabridin. Only when glabridin was combined with efflux pump inhibitor (EPI), *E. coli* became susceptible (no experiment with *Salmonella* and EPI was performed). Differences in intrinsic resistance observed can be analysed from two aspects: entry and half-life of the antibacterial compound. These two aspects are influenced by the architecture of the cell envelope. Specifically, the cell wall composition of Gram positive bacteria and the composition of the outer membrane of Gram negative bacteria influence the entry of antibacterials. The half-life is determined to a large extent by the presence of efflux pump systems from one of the efflux pump superfamilies.

Table 6.3. Antibacterial activity of glabridin against Gram positive and Gram negative bacteria.

Bacteria	Glabridin ^a (µg/mL)		Teichoic acids in cell wall (% w/w)	Main efflux pump systems ^b	Ref.
	MIC	MBC			
<i>Bacillus cereus</i> (ATCC 14579)	6	8	5	SMR (single component)	[23,24]
<i>S. aureus</i> (ATCC 25923)	8	15	21-40	MFS (single component)	[25,26]
<i>L. monocytogenes</i> (EGD-e)	15	20	30-40	MFS (single component)	[27-29]
<i>E. coli</i> (K12)	> 100	-	- ^c	RND (multicomponent)	[30]
<i>E. coli</i> (K12 + EPI ^d)	10	15	-	-	-
<i>Salmonella</i> Typhimurium (S2 505)	> 100	-	-	RND (multicomponent)	[31]

^a Antibacterial activity measured in this thesis by the broth microdilution assay. ^b SMR, small multidrug resistance superfamily; MFS, major facilitator superfamily; RND, resistance-nodulation-division superfamily. ^c Gram negative cell wall do not contain teichoic acids. ^d EPI, efflux pump inhibitor.

1) Role of cell wall composition in the entrance of prenylated phenolics

The cell wall (i.e. peptidoglycan layer) is generally considered to exert low barrier effects to the influx of antibacterials. Nevertheless, the differences in composition of the cell wall can be partly responsible for the differences in susceptibility between the Gram positive

bacteria. Partitioning to the inner membrane in Gram positives requires first the diffusion through the cell wall, which is composed of peptidoglycan, crosslinked with pentapeptide chains, and teichoic acids, polymers composed of glycosylated polyglycerol or polyribitol phosphate chains.^[22] Studies on the cell wall of (methicillin-resistance) *S. aureus* revealed important functions of wall teichoic acids (WTA), including resistance to antibacterials.^[32,33]

B. cereus cell walls contain around 5% (w/w) of teichoic acids.^[24] In contrast, *S. aureus* and *L. monocytogenes* cell walls can contain between 20-40% (w/w) of teichoic acids.^[26,29,34] This reduced content of teichoic acids makes *B. cereus* cell wall more hydrophobic and, therefore, more susceptible to diffusion of hydrophobic compounds, than *S. aureus* and *L. monocytogenes*.

Teichoic acids can have different types of substitutions (e.g. D-alanyl esters or glycosyl moieties).^[32] The nature and extent of substitutions affect the cell wall's overall charge and hydrophobicity.^[22] *L. monocytogenes* teichoic acids are known to be more glycosylated than those of *S. aureus*.^[35,36] Glycosyl residues found in teichoic acids of *L. monocytogenes* include galactose, glucose, N-acetylglucosamine and rhamnose.^[37] It is hypothesized that this higher glycosylation will make *L. monocytogenes* cell walls less hydrophobic than those from *S. aureus*. As a result, it will be less prone to diffusion of hydrophobic compounds, such as glabridin.

As the cell wall of Gram negatives does not contain teichoic acids and is thinner (5-10 nm thick) than that of Gram positives (30-100 nm),^[22] the diffusion through the cell wall is of low importance with regard to the intrinsic resistance of Gram negatives.

2) Role of the outer membrane in the entrance of prenylated phenolics

In addition to crossing the cell wall, prenylated phenolic compounds must cross the outer membrane (OM) to reach the cytoplasmic membrane. For Gram positives this does not apply as they do not possess an outer membrane. Regarding the number of prenyl groups, diprenylated molecules were less effective against *E. coli* than against Gram positive bacteria. This has been observed in other studies as well.^[11,38,39] This was proposed (**Chapter 4**) to be related to the influx restriction imparted by porins.

Figure 6.5 shows the molecular surface of ampicillin, an antibiotic known to enter via porins, and four prenylated isoflavones. Molecules are ranked based on their activity against *E. coli*. Additionally, a model of the main porin in *E. coli* with ampicillin bound inside is shown for comparison of molecular surfaces. It is speculated that the trend observed for antibacterial activity may be partly explained by the affinity of the compounds towards the porin channels. These open channels allow molecules of MW < 600-700 to cross.^[40] Therefore, we can conclude that crossing of prenylated phenolic compounds through porins is not limited by their size. These channels favour the diffusion of polar and charged molecules. The lower total polar surface area (TPSA) and higher hydrophobicity ($\log D$) of prenylated phenolic compounds in comparison with ampicillin may hinder their efficient permeation via porins.

Some antibiotics are thought to use both porin- and lipid-mediated influx, depending on their protonation.^[41] The possibility of permeation of prenylated phenolic compounds through the lipid bilayer of the outer membrane cannot be excluded. However, as an important effect on the antibacterial activity was observed when hydrophobicity was decreased (Chapter 4), porin influx is thought to be the most important influx pathway for prenylated phenolic compounds. Therefore, taking into the account the above, slow penetration through the porins is thought to be partly responsible for the intrinsic resistance of Gram negatives towards some prenylated phenolics.

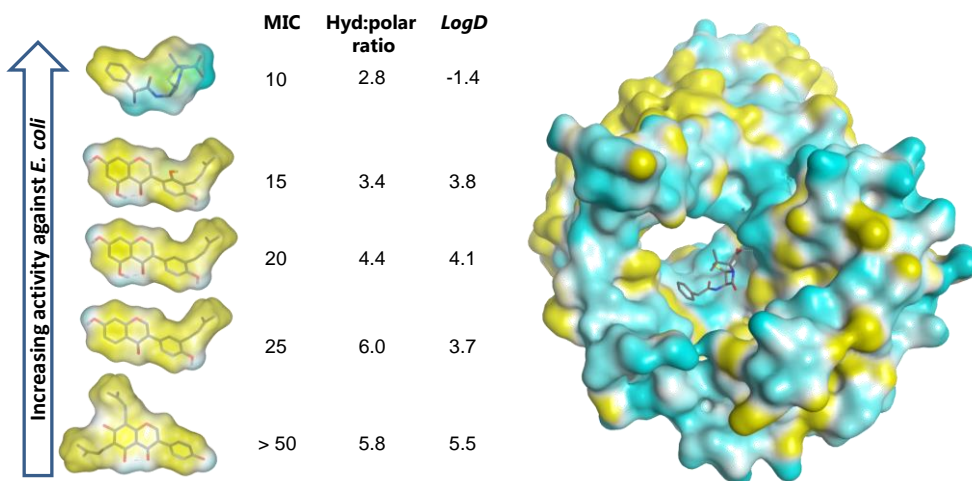


Figure 6.5. Molecular surface and properties of ampicillin and prenylated phenolic compounds (MOPAC energy minimization), ranked based on their MIC values against *E. coli* (left). Model of porin OmpF (PDB 4GCP)^[42] from *E. coli* with ampicillin bound (right). Surfaces are coloured based on hydrophilicity (light blue) and hydrophobicity (yellow).

3) Role of the efflux pumps in the half-life of prenylated phenolics

One of the main findings of this thesis is that the intrinsic resistance of *E. coli* towards prenylated phenolic compounds can be reversed by using an efflux pump inhibitor. Moreover, this finding confirms that prenylated phenolic compounds are able to cross the outer membrane of this Gram negative bacterium, via the porins as previously discussed.

Differences in susceptibility can be partly explained by the superfamily of efflux pump systems present in bacteria. Prenyated phenolics are efficiently secreted from *E. coli* by the AcrAB-TolC multidrug efflux pump as susceptibility to prenylated compounds increased when an efflux pump inhibitor of this pump was used (PABN, Chapters 3 and 4). *E. coli* and *Salmonella* contain this multicomponent multidrug efflux pump from the Resistance-Nodulation-Division (RND) superfamily (Table 6.3), which spans both the inner and outer membranes and has broad substrate specificity. This efflux pump is

important for the intrinsic resistance of Gram negative bacteria towards conventional antibacterials.^[43] The effect of efflux pump deletion in *E. coli*'s susceptibility to antibacterials has been shown to be more prominent for hydrophobic or large antibacterials (e.g. the prenylated antibiotic noboviocin, *logD* 2.8)^[41] than for hydrophilic and small antibacterials (e.g. ampicillin, *logD* -1.4). This is due to their higher efflux than influx rate under normal conditions. In contrast, for hydrophilic or small compounds, which enter rapidly via porins, deletion of efflux pumps systems did not improve their antibacterial properties to a significant extent. Their influx rate is higher than their efflux rate under normal conditions.^[41] For prenylated phenolic compounds, the inhibition of efflux pumps had a prominent effect on the antibacterial activity of the compounds. MIC values for *E. coli* decreased to similar levels as those of *L. monocytogenes*. Thus, it is postulated that under normal conditions most prenylated phenolic compounds are inactive against Gram negatives due to their relatively low influx rate in comparison to their high efflux rate.

In contrast to Gram negatives, Gram positive bacteria do not have multicomponent efflux systems (**Table 6.3**). Instead, *S. aureus* and *L. monocytogenes* contain single component efflux pump systems from the major facilitator (MFS) superfamily, which are known to secrete antimicrobials (e.g. fluoroquinolones, macrolites).^[25,27] It is known that some of these pumps have a basal level of expression.^[25] This accounts for some level of reduced susceptibility towards antimicrobial compounds for these two bacteria. *Bacillus* sp. contain single component efflux pumps from the small multidrug resistance (SMR) superfamily. Nevertheless, intrinsic multidrug resistance (MDR) in *Bacillus* has not been reported.^[23,44] The lack or low level of expression of MDR efflux pumps in *B. cereus*, besides cell wall composition as previously explained, might explain the higher susceptibility of this bacterium towards glabridin than that of *L. monocytogenes* and *S. aureus* (**Table 6.3**).

In conclusion, the type of bacteria being targeted will determine the effectiveness of prenylated phenolic compounds as antibacterials. It is essential to perform further (Q)SAR studies with other bacterial species to confirm and extend the main relationships found in this thesis.

EFFECT OF NON-PHENOLIC PLANT COMPONENTS ON ANTIBACTERIAL ACTIVITY

Chemical diversity might be advantageous for plant extracts as the presence of different types of phytochemicals might induce stronger antibacterial effects, evolving from synergy between molecules with different mode of action. Conversely, when other non-antibacterial phytochemicals are present in an antibacterial extract, counteraction of activity by those non-antibacterials must be taken into consideration.

In this thesis, two main types of phytochemicals in legume seedling extracts were identified: phenolic compounds, especially from the isoflavonoid class, and saponins (**Chapter 2**). Prenylated isoflavonoids were correlated with the antibacterial

activity, whereas saponins were not. In literature, saponins are thought to have membranolytic activity due of their amphiphilic structure. The most accepted mechanism of antimicrobial action of saponins involves their partitioning to membranes and complexation with membrane sterols.^[45]

To investigate if soyasaponins present in extracts from legume seedlings have by themselves an effect on the antibacterial properties of the extracts and of prenylated phenolic compounds, the antibacterial activities of a commercial mixture of soyasaponins and of a purified saponin were tested against *L. monocytogenes* (Figure 6.6), in combination with a legume seedling extract (i.e. white lupine) and monoprenylated isoflavone lupiwighteone, respectively. As observed, *L. monocytogenes* was insusceptible to soyasaponins. This confirms the lack of (positive) correlation found between the content of saponins and the antibacterial activity of legume seedling extracts against this bacterium (Chapter 2).

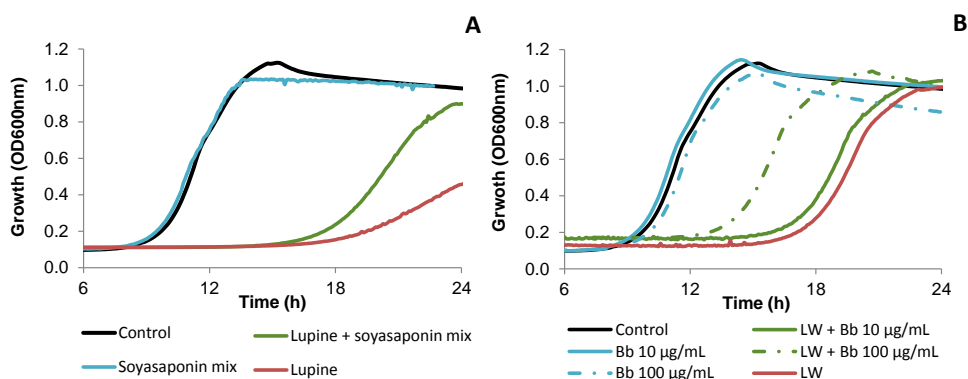


Figure 6.6. *L. monocytogenes* growth (OD_{600nm}) over time in the presence of (A) extracts containing soyasaponins (1000 µg/mL) and/or prenylated phenolic compounds (i.e. white lupine seedling extract, 1000 µg/mL); (B) soyasaponin Bb (Bb) and/or lupiwighteone (LW, 100 µg/mL). Control refers to the untreated cells. Commercial soyasaponin mixture is from Riedel-de Haën AG and soyasaponin Bb from Sigma-Aldrich.

Notably, the growth inhibitory action of white lupine and lupiwighteone was counteracted by the saponins. This detrimental effect of saponins on the antibacterial properties of prenylated phenolic compounds might be explained by the saponin's nature to form unimolecular or mixed micelles. The critical micelle concentration (CMC) of soyasaponin Bb is between 70-100 µg/mL.^[46] Therefore, saponin Bb most probably formed micelles when added at 100 µg/mL. These micelles can compete with the bacterial cell membrane for the partitioning of prenylated phenolic compounds, resulting in less prenylated molecules interacting with the bacterial membrane. In Chapter 2, the concentrations of saponins present in the extracts in the antibacterial assays were generally lower than the aforementioned CMC, except for 2 extracts (soybean G and blue lupine GF when tested at 1.0 mg/mL). This might explain the lack of negative correlation between the content of saponins and antibacterial activity.

Overall, the presence of saponins together with prenylated phenolic compounds in antibacterial plant extracts needs to be evaluated, regardless of the target bacteria. Hydrolysis of the glycosidic chains of saponins can reduce their tendency to form micelles, depending on the sapogenin skeleton. If so, this might allow the reduction of the detrimental effects of saponins on prenylated phenolic compounds antibacterial activity, when present above their CMC.

IN VITRO ENZYMATIC PRENYLATION OF PHENOLICS

O-Prenylation may be detrimental for antibacterial activity

The third aim of this thesis was to evaluate the *in vitro* production of diprenylated phenolic compounds using microbial prenyltransferases, as those compounds showed the highest antibacterial activity (**Chapter 4**). Microbial prenyltransferases are considered potential biotechnological tools to produce diprenylated phenolic compounds because of their broader substrate specificity and robustness in comparison with plant prenyltransferases.^[47] One of the main findings of this thesis was that prenyltransferase SrCloQ could either C- or O-prenylate different phenolic compounds from the flavonoid, isoflavonoid and stilbenoid classes. However, conversion yields were rather low (i.e. < 10% (w/w)) and no diprenylated molecules were produced. Nevertheless, some prenylated phenolics produced in this thesis were, to our knowledge, novel as they have not been reported in plants before. This includes the O-prenylated phenolic compounds, such as O-prenylated forms of luteolin, resveratrol and 3'-OH-daidzein; as well as some C-prenylated ones, such as C-prenylated equol.

In **Chapter 5** chain prenylated equol was one of the most abundant reaction products obtained by means of SrCloQ (i.e. A_{ring} and B_{ring} chain prenylated equol). To our knowledge, chain prenylated equol has neither been isolated nor tested for its antibacterial activity. It is hypothesized that C8 chain prenylated equol is a potentially interesting antibacterial compound as isoflavan skeletons were some of the most effective (iso)flavonoids tested in this thesis. Also, chain prenylation was shown to be better than pyran prenylation (**Chapters 3 and 4**).

Based on our active site modelling (**Chapter 5**), it was concluded that a flavone skeleton is better than an isoflavone skeleton for prenylation with SrCloQ. This is due to the orientation of the A- and C-rings in the flavone. These rings are able to make contacts with Arg160, Arg176 and Tyr233 in the active site, whereas with the isoflavone only the contact with Arg160 is possible. Considering these contacts, it can be speculated that a flavanone (e.g. 7,4'-dihydroxyflavanone, also known as liquiritigenin) is a potentially good acceptor substrate for SrCloQ. This is because it has the configuration to make the appropriate interactions with the key amino acid residues. Moreover, flavanones are more flexible than flavones, which might improve the interactions with the enzyme even further. As SrCloQ favoured B-ring prenylation, a δ -chain C-prenylated flavanone would be expected as main reaction product. According to

our SAR findings, this position and configuration of prenylation are potentially favourable for antibacterial activity.

O-prenylated natural compounds represent a new group of secondary metabolites recently recognized to have interesting and valuable biological activities, including antimicrobial and anti-cancer activity.^[48] Many of the described O-prenylated compounds have been found in a limited number of plant families, especially Rutaceae. Far less examples of O-prenylated flavonoids, isoflavonoids and stilbenoids have been isolated from legumes.^[49-51] O-Prenylated phenolic compounds have shown moderate antimicrobial activity against fungi, Gram positive and Gram negative bacteria.^[52,53] Nevertheless, in depth research on their activity is still lacking, partly because of their scarce availability. In this respect, production of novel O-prenylated phenolic compounds with SrCloQ can be a good alternative. Extending our knowledge of QSAR of prenylated phenolic compounds, O-prenylation of phenolic compounds will increase their hydrophobicity, which was related to good antibacterial activity against *L. monocytogenes* and bad against *E. coli*. On the other hand, the loss of free hydroxyl groups, depending on the position and subclass as previously shown in the SAR section of this chapter, might be detrimental for activity. To this end, C-prenylation seems the preferred option as there is no possibility of losing free hydroxyl groups essential for antibacterial activity.

Comparison of different production methods for prenylated phenolics

Diprenylated phenolic compounds were some of the most active antibacterials studied in this thesis (**Chapter 4**). In **Table 6.4**, a comparison of production methods of (di)prenylated phenolic compounds is shown, highlighting advantages, disadvantages and yields.

Elicitation of plants is a good strategy to promote the production of prenylated phenolic compounds. Unfortunately, diprenylated compounds occurred at low levels in our plant extracts, and this complicates their isolation and further evaluation. Nevertheless, legume seedling extracts containing mixtures of different prenylated phenolic compounds, including diprenylated compounds, proven to be very promising as antibacterials (**Chapter 2**).

Enzyme catalysis with promiscuous prenyltransferases can lead to novel natural products, not produced by plants, with perhaps enhanced/modified activity profiles.^[54] Although prenylation with SrCloQ did not give the results expected, other microbial prenyltransferases have shown good conversion yields (e.g. 90% for SsNovQ)^[55] and diprenylation of molecules (e.g. for Sc/NphB).^[56] NphB produced a double C-geranylated stilbenoid. Such compounds are very hydrophobic ($\log D$ 10) and relatively large (MW 500). For antibacterial purposes it might be active only against Gram positive bacteria. The geranyl chains (ten-carbon isoprenoid) might improve the activity of stilbenoid in comparison with prenyl chains, as longer flexible substituents might be more effective in interacting with the phospholipid bilayer and disrupt the membrane integrity.

Another alternative for production of diprenylated compounds is chemical synthesis. As determined in this thesis, prenylated phenolic compounds showed antibacterial activity only when the prenyl group is attached to specific positions, depending to the phenolic subclass. For research purposes, such as for QSAR studies, chemical prenylation coupled with purification is an attractive tool as availability of compounds bearing prenyl groups at diverse positions is desired for understanding QSAR. For scaling up production, one of the main limitations of chemical prenylation is selectivity of the reaction. This problem might be tackled by performing subsequent steps of functional group protection and deprotection to obtain the right reaction product.^[57] Each step, with its own special conditions of e.g. temperature, pressure and atmosphere, will make the overall process of chemical prenylation laborious.^[58]

Is double prenylation an efficient strategy to increase antibacterial activity?

In this thesis, it was found that the most active prenylated phenolic compounds against Gram positive bacteria were diprenylated (**Chapter 4**). In line with this, enzymatic prenylation as a tool for producing diprenylated compounds was investigated (**Chapter 5**). Nevertheless, when analysing the decrease in MIC values after addition of a second prenyl group to a compound, it seemed that activity mainly originated from the presence of a single prenyl group. MIC values can be >10-fold decreased by the addition of one prenyl group to a non-prenylated phenolic compound. (**Chapter 4**,^[59]). For example, genistein (non-prenylated isoflavone) was not active against *L. monocytogenes* (MIC > 100 $\mu\text{g}/\text{mL}$). Wighteone (β -prenylated genistein) showed good antibacterial activity (MIC 10-15 $\mu\text{g}/\text{mL}$, 30-45 μM). The addition of a second prenyl group to form 6,8-diprenylgenistein (or 8-prenylwighteone) ($\alpha + \beta$ prenylation) improved the activity further, but not drastically (MIC 6 $\mu\text{g}/\text{mL}$, 14 μM). For isoflavans, the addition of a second prenyl group to glabridin (MIC 15 $\mu\text{g}/\text{mL}$, 46 μM) had very little effect (hispaglabridin A, MIC 12.5 $\mu\text{g}/\text{mL}$, 32 μM).

In general, it seems that the presence of a single prenyl moiety (at the right position) is enough to provide antibacterial properties to a phenolic compound (i.e. partitioning to membranes and disruption of membrane integrity), but a second prenyl group will make it slightly more efficient. No triple prenylated compounds were tested in this thesis. Nevertheless, the few examples in literature demonstrated that triple prenylation does not improve the antibacterial properties of prenylated compounds beyond that of diprenylated molecules.^[60] On the contrary, most triple prenylated compounds reported were inactive.^[61] In conclusion, diprenylated phenolic compounds may not yield the increase in potency expected in relation to the research and production efforts required (e.g. plant, enzymatic or chemical prenylation). Nevertheless, to this end, diprenylated phenolic compounds have shown the highest antibacterial activity against human pathogenic bacteria, with MIC values similar to those of traditional antibacterials.

Table 6.4. Comparison of different production methods of prenylated phenolic compounds.

Method	Advantages	Disadvantages	Yields (%)
<i>In planta</i> prenylation ^a	Large molecular diversity (valuable for application of extracts as antibacterials) Low production and scale up costs	Low concentrations of each individual compound	10-60% prenylated compounds in extracts of elicited legume seedlings (this thesis)
Enzymatic prenylation	Aqueous conditions Stereo- and regiospecificity Broad substrate specificity of some microbial PTs (novel natural prenylated compounds)	Stability of enzyme (substrate/product inhibition) Low initial substrate concentrations (solubility problems)	<10% <i>SrCloQ</i> (this thesis) 10-90% <i>ScINphB</i> ^[56,59] 5-90% <i>SsNovQ</i> ^[55] 10-27% <i>Sco7190</i> ^[59]
Chemical prenylation	High yields Racemic mixtures (<i>cis/trans</i> , different conjugation of prenyl) (valuable for SAR purposes)	Successive steps for functional group protection and deprotection Long step-sequences (> 48-72 h) with extreme temperatures (e.g. -70 °C, 170 °C)	20-50 % ^[60] 20 % ^[57] 50% ^[58] 60-90% ^[61]

^a Not including transgenic plants.

PROSPECTS

Prenylated phenolic compounds have very good potential as natural antibacterial agents, as they showed MIC values $\leq 15 \mu\text{g/mL}$. Additionally, these compounds are proposed to target the cytoplasmic membrane integrity with a different mechanism than other conventional antibacterials targeting this membrane.

Pathogenic bacteria have been treated with antibacterials that affect a single target and this approach is partly responsible for the antibacterial resistance observed nowadays. A new concept consists of using antimicrobials with different targets in order to reduce the probability of resistance development.^[65] In this context, non-prenylated flavonoids, such as kaempferol (present in many edible and medicinal plants)^[66], which have shown strong inhibition of the bacterial enzyme DNA gyrase,^[67] can be combined with prenylated isoflavonoids, e.g. from elicited lupine seedlings. In this way, the membrane integrity and DNA production are targeted simultaneously.

In this thesis, compounds were tested against *E. coli* and no susceptibility was observed under normal growth conditions. As addition of an efflux pump inhibitor restored the susceptibility of *E. coli* towards prenylated phenolic compounds, the combination of these antibacterials with natural efflux pump inhibitors is a promising tool to target Gram negatives. Natural compounds, such as epigallocatechin-gallate (EGCg, present in tea) and daidzein (present in soybean), have been identified as natural efflux pump inhibitors.^[68-70] EGCg showed significant efflux pump inhibition at $50 \mu\text{g/mL}$. This is only two times higher than the concentration commonly used of the traditional efflux pump inhibitor PA β N (**Chapters 3 and 4**). Thus, addition of such compounds to *multi-targeted* antibacterial preparations might be a promising strategy to increase the spectrum of activity (Gram positive and Gram negatives), as well as to increase their potency. It should be emphasized that prenylated phenolic compounds have shown good antibacterial activity against other Gram negative bacteria, mainly *Klebsiella* sp., *Proteus* sp. and *Pseudomonas* sp., without the need of efflux pump inhibitors. Therefore, the spectrum of activity of these molecules can be broader than observed in this thesis.

For clinical applications, prenylated phenolic compounds have shown synergistic activity *in vitro* when combined with conventional antibacterials and have restored the susceptibility of resistant bacteria.^[71] These antibacterial compounds can be given as part of a combinatorial therapy for gastrointestinal infections together with antibacterials targeting other bacterial cell components besides the cytoplasmic membrane. For example, they might be combined with antibacterials targeting protein synthesis, DNA production or cell wall synthesis.

The proposed mode of action of prenylated phenolics in the cytoplasmic membrane (including permeabilization and alteration of membrane fluidity), appears complementary to that of conventional antibacterials. Furthermore, the spectrum of activity of conventional antibacterials targeting the cytoplasmic membrane (i.e. antimicrobial peptides) is restricted to Gram positive bacteria, as the large size of these

antibiotics prevents them to cross the outer membrane of Gram negative bacteria. In this respect, prenylated compounds have an advantage over that class of antibiotics, as they are able to enter the Gram negative cell envelope and be effective in disrupting the cytoplasmic membrane integrity.

The low MIC values and broad spectrum of activity that some prenylated compounds have shown makes these phytochemicals promising natural antibacterial agents. The MOA of prenylated phenolics in the bacterial cell membrane needs to be further investigated. Additionally, aspects, such as emergence of resistance after repeated exposure, cytotoxicity, pharmacokinetic properties, product and process conditions, have yet to be evaluated for these natural antibacterials.

REFERENCES

- [1] Kosters, H.A.; Wierenga, P.A.; de Vries, R.; Gruppen, H. Characteristics and effects of specific peptides on heat-induced aggregation of β -lactoglobulin. *Biomacromolecules*, 2011, **12**, 2159-2170.
- [2] Johns, C.; Macka, M.; Haddad, P.R.; King, M.; Paull, B. Practical method for evaluation of linearity and effective pathlength of on-capillary photometric detectors in capillary electrophoresis. *Journal of Chromatography A*, 2001, **927**, 237-241.
- [3] Doerge, D.R.; Chang, H.C.; Churchwell, M.I.; Holder, C.L. Analysis of soy isoflavone conjugation *in vitro* and in human blood using liquid chromatography-mass spectrometry. *Drug Metabolism and Disposition*, 2000, **28**, 298-307.
- [4] CLSI. Methods for dilution antimicrobial susceptibility test for bacteria that grow aerobically; approved standard-ninth edition. 2012. Clinical and Laboratory Standards Institute: Wayne, PA, USA.
- [5] Golus, J.; Sawicki, R.; Widelski, J.; Ginalska, G. The agar microdilution method – a new method for antimicrobial susceptibility testing for essential oils and plant extracts. *Journal of Applied Microbiology*, 2016, DOI: 10.1111/jam.13253.
- [6] Paterlini, S.; Minerva, T. Regression model selection using genetic algorithms. In Proceedings of the 23rd workshop of the Italian Neural Networks Society 2010. World Scientific and Engineering Academy and Society (WSEAS): Iasi, Romania.
- [7] Hibbert, D.B. Genetic algorithms in chemistry. *Chemometrics and Intelligent Laboratory Systems*, 1993, **19**, 277-293.
- [8] Awouafack, M.; McGaw, L.; Gottfried, S.; Mbouangouere, R.; Tane, P.; Spitteller, M.; Eloff, J. Antimicrobial activity and cytotoxicity of the ethanol extract, fractions and eight compounds isolated from *Eriosema robustum* (Fabaceae). *BMC Complementary and Alternative Medicine*, 2013, **13**, 1-9.
- [9] Aslam, S.N.; Stevenson, P.C.; Kokubun, T.; Hall, D.R. Antibacterial and antifungal activity of cicerfuran and related 2-arylbenzofurans and stilbenes. *Microbiological Research*, 2009, **164**, 191-195.
- [10] Tsuchiya, H.; Sato, M.; Miyazaki, T.; Fujiwara, S.; Tanigaki, S.; Ohyama, M.; Tanaka, T.; Inuma, M. Comparative study on the antibacterial activity of phytochemical flavanones against methicillin-resistant *Staphylococcus aureus*. *Journal of Ethnopharmacology*, 1996, **50**, 27-34.
- [11] Hatano, T.; Shintani, Y.; Aga, Y.; Shiota, S.; Tsuchiya, T.; Yoshida, T. Phenolic constituents of licorice. VIII. Structures of glicophenone and glicoisoflavanone, and effects of licorice phenolics on methicillin-resistant *Staphylococcus aureus*. *Chemical & Pharmaceutical Bulletin*, 2000, **48**, 1286-1292.
- [12] Tanaka, H.; Sato, M.; Fujiwara, S.; Hirata, M.; Etoh, H.; Takeuchi, H. Antibacterial activity of isoflavonoids isolated from *Erythrina variegata* against methicillin-resistant *Staphylococcus aureus*. *Letters in Applied Microbiology*, 2002, **35**, 494-498.
- [13] Tanaka, H.; Sato, M.; Oh-Uchi, T.; Yamaguchi, R.; Etoh, H.; Shimizu, H.; Sako, M.; Takeuchi, H. Antibacterial properties of a new isoflavonoid from *Erythrina poeppigiana* against methicillin-resistant *Staphylococcus aureus*. *Phytomedicine*, 2004, **11**, 331-337.

- [14] Kato, R.; Kajiya, K.; Tokumoto, H.; Kumazawa, S.; Nakayama, T. Affinity of isoflavonoids for lipid bilayers evaluated with liposomal systems. *Biofactors*, 2003, **19**, 179-187.
- [15] Movileanu, L.; Neagoe, I.; Flonta, M.L. Interaction of the antioxidant flavonoid quercetin with planar lipid bilayers. *International Journal of Pharmaceutics*, 2000, **205**, 135-146.
- [16] Sohn, H.Y.; Kwon, C.S.; Son, K.H. Fungicidal effect of prenylated flavonol, papyriflavonol A, isolated from *Broussonetia papyrifera* (L.) Vent. against *Candida albicans*. *Journal of Microbiology and Biotechnology*, 2010, **20**, 1397-1402.
- [17] Liu, L.; Fang, Y.; Wu, J. Flexibility is a mechanical determinant of antimicrobial activity for amphipathic cationic α -helical antimicrobial peptides. *Biochimica et Biophysica Acta (BBA) - Biomembranes*, 2013, **1828**, 2479-2486.
- [18] Selvaraj, S.; Krishnaswamy, S.; Devashya, V.; Sethuraman, S.; Krishnan, U.M. Influence of membrane lipid composition on flavonoid-membrane interactions: Implications on their biological activity. *Progress in Lipid Research*, 2015, **58**, 1-13.
- [19] Hendrich, A.B.; Malon, R.; Pola, A.; Shirataki, Y.; Motohashi, N.; Michalak, K. Differential interaction of *Sophora* isoflavonoids with lipid bilayers. *European Journal of Pharmaceutical Sciences*, 2002, **16**, 201-208.
- [20] Wesołowska, O.; Gašiorowska, J.; Petrus, J.; Czarnik-Matusewicz, B.; Michalak, K. Interaction of prenylated chalcones and flavanones from common hop with phosphatidylcholine model membranes. *Biochimica et Biophysica Acta (BBA) - Biomembranes*, 2014, **1838**, 173-184.
- [21] Sinha, R.; Joshi, A.; Joshi, U.J.; Srivastava, S.; Govil, G. Localization and interaction of hydroxyflavones with lipid bilayer model membranes: A study using DSC and multinuclear NMR. *European Journal of Medicinal Chemistry*, 2014, **80**, 285-294.
- [22] Silhavy, T.J.; Kahne, D.; Walker, S. The bacterial cell envelope. *Cold Spring Harbor Perspectives in Biology*, 2010, **2**, 1-16.
- [23] Jack, D.L.; Storms, M.L.; Tchieu, J.H.; Paulsen, I.T.; Saier, M.H. A broad-specificity multidrug efflux pump requiring a pair of homologous SMR-type proteins. *Journal of Bacteriology*, 2000, **182**, 2311-2313.
- [24] Amano, K.-i.; Hazama, S.; Araki, Y.; Ito, E. Isolation and characterization of structural components of *Bacillus cereus* AHU 1356 cell walls. *European Journal of Biochemistry*, 1977, **75**, 513-522.
- [25] Costa, S.S.; Viveiros, M.; Amaral, L.; Couto, I. Multidrug efflux pumps in *Staphylococcus aureus*: an update. *The Open Microbiology Journal*, 2013, **7**, 59-71.
- [26] Wilkinson, B.J.; Dorian, K.J.; Sabath, L.D. Cell wall composition and associated properties of methicillin-resistant *Staphylococcus aureus* strains. *Journal of Bacteriology*, 1978, **136**, 976-982.
- [27] Gahan, C.G.M.; Hill, C. *Listeria monocytogenes*: survival and adaptation in the gastrointestinal tract. *Frontiers in Cellular and Infection Microbiology*, 2014, **4**, 1-7.
- [28] Uchikawa, K.; Sekikawa, I.; Azuma, I. Structural studies on lipoteichoic acids from four *Listeria* strains. *Journal of Bacteriology*, 1986, **168**, 115-122.
- [29] Uchikawa, K.; Sekiawa, I.; Azuma, I. Structural studies on teichoic acids in cell walls of several serotypes of *Listeria monocytogenes*. *Journal of Biochemistry*, 1986, **99**, 315-327.
- [30] Anes, J.; McCusker, M.P.; Fanning, S.; Martins, M. The ins and outs of RND efflux pumps in *Escherichia coli*. *Frontiers in Microbiology*, 2015, **6**, 587.
- [31] Nikaido, E.; Yamaguchi, A.; Nishino, K. AcrAB multidrug efflux pump regulation in *Salmonella enterica* serovar Typhimurium by RamA in response to environmental signals. *The Journal of Biological Chemistry*, 2008, **283**, 24245-24253.
- [32] Winstel, V.; Xia, G.; Peschel, A. Pathways and roles of wall teichoic acid glycosylation in *Staphylococcus aureus*. *International Journal of Medical Microbiology*, 2014, **304**, 215-221.
- [33] Brown, S.; Xia, G.; Luhachack, L.G.; Campbell, J.; Meredith, T.C.; Chen, C.; Winstel, V.; Gekeler, C.; Irazoqui, J.E.; Peschel, A.; Walker, S. Methicillin resistance in *Staphylococcus aureus* requires glycosylated wall teichoic acids. *Proceedings of the National Academy of Sciences*, 2012, **109**, 18909-18914.
- [34] Fujii, H.; Kamisango, K.-I.; Nagaoka, M.; Uchikawa, K.-I.; Sekikawa, I.; Yamamoto, K.-I.; Azuma, I. Structural study on teichoic acids of *Listeria monocytogenes* Types 4a and 4d. *Journal of Biochemistry*, 1985, **97**, 883-891.
- [35] Greenberg, J.W.; Fischer, W.; Joiner, K.A. Influence of lipoteichoic acid structure on recognition by the macrophage scavenger receptor. *Infection and Immunity*, 1996, **64**, 3318-25.
- [36] Xia, G.; Kohler, T.; Peschel, A. The wall teichoic acid and lipoteichoic acid polymers of *Staphylococcus aureus*. *International Journal of Medical Microbiology*, 2010, **300**, 148-154.
- [37] Fiedler, F. Biochemistry of the cell surface of *Listeria* strains: A locating general view. *Infection*, 1988, **16**, S92-S97.

- [38] Fukai, T.; Marumo, A.; Kaitou, K.; Kanda, T.; Terada, S.; Nomura, T. Antimicrobial activity of licorice flavonoids against methicillin-resistant *Staphylococcus aureus*. *Fitoterapia*, 2002, **73**, 536-539.
- [39] Kirmızibekmez, H.; Uysal, G.B.; Masullo, M.; Demirci, F.; Bağcı, Y.; Kan, Y.; Piacente, S. Prenylated polyphenolic compounds from *Glycyrrhiza ionicica* and their antimicrobial and antioxidant activities. *Fitoterapia*, 2015, **103**, 289-293.
- [40] Galdiero, S.; Falanga, A.; Cantisani, M.; Tarallo, R.; Pepa, M.E.; D'Oriano, V.; Galdiero, M. Microbe-host interactions: structure and role of Gram-negative bacterial porins. *Current Protein & Peptide Science*, 2012, **13**, 843-854.
- [41] Li, X.-Z.; Plésiat, P.; Nikaïdo, H. The challenge of efflux-mediated antibiotic resistance in Gram-negative bacteria. *Clinical Microbiology Reviews*, 2015, **28**, 337-418.
- [42] Ziervogel, Brigitte K.; Roux, B. The binding of antibiotics in OmpF porin. *Structure*, 2013, **21**, 76-87.
- [43] Kumar, A.; Schweizer, H.P. Bacterial resistance to antibiotics: Active efflux and reduced uptake. *Advanced Drug Delivery Reviews*, 2005, **57**, 1486-1513.
- [44] Kroeger, J.K.; Hassan, K.; Vörös, A.; Simm, R.; Saidijam, M.; Bettaney, K.E.; Bechthold, A.; Paulsen, I.T.; Henderson, P.; Kolstø, A.-B. *Bacillus cereus* efflux protein BC3310 - a multidrug transporter of the unknown major facilitator family, UMF-2. *Frontiers in Microbiology*, 2015, **6**, 1-12.
- [45] Osbourn, A.; Goss, R.J.M.; Field, R.A. The saponins - polar isoprenoids with important and diverse biological activities. *Natural Product Research*, 2011, **28**, 1261-1268.
- [46] Decroos, K.; Vincken, J.-P.; van Koningsveld, G.A.; Gruppen, H.; Verstraete, W. Preparative chromatographic purification and surfactant properties of individual soyasaponins from soy hypocotyls. *Food Chemistry*, 2007, **101**, 324-333.
- [47] Winkelblech, J.; Fan, A.; Li, S.-M. Prenyltransferases as key enzymes in primary and secondary metabolism. *Applied Microbiology and Biotechnology*, 2015, **99**, 7379-7397.
- [48] Epifano, F.; Genovese, S.; Menghini, L.; Curini, M. Chemistry and pharmacology of oxyprenylated secondary plant metabolites. *Phytochemistry*, 2007, **68**, 939-953.
- [49] Veitch, N.C. Isoflavonoids of the Leguminosae. *Natural Product Reports*, 2013, **30**, 988-1027.
- [50] Veitch, N.C.; Grayer, R.J. Flavonoids and their glycosides, including anthocyanins. *Natural Product Reports*, 2011, **28**, 1626-1695.
- [51] Shen, T.; Wang, X.-N.; Lou, H.-X. Natural stilbenes: an overview. *Natural Product Reports*, 2009, **26**, 916-935.
- [52] Hayashi, K.; Tokura, K.; Okabe, K.E.I.; Yamamoto, K.; Tawara, K. Syntheses and antimicrobial activities of Fomecins A and B, Asperugin, and related compounds. *Chemical & Pharmaceutical Bulletin*, 1982, **30**, 2860-2869.
- [53] Bonifait, L.; Marquis, A.; Genovese, S.; Epifano, F.; Grenier, D. Synthesis and antimicrobial activity of geranyloxy- and farnesyloxy-acetophenone derivatives against oral pathogens. *Fitoterapia*, 2012, **83**, 996-999.
- [54] Tian, L.; Pang, Y.; Dixon, R. Biosynthesis and genetic engineering of proanthocyanidins and (iso)flavonoids. *Phytochemistry Reviews*, 2008, **7**, 445-465.
- [55] Ozaki, T.; Mishima, S.; Nishiyama, M.; Kuzuyama, T. NovQ is a prenyltransferase capable of catalyzing the addition of a dimethylallyl group to both phenylpropanoids and flavonoids. *The Journal of Antibiotics*, 2009, **62**, 385-392.
- [56] Kumano, T.; Richard, S.B.; Noel, J.P.; Nishiyama, M.; Kuzuyama, T. Chemoenzymatic syntheses of prenylated aromatic small molecules using *Streptomyces* prenyltransferases with relaxed substrate specificities. *Bioorganic & Medicinal Chemistry*, 2008, **16**, 8117-8126.
- [57] Hossain, M.M.; Tokuoka, T.; Yamashita, K.; Kawamura, Y.; Tsukayama, M. Regioselective synthesis of 6-prenylpolyhydroxyisoflavone (wightone) and wightone hydrate with hypervalent iodine. *Synthetic Communications*, 2006, **36**, 1201-1211.
- [58] Tischer, S.; Metz, P. Selective C-6 prenylation of flavonoids via europium(III)-catalyzed Claisen rearrangement and cross-metathesis. *Advanced Synthesis & Catalysis*, 2007, **349**, 147-151.
- [59] Rukachaisirikul, T.; Innok, P.; Aroonrerk, N.; Boonamnuyap, W.; Limrangsun, S.; Boonyon, C.; Woonjina, U.; Suksamrarn, A. Antibacterial pterocarpanes from *Erythrina subumbrans*. *Journal of Ethnopharmacology*, 2007, **110**, 171-175.
- [60] Hufford, C.D.; Jia, Y.; Croom, E.M.; Muhammed, I.; Okunade, A.L.; Clark, A.M.; Rogers, R.D. Antimicrobial compounds from *Petalostemum purpureum*. *Journal of Natural Products*, 1993, **56**, 1878-1889.
- [61] Madan, S.S., G.N.; Kohli, K.; Ali, M.; Kumar, Y.; Singh, R.M.; Prakash, O. Isoflavonoids from *Flemingia strobilifera* (L) R. BR. roots. *Acta Poloniae Pharmaceutica-Drug Research*, 2009, **66**, 297-303.
- [62] Shindo, K.; Tachibana, A.; Tanaka, A.; Toba, S.; Yuki, E.; Ozaki, T.; Kumano, T.; Nishiyama, M.; Misawa, N.; Kuzuyama, T. Production of novel antioxidative prenyl naphthalen-ols by

- combinational bioconversion with dioxygenase PhnA1A2A3A4 and prenyltransferase NphB or SCO7190. *Bioscience, Biotechnology, and Biochemistry*, 2011, **75**, 505-510.
- [63] Xu, J.; Wang, H.; Sim, M.M. First synthesis of (\pm)-C-3-prenylated flavanones. *Synthetic Communications*, 2003, **33**, 2737-2750.
- [64] Zhao, L.M.; Zhang, S.Q.; Jin, H.S.; Wan, L.J.; Dou, F. Zinc-mediated highly alpha-regioselective prenylation of imines with prenyl bromide. *Organic Letters*, 2012, **14**, 886-889.
- [65] Medina-Franco, J.L.; Giulianotti, M.A.; Welmaker, G.S.; Houghten, R.A. Shifting from the single to the multitarget paradigm in drug discovery. *Drug Discovery Today*, 2013, **18**, 495-501.
- [66] Calderon-Montano, J.M.; Burgos-Moron, E.; Perez-Guerrero, C.; Lopez-Lazaro, M. A review on the dietary flavonoid kaempferol. *Mini-Reviews in Medicinal Chemistry*, 2011, **11**, 298-344.
- [67] Fang, Y.; Lu, Y.; Zang, X.; Wu, T.; Qi, X.; Pan, S.; Xu, X. 3D-QSAR and docking studies of flavonoids as potent *Escherichia coli* inhibitors. *Scientific Reports*, 2016, **6**, 1-13.
- [68] Prasch, S.; Bucar, F. Plant derived inhibitors of bacterial efflux pumps: an update. *Phytochemistry Reviews*, 2015, **14**, 961-974.
- [69] Aparna, V.; Dineshkumar, K.; Mohanalakshmi, N.; Velmurugan, D.; Hopper, W. Identification of natural compound inhibitors for multidrug efflux pumps of *Escherichia coli* and *Pseudomonas aeruginosa* using *in silico* high-throughput virtual screening and *in vitro* validation. *Plos One*, 2014, **9**, 1-13.
- [70] Sudano Roccaro, A.; Blanco, A.R.; Giuliano, F.; Rusciano, D.; Enea, V. Epigallocatechin-gallate enhances the activity of tetracycline in Staphylococci by inhibiting its efflux from bacterial cells. *Antimicrobial Agents and Chemotherapy*, 2004, **48**, 1968-1973.
- [71] Sakagami, Y.; Mimura, M.; Kajimura, K.; Yokoyama, H.; Iinuma, M.; Tanaka, T.; Ohyama, M. Anti-MRSA activity of sophoraflavanone G and synergism with other antibacterial agents. *Letters in Applied Microbiology*, 1998, **27**, 98-100.

Summary

Currently, there is a significant increase in antibacterial resistance coupled with a decrease in discovery and innovation in antibacterial research. The legume plant family is a potential source of novel antibacterials. Prenylated phenolic compounds from the flavonoid class, the stilbenoid class and, especially, the isoflavonoid class are important secondary metabolites in this family. Prenylation of phenolics, i.e. substitution with a C₅-isoprenoid (*prenyl*) group, is known to be a response of legumes upon infection. Prenyl groups can be attached to phenolics in different configurations, i.e. as a chain (3,3-dimethylallyl) or as a ring (e.g. 2''-isopropenylfuran or 2,2-dimethylpyran). Prior to our research, it was already known that prenylation can modulate the antibacterial properties of phenolic compounds. This was mainly related to their increase in hydrophobicity. However, their quantitative structure-activity relationships (QSAR) and mode of action were still poorly established. Therefore, this study investigated the antibacterial properties of prenylated phenolic compounds from legumes against human pathogenic bacteria. The aims of this thesis were to (i) establish systematic QSAR with regard to the antibacterial activity of prenylated phenolics, and (ii) to elucidate the mode of action of these compounds. An additional aim was to (iii) study the *in vitro* production of prenylated phenolics, as availability is one of the main limiting factors for QSAR studies and, ultimately, for their applicability. The main hypothesis of this thesis was that, besides hydrophobicity, other molecular characteristics are required to understand the antibacterial action of prenylated phenolic compounds.

In **Chapter 1** the main factors influencing the effective action of antibacterials in bacteria were described, as well as the chemical diversity of prenylated phenolic compounds present in legumes. An overview of prenylated phenolic compounds which have shown very good antibacterial activity in comparison with conventional antibacterials was presented. Additionally, the tentative mode of action of these compounds in the bacterial cell were described. Finally, different methods used to produce these compounds were presented.

In **Chapter 2** molecular diversity of phytochemicals of legume extracts was enhanced by germination and fungal elicitation of seven legume species, as established by RP-UHPLC-UV-MS. The relationship between phytochemical composition, including different types of skeletons and substitutions, and antibacterial activity of extracts was investigated. Extracts rich in prenylated isoflavonoids and stilbenoids showed potent activity against the Gram positives *Listeria monocytogenes* and methicillin-resistant *Staphylococcus aureus* at concentrations between 0.05-0.1% (w/v). Prenylated phenolic compounds were significantly correlated with the antibacterial properties of the extracts, unlike other types of phytochemicals. Furthermore, the position of the prenyl group within the phenolic skeleton was shown to influence the antibacterial activity.

In **Chapter 3** different pools enriched in prenylated phenolic compounds were made from extracts of elicited lupine, peanut and soybean seedlings. One pool was rich in chain prenylated isoflavones (isoflavonoid class), one in chain prenylated stilbenoids, one in chain prenylated 6 α -OH-pterocarpanes (isoflavonoid class), and one in ring-closed prenylated 6 α -OH-pterocarpanes. Pools showed high antibacterial activity against

L. monocytogenes, but not against *Escherichia coli* (Gram negative). The isoflavone pool was the most efficient with a minimum inhibitory concentration (MIC) of 10 $\mu\text{g}/\text{mL}$ of chain prenylated isoflavones against *L. monocytogenes*, followed by the chain prenylated pterocarpan pool (MIC 25 $\mu\text{g}/\text{mL}$), and chain prenylated stilbenoid pool (MIC 35 $\mu\text{g}/\text{mL}$). Intrinsic resistance of the Gram negative bacterium was overcome with an efflux pump inhibitor (EPI). This demonstrated that prenylated phenolic compounds are able to enter the Gram negative outer membrane (OM), and that the common intrinsic resistance observed is mainly due to the active efflux. In the presence of an EPI, *E. coli*'s susceptibility to chain prenylated isoflavones was increased to the same level as that of *L. monocytogenes*. With regard to the mode of action of these compounds, chain prenylated isoflavones permeabilized the cytoplasmic membrane of *L. monocytogenes* and *E. coli* (when combined with the EPI) within minutes of exposure, whereas the conventional antibacterial ampicillin did not. The antibacterial properties of the pools could not be explained solely by the hydrophobicity of the prenylated compounds. Intermediate skeleton flexibility and bent configuration were found to be key molecular features of the compounds present in the antibacterially active pools.

In **Chapter 4** the antibacterial properties of 30 prenylated (iso)flavonoids, which differed in phenolic skeleton and substitution with hydroxyl and methoxyl groups, as well as in configuration, number and position of prenyl substituents, were tested against *L. monocytogenes* and *E. coli*, the latter one in combination with an EPI. Diprenylated phenolic compounds were the most potent antibacterials against *L. monocytogenes*, whereas they were inactive against *E. coli* with EPI. Therefore, intrinsic resistance of this Gram negative bacterium towards diprenylated phenolic compounds was attributed to their reduced influx through porins. MIC values of the most active prenylated compounds ranged between 6.3-12.5 $\mu\text{g}/\text{mL}$ for *L. monocytogenes*, and between 10.0-15.0 $\mu\text{g}/\text{mL}$ for *E. coli*. Using QSAR analysis, significant linear and binary classification models were obtained to predict activity. The linear models accounted for $\geq 60\%$ of the variance observed, and the classification models had $\geq 83\%$ accuracy. Hydrophobicity and shape (including flexibility and globularity) were the main molecular characteristics related to antibacterial activity. The molecular shape (including specific distribution of hydrophobic and hydrogen bond acceptor groups) was illustrated by a 3D pharmacophore model for both bacteria. With this pharmacophore model, differences in activity for similar compounds, but prenylated at different positions, could be explained. With regard to the mode of action of antibacterially active prenylated (iso)flavonoids, we found that monoprenylated compounds were better membrane permeabilizers than diprenylated ones, highlighting potential differences in interaction of the mono and diprenylated molecules with the cytoplasmic membrane. The ratio of hydrophobic : polar surface area was found to correlate with the permeabilization capacity of these compounds.

Because diprenylated phenolic compounds showed the most promising antibacterial activity and availability of those compounds is limited in plants, in **Chapter 5** the production of novel diprenylated phenolic compounds was evaluated by *in vitro* enzymatic prenylation. *Streptomyces roseochromogenes* prenyltransferase SrCloQ, known to have broad acceptor substrate specificity, was used. Acceptor substrate

specificity of SrCloQ was investigated using different non-genuine phenolic compounds. RP-UHPLC-UV-MSⁿ was used for the tentative annotation and quantification of the prenylated products. Flavonoids, isoflavonoids and stilbenoids with different types of substitution were prenylated by SrCloQ, although with less efficiency than the genuine substrate. No diprenylated compounds were obtained. Nevertheless, some monoprenylated compounds produced were, to our knowledge, novel. The isoflavan equol, followed by the flavone 7,4'-dihydroxyflavone, were the best non-genuine acceptor substrates. Docking studies were performed to explain the non-genuine acceptor substrate specificity observed *in vitro* and important active site-phenolic contacts were identified. Finally, the insights obtained on acceptor substrate specificity and regioselectivity for SrCloQ were extended to other members of the CloQ/NhpB prenyltransferase family.

In **Chapter 6** the main findings presented in this thesis are discussed. The main considerations of the techniques used to quantify chemical composition and antibacterial activity were examined. Main structural characteristics and bacterial aspects found to influence the antibacterial activity of prenylated phenolics were addressed. The mode of action of these compounds was discussed in relation to the main QSAR established. Additionally, the effects of saponins on the antibacterial activity of prenylated phenolics were explained. A comparison between different production methods for diprenylated compounds was given and, finally, prospects of prenylated phenolic compounds as antibacterials were elaborated.

In conclusion, the antibacterial activity of prenylated phenolics is modulated by the type of skeleton, prenyl configuration and prenyl position. It is postulated that hydrophobicity influences the partitioning of the compounds to the cytoplasmic membrane, and that molecular shape influences the antibacterial activity and disruption of membrane integrity. Membrane permeabilization is one of the main mechanism of disruption of these compounds. Although, other forms of disruption of membrane integrity need to be further addressed. These findings provide valuable insight into the antibacterial activity and mode of action of these natural compounds. The quantitative models developed can be useful for prediction of antibacterial activity of untested molecules and provide valuable information for the design of novel prenylated phenolic compounds as antibacterials.

Acknowledgments

I would like to express my gratitude to many people who, in one way or another, supported me during this period of time.

A successful PhD is only possible with excellent leadership and for this I am especially grateful for my project supervisors Harry, Jean-Paul and Heidy. Harry thank you for the opportunity to work at the Laboratory of Food Chemistry and for being actively involved in this PhD project. Our scientific discussions challenged and improved this thesis greatly. Furthermore, your dedication for the Laboratory of Food Chemistry inspires excellent, passionate research, which is the best atmosphere I could have as a “young” scientist. Jean Paul I am grateful and happy for having you as my daily supervisor. Your knowledge, guidance and patience made this PhD fruitful and, more important, enjoyable. I had and will continue to have the best mentor I could ask for. Heidy without your involvement this project would not have progress this far. Your microbiological perspective was very valuable as well as your guidance and support throughout these years. I sincerely hope we continue to collaborate.

Special thanks to all the staff of the Laboratory of Food Chemistry. To the (associate and assistant) professors, postdocs, PhD students and technicians, thanks for sharing your knowledge so willingly and so enthusiastically. To our dear Jolanda, thank you for making things so easy and efficient for us at FCH. The pleasant social atmosphere of the Laboratory made these four years fly past by and made the decision to stay longer an easy one. Thank you all for the pleasant coffee breaks, delicious birthday cakes, fun lab trips and interesting (scientific) conversations shared.

Thanks to all the people from the Laboratory of Food Microbiology who made me feel welcome. Special thanks to Ingrid, Monica, Irma, Oscar, Judith, Eddy and Tjakko for your help in the lab and scientific advice.

My gratitude also goes to my co-authors. Gijs Schaftenaar thank you for your involvement in this project, for explaining very patiently all the details about molecular modelling and for your time improving our manuscripts. Thanks to Jos Hageman for accepting to collaborate in this project with such a short notice, and for providing very valuable statistical expertise. Furthermore, thanks to Franziska Leipoldt and professor Lutz Heide for kindly providing the prenyltransferase plasmids and for your input during the preparation of the manuscript.

Special thanks to my “isoflavonoid team” and co-authors Milou and Aisyah. You were actively part of this PhD project. Without your input I could not have done part of this research. Thank you for your feedback and also for making me part of your own projects. Furthermore, thanks to the “new” members, Wouter, Silvia and Sylvia. Thank you all for always being willing to help and for making such a pleasant working team.

I am grateful for all the BSc and MSc students I had the opportunity to work with. Bianca, Jing Jang, Bake, Tom, Pieter-Paul, Anita, Roan, Wouter and Judith, this research project would not have progress this far without your work and your scientific curiosity. Being your supervisor was a great learning experience for me and I hope I was able to transmit, at the least, my passion for science to you.

Special thanks to my officemates from Biotechnion and Axis, Annemieke, Elisabetta, Melliana, Patricia, Claire, Yuxi, Abhishek, Bianca, Moheb and Wouter. Our scientific discussions, interesting random conversations, stupid jokes, chocolate, birthday decoration, made PhD student life very fun.

To my colleagues but more important my friends, Alexandra, Patricia and Elisabetta. Your friendships are one of best things I got from this time. Thanks for all the crazy fun moments and long live “el trio de la muerte”.

Special thanks to Pepe, my grandfather who is responsible for my passion for science. Pepe thank you for sharing your wisdom and immense knowledge with me; for always encouraging me to ask questions. I feel very privileged to have you and I promise to never stop learning.

A mi familia de Holanda, Irene, Marce V., Rafita, Made, Serguis, Marce F., Francito, Peter, Vicky, Pieter, Xio y Coen. Muchas gracias por adoptarme desde que llegue hace más de 6 años. Les agradezco de corazón todo el apoyo incondicional. Son parte de mi vida y espero seguir compartiendo logros, bendiciones y retos. Los quiero mucho.

Gracias a mi familia en Costa Rica y Panamá por el amor que siempre me han mostrado. A mis padres, en cada paso o decisión tomada los he tenido siempre muy presentes en mi corazón. Hoy soy quien soy gracias a ustedes y es una bendición tenerlos en mi vida. Los quiero mucho a todos y los extraño todos los días.

Un logro compartido se disfruta mejor y soy muy afortunada de tener un compañero de vida para hacerlo. Carlos Iván gracias por compartir sueños, por la paciencia y por el amor durante todos estos años. Te amo.

CARLA

About the author

CURRICULUM VITAE

Carla Maria Araya-Cloutier was born on June 23rd 1986 in Tilarán, Costa Rica. In 2004 she started her studies in Food Technology at University of Costa Rica. Her major thesis was conducted at the National Centre of Food Science and Technology (Centro Nacional de Ciencia y Tecnología de Alimentos, CITA) and focused on the development of a fermentation process for production of lactic acid using an industrial waste product from pineapple and *Lactobacillus casei* subspecies *rhannosus*. In 2010 she graduated and received an NFP fellowship to study the MSc in Food Technology with the specialization in Food Ingredient Functionality at Wageningen University. Her major thesis focused on the effect of galactooligosaccharides on the composition and metabolism of antibiotic-treated gut microbiota, and it was performed at the Laboratory of Food Chemistry. As part of her MSc program she conducted an industrial internship at Unilever R&D, Vlaardingen, the Netherlands, where she studied mild cell-opening techniques for the extraction of soybean oil. After graduating with honours in 2012, she started her PhD research at the Laboratory of Food Chemistry. The results of her PhD research are presented in this thesis. Carla continues to work at the Laboratory of Food Chemistry as postdoctoral researcher.



Contact: caraya86@gmail.com

LinkedIn: www.linkedin.com/in/carla-araya-cloutier

LIST OF PUBLICATIONS

Araya-Cloutier, C.; Vincken, J-P.; van de Schans, M.G.M.; Schaffenaar, G.; Hageman, J.; den Besten, H.M.W.; Gruppen, H. 2017. QSAR-based molecular signatures of prenylated (iso)flavonoids underlying antimicrobial potency against and membrane-disruption in Gram positive and Gram negative bacteria: *Listeria monocytogenes* and *Escherichia coli*. *To be submitted for publication*.

Araya-Cloutier, C.; Vincken, J-P.; van Ederen, R.; den Besten, H.M.W.; Gruppen, H. 2017. Rapid membrane permeabilization of *Listeria monocytogenes* and *Escherichia coli* induced by prenylated phenolic compounds: influence of skeleton structure and prenyl configuration. *Submitted for publication*.

Araya-Cloutier, C.; Martens, B.; Schaffenaar, G.; Leipoldt, F.; Gruppen, H.; Vincken, J-P. 2017. Structural basis for non-genuine phenolic acceptor substrate specificity of *Streptomyces roseochromogenes* prenyltransferase CloQ from the ABBA/PT-barrel superfamily. *Accepted in PLOS ONE*.

Araya-Cloutier, C.; den Besten, H.M.W.; Aisyah, S.; Gruppen, H.; Vincken, J-P. 2017. The position of prenylation of isoflavonoids and stilbenoids from legumes (Fabaceae) modulates the antimicrobial activity against Gram positive pathogen. *Food Chemistry* 226:193-201.

Zderic, A.; **Araya-Cloutier, C.;** Zondervan, E. 2016. Mild disclosure of oil bodies from soybeans: From operating window towards process design. *Journal of Food Technology and Preservation* 1(1): 18-24.

Araya-Cloutier, C.; Rojas-Garbanzo, C.; Velázquez-Carillo, C. 2012. Effect of initial sugar concentration on the production of L (+) lactic acid by simultaneous enzymatic hydrolysis and fermentation of an agro-industrial waste product of pineapple (*Ananas comosus*) using *Lactobacillus casei* subspecies *rhamnosus*. *International Journal of Biotechnology for Wellness Industries* 1(1):91-100

Araya-Cloutier, C.; Rojas-Garbanzo, C.; Velázquez-Carillo, C. 2010. Síntesis de ácido láctico, a través de la hidrólisis enzimática simultánea a la fermentación de un medio a base de desecho de piña (*Ananas comosus*) para uso como materia prima para la elaboración de ácido poliláctico. *Revista Iberoamericana de Polímeros* 11(7): 407-416.

OVERVIEW OF COMPLETED TRAINING ACTIVITIES

Discipline specific activities

Courses

Advanced Food Analysis	VLAG, Wageningen, 2013
Ion Trap Operations	Thermo Scientific, London, 2013
Genetics and Physiology of Food Associated Microorganisms	VLAG, Wageningen, 2013
International Chemical Design and Discovery course	CMBI, Nijmegen, 2014
Multivariate Analysis of Food Data	VLAG, Wageningen, 2014
Diversity in Science Symposium	WPC, Wageningen, 2016

Conferences

Polyphenol Applications	ISANH, Bonn, 2013
International Symposium on Phytochemicals in Medicine and Food ^b	PSA, Shanghai, 2015

General Courses

VLAG PhD Introduction Week	VLAG, Baarlo, 2013
Techniques for Writing and Presenting a Scientific Paper	WGS, Wageningen, 2013
Project and Time Management	WGS, Wageningen, 2013
Mobilising your Scientific Network	WGS, Wageningen, 2013
Teaching and Supervising Thesis Students	ESD, Wageningen, 2014
WGS PhD Workshop Carousel	WGS, Wageningen, 2014
Scientific Writing	WUR in'to Languages, Wageningen, 2015

Optionals

Research proposal preparation	FCH, Wageningen, 2012
PhD study trip	FCH, Singapore and Malaysia, 2012
PhD study trip ^{a, b, c}	FCH, Germany, Denmark, Sweden and Finland, 2014
BSc and MSc thesis student supervision, presentations and colloquia	FCH, Wageningen, 2012-2016
PhD presentations and seminars	FCH, Wageningen, 2012-2016

^a Poster presentation. ^b Oral presentation. ^c Organizing committee

Abbreviations: CMBI, Centre for Molecular and Biomolecular Informatics. ESD, Educational Staff Development Wageningen University. FCH, Laboratory of Food Chemistry, Wageningen University. ISANH, International Society of Antioxidants in Nutrition and Health. PSA, Phytochemical Society of Asia. VLAG, Graduate School for Nutrition, Food Technology, Agrobiotechnology and Health Sciences. WGS, Wageningen Graduate Schools. WPC, Wageningen PhD Council. WUR, Wageningen University & Research.

The work described in this thesis was performed at the Laboratory of Food Chemistry, Wageningen University & Research, the Netherlands.

Financial support from Wageningen University for printing this thesis is gratefully acknowledged.

Cover design by Carla Araya-Cloutier and Soledad Cook-Ordonez

Printed by Proefschrift-AIO, the Netherlands

Edition: 250 copies

Carla Araya-Cloutier, 2017

